UNIVERSITÀ DEGLI STUDI DI MILANO

Scuola di Dottorato in Scienze Biologiche e Molecolari

XXVIII Ciclo

Immunopathological response to *Pseudomonas aeruginosa* and potential therapies in respiratory infections

Camilla Riva

PhD Thesis

Scientific tutor: Prof. Giovanni Bertoni

Scientific co-tutor: Dr. Alessandra Bragonzi

Academic year: 2015-2016

SSD: [BIO/11; BIO/19]

Thesis performed at San Raffaele Scientific Institute; Division of Immunology, Transplantation and Infectious Diseases; Infections and Cystic Fibrosis Unit.

Contents

Part I

Part II

Published Paper

ASCRONYMS and ABBREVIATION

ASL: airway surface liquid

BALF: bronchoalveolar lavage fluid

BALT: broncus associated lymphoid tissue

CF: cystic fibrosis

cftr: cystic fibrosis trasmembrane regulator gene

COPD: chronic obstructive pulmonary disease

ENaC: epithelial sodium channel

GAG: glycosaminoglycans

sGAG: sulphated glycosaminoglycans

HNE: human neutrophil elastase

HS: heparin sulphate

HEP/HS: heparin/heparin sulphate

IPF: idiopathic pulmonary fibrosis

LPS: lipopolysaccharide

LTB4: leukotriene B4

MMPs: metalloproteases

MRSA: methicillin-resistant *Staphylococcus aureus*

NCFB: non-cystic fibrosis bronchiectasis

NF-Kb: nuclear factor κB

PAMPs: pathogen-associated molecular patterns

PGN: peptidoglycan

PGP: proline-glycine-proline

PCL: periciliary liquid layer

RBM: reticular basement membrane

TLRs: toll like receptors

TGF-β: transforming growth factor-beta

TNFα: tumor necrosis factor

FEV_1: forced expiratory volume 1

PS: polysaccharide

FDA: Food and Drug Administrartion

A. Abstract

Repeated cycles of infections, caused mainly by *Pseudomonas aeruginosa,* combined with a robust host immune response and tissue injury, determine the course and outcome of cystic fibrosis (CF) lung disease. The initial acute infection disease is kept in check by an excessive neutrophil-dominated inflammation, while as the disease progresses *P. aeruginosa* adapts to the airways and dramatically modifies its phenotype causing permanent chronic infection. The persistent *P. aeruginosa* infection escapes the innate immune responses and causes damage to the host. Airways remodelling is characterized by mucus hypersecretion, degradation of its structural components, caused by the activity of matrix metalloproteinases, and high level of sulphated glycosaminoglycans (GAG). However, whether, how and at to what extent bacterial adaptive variants and their persistence influence the pathogenesis and disease development, and the role played by GAG in this context remain largely unknown.

Using *in vitro* and murine models of acute and chronic lung infection, we showed that *P. aeruginosa* CF-adaptive variants shaped the innate immune response favoring their persistence. Next, we refined a murine model of chronic pneumonia extending *P. aeruginosa* infection up to three months. In this model we observed that the *P. aeruginosa* persistence lead to CF hallmarks of airway structural degeneration and fibrosis, including epithelial hyperplasia, goblet cell metaplasia, collagen deposition, elastin degradation, GAG remodelling and several additional markers of tissue damage. This murine model was further exploited to test the effect of a library of compounds that could compete with GAG present in the lung (GAG mimetics), with attenuated anticoagulant properties, on host response to *P. aeruginosa* infection. GAG mimetics C3 and C23 demonstrated a remarkable efficacy in reducing inflammation and tissue damage. These molecules contained also the bacterial load during *P. aeruginosa* chronic infection, probably acting on biofilm formation. Overall, the murine model of *P. aeruginosa* chronic infection, reproducing CF lung pathology, established in this work has been instrumental to identify novel molecular targets and to test newly tailored molecules inhibiting chronic inflammation and tissue damage processes in pre-clinical studies. In addition, the results obtained with GAG mimetics support the developments of these compounds as novel therapy in CF and potentially for the treatment of other chronic respiratory pathologies.

B. State of the Art

B.1. Chronic lung diseases: epidemiology and pathogenesis

Chronic lung disease is the term for a wide variety of persistent lung disorders. Airway diseases are some of the most common medical conditions in the world but their prevalence is underestimated according to epidemiological surveys, which further increases the complexity of managing these diseases. Despite the presentation of similar symptoms (dyspnea, coughing, wheezing and expectoration) airway diseases have different underlying pathophysiological processes and must be distinguished to enable the administration of appropriate treatment (Athanazio, 2012). This section aims to present the main features of the most common chronic respiratory illnesses: bronchiectasis, chronic obstructive pulmonary disease (COPD), asthma, idiopathic pulmonary fibrosis (IPF) and cystic fibrosis (CF) (**Fig. 1**).

Bronchiectasis is a respiratory disease characterized by irreversible widening of thick-walled-bronchi, periods of acute infective exacerbations (short periods, at least 48 h, of increased cough, dyspnea, and production of sputum that can become purulent), inflammation, and purulent sputum-expectoration (Bilton, 2008). Respiratory infections are the leading causes of bronchiectasis. The main bacterial pathogens that are commonly isolated in bronchiectasis are *Haemophilus influenza*, *Pseudomonas aeruginosa*, *Streptococcus pneumoniae*, *Haemophilus parainfluenzae*, *Staphylococcus aureus and Moraxella catarrhalis* (Feldman, 2011). About one-third of the patients with bronchiectasis are chronically colonized with *P. aeruginosa* and are known to experience an accelerated decline in lung function and more frequent exacerbations than those infected with other microorganisms (Chawla et al., 2015). However, other pro-inflammatory attacks can trigger or accelerate bronchiectasis disease, such as a toxin inhalation, smoking or changes in immune responses (O'Donnell, 2008). The prevalence and severity of the non-cystic fibrosis bronchiectasis (NCFB) intensifies with age and when in association with other diseases or autoimmune symptoms, including COPD or rheumatoid arthritis respectively, the relative risk of death increases (Bergin et al., 2013).

COPD is a major cause of chronic morbidity and mortality worldwide. COPD is a pulmonary disease characterized by airflow limitation that is not fully reversible (Cukic et al., 2012). The airflow limitation is often ascribed to remodeling, which consists of airway wall thickening by fibrosis and/or emphysema, airway epithelial cell hyperplasia, squamous cell and goblet cells metaplasia, reticular basement membrane (RBM) thickening and angiogenesis (Hirota and Martin, 2014).

Despite the morphologic and clinical heterogeneity of COPD, one common feature is inflammation in the small airways (characterized mainly by infiltration of neutrophils, macrophages, $CD8^+$ T-cells and B-cells), which intensifies with disease progression (Brightling et al., 2000). Approximately 90% of COPD cases are related to smoking, whereas other less common risk factors include occupational exposure and biomass burning (Athanazio, 2012). The chronic and progressive course of COPD is frequently aggravated by exacerbations. *H influenzae*, *S. pneumoniae*, *M. catarrhalis* and *P. aeruginosa* are associated with increased bronchial and systemic inflammation and the development of exacerbations (Sethi et al, 2008). Opportunistic bacteria (approximately 50%) and also virusis (approximately 30%) can, therefore, accelerate the progression of COPD through an increase in the frequency of exacerbations and also through direct injury to the lung tissue (Decramer et al., 2012).

Asthma is a common chronic lung disease characterized by intermittent airway obstruction and inflammation (in particular characterized by $CD4^+$ T cells, eosinophils and mast cells) that affects more than 300 million people worldwide (Martinez and Vercelli, 2013). In severe cases, the sub-epithelial basement membrane is thickened, smooth-muscle mass is increased through hypertrophy and hyperplasia, the airways undergo fibrosis with increased deposition of connective tissue, and fibroblast and myofibroblast (cells with contractile properties) proliferation occurs (Wadsworth, 2013). In atopic individuals, the main risk factor for developing asthma is exposure to allergens. For individuals with non-atopic asthma, several risk factors have been found, including smoking, advanced age, an unfavorable socio- economic condition and housing in an urban center (Court et al., 2002). Bacterial infections (*S. pneumonia*, *S. pyogenes*, *S. aureus*, *M. catarrhalis* and *H. influenzae)* may also contribute to airway wall remodeling through the activation of fibrosis by the release of growth factors such as transforming growth factor β (TGF-β), leading to fibroblast activation and release of extracellular matrix proteins (Rossol et al., 2011; Zhang 2012).

IPF is a chronic, progressive, irreversible, and usually lethal lung disease of unknown cause. Injury to the alveolar epithelium followed by aberrant repair is a central pathogenic mechanism in IPF and this dysregulated repair is characterized by 'fibroblast foci', aggregates of activated myofibroblasts whose extent correlates with poorer prognosis (King Jr et al., 2011). IPF occurs primarily in older adults, many of whom have been smokers, and polymorphisms in genes related to epithelial integrity and host defense predispose to the disease (Noth et al, 2013). Although viruses may play a part in the initiation and progression of disease and may also be responsible for a proportion of acute exacerbations (Wootton et al., 2011), the role of bacteria in the

pathogenesis and progression of IPF has not yet been studied in detail. Active infection in IPF is, however, known to carry a high morbidity and mortality (Molyneaux and Maher, 2013) suggesting that bacteria may play a role in driving IPF disease progression.

CF disease is caused by mutations in the in the cystic fibrosis transmembrane regulator (*cftr*) gene and remains one of the most common fatal hereditary disorders worldwide. Although CF is a complex multi-organ disease, morbidity and mortality are mainly determined by chronic obstructive lung disease that evolves from early onset mucus plugging in the small airways, chronic neutrophilic airway inflammation and bacterial infection (Mall and Hartl, 2014). The destruction of lung function due to the hyperactive inflammatory response, possibly exacerbated by bacterial toxins, causes the progressive deterioration of lung function and ultimately makes these lung infections fatal (Gellatly and Hancock, 2013). The most common bacterial pathogens isolated from the CF airways are *H. influenza*, *S. aureus* and *P. aeruginosa*. About 80% of adult CF patients suffer from chronic *P. aeruginosa* lung infections which are responsible for their short life expectancy with a median predicted survival of 40.7 years (Cystic fibrosis foundation patient registry Annual Report 2014). CF disease will be further described in the next paragraph.

Although these diseases present several common characteristics, they have different pathological origins and may present diverse clinical outcomes. Improved understanding of the pathophysiological pathways, the role of bacterial pathogens, and airway remodeling are needed to explore therapies that can be shared by patients affected by diverse respiratory diseases.

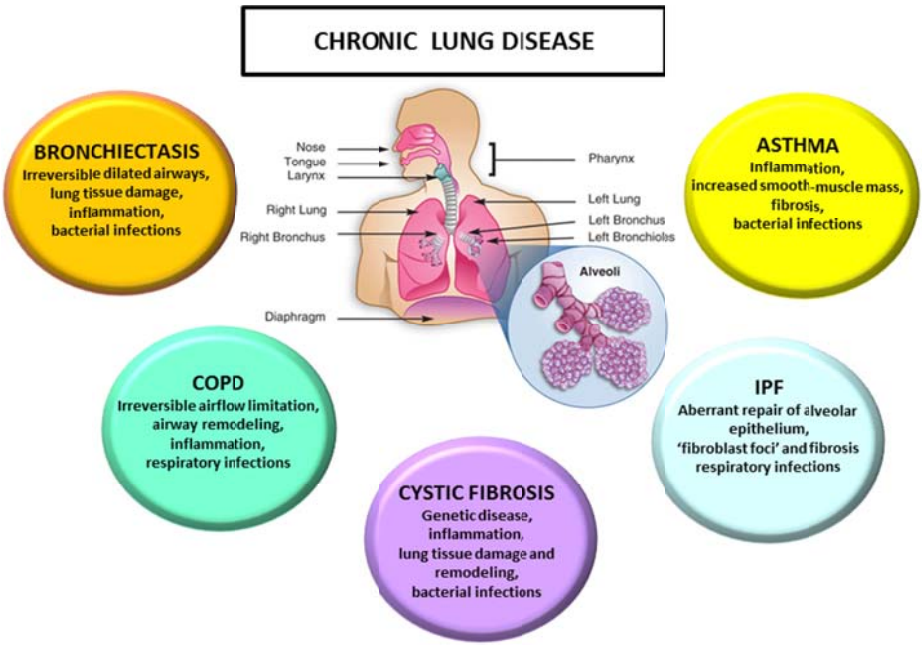

Figure 1. Main features of chronic lung diseases.

B.2 Cystic fibrosis

B.2.1 Epidemiology of CF and relevant aspects of CF lung pathogenesis

Although classified as a rare disease, CF is the most common life-threatening monogenic condition in Caucasians. The estimated incidence of CF is 1 in 2500-4000 newborns, with a recognized heterogeneity in the geographic distribution. CF affects >70,000 individuals worldwide, including 30,000 in Europe. There is a wide clinical variability in organ involvement; the dominant cause of morbidity and mortality is lung disease, but other CF symptoms include pancreatic insufficiency, intestinal obstruction, elevated electrolyte levels in sweat (the basis of the most common diagnostic test) and male infertility (Amaral, 2015).

This inherited condition is caused by the mutation in the *cftr* gene that encodes a 1480 amino-acid CFTR protein with a mass of about 170 Kda. The large glycoprotein CFTR (**Fig. 2**) is a cAMP-regulated Cl^- and bicarbonate ($HCO3^-$) channel and is expressed primarily in lipid bilayer at the apical membrane of epithelial cells but also in many other cell types, including immune system cells (Gadsby et al., 2006).

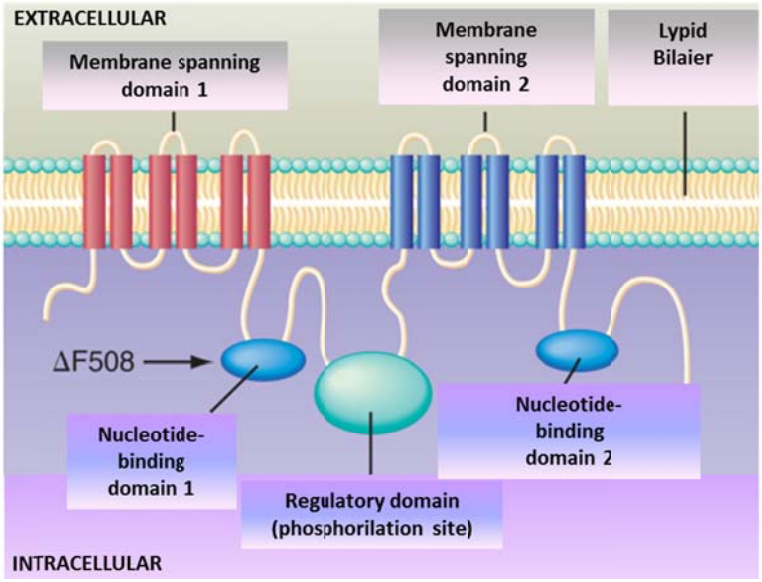

Figure 2. CFTR protein chloride channel expressed in lipid bilayer at the apical membrane of epithelial cells. The CFTR protein is a member of the ATP-binding cassette (ACB) family of transporters. It contains two nucleotide-binding domains that bind and hydrolize ATP, two trasmembrane domains that form the channel, and a central regulatory (R) domain. The R domain, unique to CFTR, is highly charged with numerous phosphorylation sites for protein kinase A or C (Gibson et al., 2003).

Although CFTR mainly functions as a chloride channel, it has many other regulatory roles, including inhibition of sodium transport through the epithelial sodium channel (ENaC), regulation of ATP channels, regulation of intracellular vesicle transport, acidification of intracellular organelles, and inhibition of endogenous calcium-activated chloride channels. Consequently, CFTR regulates the hydration of the airways' surface fluid (O'Sullivan and Freedman, 2009; Sagel and Accurso, 2002).

A defect of CFTR protein impacts on airway physiology and mucociliary clearance. The airway surface liquid (ASL) is the first line of defense against inhaled or aspirated pathogens providing a barrier between the epithelium and inspired air and its regulation reflects the balance between sodium (Na^+) absorption and chloride (Cl^-) secretion mediated by EnaC and CFTR channels respectively. ASL consists of two layers above the epithelial surface – a periciliary liquid layer (PCL) with a height of the extended cilium (about 7 um) and a thin and hydrated mucus layer. The PCL volume is tightly regulated to provide a low viscosity solution for ciliary beat and to lubricate gel forming mucins secreted from cell surface. Within the PCL the rate of epithelial O_2 consumption is homogeneous. The mucus layer consists of high molecular weight mucins, produced by surface goblet cells and submucosal gland epithelia, whose properties are altered by water content, ion concentrations, and pH. The diversity of the carbohydrate side chains within the mucin gel is suited for binding a wide variety of particles for ultimate clearance from the airway (Gibson et al., 2003). In CF, the airway epithelium absorbs the Na^+ and Cl^- ions and water from the lumen, depletes the PCL and slow down or even stop the mucus transport (**Fig. 3**).

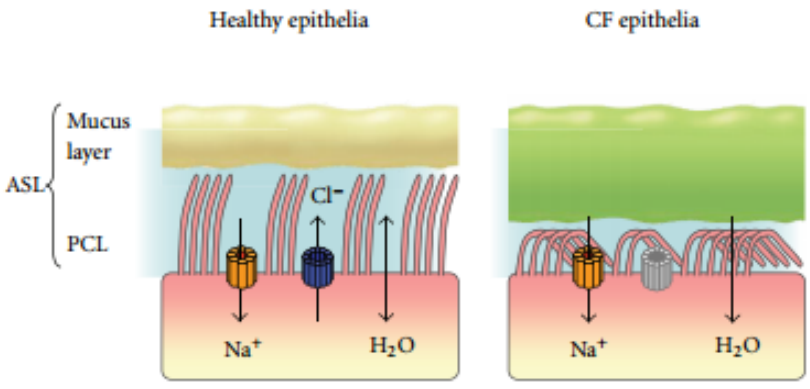

Figure 3. **Effect of CFTR dysfunction on the airway surface liquid (ASL)**. (**a**) In healthy airway epithelia, CFTR is intact and plays a vital role in regulating hydration of the ASL that consists of the periciliary layer (PCL) and the mucus layer. (**b**) Due to defective CFTR in CF, Cl^- secretion is impaired and Na^+ absorption through ENaC is upregulated resulting in dehydration of the ASL with thick mucus accumulating and causing the PCL to collapse (Reeves et al., 2012).

Increased CF epithelial O_2 consumption, associated with accelerated CF ion transport, generates steep hypoxic gradients in the thickened mucus layer with zones ranging from aerobic (generally located at the top) and microaerobic and/or even completely anaerobic (located in the deeper layers) (Worlitzsch et al., 2002; Hassett et al., 2002; Boucher, 2004). Moreover, an impaired bicarbonate (HCO_3^-) secretion leads to a decrease of ASL pH. Of note, mucins become more viscous at acidic pH, thus probably contributing to the thick hypoxic mucus plaque formation that characterizes CF airways. The hypoxic gradient in the thickened mucus layer creates a favorable environment for the opportunistic pathogen *P. aeruginosa* that is considered the key pathogen in CF. *P. aeruginosa*, deposited on the mucus surfaces, penetrates actively (e.g., by inhalation, flagellum- or pili-dependent motility) and/or passively (due to mucus turbulence) into hypoxic zones of the mucus masses (Gibson et al., 2003). Subsequent chronic airway infections with *P. aeruginosa,* are usually preceded by a period of recurrent, intermittent of the airway. In this phase the infection can be effectively combated with aggressive antibiotic therapy, and this can substantially delay the onset of chronic infection (Folkesson et al., 2012). For unknown reasons, this intermittent colonization phase, which can last for years, sooner or later turns into a chronic infection (Burns et al., 2001; Doring et al., 2006) that is characterized by the adaptation of the bacterium to hypoxic niches with increased alginate production and macro-colonies creation (**Fig. 4**). These macro-colonies are often embedded within a self-produced matrix of extracellular polymeric substance (known as biofilm mode of growth), becoming resistant to secondary defenses including neutrophils and antibiotic treatment. These pathogenic events favor the persistence of *P. aeruginosa*, setting the stage for the establishment of chronic infection and increased lung obstruction and destruction (Gibosn et al., 2003; Folkesson et al., 2012).

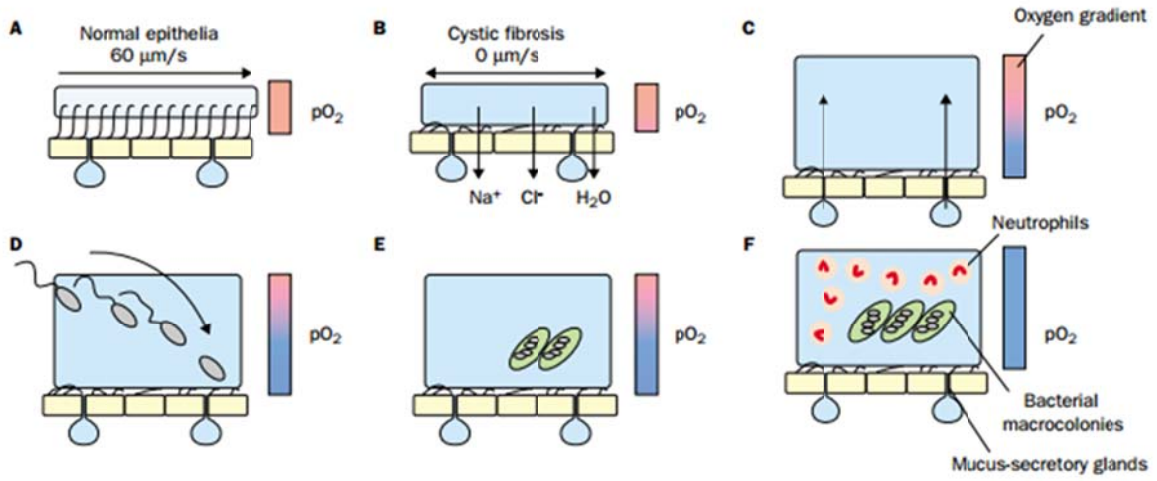

Figure 4. Schematic view of the pathogenic events that leads *P. aeruginosa* to establish chronic infection in airways of CF patients. Because of blocked chloride secretion, excessive sodium absorption and water absorption, normal mucociliary clearance (A) is defective in cystic fibrosis (B). Mucus secretion leads to plug formation (C). Steep hypoxic gradients (blue bar) are sensed by penetrating bacteria (D) leading to increased alginate (**E**) and macrocolony formation (F). The macro-colonies are resistant to secondary defens including neutrophils and antibiotic treatment. (F). (Legend: Blue circles=mucus layer; yellow squares=airway epithelial cells. For oxygen gradient: red=no gradient; blue=steep, hypoxic gradient) (Ratjen and Doring, 2003).

B.2.3 Microbial infections in CF

CF has a unique set of bacterial pathogens that are frequently acquired in an age-dependent sequence (**Fig. 5**)(Cystic Fibrosis Foundation Patient Registry 2013). For many decades, the microbiology of CF airway infections has been determined by bacterial and fungal culture methods, focusing on the most commonly isolated organisms including *S. aureus*, *H. influenza* and *P. aeruginosa* (Hauser et al., 2011). Early infections in CF airways are most frequently caused by *H. influenzae* and *S. aureus*, microorganisms detected also in the airways of other young children with chronic illnesses and adults with NCFB (Burns et al., 2001). *S. aureus* is often the first organism cultured from the respiratory tract of young children with CF (Armstrong et al., 1997) and remains an important pathogen through adulthood. The CF community is particularly concerned about methicillin-resistant *S. aureus* (MRSA). Some data suggest slightly worse clinical outcomes in patients with chronic MRSA infections than in those with methicillin-sensitive *S. aureus* infections (MSSA), as greater airflow obstruction, increased hospital admissions and extended courses of antibiotics (Ren et al., 2007). *P. aeruginosa* is the most significant pathogen in CF (Gibson et al., 2003). Pediatric CF patients with respiratory culture positive for *P. aeruginosa* experience higher mortality, increased frequency of infection, hospitalization for acute respiratory exacerbations, and decreased lung function with a significantly lower percent of predicted forced

expiratory volume 1 (FEV_1) when compared to those without *P. aeruginosa* (Emerson et al., 2002). The source of *P. aeruginosa* isolates in patients with CF has not been clearly established. There is a wide distribution of *P. aeruginosa* genotypes that have been demonstrated in young children (Burns et al., 2001), suggesting acquisition from environmental reservoirs, and sometimes do patients with CF appear to share genotypes (Armstrong et al., 2002; Speert et al., 2002). Colonization can occur both in paranasal sinuses and in the lungs. Comparison of genotypes from upper and lower airway sources, collected simultaneously from patients, could indicate the same genotype. After waves of antibiotic treatment, it was demonstrated that the lung can be recolonized by the same *P. aeruginosa* genotype, which has survived the immune and antibiotics attack in the paranasal sinuses (Folkessons et al., 2012).

Many other opportunistic organisms not commonly recovered from healthy individuals have been associated with evolution of the airway disease in CF individuals over the last decade. It was recently demonstrated that *Achromobacter xylosoxidans* is a clinically important pathogen in CF patients causing inflammation and clinical deterioration similar to the changes found in CF patients infected with *P. aeruginosa* (Hansen et al., 2010). The prognosis dramatically becomes worst after the acquisition of *Burkholderia cepacia* complex that causes a sepsis-like syndrome characterized by high fever, bacteremia and rapid progression to severe necrotizing pneumonia leading to death. Recent studies on fungal colonization/infection of the CF airway show the presence of *Aspergillus fumigatus* in up 50% of subjects and its association with a lower FEV_1 and an increased exacerbations requiring hospitalization (Amin et al., 2010).

More recently, non-culture based methods have contributed to our understanding of the polymicrobial nature of CF airway infections. Many organisms not previously recovered from the CF airway have been reported from patient samples using polymerase chain reaction (PCR) and deep sequencing (Bittar et al., 2010; Salipante et al., 2013) including viridans streptococcus, *Prevotella* spp., *Veillonella* spp. and other anaerobic organisms. While *Streptococcus milleri* has been reported to be a clinically relevant pathogen in CF because of its association with pulmonary exacerbations (Sibley et al., 2010), studies by Zemanick and others have reported that anaerobes identified from sputum by sequencing are associated with less inflammation and higher lung function than *P. aeruginosa* (Sibley et al., 2010; Zemanick et al., 2013).

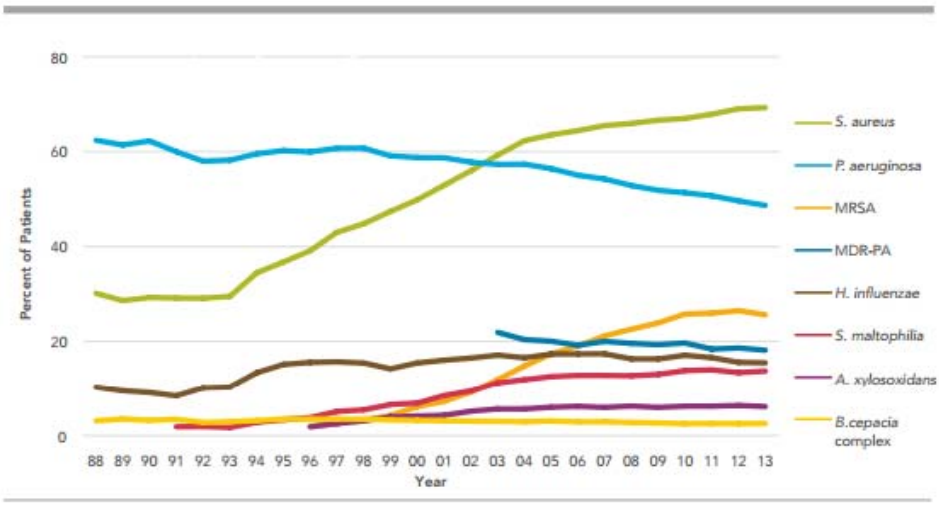

Figure 5. Prevalence of respiratory microorganisms in patients with CF as a function of age. The prevalence of multi-drug resistant *P. aeruginosa* (MDR-PA) and methicillin-resistant S. aureus (MRSA) are also included in the graph (Cystic Fibrosis Foundation Patient Registry 2013).

B.2.4 Adaptation of *P. aeruginosa* to CF airways

Several studies have followed the progression of *Pseudomonas* infections in patients with CF over the course of many years. The capacity of *P. aeruginosa* to cause infections in CF patients and other hosts can be traced back to its considerable adaptability to specific environment conditions, such as micro-anaerobic condition of CF airways, and the production of numerous virulence factors (Lee *et al*., 2006) (**Fig. 6**).

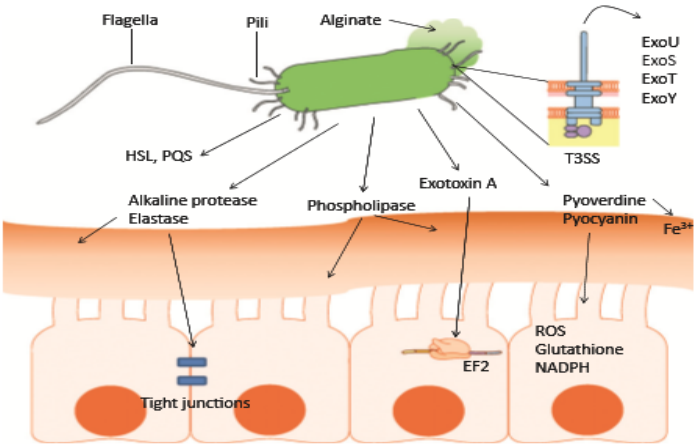

Figure 6. **Virulence factors produced by *P. aeruginosa*.** Flagella and type 4 pili are the main adhesins, capable of binding to host epithelial gangliosides, asialoGM1 and asialoGM2. Along with lipopolysaccharide (LPS), these surface appendages are also highly inflammatory. Once contact with host epithelia has occurred, the T3SS can be activated, which is able to inject cytotoxins directly into the host cell. Several virulence factors are secreted by *P. aeruginosa* and have varying effects on the host. Several proteases are produced, which can degrade host complement factors, mucins, and disrupt tight junctions between epithelial leading to dissemination of the bacteria. Lipases and phospholipases can target lipids in the surfactant as well as host cell membranes. Pyocyanin, a blue-green pigment, can interfere with host cell electron transport pathways and redox cycling. Pyoverdine captures $Fe3^{+}$ to allow for a competitive edge in an environment in which free iron is scarce (Gellatly SL and Hancock RE, 2013).

P. aeruginosa possesses a 6,3 Mb genome encoding 5,570 predicted ORFs and 521 putative regulatory genes suggesting that its adaptability is linked to a highly complex gene regulation (Stover et al., 2000). The accessory genome, that can be horizontally transferred among strains, represents the flexible gene pool (e.g. bacteriophages, plasmids, insertion elements, transposons, conjugative transposons, integrons and genomic islands) that frequently undergoes acquisition and loss of genetic information. Therefore the flexible gene pool plays an important role in the adaptive evolution of bacteria (Klockgether et al., 2007; Wiehlmann et al., 2007).

CF lung disease follows a characteristic patter. Chronic CF airway infection with *P. aeruginosa* is usually preceded by a period of recurrent, intermittent colonization of the airway. In this phase, which can lasts from birth until the patients acquires a chronic infection, the infection can be effectively combatted with aggressive antibiotic therapy, and this can substantially delay the onset of subsequent chronic infection (Hoiby et al., 2005). The patient is often re-infected at later time points with other *P. aeruginosa* strains of different genotypes, but in approximately 25% of cases re-colonization occurs with the same genotypes (Doring et al., 2006; Gibson et al., 2003; Munck et al., 2001). Given the plasticity of *P. aeruginosa* and the prolonged infections characteristic of CF, it is not surprising that this pathogen undergoes significant adaptation within the CF lung. Although initial infection may be facilitated by the large genome of *P. aeruginosa* and its superior ability to sense and respond to a broad variety of environmental conditions (Stover et al., 2000), later adaptation results at least in part from the selection of clonal lineages containing spontaneously arising mutations. Mutations result in the generation of a diverse array of *P. aeruginosa* lineages, many of which exhibit altered phenotypes (Smith et al., 2006). Then, conditions within the CF airways favor the growth and selection of strains with phenotypic traits that confer an adaptive advantage. Such selection is relatively common in CF but apparently differs in its nature from one portion of the respiratory tract to another, resulting in heterogeneous populations of bacteria that are closely related but possess unique sets of mutated genes (Hogardt et al., 2004; Nguyen and Singh, 2006; Smith et al., 2006).

Single, motile *P. aeruginosa* cells expressing high amounts of toxins are characteristic for acute and generalized types of infections. Whereas, various morphotypes, that are not normally present in environmental *P. aeruginosa* strains, have been described in strains isolated from chronically infected CF patients, including strains that are mucoid, smooth, rough, dwarf, colorless or present as small colony variants (SCV) (Lory et al., 2009; Starkey et al., 2009). Studies in the agar beads murine model by using the *P. aeruginosa* isolates from patients with CF demonstrated that the risk

of chronic infection is increased by the absence of pili and flagella (Bragonzi et al., 2009). These studies provide an explanation for the clinical observation that *P. aeruginosa* isolates obtained from CF hosts often exhibit a non-motile phenotype (Luzar et al., 1985; Rau et al., 2010) and explain how this phenotype can confer a survival advantage for bacteria during chronic infection. A consistent finding in CF airways is the presence of mucoid *P. aeruginosa* strains that overproduce the exopolysaccharide alginate, a negatively charged polymer of b-1-4-linked D-mannuronate, and its C5 epimer, L-guluronate (Deretic et al., 1995; Boucher et al., 1997). Alginate expression is upregulated by microaerobic environmental conditions that are present in the viscous mucus of CF patients (Worlitzsch et al., 2002). Alginate expression is considered to be an important factor for the persistence of *P. aeruginosa* in the airways of CF patients as alginate protects the pathogen not only against innate immune functions but also against opsonophagocytosis involving specific antibodies, produced by the adaptive immune system. Other phenotypic changes of *P. aeruginosa* strains occurring during the course of chronic CF lung infection include decreased exotoxin A expression (Suh et al., 1999), lipolysaccharide (LPS) and peptidoglycan (PGN) modifications (Hancock et al., 1983; Cigana et al., 2009) and altered lipid moieties (Sabra et al., 2003). Furthermore, increased auxotrophy (Thomas et al., 2000), defects in type II (Woods et al., 1986) and III secretion (Jain et al., 2004; Lee et al., 2005; Hogardt et al., 2007; Rau et al., 2010), reduced production of proteases and phospholipase C, loss of pyoverdine, pyocins and elastase expression (Hogardt et al., 2007), altered metabolic activities (Silo-Suh et al., 2005) and antibiotic resistance (Smith et al., 2006; Hogardt et al., 2007) have been described in *P. aeruginosa* strains from CF patients. Thus, chronic exposure to the CF environment selects for a variety of adapted phenotypes in *P. aeruginosa* strains (**Fig. 7**).

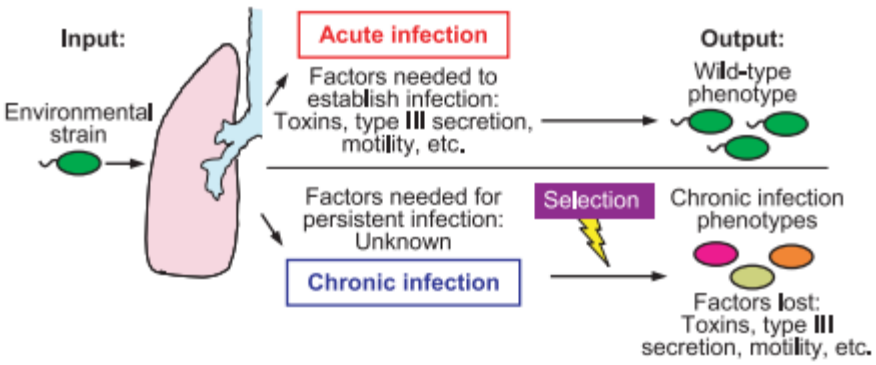

Figure 7. **Evolution of *P. aeruginosa* acute and chronic lung infection in CF disease**. The factors needed for acute infections are generally well understood, whereas those needed for chronic infection are not. Bacterial functions needed for acute infection are usually selected against in chronic CF infections (Nguyen and Singh, 2006).

So far, also whole-genome analysis indicates that *P. aeruginosa* adapts genetically to CF airways, suggesting that most phenotypic varieties of chronic *P. aeruginosa* isolates are genetically determined by mutation and selection. When a *P. aeruginosa* isolate was compared with its clonal variants, isolated 90 months later from a single CF patient, revealing 68 mutations, the analysis suggested a reduced virulence of the latter strains with regard to their ability to induce acute infections, based on mutations in many virulence genes including type III secretion, quorum sensing and motility (Smith et al., 2006).

Thus the long-term persistence of *P. aeruginosa* in CF lung, known as adaptive radiation, has been interpreted as an *in vivo* selection process, resulting in less virulent variants that consequently do less harm to their host than the original colonizing strain (Smith et al., 2006).

B.3 Host-pathogen interplay in CF lung disease pathogenesis

B.3.1 Innate immunity

Respiratory failure resulting from chronic infection and inflammation of the airways still represent the primary cause of death for most individuals with CF (Gibson et al., 2003). Respiratory tract infection contributes to a dysregulated host immune response in CF, impacting on both innate and adaptive immunity and perpetuating inflammation (**Fig. 8**), finally leading to progressive pulmonary damage with bronchiectasis and emphysema (Pillarisetti et al., 2011). Innate immunity operating in the lung pairs physical barriers to infection with the ability of resident cells to sense and respond to infection inducing the mucosal recruitment of effector cells that facilitate rapid clearance (Yonker et al., 2015). Since mucous barrier and mucociliary clearance act as an important integral part of the innate pulmonary defense system, the mucociliary dysfunction due to airway surface dehydration constitutes a disease-causing mechanism that links the basic CF defect to impaired airway defense and CF lung disease (Hartl et al., 2012).

In healthy airways, epithelial cells, macrophages, and dendritic cells recognize pathogen-associated molecular patterns (PAMPs) that evade mucociliary clearance. Pattern recognition receptors (PRRs), including toll like receptors (TLRs) and intracellular nod like receptors (NLRs), recognize PAMPs, such as cell wall lipoproteins (typically recognized by TLR2), LPS (recognized by TLR4 although some LPS species can be recognized by TLR2), and flagellin (recognized by TLR5), facilitating pathogen identification. NLR Nod1 exhibits specificity for Gram-negative bacterial PGN, while NLR Nod2 binds muramyl dipeptide (MDP) motif that is common to Gram-positive and

Gram-negative bacteria (Akira et al., 2006; Cigana et al., 2011). These interactions result in immune signaling through the adapter proteins myeloid differentiation factor 88 (MyD88) or apoptosis-associated speck-like protein containing a caspase recruitment domain (ASC), triggering cascades resulting in activation of transcription factors, including the nuclear factor κB (NF-κB), and ultimately in the production of pro-inflammatory mediators, such as tumor necrosis factor α (TNFα), interleukin (IL)-8, and IL-1β (Skerrett et al., 2007). In CF, many aspects of this process appear to be dysregulated. For example, CF bronchial epithelial cell lines display aberrant PRR signaling and constitutively elevated NF-κB activity. Sputum and brochoalveolar lavage fluid (BALF) from CF patients reveal increased level of pro-inflammatory cytokines, such as TNF-α, IL-6 and IL-1β, and decreased levels of anti-inflammatory cytokines, such as IL-10 (Yonker et al., 2015).

As a consequence of epithelial dysfunction and pathogen sensing, a pro-inflammatory cascade is initiated in CF airways leading to the recruitment of neutrophils from the bone-marrow niche via the circulation into the airways. Tissue-released chemokines, mainly released by epithelial cells and macrophages, attract neutrophils via chemokine gradients to the site of inflammation, putting chemokines and their G-protein coupled receptors in the spotlight of targeted anti-inflammatory strategies (Owen, 2001; Charo et al., 2006). The best studied chemokine in CF lung disease is IL-8. Many groups have reported elevated levels of this chemokine in the BALF and sputum of both CF adults and children (Sagel, 2003; Hartl et al., 2007). This chemokine exhibits pleotropic effects on neutrophils, acting as a potent chemoattractant and inducing degranulation and superoxide production (Winkler, 2003). Furthermore adult mice that overexpress the sodium channel ENaC showed a sustained neutrophilic airway inflammation and the neutrophil-attracting chemokines macrophage inflammatory protein-2 (MIP-2) and KC (functionally similar to the human IL-8 chemokine) were significantly increased in BALF and lung homogenates (Mall et al., 2004). Beyond this canonical pathways of preformed cytokines/chemokines regulating inflammatory response in CF, evidence suggests significant non-canonical pathways responsible of neutrophil influx. A recently identified collagen breakdown product, proline-glycine-proline (PGP), has been established as a neutrophil chemoattractant, producing superoxide, and inducing the release of proteases from neutrophils (Weathington et al., 2006). Additional intercellular signaling among neutrophils occurs via leukotriene B4 (LTB4), an arachidonic acid metabolite generated by 5-lipoxygenase that serves as a potent neutrophil chemoattractant capable of amplifying recruitment (Lammermann et al., 2013; Pazos et al., 2015). CF patients display abnormalities in

levels of PGP peptides (Gaggar et al., 2008) and LTB4 (Bodini et al., 2005), although the effect of these alterations are not fully appreciated.

B3.1.2 Neutrophils

Upon entering the airspace of the CF lung, neutrophils seek to eradicate the inciting infection. In general, the pathophysiological role of airway neutrophils in CF and other chronic neutrophilic lung diseases is two-faced: on the one hand they are required for antibacterial and antifungal host defense, on the other hand they can cause significant parenchymal lung tissue damage when they accumulate over longer time periods and liberate their toxic granule contents, mainly serine and metalloproteases (MMPs) (e.g. neutrophil elastase and MMP-9) as well as oxidants, in an uncontrolled fashion (Mantovani et al., 2011). Animal models and *in vivo* human studies have also demonstrated an important role for the neutrophil in mediating lung damage in CF, but have not established whether this is a primary or secondary phenomenon (McKeon et al., 2010).

In the airway microenvironment of chronic *P. aeruginosa* infections, infiltrated neutrophils are faced with quorum sensing-induced bacterial biofilms (Donlan et al., 2002) and this interaction substantially modulates the phagocyte's behavior. Biofilms are organized by microorganisms and contain a matrix extracellular DNA, proteins and polysaccharides. Biofilms factors, such as 3OC12-HSL N-(3oxododecanoyl)-L-homoserine lactone (Zimmermann et al., 2006), and extracellular DNA from microorganisms induce neutrophil migration and further activate neutrophils (Trevani et al., 2003). Recruited neutrophils associated with biofilm are less effective at eradicating bacteria: indeed, biofilm-entrapped neutrophils have decreased mobility, decreased enzyme production and ineffective oxidative burst (Jesatis et al., 2003). An important part of the immune response includes the ability of neutrophils to form antimicrobial neutrophils extracellular traps (NETs). NETs are made up of neutrophil DNA, histones, and proteolytic enzymes, actively released by the neutrophil as a means to ensnare nearby microbes including those that are predominant in the CF airspace, such as *P. aeruginosa*, *H. influenzae* and *S. aureus*, as well as fungal pathogen *A. fumigatus* and *Candida albicans* (Brinkmann et al., 2004). However, in CF, NETs are detrimental and contribute to thick tenacious airway secretions that lead to progressive lung disease, entangling, rather than clearing airway infection. Thus, in CF, NETs formation most likely fails to destroy the plethora of pathogens encountered in the airspace and may only contribute to neutrophil-mediated damage of lung tissue. Furthermore, the formation of NETs likely reinforces

microbial biofilms in CF, facilitating microbial persistence and contributing to the dysregulation of the innate immune system (Langereis et al., 2013).

Therefore, despite the pronounced recruitment of neutrophils into the CF airway, these phagocytes are ineffective in clearing the inciting infection and ultimately serve to the detriment of the lung by contributing to biofilm formation and host tissue destruction.

B3.1.3 Macrophages

Macrophages, together with the epithelium, are part of the lung's innate cellular surveillance system. They efficiently phagocytize bacteria, dead cells and debris. In addition, their activation by external triggers (viruses, bacteria, bacterial products, etc.) leads to a cascade of events that contribute to the migration of neutrophils into the alveolar space and, eventually, to the activation of dendritic cells and T cells, initiating the adaptive arm of immune response. In CF, macrophages likely play a significant yet underappreciated role, via aberrant scavenger signaling cascades, resulting in chronic inflammation yet ineffective clearance of infection. In addition, CFTR mutations result in impaired bacterial killing in murine and human macrophages with dysregulated cytokine production (Hartl et al., 2012; Del Porto et al., 2011) including high concentrations of pro-inflammatory cytokines released by macrophages, such as IL-1α, IL-6, granulocyte-colony stimulating factor **(**G-CSF), and IL-8. Elevated production of these cytokines was also confirmed in bone marrow and alveolar macrophages from *cftr*-deficient mice after *in vitro* stimulation with LPS from *P. aeruginosa.* There is also evidence that virulence factors released from *P. aeruginosa*, as pyocyanin, compromise macrophage efferocytosis of apoptotic neutrophils indicating that the microbial environment could further suppress phagocytic functions (Bianchi et al., 2008). These data suggest that CFTR directly contributes to microbicidal dysfunction of macrophages.

B.3.2 Adaptive immunity

While neutrophils are the dominant cell population in the broncho-alveolar compartment of CF patients, recent studies indicate that T lymphocytes accumulate within the subepithelial bronchial tissue, while the bronchial space is almost devoid of T cells, supporting the notion that the pulmonary immune system is compartmentalized and the role of T cells has probably been under-appreciated in CF lung disease due to their paucity in sputum or BALF (Tschernig et al., 1997; Schuster et al., 2000). T cell function is also affected by defects in CFTR, although the specific mechanisms involved in this effect have not been defined. Historically, the predilection to mount a Th2 response appeared to be central to the CF T-cell phenotype. A Th2-dominated immune response in CF patients with chronic *P. aeruginosa* lung infection as compared with CF patients without chronic infection was observed, whereas Th1 responses were accompanied by a better pulmonary outcome (Hartl et al., 2006; Moser et al., 2000). Although there is growing evidence that a Th1-dominated immune response might improve the prognosis of CF patients with chronic *P. aeruginosa* lung infection, the host would presumably benefit also of a Th17 response. Recently, the potential key role of Th17 signaling in the host response to this extracellular pathogen is increasingly emerging. Higher levels of IL-17 and IL-23 cytokines were described in patients chronically infected with *P. aeruginosa* as compared to those who were not chronically infected with *P. aeruginosa* (Decraene et al., 2010). Furthermore, increased levels of IL-17 in BALF during exacerbations were found associated with positive *Pseudomonas* species sputum cultures (Chan et al., 2013). In addition, a crucial role has been proposed for IL-17 producing cells in inflammation in the lung of patients with CF promoting inflammation-related destruction of lung tissue, supporting neutrophil recruitment, and defined IL-17A to be a marker preceding infection with *P. aeruginosa* (Tiringer et al., 2013). How different Th cell subtypes respond to different and emerging pathogens is still unknown. Novel insight in new T-cell subsets (Th17-Th2, Th17-Th1) and the capacity of Th17 cells to produce Th2-type cytokines strengthen the complexity and plasticity of the adaptive immune system (Tiringer et al., 2013). Moreover, the presence of a complex microbiota and multiple pathogens, which vary among CF patients, combined with a lack of comprehensive clinical studies on adaptive immune responses, aligns to complicate characterization of the adaptive immune response in CF.

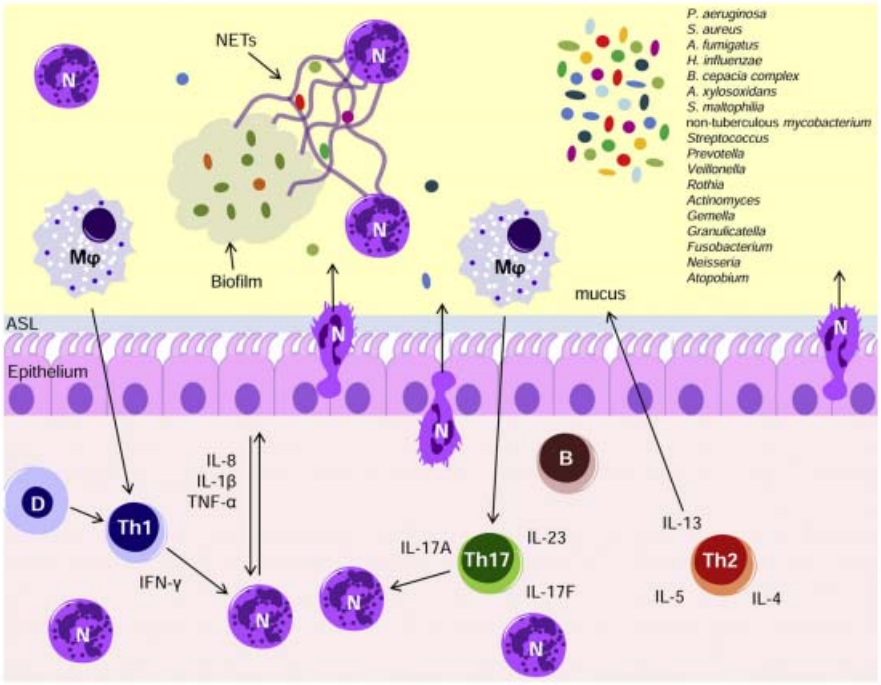

Figure 8. Innate and adaptive immune response to infections in CF. Infection by several different pathogens triggers perpetual bouts of neutrophil recruitment and breach of the airway epithelium. In the airspace, neutrophils encounter persistent microbial biofilms and release neutrophil extracellular traps (NETs) that are ineffective and ultimately repurposed for the benefit of the microbial biofilms. Following continuous cycles of acute infection or once chronic infection is established, T lymphocytes are recruited and polarized to Th1, Th2 and/or Th17 cells. IL-17A and related cytokines as well as interferon γ (IFN-γ) play an important role in the excessive recruitment of neutrophils. The effector phase of allergic bronchopulmonary aspergillosis (ABPA), associated to *Aspergillus fumigatus* infections, is determined by Th2-mediated allergic responses, including eosinophilia, mucus production, and airway hyperresponsiveness. The relevance of other emerging pathogens in CF lung disease progression still remains to be fully elucidated. N, neutrophils; Mφ, macrophages; D, dendritic cells; B, B cells (Yonker et al, 2015).

B.4 CF airway remodeling

Most patients with CF die from respiratory failure with extensive airway destruction. Repeated cycles of infection and inflammation are traditionally been thought as the cause of tissue lung damage. Pulmonary disease in CF is characterized by extensive structural airway changes including bronchiectasis, bronchiectatic pus-filled cystis, mucoid impaction, atelectasis (collapse or closure of a lung resulting in reduced or absent gas exchange), RBM thickening, fibrosis and vascular changes. These structural changes in the airway wall are referred to as remodeling which, in this context has been defined as an alteration in size, mass or number of tissue structural components inappropriate to the maintenance of normal function (Hirota and Marin, 2014). All of these pathologic changes involve extensive alterations of lung extracellular matrix (ECM), that plays a key role in tissue architecture and homeostasis (Atkinson and Senior, 2003). The ECM is a complex network within the airway wall consisting of fibrous (collagen and elastin) and adhesive

(fibronectin and laminin) proteins embedded in a hydrated polysaccharide gel containing GAG which provide rigidity to the airway wall (Bousquest J et al., 2000). GAG are long linear structures composed of heterogeneous polysaccharides (PS) and are formed by long disaccharide units with varying degrees of linkage, acetylation and sulphation. GAG act by binding selectively to a variety of proteins and pathogens and are crucially relevant to many disease processes, such as inflammation (Lever and Page, 2002; Young, 2008; Rek et al., 2009), cancer (Yip et al., 2006) and infectious diseases (Rostand and Esko, 1997; Wadstrom and Ljungh, 1999). Heparin and heparan sulphate (HS) are GAG consisting of 1–4 linked uronic acid and glucosamine and encompassing varying degrees of sulphation, and they are involved in many of these activities (Gandhi and Macera, 2010). In particular it was described that HS chains play key roles at different stages during the entry of leukocytes into sites of inflammation: they facilitate L-selectin-dependent cell rolling, promote chemokine transport across the endothelium, and assist chemokine presentation to leukocytes, which results in integrin activation (Wang et al., 2005; Borsing, 2004).

Recent studies suggest that GAG remodeling may be an important mechanism leading to CF airways tissue damage and destruction. Increased concentration and sulphation of GAG have been found in BALF from children with CF, and secretion of GAG, such as HS (Solic et al., 2005), chondroitin sulphate (CS) (Khatri et al., 2003), and hyaluronic acid (HA) (Wyatt et al., 2002), is markedly increased in bronchial cells and CF tissues (**Fig 9**). Furthermore, it has been shown that binding to GAG renders IL-8 impervious to proteolysis, thus increasing the half-life and activity of the chemokine at the site of inflammation and sustaining neutrophil recruitment in CF airways (Solic et al, 2005). GAG could also bind and stabilize other cytokine like monocyte chemoattractant protein 1 (MCP-1), RANTES and MIP-1β, thus amplifying chronic neutrophil recruitment and inflammation (Lau et al., 2004).

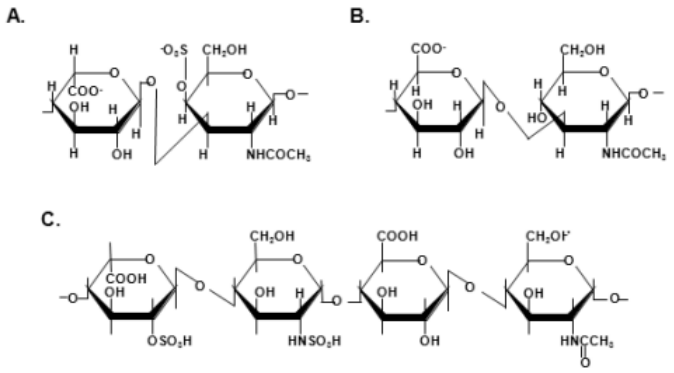

Figure 9. Structural formulas of GAGs up-regulated in CF. Structures represent the repeating units of CS B (A), HA (B), and HS (C) (Reeves et al, 2011).

The presence of GAG and desmosine in sputum, raised levels of urinary desmosines and collagen metabolites, and ultrastructural evidence of lysis of elastic and collagen fibers in endobronchial biopsies (Laguna et al., 2009) reflect the degradation of the ECM in the CF lung. This breakdown of the airway tissue is likely to be functionally relevant, leading to a loss of lung function and favoring the development of bronchiectasis. Degradation of the bronchial tissue matrix is associated with an early protease/antiprotease imbalance in CF linked to inflammation and infection (Hillard at al., 2007). While the role of serine proteases, such as human neutrophil elastase (HNE), cathepsin G and proteinase 3 have been characterized in detail in murine and human studies, there is emerging evidence that MMPs, mainly released by neutrophils and macrophages could play a key role in the pathogenesis of CF lung disease (Gaggar, 2011). MMP-9 has been extensively examined in the lower airway secretions of CF patients and has been found to be increased in both quantity and activity (Gaggar et al., 2007; Ratjen et al., 2002). Furthermore increased levels of MMP-9 have been found in sputum and BALF from children with CF (Sagel et al., 2005; Roderfeld et al., 2009) and it has also been found that MMP-9 levels inversely correlate with lung function (Sagel et al., 2005). Gaggar and colleagues further described an increase in MMP-9 activity with a concomitant decrease of the presence of its prominent natural inhibitor, TIMP-1. This imbalance was thought to be, in part, due to a mechanism of MMP-9 activation and TIMP-1 degradation via HNE (Jackson et al., 2010) (**Fig 10**).

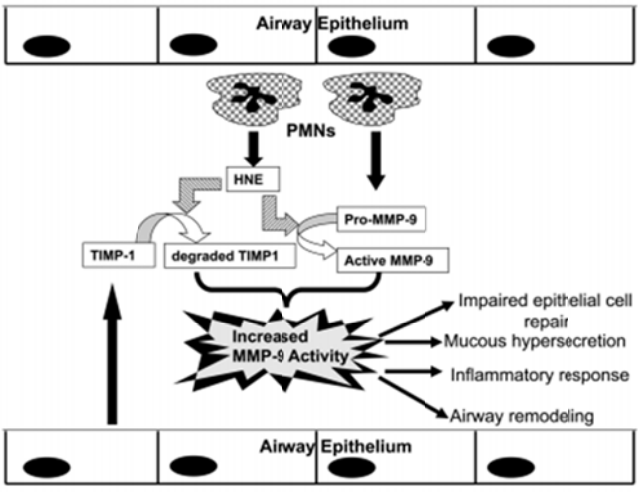

Figure 10. Increased MMP-9 activity augments potential mechanisms of CF related pathobiology: ongoing dysregulation of MMP-9 activity in CF airways impacts various aspects of CF related pathophysiology including airway remodeling, epithelial cell damage, increased mucous production and augmentation of inflammatory response (Jackson et al., 2010).

In this context, the increased activation of MMP-9 in CF lung disease has many possible downstream inflammatory effects including the release of PGP (Weathington et al., 2006; Gaggar et al, 2008), previously described, and the activation of latent TGF-β (Yu Q. and Stamenkovic, 2000). TGF-β is a potent pro-fibrotic cytokine, known to mediate fibroblast pathobiology in human lungs and is also a modifier of disease severity among CF individuals. Harris and colleagues found that plasma (but not serum) TGF-β is increased in association with *P. aeruginosa* infection and lung disease, and is reduced in response to therapy in CF pediatric patients (Harris et al., 2011). TGF-β induces the differentiation of fibroblasts into myofibroblast phenotype (fibroblasts with α-smooth muscle actin among other contractile elements) and this process arises secondary to chronic epithelial injury of inflammation, two well described features of CF respiratory deterioration. Harris and colleagues for the first time indicated the importance of TGF-β mediated pulmonary fibrosis in human CF lung disease and described a novel mechanism by which TGF-β associated myofibroblast differentiation contributes to the progression of CF lung disease (**Fig. 11**) (Harris et al., 2013).

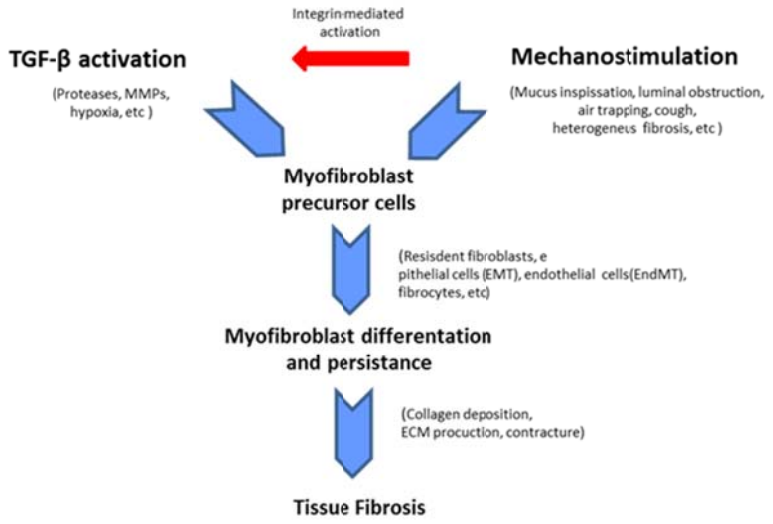

Figure 11. **Schematic model depicting myofibroblast differentiation in cystic fibrosis (CF).** TGF-β signaling and mechanostimulation in CF lungs induce precursor cells such as resident fibroblasts to undergo myofibroblast differentiation. TGF-β activation is robust and likely multifactorial due to well-established mechanisms including integrin expression and proteases such as the matrix metalloproteases (MMPs). Mechanical strain (e.g. from luminal obstruction, tissue fibrosis and persistent coughing) further augments TGF-β activation and contributes to development and persistence of the myofibroblast phenotype. Sources of myofibroblast precursors include resident lung tissue fibroblasts, circulating fibrocytes, epithelial mesenchymal transition (EMT) or endothelial mesenchymal transition (EndMT). Persistence of the myofibroblast leads to progressive tissue fibrosis with collagen production, extracellular matrix synthesis and tissue contracture (Harris et al., 2013).

B.5. Therapeutic options to target pathogens and detrimental host responses in CF

When CF was first described in 1938, the predicted survival age of a CF patient was only 6 months**.** There has been a significant improvement in the survival of individuals with CF over the last half century, from a median age of survival of 5 years in the 1970s to approximately 40 years of age as of 2011. The reasons for the improvement in clinical outcomes are multifactorial but include the intense use of antibiotic and anti-inflammatory therapy in this patient population. Despite these improvements, however, the majority of CF deaths still occur in young adulthood, typically between the ages of 21 and 30 years. Several novel approaches are being developed to control the severe infection and inflammation characteristic of the CF lung that are essential to improve the quality of life and survival of people with CF (Waters and Smyth, 2015). Today, the CF Foundation maintains a robust pipeline of therapies that target CF from every angle, including the root cause of the disease. The drug development pipeline shows the progress of potential CF treatments through the different phases of clinical research and, in some cases, approval by the U.S. Food and Drug Administration (FDA) for use by people with CF.

B.5.1 Antimicrobial therapies

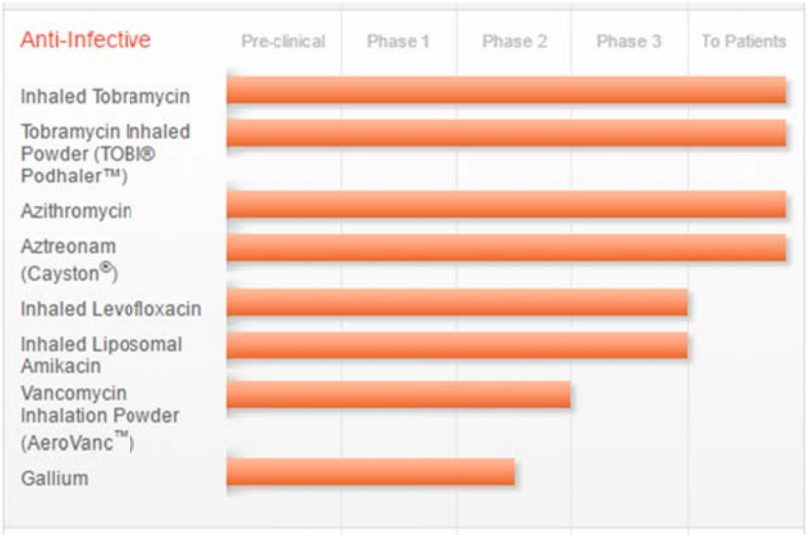

Figure 12. Anti-infective drug pipeline from CF Foundation 2015.

Several new inhalational antibiotics have recently become available for the treatment of *P. aeruginosa* pulmonary infections in CF patients. New aerosolized formulation have recently been introduced, such as inhaled tobramycin (aminoglycoside antibiotic) and aztreonam (beta lactam antibiotic), being able to achieve very high intrapulmonary concentrations with few associated systemic side effects (Waters and Smyth 2015). Aerosolized levofloxacin is another new

pharmaceutical agent developed for the treatment of *P. aeruginosa* pulmonary infections in patients with CF. In comparison to aztreonam and aminoglycosides, levofloxacin has the most rapid rate of killing among *P. aeruginosa* isolates and is more potent against *P. aeruginosa* biofilms (King et al., 2010). Azithromycin is a macrolide antibiotic that has been shown to reduce pulmonary exacerbations and improve CF lung function (Saiman et al., 2003). Despite its unknown mechanism of action, azithromycin appears to be of benefit to patients with CF. Indeed, the CF Foundation recommends the chronic administration of azithromycin to CF patients aged 6 years and older who are infected with *P. aeruginosa*, and that it should be considered also for those patients who are not infected with *P. aeruginosa* (Cantin et al., 2015).

In addition to new types of antibiotics of differing classes, there have also been developments in the way these drugs are formulated and delivered. A currently available example is tobramycin inhalation powder (TIP) that has the advantages of being able to be delivered very quickly (in approximately 5 min) using a "podhaler™" inhalation device and having good lung delivery (Parkins et al., 2011). The inhaled dry powder version of the antibiotioc vancomycin (AeroVanc^{TM}) was also develop for treatment of MRSA airway infection.

Another novel method of delivery is the packaging of antibiotics within liposomes for aerosolization and an example of this is inhaled liposomal amikacin (aminoglycoside antibiotic). Because the liposome is very small and has a neutral charge (shielding the positively charged amikacin from the negatively charged CF sputum), the drug is able to effectively penetrate into CF sputum and bacterial biofilms (Meers et al., 2008). Once at the site of infection, liposomes release the active drug, amikacin, upon exposure to rhamnolipids, a by-product of the *P. aeruginosa* bacteria itself.

Antimicrobial resistance might be further prevented by using non-antibiotic treatments and there are diverse group of novel agents which act by increasing the organism's antibiotic susceptibility; by reducing virulence; or by rendering the organism more susceptible to the host immune system (Hurly et al., 2010). These agents includes for example gallium metal that has already been approved by the FDA for intravenous use in people. Gallium can substitute itself in many of the iron (Fe^{+}) dependent pathways essential in the growth and functioning of many bacteria such as *P. aeruginosa* (Kaneko et al., 2007). In such a way, gallium can inhibit the growth of bacteria such as *P. aeruginosa*.

B.5.2 Anti-inflammatory therapies

Figure 13. Anti-inflammatory drug pipeline from CF Foundation (2015).

On the other side, a direct assault on the airway inflammatory response seems warranted given that drugs that target inflammation have been shown to slow the decline in lung function and improve survival (Cantin et al., 2015).

Ibuprofen is the only anti-inflammatory drug currently recommended for the long term treatment of CF airway inflammation (Mogayzel et al., 2013). High-dose ibuprofen decreases neutrophil migration as measured through oral mucosal washes in clinical trials and slows the progression of CF lung disease, particularly in children (Lands et al., 2007). Despite these beneficial effects, ibuprofen has not been widely adopted, largely due to the challenges associated with obtaining a pharmacokinetic study for appropriate dosing and concerns over adverse effects (Konstan, 2008). Although ibuprofen is associated with gastrointestinal bleeding, its occurrence is rare (Konstan et al., 2007). Concomitant use of antacids, proton pump inhibitors, or prostaglandin E1 analogues would likely limit this adverse event. Thus, the benefits of ibuprofen outweigh its risks (Cantin et al., 2015). Currently the CF drug pipeline proposed also other two oral anti-inflammatory molecules that are in a phase 2 trial: CTX-4430 and JBT-101. CTX-4430 reduces the production of LTB4, a potent neutrophil chemoattrant present in CF airway (Snelgrove et al., 2010), while JBT-101 (Resunab^{TM}) is a preferential agonist to the CB2 receptor that is expressed on immune cells to resolve inflammation without immunosuppression. According to the release, the drug increases the production of “specialized pro-resolving lipid mediators of inflammation” (Tepper et al., 2014).

The inflammatory response in CF provides a wide plethora of potential targets for new drug development. Determining which targets will have the major impact without resulting in untoward effects remains the objective (Cantin et al., 2015).

B.5.3 Anti-tissue damage drugs

Other interesting therapeutic goals in CF management are targeting the imbalance of protease/antiprotease and also tissue remodeling observed in CF lung, to prevent tissue damage. These treatments are not listed in the CF foundation pipeline, so intensive research have to be done to develop these approaches.

The CF lung environment is associated with a disproportionate inflammatory response and one aspect of this complex inflammatory environment is the high protease burden. HNE is a serine protease that is found in high abundance in CF BALF (Birrer et al., 1994) and is capable of degrading major components of connective tissue, including elastin (Kelly et al., 2008). It has been suggested that HNE is the most important protease in the inflammatory lung and is placed at the apex of the protease hierarchy (Geraghty et al., 2007). Anti-proteases have been under investigation in CF since the early 1990s. Aerosolized plasma-purified Alpha 1 anti-trypsin (AAT) has been shown to significantly decrease key inflammatory mediators (IL-8, TNF-α, LTB4, and IL-1β), elastase activity, and incidence of *Pseudomonas* infection (Griese et al., 2007). Human recombinant AAT (rAAT) is currently under investigation in patients with CF (Griese et al., 2007). Taggart and colleagues have proposed secretory leucoprotease inhibitor (SLPI) as a multifunctional therapeutic for chronic inflammatory lung disease characterized by a high protease burden (Taggart et al., 2002; Greene et al., 2004). Their studies showed how SLPI acts not only as an antiprotease but also as an anti-inflammatory by directly inhibiting TLR signalling and NF-kB activation in macrophages (Taggart et al., 2005).

In addition, a large number of *in vitro* (Baici et al., 1993; Fryer et al., 1997) and *in vivo* (Fryer et al., 1997; Tian et al.,1995) studies have been performed looking at the antiprotease effects of heparin. The theory behind using heparin to bind and inactivate HNE is not dissimilar to what happens naturally *in vivo*. By way of explanation, exposure of HS proteoglycans to HNE causes release of HS chains and fragments of HS proteoglycans (Buczeck-Thomas et al., 1999), which in turn bind and limit HNE activity (Spencer et al., 2006). However, under chronic inflammatory conditions and high HNE burden, this natural feedback loop is destroyed, tilting the balance in favor of HNE-mediated tissue destruction. Walsh et colleagues demonstrated that heparin and HS have the ability to inhibit lung elastin breakdown by HNE of, thus suggesting a role of these GAG in protecting structural proteins (Walsh et al., 1991). This inhibition of HNE activity by heparin was initially deemed to be influenced by charge interactions, where correlations were observed between charge density and N-sulphate groups on the heparin molecules and HNE activity (Volpi, 1996).

However, more recent studies suggest that heparin binds to HNE by a competitive tight binding mechanism corresponding to length of saccharides, with 12–14 being required for HNE inhibition (Spencer et al., 2006). In addition, semi-synthetic or GAG derivatives have also demonstrated antiprotease activity against HNE (Becke et al., 2003) and cathepsin G (Sissi et al., 2006). Moreover, a role for GAG in stabilising interaction of SLPI with HNE has been reported (Ying et al., 1997), augmenting SLPI antiprotease activity *in vivo* (Fath et al., 1998) . These studies promote the idea that antiprotease therapies are likely to have significant benefit for CF.

There are no studies reporting efficacy of therapies for CF airway remodeling but the effect of current therapeutic molecules used in IPF and COPD to control airway remodeling could may also be extended to CF field. Pirfenidone (5-methyl-1-phenyl-2-[1H]-pyridone), a novel compound with combined anti-inflammatory, antioxidant, and antifibrotic effects in experimental models of pulmonary fibrosis could have a therapeutic potential for CF (King Jr et al., 2011). This molecule showed encouraging results in phase II clinical study in patients with advanced IPF (Taniguchi et el., 2010; Noble et el., 2011).

Tiotropium, a long-acting muscarinic receptor antagonist, inhibited the increase of airway smooth muscle (ASM) mass and goblet cell metaplasia in allergen challenged guinea pigs (Gosens et al., 2005) and mice (Kang et al., 2012). In animal COPD models, tiotropium has been shown to inhibit goblet cell metaplasia, mucin production, and vascular remodeling but to have no effect on airspace enlargement (Pera et al., 2011). Although bronchoconstriction per se may release growth-promoting molecules from airway epithelium, it is not clear whether the effects of tiotropium are mediated by affecting airway mechanics or through predominantly biochemical processes. The effect of tiotropium on airway remodeling has not been evaluated in human subjects.

With the discovery of small molecules that can restore the function of CFTR (Ikpa et al., 2014), it is hoped that one day individuals with CF will no longer be afflicted with these difficult to treat pulmonary infections caused by opportunistic, multidrug resistant pathogens. However, until the underlying defect can be corrected in all CF patients, treatments that decrease infection, pulmonary hyper-inflammation and airways structural damage are vital to the quality of life and survival of individuals with CF (Waters and Smith, 2015).

C. Aim of the Project

Pulmonary disease is the main cause of morbidity and mortality in CF patients. During the course of chronic colonization *P. aeruginosa* adapts to the airways and dramatically modifies its phenotype avoiding the host immune recognition. In this context structural changes of the airways, including accumulation and degradation of ECM components and GAG remodelling, are associated to the progression of CF lung disease. However it is still not clear whether and how *P. aeruginosa* CF-adapted isoletes, persisting in CF airways, affect the host immune response and favor airway damage and the remodeling processes. Moreover, whether GAG remodeling may contribute to lung pathology and may be considered a potential therapeutic target, remains unclear. The main objectives of this PhD work were:

- ✓ **To track the host immunopathological response to *P. aeruginosa* variants *in vitro* and in murine models of infection**. Sequential clonal *P. aeruginosa* isolates recovered from CF patients were tested in human CF bronchial epithelial cells IB3-1 and in macrophage-like cells THP-1 to evaluate inflammatory response and tissue damage markers. Mice were intratracheally infected with *P. aeruginosa* isolates as planktonic bacteria for short term to reproduce the acute infection; whereas, to establish *P. aeruginosa* chronic lung infection, mice were intratracheally infected with bacteria embedded in agar beads for long term up to three months. Bacterial load, histopathology and markers of inflammation and tissue damage were evaluated in murine lungs.

- ✓ **To determine the pathophysiological relevance of GAG and test the efficacy of competitors (GAG mimetics) in reducing inflammation, tissue damage and infection burden in murine models of *P. aeruginosa* infection.** Different GAG species were identified by HPLC-MS in lung pellet and supernatants of wt and CF mice chronically infected with *P. aeruginosa* CF-adapted isolate. Furthermore, GAG mimetics were synthetized and their activities tested subcutaneously in mice during *P. aeruginosa* acute and chronic lung infection. Bacterial count, lung inflammation and markers of tissue damage were evaluated. Finally, these compounds were tested *in vitro* to evaluate their antibacterial potential.

D. Main Results

D.1 Immunopathological response to *P. aeruginosa* during lung infection

D.1.1 *P. aeruginosa* CF-adapted variants shape the host response during the progression of infection

In order to investigate the host response to *P. aeruginosa* infection we set up acute (planktonic bacteria) (Lore` et al., 2012) and chronic (agar-bead embedded bacteria) lung infection (Bragonzi, 2010) in C57BL/6NCrlBR mice with the early AA2 isolate and CF-adapted variants AA43 and AA44 (**Fig. 14**). In particular, CF-adapted variants carry i) mutations within the genome temporally associated with CF lung infection (Bianconi et al., 2011), ii) several phenotypic changes in virulence factors production (Bragonzi et al., 2009) iii) PAMPs (Cigana et al., 2009).

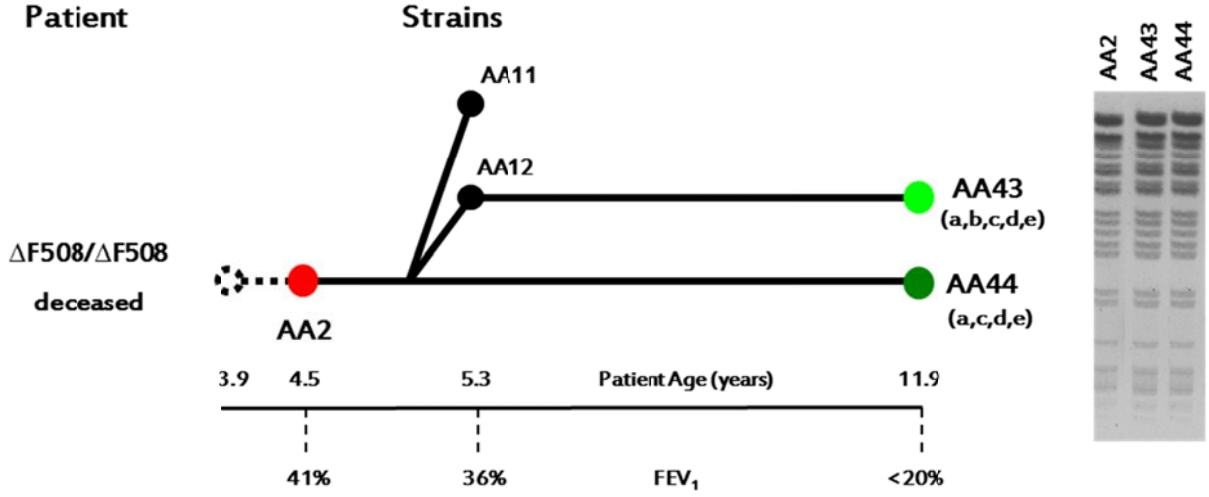

Figure 14. *P. aeruginosa* sequential isolates from patient AA. AA2 isolate was recovered at the first *P. aeruginosa*–positive culture for the **Δ**F508/**Δ**F508 CF patient (4.4 years old). AA11 and AA12 were sequential isolates recovered after 5 month while AA43 and AA44 were isolated after 7.5 years. AA43 and AA44 isolates were clonal to AA2 but carried different phenotypic traits, such as a) motility defect, b) mucoid phenotype, c) protease reduction, d) LPS modification and e) PGN modification.

In the murine model of acute lung infection the early isolate AA2 disseminated systemically leading mice to mortality, while CF-adapted variants AA43 and AA44 were avirulent and were almost completely cleared by the host immunosystem within 2 days. In the agar-beads model, only CF-adapted isolates were able to establish long term chronic infection up to 90 days with a stable bacterial load (≈10^4 colony forming units/lungs), while the early isolate AA2 was lethal. Thus, in these murine models, the susceptibility to *P. aeruginosa* is isolate-dependent (**Fig. 15A and B**). Then, we investigated the bacterial localization, the immune host response and the

histopathological lesions during the course of chronic infection. Immunofluorescent staining and Haematoxylin and Eosin (H&E) showed that on day 2 *P. aeruginosa* was confined to bronchial lumens in the agar beads, while after long term-infection AA43 and AA44 were localized as macrocolonies in the beads deposited in the bronchial lumen and in biofilm-like structures (**Fig. 15C).** In the initial phases of the infection, CF-adapted variants AA43 and AA44 involved less innate immune cells recruitment, including neutrophils and macrophages (**Fig. 16A and B**), than early AA2 isolate. Furthermore cytokines/chemokines profile analysis showed that AA43 and AA44 induced lower levels of MIP-2, KC, MIP-1α, IL-6, MCP-1 and TNFα in comparison to AA2 during acute infection and at the onset of chronic infection. At the later stage of chronic infection, induced by CF-adapted variants, these cytokines/chemokines decreased further, although not to the basal level, while IL-17A and IFN-γ concentration remained sustained up to 28 days (**Fig. 17A-H**). Taking into consideration that IL-17A and IFN-γ are key-signature cytokines of T helper cells polarization, these results highlight the potential involvement of adaptive immunity during *P. aeruginosa* chronic infection, confirmed by the high recruitment of T and B cells as indicated by the adaptive immune cells infiltration score on lung histopathological analysis (**Fig. 16C**). Furthermore the adaptive immune response was characterized by the formation of bronchus associated lymphoid tissue (BALT)-like structures (**Fig. 16A and D**) promoted by the persistence of CF-adapted variants. Overall these data suggest that *P. aeruginosa* CF-adapted variants with their ability to persist in bronchial lumen, determine a weakening of the innate immune recognition and lead to the adaptive immune response during the course of airway diseases.

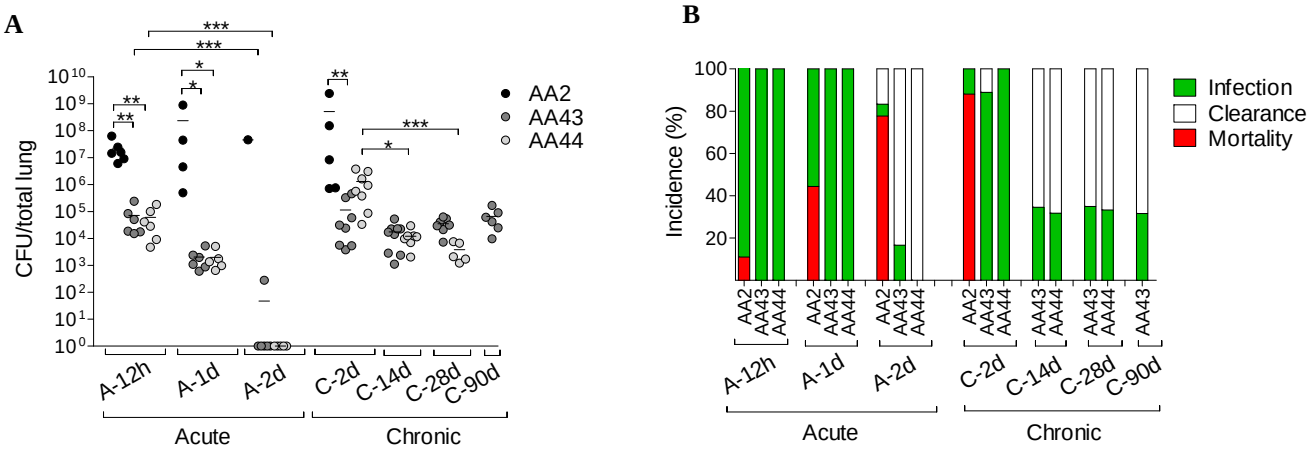

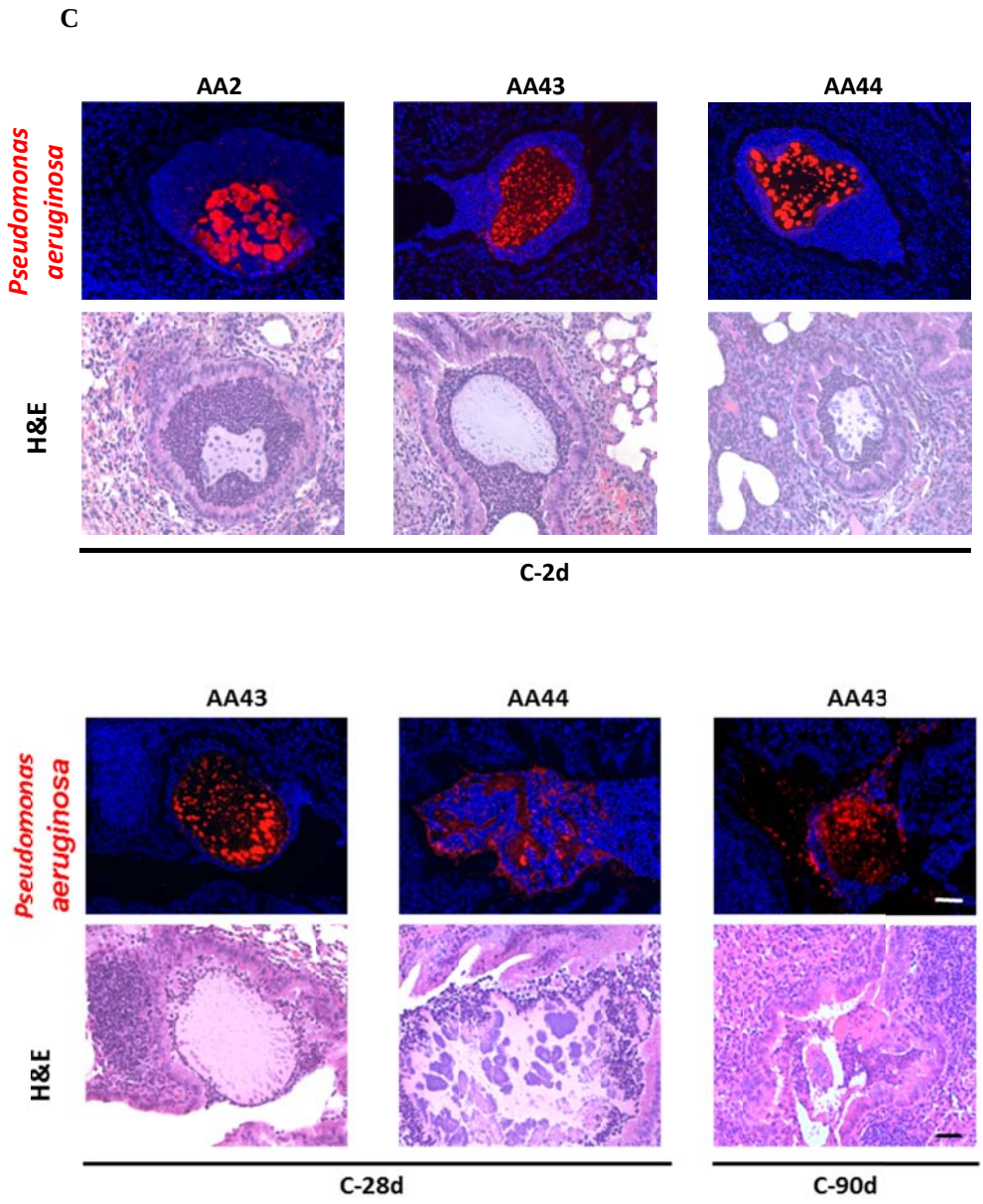

Figure 15. Virulence of *P. aeruginosa* isolates and bacterial localization in murine models of airways infection. Two groups of minimum five C57Bl/6NCrlBR mice were intratracheally infected with $5x10^6$ colony forming units (CFU) as planktonic bacteria (acute infection) for 12, 24 and 48 hours, or with $1\text{-}2x10^6$ CFU embedded in agar beads (chronic infection) for 2, 14, 28 and 90 days. BALF was performed and lungs recovered and homogenized. **A**) CFUs were evaluated in total lung. Dots represent CFUs in individual mice and horizontal lines represent median values. The data are pooled from at least two independent experiments (n=1-9). Statistical significance by ANOVA is indicated: *p<0.05, **p<0.01, ***p<0.001. **B**) The incidences of mortality induced by bacteremia (red), clearance (white) and airway infection (green) were determined. The data are pooled from at least two independent experiments (n=8-24). **C**) Bacterial and agar-beads localization in the lung were evaluated on challenged mice by immunofluorescence (with specific antibody against *P. aeruginosa*, stained in red, and with 4,6-Diamidino-2-phenylindole dihydrochloride, stained in blue) and H&E staining. Scale bar: 25 µm.

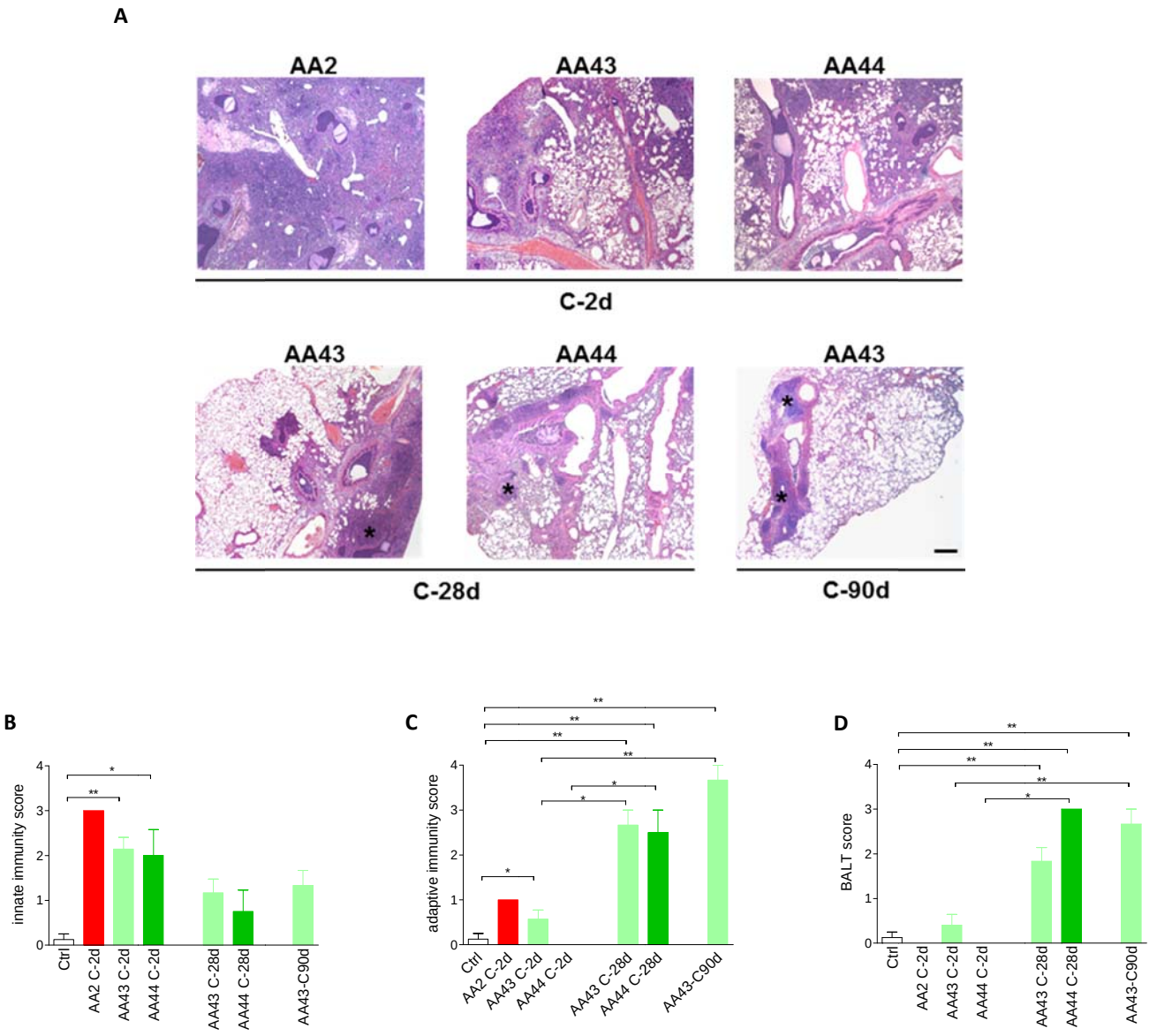

Figure 16. Lung histology and histopathological score of immune cells recruitment in the murine model of *P. aeruginosa* chronic airways infection in C57Bl/6NCrlBR mice . Mice were infected with 1 to 2x10^6 CFU/lung of isolates embedded in agar beads for the chronic infection and analyzed during a time course post-infection (2, 28 and 90 days). **A**) Lung histopathology was performed on challenged mice by H&E staining. Scale bars: 200 µm. BALT-like structures are indicated by asterisks. Innate (**B**) and adaptive (**C**) immune cells infiltration and BALT activation (**D**) were scored in tissue section of murine lungs stained with H&E. The data are pooled from at least two independent experiments (n= 2-7). Values represent the mean ± standard error of the mean (SEM). Statistical significance by ANOVA and Mann Withney is indicated: *p<0.05, **p<0.01.

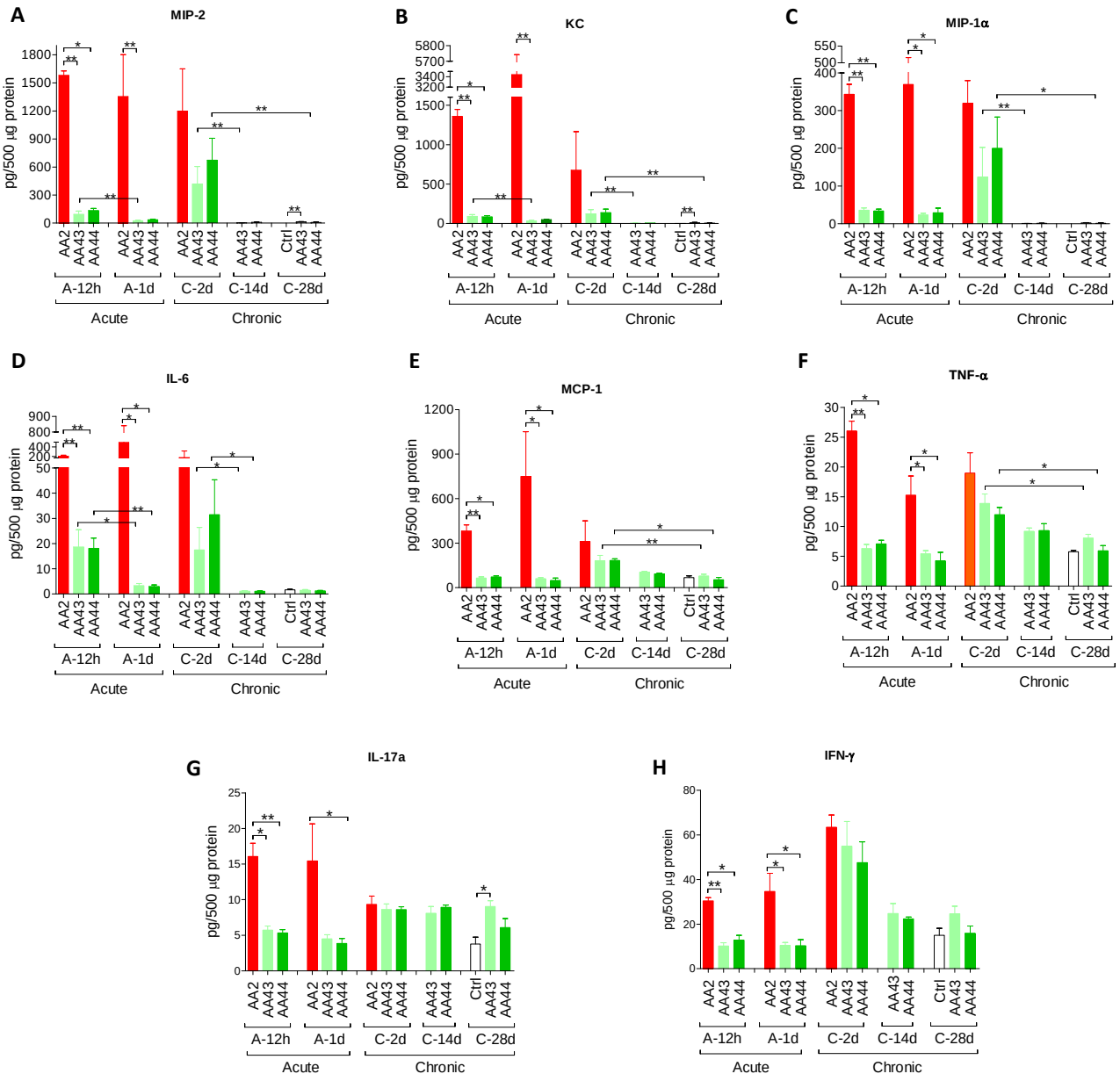

Figure 17. Lung inflammatory response after acute and chronic *P. aeruginosa* lung infection in C57BL6/NCrl mice. Mice were infected with 5x10^6 CFU/lung of planktonic bacteria for the acute infection or 1 to 2x10^6 CFU/lung of strains embedded in agar beads for the chronic infection and analyzed during a time course post-infection (12 hours and 1 day of acute infection and 2, 14 and 28 days of chronic lung infection). Cytokines and chemokines, including MIP-2 (**A**), KC (**B**), MIP-1α (**C**), IL-6 (**D**), MCP-1 (**E**), TNF-α (**F**), IL-17A (**G**), IFN-γ (**H**) were measured by Bioplex in lung homogenates. The data are pooled from at least two independent experiments (n=3-6). Values represent the mean ± SEM. Statistical significance by ANOVA and Mann Whitney test is indicated: *P<0.05, **P<0.01.

D.1.2 Differential cell host response to *P. aeruginosa* phenotypic variants

Next, we performed *in vitro* analysis to exclude the confounding variables (e.g. different bacterial load) during the course of the infection that cannot be controlled in mouse models. Thus, using a RNA macroarray, we performed a global transcriptional analysis of human IB3-1 CF bronchial epithelial cells, widely investigated in CF inflammation, infected with early AA2 and CF-adapted variants AA43 and AA44. We identified a total of 20 genes whose expression changed more than 2-fold in cells infected with AA43 and AA44 in comparison to cells infected with AA2, but with equal bacterial load. Only five genes were up-regulated after infection with the AA43 and AA44 CF-adapted variants in respect to AA2 infection, while the majority (15 out of 20) were down-regulated, including several chemokines and cytokines and their receptors (TNF-α, Gro-β and γ, IP-10, IL-8, FPR2, CCR6, CCR7, CCR9), and adhesion molecules involved in the process of leukocytes extravasation and recruitment (VCAM-1 and ICAM-1). In addition, although AA2 isolate induced higher expression of elastase 2, liable for collagen-IV and elastin proteolysis, AA43 and AA44 induced much higher expression of the matrix metalloprotease 9 (MMP-9), suggesting a contribution of *P. aeruginosa* CF-adapted variants in matrix degradation **(Fig. 18A).** Validation of RNA macroarray results was performed by real time PCR and/or ELISA for selected targets (IL-8, TNF-α, IP-10, VCAM-1, ICAM-1, Gro-β) in IB3-1 and their isogenic wt cells, namely C38, while MMP-9 target was validated in macrophagic-like cells THP-1. The validation confirmed the RNA macroarray results (**Fig. 18B-H**) indicating that CF-adapted variants AA43 and AA44 induced a significant waekening of the host response and contributed in matrix degradation. Next we extended our investigation with other *P. aeruginosa* early and CF-adapted isolates: KK1 and KK2, isolated at the onset of chronic colonization, and KK71 and KK72, isolated after a period of 12.6 years and before patient's death. Results showed that CF-adapted variants KK71 and KK72 induced a lower expression of IL-8, TNF-α, Gro-β, VCAM-1, ICAM-1 and IP-10 in comparison to early isolate KK1 and KK2 (**Figure 18B-H)**. In addition, confirming the results obtained with the AA clonal lineage, infection with KK71 and KK72 stimulated lower IL-8 proteic levels in comparison to early strain KK1 and KK2 (**Fig. 18C**).

Overall, these results unravel that different *P. aeruginosa* CF-adapted variants are able to rewrite the host response in host cells *in vitro* and in particular attenuate the expression of a set of genes involved in inflammation, confirming our results obtained in *in vivo* models.

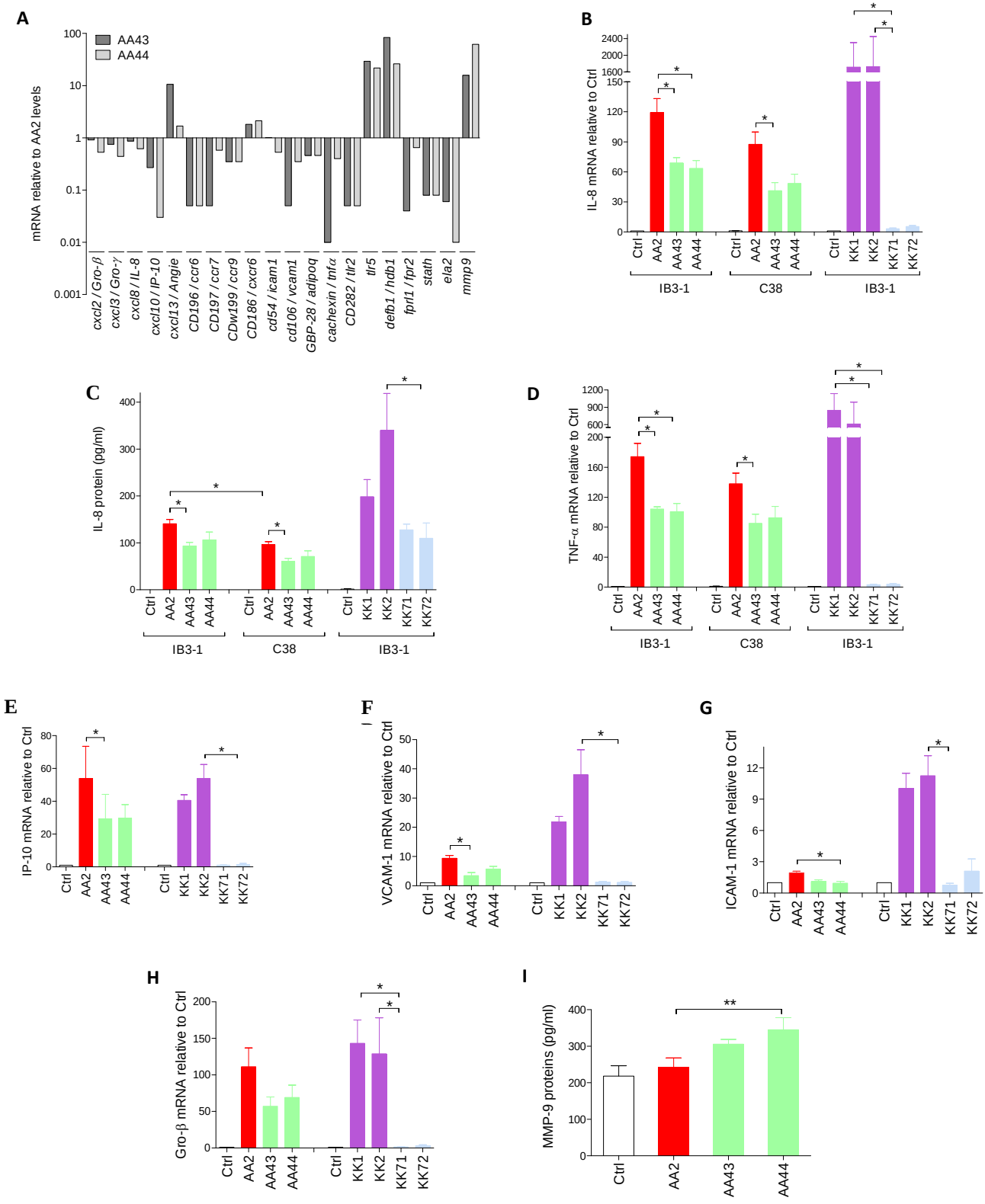

Figure 18. Expression/release of markers of inflammation and tissue damage in cell lines after infection with *P. aeruginosa*. Bronchial epithelial CF cells, IB3-1, were infected for 4 hours with *P. aeruginosa* AA2-AA43-AA44 isolates, RNA extracted and retrotranscribed, and macroarray conducted. **A**) Genes expression is expressed after normalization on expression induced by AA2. Validation of gene expression was performed by real time PCR in IB3-1 (**B, D-H**) and isogenic non-CF cells C38 (**B, D**) after infection with AA2, AA43, AA44, KK1, KK2, KK71 and KK72. **C**) Validation of IL-8 protein release in culture medium of IB-3 and C38 and **I**) MMP-9 protein release in supernatants of THP-1 cells was performed by ELISA. Values represent the mean ± SEM. The data are pooled from at least three independent experiments. Statistical significance by ANOVA is indicated: * p<0.05, ** p<0.01.

D.1.3 *P. aeruginosa* persistence promotes airway tissue damage in mice that mirrors human CF pathology

Next, we investigated the impact of *P. aeruginosa* CF-adapted variants on murine lungs in terms of tissue remodelling and damage. Mice retaining infection with AA43 and AA44 for one-month showed typical features of human CF airways pathology: intraluminal and peribronchial inflammation, epithelial hyperplasia and structure degeneration, goblet cells metaplasia, collagen deposition and elastin degradation (**Fig. 19A-C**). Then biochemical markers of tissue damage typical of human CF lung disease were investigated in BALF and in lung homogenate. The analysis showed an increase of MMP-9 activity and protein (**Fig. 20A-C**), TGF-β release and sulphated GAG (sGAG) (**Fig. 20D-F**) during long-term infection with CF-adapted variants AA43 and AA44. So the above described mouse model of long-term airway chronic infection established with *P. aeruginosa* CF-adapted variants is able to reproduce several traits of human CF lung pathology. Furthermore, taking into consideration our previous results in chronic infection model and cell culture and the emerging relevance of MMPs to impaired lung function in CF patients (Gaggar et al., 2006) we evaluated whether MMP-9 could play a key role in tissue damage induction during chronic lung infection. For this purpose we infected *Mmp9*$^{-/-}$ and their congenic wt mice with CF-adapted isolate AA43 embedded in agar beads for 28 days. No difference in bacterial load, total cells recruitment, sGAG and TGF-β was observed while lower collagen levels in *Mmp*9$^{-/-}$ mice than in congenic wt mice were found (**Fig. 21A-E**). These results suggest a role of MMP-9 in the process of collagen deposition during *P. aeruginosa* chronic persistence.

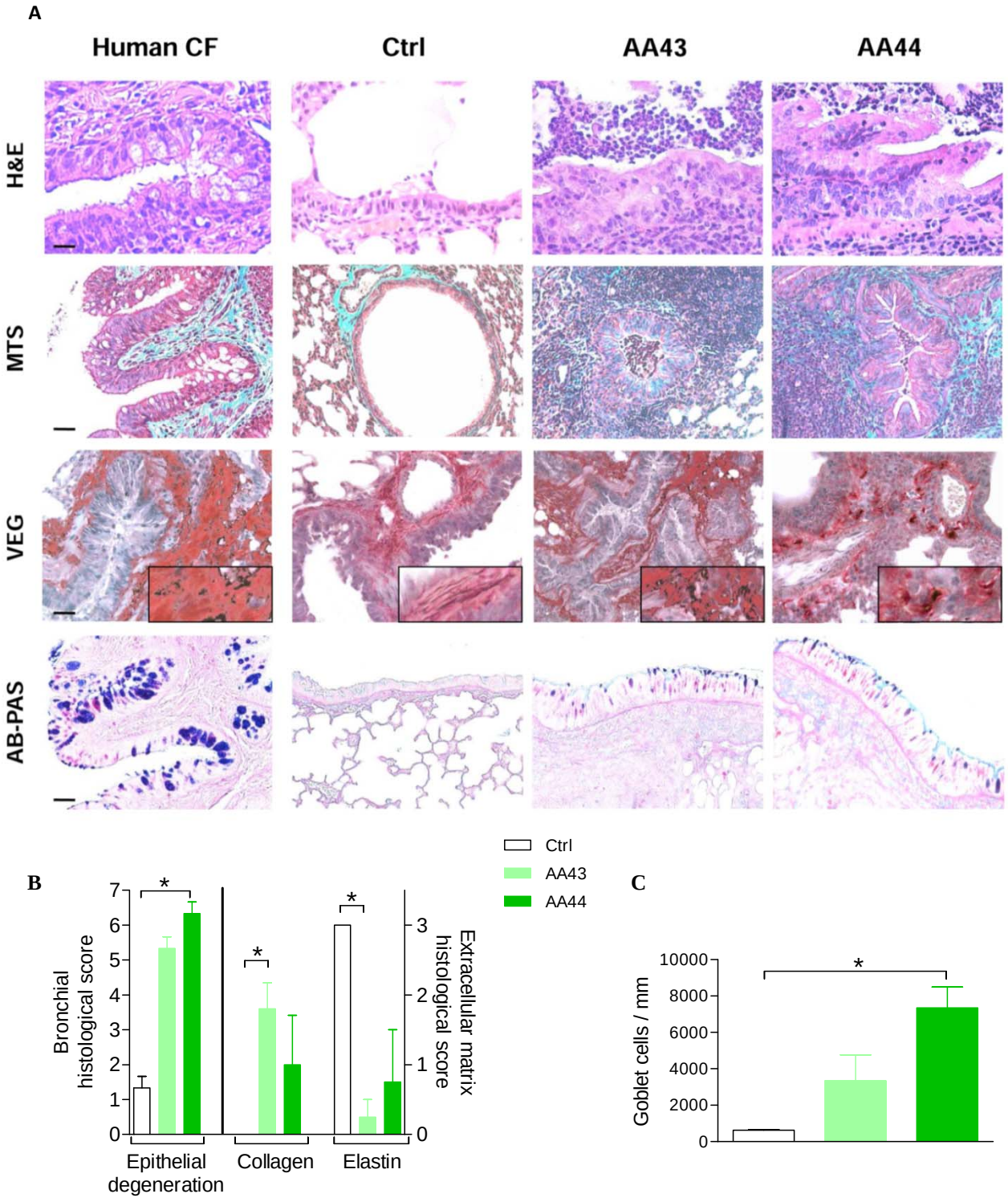

Figure 19. Lung histology and histopathological score of tissue damage in murine lung after infection with *P. aeruginosa*. C57Bl/6NCrlBR mice were infected with 1 to 2x10^6 CFU/lung of isolates embedded in agar beads and analyzed 28 days post-infection. Sections of airways from transplanted CF patients and from C57Bl/6NCrlBR infected with CF-adapted isolates AA43 and AA44 and sterile beads were stained with H&E, Masson's trichrome staining (MTS) for collagen, Van Gielson elastic (VEG*)* for elastic fibers and Alcian blue periodic acid-Schiff (AB/PAS) for mucopolysaccarides, according to the standard procedures (**A**). Scale bars: 12.5 µm for H&E, 25 µm for MTS, VEG and AB-PAS. Scorings of bronchial epithelial degeneration, collagen deposition and elastin degradation (**B**) were performed on slices stained with H&E, MTS and VEG, respectively. Goblet cells numbers were evaluated on slices stained with AB-PAS (**C**). The data are pooled from at least two independent experiments (n=2-6). Values represent the mean ± SEM. Statistical significance by ANOVA is indicated: *p<0.05.

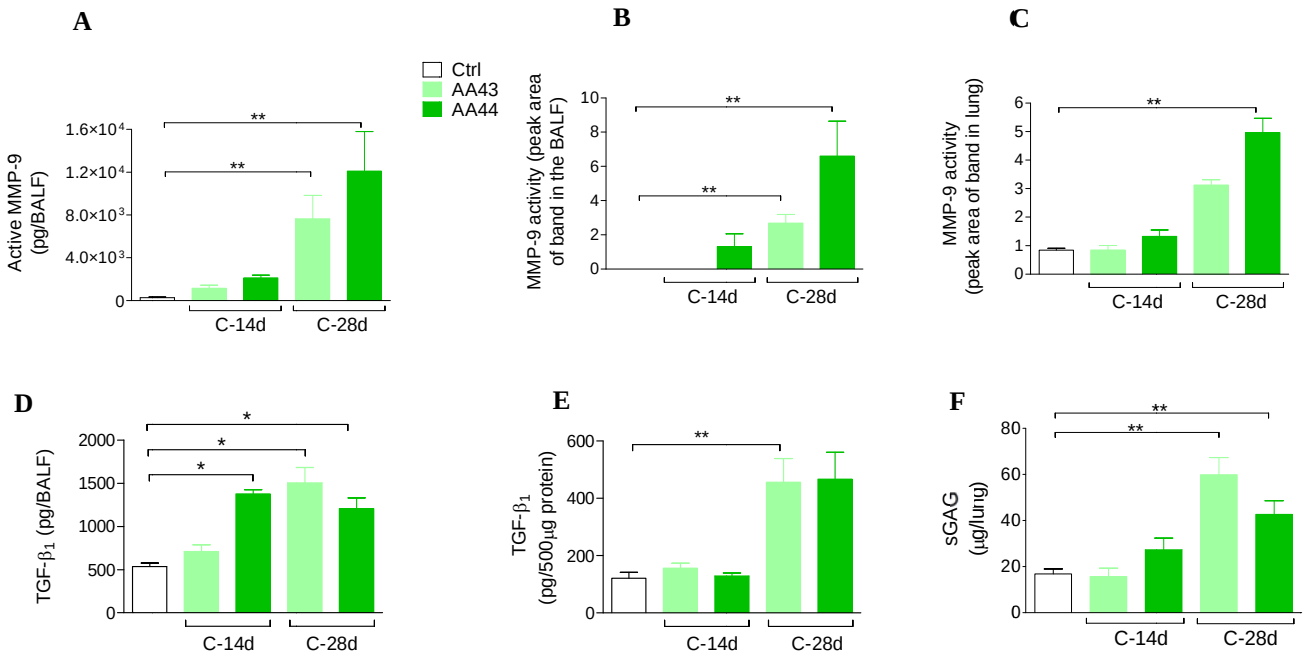

Figure 20. Tissue damage markers, including MMP-9, in murine models after *P. aeruginosa* infection. C57Bl/6NCrlBR mice were infected with 1 to 2x10^6 CFU/lung of CF-adapted isolates embedded in agar beads for 14 and 28 days. Levels of MMP-9 protein (**A**) in BALF by ELISA, MMP-9 activity (**B**) in BALF and (**C**) lung homogenate by zymography, TGF-β_1 (**D**) in BALF and (**E**) lung homogenate by Bioplex and sGAG (**F**) in lung homogenate by a dye-binding colorimetric assay were measured after 14 and 28 days of chronic lung infection. Values represent the mean ± SEM. The data are pooled from at least two independent experiments (n=3-12). Statistical significance by ANOVA and Mann Whitney test is indicated: * p<0.05, ** p<0.01.

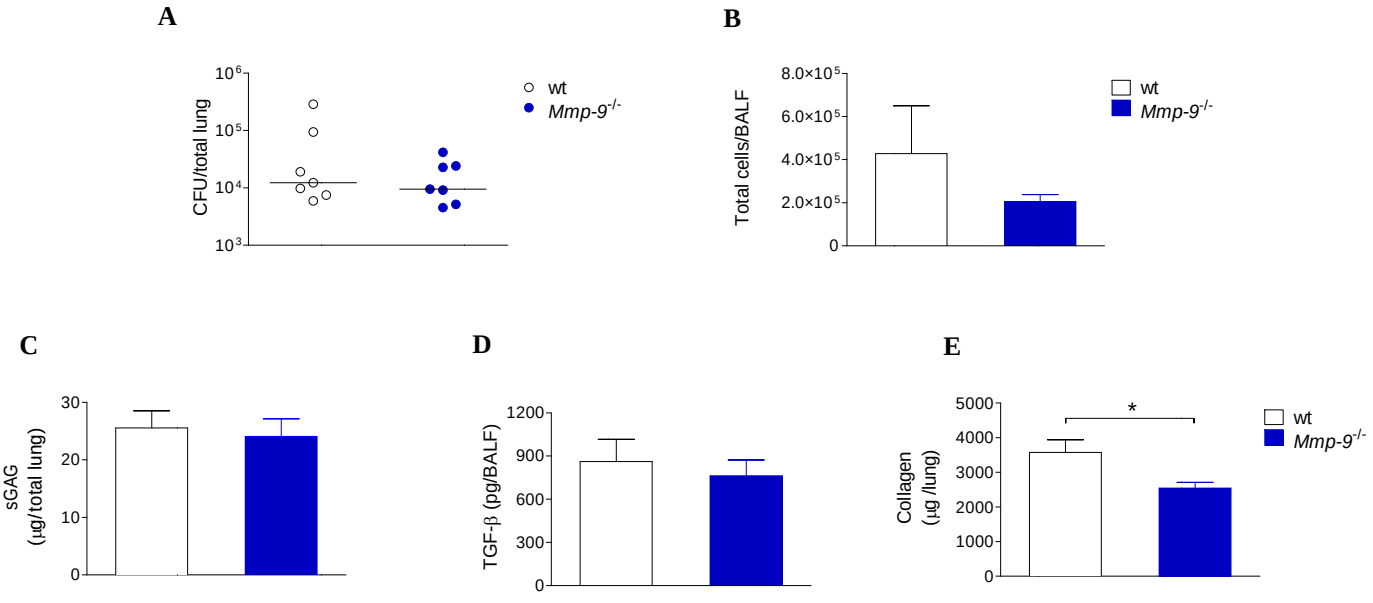

Figure 21. Bacterial load, leukocytes recruitment and tissue damage in lungs of *Mmp-9*$^{-/-}$ and congenic wt mice after *P. aeruginosa* long-term chronic infection. B6.FVB(Cg)-Mmp9tm1Tvu/J and congenic mice were infected with 2x10^6 CFU/lung of CF-adapted isolate AA43 embedded in agar beads. **A**) CFU in total lung, (**B**) total cells recruitment in BALF, (**C**) sGAG in lung homogenate by a colorimetric assay (**D**) TGF-β_1 by Bioplex and (**E**) collagen by the dye-binding Sircol Insoluble Collagen assay were evaluated after 28 days of chronic lung infection. Dots represent CFUs in individual mice and horizontal lines represent median values. Total leukocytes, sGAG and TGF-β_1 values are represented as mean ± SEM. The data derive from one experiment (n=6-7). Statistical significance by Mann Whitney test is indicated: * p<0.05.

D.2 Characterization of GAG species in the lung of mice after long-term chronic infection with *P. aeruginosa* CF-adapted isolate

Our previous results (shown above) highlighted an increase in sGAG levels in the lungs of mice chronically infected with *P. aeruginosa* for 28 days. Based on these data we investigated the levels of specific GAG disaccharides in this mouse model. Murine lungs were perfused, to avoid the detection of circulating GAG present in the blood, and then recovered. Then, pellets and supernatants of lung homogenates were analysed separately to distinguish released GAG from those present as structural components of the ECM. After 28 days of chronic infection with CF-adapted isolate AA43, disaccharides analysis showed an increase in heparin/heparan sulphate (HEP/HS) products in infected C57Bl/6NcrlBR (wt) mice compared to uninfected controls (**Fig. 22A**). In particular, in the pellet we observed the prevalence of the monosulphated disaccharides Δ2,1,0 (1 sulphates and 0 acetyl) and Δ2,1,1 (1 sulphate and 1 acetyl) over the other three species detected. No significant differences were found between the supernatants of the control and infected mice suggesting that *P. aeruginosa* long-term chronic infection modulates levels of specific structural GAG present in ECM.

In addition, to evaluate whether CFTR background may contribute to GAG remodelling, we infected $Cftr^{tm1Unc}$TgN(FABPCFTR) (CF) mice with *P. aeruginosa* isolate AA43 for 28 days (**Fig. 22B**). Analysis of lung samples revealed that the HEP/HS were the most prevalent products detected also in infected and non-infected CF mice. Notably, we observed more digestion products in supernatants of CF mice compared to wt mice. In addition, the most represented disaccharide in CF mice was Δ2,2,1 (2 sulphates and 1 acetyl), absent in wt mice. Overall these results indicated significant diversity between wt and CF mice: in particular, CF mice showed structural HEP/HS with an overall degree of sulphation higher than wt mice as well as a higher release of HEP/HS, that could potentially represent mediators of the excessive inflammation observed in CF.

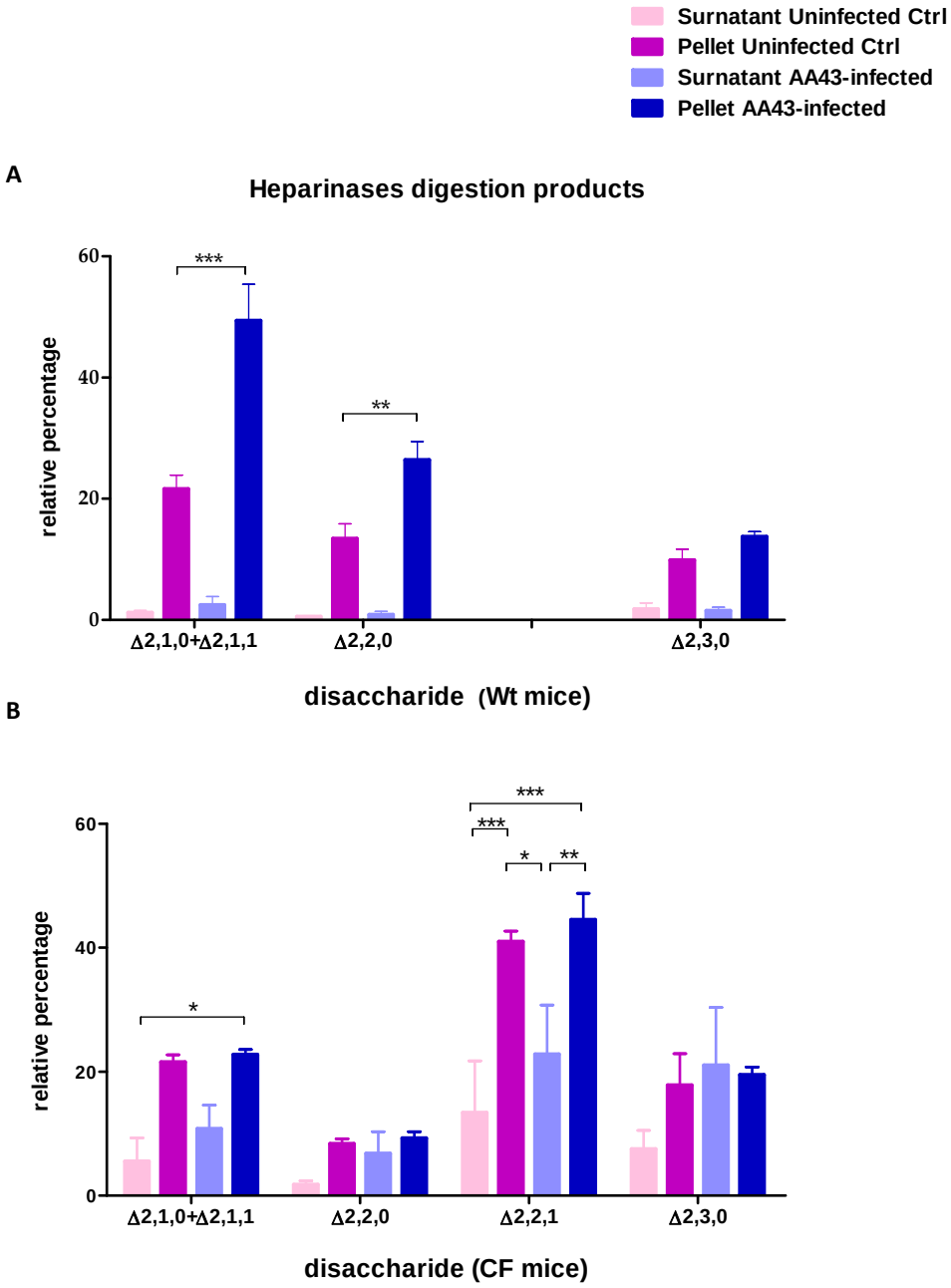

Figure 22. Disaccharide products of the digestion of HEP/HS from lungs of C57Bl/6NcrlBR (wt) mice and Cftr^{tm1Unc}TgN(FABPCFTR) (CF) mice after *P. aeruginosa* chronic lung infection. Lung homogenates of wt and CF mice infected with CF-adapted isolate AA43 or treated with sterile agar beads for 28 days were separated into pellets and supernatants to distinguish released GAG from those present as structural components of the ECM. GAG were isolated and then digested with specific enzymes to identify GAG species: first they were digested with chondroitinase ABC that cuts chondroitin sulphate (CS) and dermatan sulphate (DS) chains, then with a heparinase cocktail (I,II,III) that cuts heparan sulphate (HS) and heparin (HEP). Recovered digestion products were lyophilized and dissolved for high performance liquid chromatography-mass spectrometry (HPLC-MS) analysis. Even if HPLC-MS analysis is not quantitative, comparison among samples was possible under identical conditions and by comparing the integrals of LC-MS peaks of disaccharides to the sum of the relative integrals. **A**, **B**) The two graphs showed the percentage of each disaccharide species relative to the disaccharide moiety in pellet and SN of lungs from wt and CF mice infected or not-infected. 100% is considered the sum of integrals of pellet of lungs from Wt **and** CF mice infected with AA43. The unsaturated bond of the terminal uronic acid is indicated by Δ, and the number of monomers, the number of sulfates and the number of acetyls are reported. Two-way ANOVA with Bonferroni's post-test was used to statistically analyze results. Data represent the mean ± SEM of three samples per type which have been processed independently.

D.3. GAG modulation of inflammation and tissue damage in in vitro and in vivo analysis

D.3.1 Preparation of chemically modified GAG mimetics

Taking into consideration the increased levels of sGAG induced by *P. aeruginosa* infection, we synthetized and characterized a library of compounds to be tested as competitors of GAG present in the lung (GAG mimetics) in mouse models of acute and chronic *P. aeruginosa* airways infection. These molecules are polysaccharides (PS) derived from heparin that have been previously shown to interact with other proteins inhibiting inflammation, while exhibiting strongly reduced anticoagulant activities (Guimond, Turnbull, & Yates 2006). In particular, the N-acetylated heparin C23 and the glycol-split heparin derivative C3 were generated (Casu et al., 2004) based on unmodified pig mucosal heparin (PMH) (at the Ronzoni Institute, Milano) (**Fig. 23A and B**). The percentage of N-acetyl substitution in glucosamine residues (% N-acetyl), the percentage of glycol-split uronate residues (% Glycol-split) and the size of the compounds (**Fig. 23C**) are important parameter that can influence the binding of PS to proteins. The average molecular weight (M_w) of the compounds (17.2 and 16,5 kDa), assured an interaction with both IL-8 and HNE (Veraldi et al., 2015).

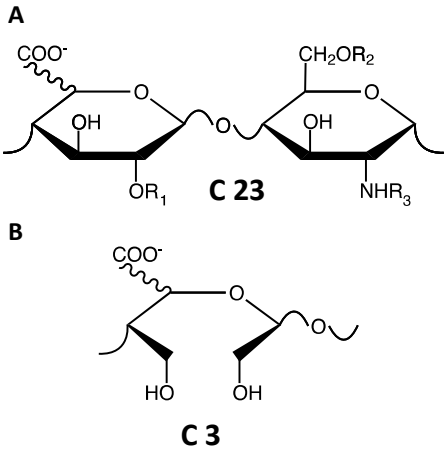

C

Compound	M_w(kDa)	% N-acetyl	% Glycol-split
C23	17,2	100	0
C3	16,5	14,6	20

Figure 23. A) The repeating disaccharide unit of compound C23 are R_1 and R_2 = H/SO_3^- and R3 = H/SO_3^-/$COCH_3$. The uronic acid is predominantly in the form L-iduronic acid (L-IdoA and L-IdoA-2-O-sulfate; ~ 80%) with D-glucuronic acid (D-GlcA; ~ 20%) making up the remainder. **B**) The glycol-split uronic acid residue present in compounds C3. **C**) The table contains the features by which these molecule differ each other: the weight average molecular weight (M_w), the percentage of N-acetyl substitution in glucosamine residues (% N-acetyl) and the percentage of glycol-split uronate residues (% Glycol-split) (cleavage by periodate oxidation of vicinal diols in unsubstituted D-GlcA and L-IdoA residues)

D.3.2 In vitro modulation of HNE activity and inflammation by GAG mimetics

First, we investigated the ability of GAG mimetics to inhibit the *in vitro* activity of HNE (**Fig. 24A**), a serine protease highly abundant in CF BALF and able to degrade major components of connective tissues, including elastin (Reeves., 2011). Results showed that C3 inhibited HNE activity of 50-60% of inhibition, comparably to HEP, the reference molecule. C23 was also efficacious in reducing HNE activity, although at a lower extent (25-30%). Then, we evaluated their anti-inflammatory potential analysing TNF-α release in the supernatants of macrophagic-like cells THP-1. Cells were infected with *P. aeruginosa* early isolate AA2 and treated with three different concentration of C3 and C23. Results showed a statistically significant reduction of TNF-α release by 10 ug/ml of C23 (**Fig. 24B**) , while the lower concentration of C3 (**Fig. 24C**) had a similar effect but without statistical significance.

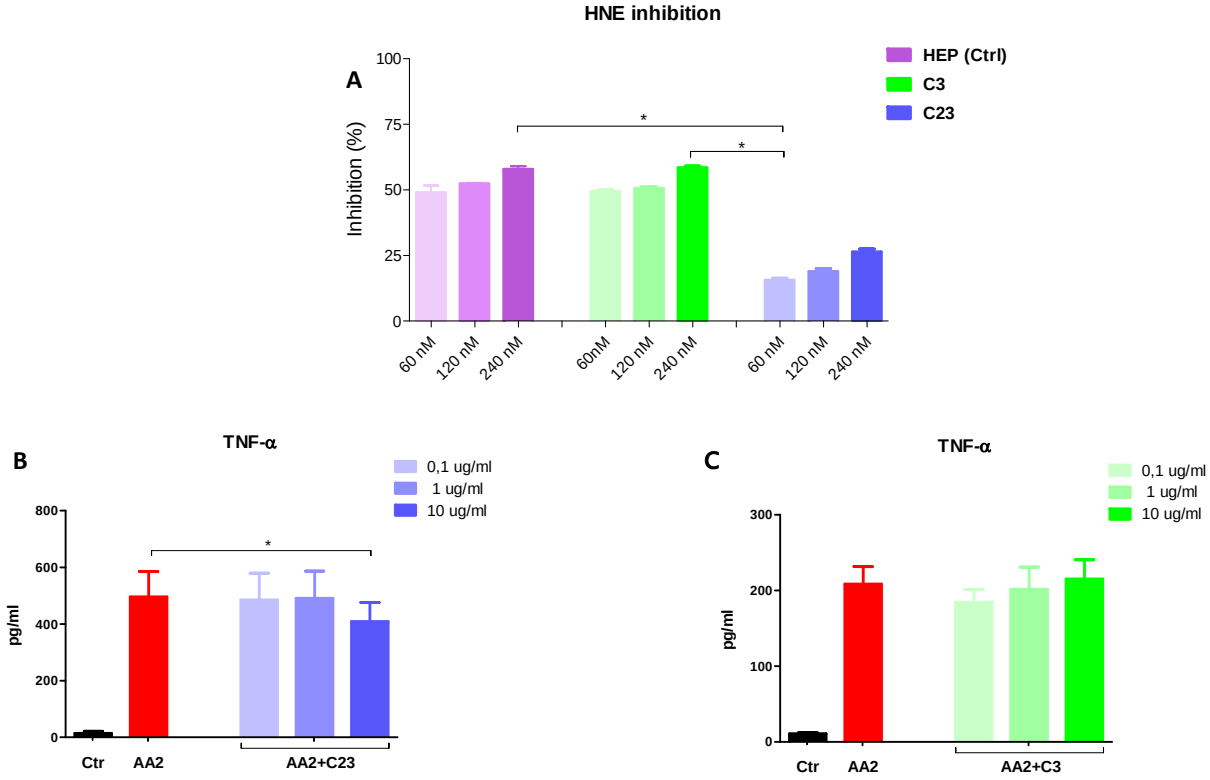

Figure 24. Modulation of human neutrophilic elastase (HNE) activity and inflammation *in vitro* by GAG mimetics C3 and C23. (**A**) To evaluate the ability of GAG mimetics to inhibit HNE activity, three different concentrations (60, 120 and 240 nM corresponding to 1:1, 2:1 and 4:1 molar ratio, respectively) of C3 and C23 were tested. The inhibition was evaluated with a colorimetric assay measuring the release of p-nitroaniline from a low molecular weight chromogenic substrate following the cleavage by HNE. The graph showed the percentage of inhibition of the elastase calculated from the regression curve of the initial speed of the reaction. TNF-α protein levels were measured by ELISA in the culture medium of macrophage-like THP-1 cells infected for 4 hours with *P. aeruginosa* AA2 strain (MOI 1:1) and treated with three different concentration (0.1, 1, 10 ug/ml) of C23 (**B**) and C3 (**C**) two hours before and two hours after the infection. Results are expressed as mean ± SEM of three independent experiments in triplicate. Statistical significance by ANOVA and Mann Whitney test is indicated: * $p<0.05$.

D.3.3 Modulation of inflammation and tissue damage by GAG mimetics in mouse models of *P. aeruginosa* infection

First, GAG mimetics C3 and C23 were tested in mice infected with *P. aeruginosa* AA2 isolate in a murine model of *P. aeruginosa* acute infection. C23 significantly reduced the number of total leukocytes (**Fig. 25A**), including neutrophils (**Fig. 25B**), in BALF in comparison to Ctrl infected mice treated with saline, while C3 had no effect. When the cytokines/chemokines profile, normalized on the bacterial burden, was evaluated, C23 reduced levels of MIP-1β, IL-6, G-CSF, IFN-γ, MCP-1, and RANTES (**Fig. 25C-H**), indicating its anti-inflammatory activity. C3 showed similar effects. Noteworthy, C3 significantly increased the bacterial load, while C23 did not affect it (**Fig. 25I**) despite its inhibitory activity on leukocytes infiltration, confirming its beneficial effect during *P. aeruginosa* acute infection.

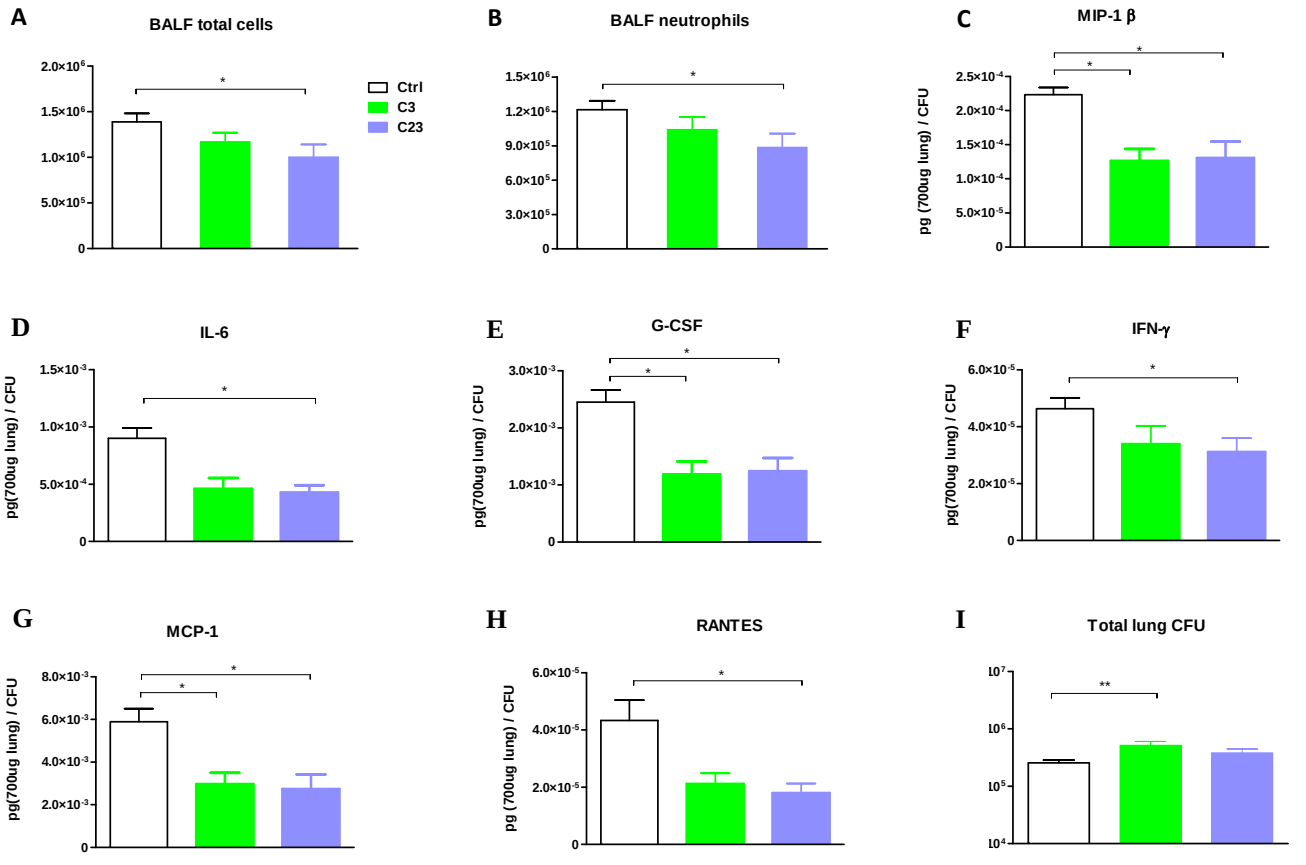

Figure 25: Inflammation modulation by C3 and C23 after *P. aeruginosa* acute lung infection. C57Bl/6NCrlBR mice were infected with 1x10^6 CFU/lung of early AA2 isolate (planktonic bacteria) and treated subcutaneously with C3 and C23 (30 mg/Kg) 2 hours before and 2 hours after the infection. Mice were sacrificed 6 hours after bacterial challenge. **A**) Total cell and and (**B**) neutrophils recruitment was analyzed in BALF. Cytokines/chemokines levels, including MIP-1β (**C**), IL-6 (**D**), G-CSF (**E**), IFN-γ (**F**), MCP-1 (**G**) and RANTES (**H**), measured by Bioplex were normalized on total CFU in the lung homogenates. (I) Total CFU were evaluated in total lungs. Values represent the mean ± SEM. Statistical significance by ANOVA and Mann Whitney test is indicated: * p<0.05, ** p<0.01.

Next, we exploited the effects of GAG mimetics during *P. aeruginosa* long-term persistence up to 28 days. In this pilot experiment, the daily subcutaneous treatment was started after one week from the infection, when chronic infection is stably set-up, to mimic the treatment in a patient already chronically colonized by *Pseudomonas aeruginosa.* After 28 days of chronic infection, both C3 and C23 had a similar anti-inflammatory activity: they decreased leukocytes infiltration in BALF, including neutrophils, and the levels of MIP-1α, IL-1β and KC in lung homogenates in comparison to Ctrl mice treated with saline, although differences did not reach statistical significance (**Fig. 26A and B, C-E**). Both compounds reduced MMP-9 active protein (**Fig. 26F**). In addition, C3 was able to significantly decrease elastin degradation (**Fig. 26G**). Overall, these results indicate that GAG mimetics can modulate lung immunopathology induced by *P. aeruginosa* chronic infection, reducing inflammation and tissue damage. Notably, despite their anti-inflammatory activity, C3 and C23 were able to contain the bacterial load, although without statistical significance (**Fig. 14H**), suggesting that these compounds could have anti-bacterial activity.

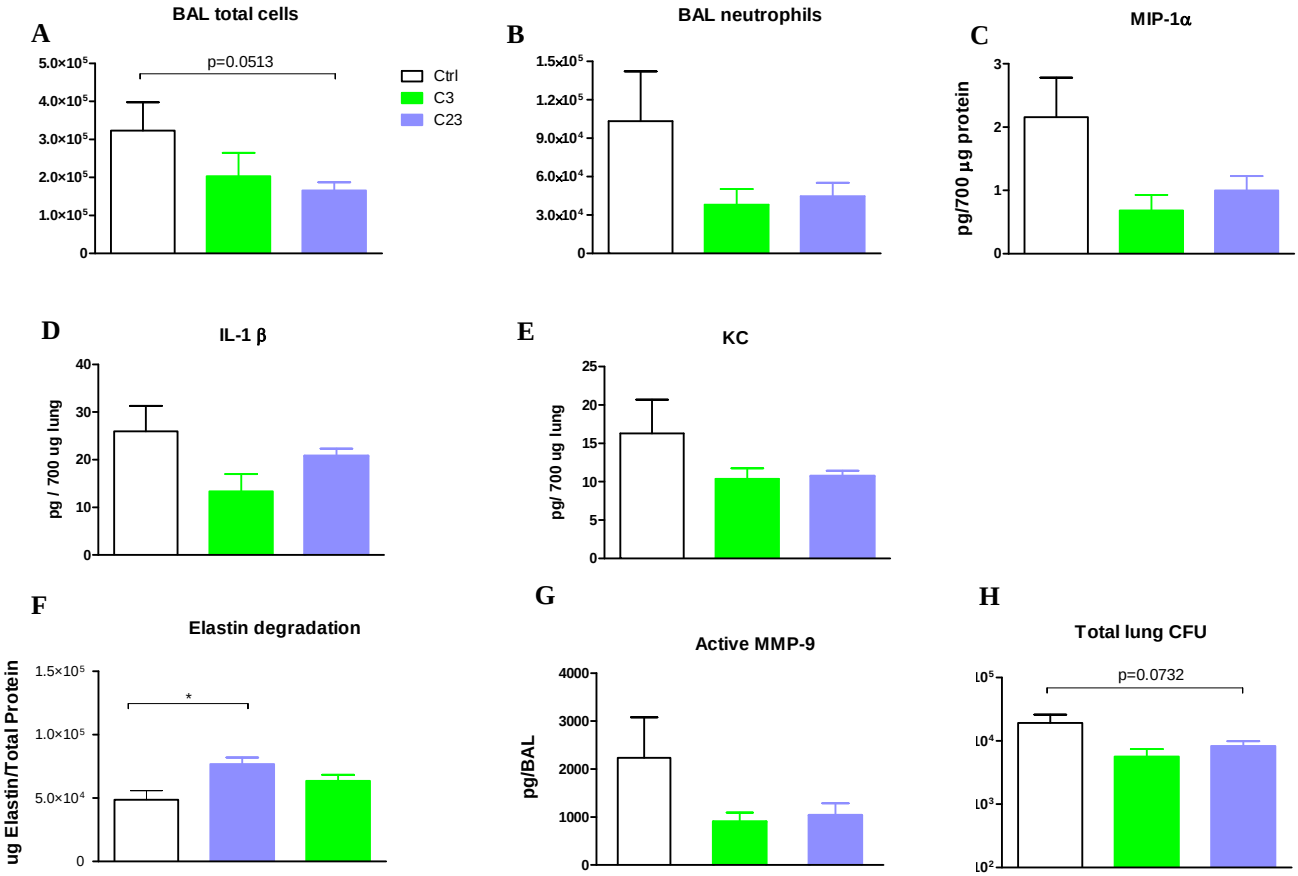

Figure 26: Inflammation, bacterial burden and tissue damage following treatment with C3 and C23 during *P. aeruginosa* long-term chronic lung infection. C57Bl/6NCrlBR mice were infected with 1-2x10^6 CFU/lung of CF-adapted isolate AA43 embedded in agar-beads and treated subcutaneously daily starting from a week after infection with C3 and C23 (30 mg/Kg) and saline (Ctrl mice) and sacrificed 28 days after bacterial challenge. **A**) Total cell and (**B**) neutrophils recruitment were analyzed in BALF. Cytokines/chemokines levels , including MIP-1α (**C**), IL-1β (**D**) and KC (**E**), measured by Bioplex were detected in lung homogenates. F Elastin levels were evaluated by a colorimetric dye-binding assay and results were indicated as the ratio between elastin measured in the lung homogenates and total protein quantified in the same samples. G) Levels of the MMP-9 active form were measured by ELISA in the BALF. (**H**) Total CFU were evaluated in total lungs. Values represent the mean ± SEM. Statistical significance by Mann Whitney test is indicated with the p value.

Taking into consideration the reduction of *P. aeruginosa* bacterial load described above, we evaluated if GAG mimetics could also have an antibacterial effect. As we did not find any minimal inhibitory concentration ($MICs_{90}$) after treatment with up to 512 ug/ml of C23 and C3 (data not shown), we investigated whether GAG mimetics could affect biofilm formation by CF-adapted isolate AA43 *in vitro*. Results revealed that C3 induced a statistically significant reduction of biofilm formation at lower concentrations, while C23 was effective at the higher concentration (10 ug/ml) (**Fig. 27A and B**). These results confirm that GAG mimetics can have anti-bacterial effects, and suggest that their administration may impact on *P. aeruginosa* chronic colonization.

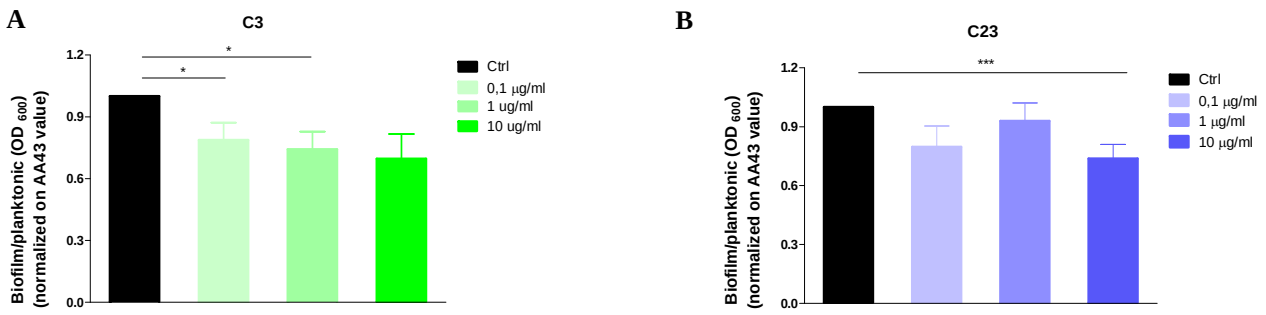

Figure 27: Effect of C3 and C23 on *P. aeruginosa* biofilm formation.AA43 was grown for 24 hours in plates at 37°C either in the absence or presence of three different concentrations (0.1, 1 and 10 ug/ml) of C3 (**A**) and C23 (**B**). Biofilm biomass was quantified by staining with crystal violet and absorbance measurements at OD_{600}. Absorbance of planktonic bacteria in the culture medium was measured at OD_{600}. Results are expressed as the ratio between biofilm absorbance and planktonic bacteria absorbance. The data are pooled from three independent assays, Values represent the mean ± SEM. Statistical significance by Mann Whitney test is indicated: * $p<0.05$, and *** $p<0.001$.

E. Conclusions and Future Prospects

CF patients are susceptible to chronic lung infections, the predominant cause of the morbidity and mortality associated with the disease. The most common pathogen in this respect is *P. aeruginosa*, a highly versatile bacterium capable of causing a wide range of mostly opportunistic infections, as well as colonising a variety of environmental niches (Lyczak et al., 2000). The ecological flexibility of *P. aeruginosa* can be attributed to its large genome (typically >6 Mb), which contains a particularly high proportion of regulatory genes, as well as a large number of genes involved in the catabolism, transport, and efflux of organic compounds (Stover et al., 2000; Silby et al., 2011). The CF lung is a heterogeneous, hostile, and stressful environment for invading bacteria, and *P. aeruginosa* populations must overcome these challenges to persist and survive. Postulated stressors in the CF lung include osmotic stress (Brocker et al., 2012) due to the viscous mucus, oxidative (Hector et al., 2014) and nitrosative (Wood et al., 2007) stresses due to host responses, sublethal concentrations of antibiotics (Andersson and Hughes, 2014), and the presence of other microorganisms (Fodor et al., 2012; Lopes et al., 2014). It has been recognized for many years that *P. aeruginosa* undergoes evolutionary changes in response to these selective forces during the chronic infection process (Winstanley et al., 2016). In this study we used sequential clonal *P. aeruginosa* isolates recovered from a CF patient. The early isolate AA2 was recovered at the onset of chronic infection while the CF-adapted variants AA43 and AA44 were isolated after years of chronic colonization. These *P. aeruginosa* clonal isolates were phenotypically typified and genetically characterized for genome rearrangements, mutations, and variations in pathogenic islands. In particular, AA43 and AA44 were, respectively, mucoid and non-mucoid variants with adaptive phenotypes, including absence of swimming motility, twitching motility and protease secretion, while the early AA2 was equipped by a wide series of virulence factors including swimming motility, twitching motility and protease secretion (Bragonzi et al., 2009; Cigana et al. 2009, Loré et al., 2012).

Previous studies investigated the virulence of these isolates in non-mammalian (*C. elegans*, *G. mellonella* and *D. melanogaster*) and in mammalian hosts (C57bl/6NCrl and Balb/cAnNCrl inbred mouse strains) (Lorè et al., 2012) during acute infection that is a short-term infection, carried out by a planktonic bacterial community. The acute infection could be eradicated by the immune system of the host or lead to mortality (Furukawa, 2006). In that work we observed that the early isolate AA2 was lethal while CF-adapted variants AA43 and AA44 were attenuated in acute

virulence. These results indicated host tolerance against *P. aeruginosa* CF adapted variants, as suggested by the high bacterial load sustained by the host. To mimic the progressive bronchopulmonary chronic infection typical of CF patients, in this work we challenged C57bl/6NCrl mice with AA2 and CF-adapted variants AA43 and AA44 embedded in agar beads (Facchini et al., 2014) and we reported, for the first time, the response to long-term *P. aeruginosa* lung infection (until 90 days) (Cigana et al., 2016). Bacteria embedded in the immobilizing agents appear to grow in the microaerobic/anaerobic conditions in form of microcolonies, similarly to the growth in the mucus of patients with CF (Bragonzi, 2010). In a chronic infection, bacterial proliferation is limited to a specific host tissue (e.g., in the CF lung or in association with medical devices), and bacteria can persist in the host for extended periods of time, adopting a slow-growing sessile lifestyle (biofilm). In the biofilm mode of growth bacteria are more resistant to the host immune system and prolonged antibiotic therapies, and they produce limited amount of virulence factors despite high cell density (Furukawa, 2006; Bondì et al., 2014). In the agar-beads model we noted that the early isolate AA2 was not able to establish long-term chronic infection while it induced mortality in mice. Conversely, CF-adapted variants AA43 and AA44, irrespective of mucoid phenotype, were able to persist in the bronchial lumen of mice as macrocolonies with a stable bacterial load (10^3/10^4 CFU) until 90 days.

When the immune response was analyzed, the histopathological analysis revealed that the bronchi and the parenchyma of mice infected with AA43 and AA44 were infiltrated by lower levels of innate immune cells (neutrophils and macrophages) after 28 and 90 days of chronic infection when compared to 2 days of chronic infection. Furthermore during the course of infection, AA43 and AA44 induced lower levels of inflammatory mediators, including MIP-2, KC, MIP-1 α, IL-6, MCP-1 and TNF-α compared with concentration induced by AA2 during acute infection and at the onset of chronic infection (2 days). In addition our results highlighted the evidence that the persistence of CF-adapted variants AA43 and AA44 involved a shift from innate to adaptive immune response as confirmed by the high levels of IL-17A and IFN-γ, indicating lymphocytes polarization, and the formation of BALT-like structures.

These data observed in mice were also supported by *in vitro* stimulation of IB3-1 CF bronchial epithelial cells with AA2, AA43 and AA44 and by the validation of targets selected from a global transcriptional analysis performed by RNA macroarray. In particular, CF-adapted variants AA43 and AA44 induced a significantly lower stimulation of IL-8, TNF-α, IP-10, VCAM-1, ICAM-1 and Gro-β transcription than early AA2 isolate. A weaker stimulation of these inflammatory targets by CF-

adapted variants was also confirmed when we extended the analysis to another *P. aeruginosa* clonal lineage from CF patient (KK). In this case, *P. aeruginosa* CF-adapted variants KK71 and KK72, isolated after many years of chronic infection, were less pro-inflammatory than early clonal isolates KK1 and KK2, isolated at the onset of infection. These *in vivo* and *in vitro* results suggest that the adaptation of *P. aeruginosa* to the CF lung niches negatively selects virulence factors able to stimulate host immune detection thus increasing immunoevasion and/or tolerance, and switches the host response to other pathways (e.g. adaptive immunity) (Cigana et al., 2009; Cigana at al., 2011, Medzhitov R et al., 2012). Furthermore, one factor of major interest was that the host response to *P. aeruginosa* adapted variants did not appear to be dependent only on a particular bacterial phenotype or clonal variant. Different *P. aeruginosa* patho-adaptive variants (e.g. mucoid and non-mucoid) or belonging to different patients, showed a similar capacity to weaken the host immune response (Cigana et al., 2016).

Interestingly, the histopathological analysis revealed that the persistence of CF-adapted variants AA43 and AA44 in the lung of mice reproduced several features typical of CF airway pathology after one month of infection (e.g. epithelial hyperplasia, goblet cells metaplasia, collagen deposition and elastin degradation). These pulmonary alterations together with others (e.g. bronchiectasis, mucoid impaction and atelectasis) are clustered as airway remodeling. These processes may already be present in children with CF and, in more than 90% of patients with CF, ultimately lead to death for respiratory failure (Regamey et al., 2011). Airway remodeling in CF is traditionally thought to be solely the consequence of repeated cycles of inflammation and infection and therapeutic approaches to preserve airway function may be required (Hillard et al., 2007). Furthermore in mice CF-adapted variants AA43 and AA44 induced an increase of MMP-9 activity and protein after one month of chronic infection. In addition, RNA macroarray analysis *in vitro* demonstrated that AA43 and AA44 adapted variants were more prone to induce MMP-9 protein release from macrophagic-like cells than the early isolate AA2. In the context of CF lung disease, MMP-9 was found to be the predominant active MMP isoform in CF patients and it was linked to impaired lung function (Gaggar et al., 2007; Ratjen et al., 2002). Our investigation in *Mmp9*$^{-/-}$ ko mice confirmed a key role of MMP-9 in tissue remodeling during *P. aeruginosa* chronic lung infection. In particular results observed in *Mmp9*$^{-/-}$ ko mice, demonstrated its involvement in the process of collagen deposition. Indeed, it has been shown that the degradation of airway wall observed in the CF lung is associated with an increase of MMP-9 activity and probably with a concomitant decrease of its natural inhibitor, TIMP-1 (Jackson et al., 2010). It was also

demonstrated that the increased activation of MMP-9 in CF lung disease cleaves latent TGF-β (Yu and Stamenkovic, 2000), a potent pro-fibrotic cytokine, that we found at high concentration in the lungs of mice chronically infected with CF-adapted variants AA43 and AA44. TGF-β activation is markedly up-regulated in CF and contributes to the progression of CF lung disease by mediating pulmonary fibrosis (Harris et al., 2013). Notably, the long-term chronic infection established in mice with AA43 and AA44 adapted variants induced also higher concentration of sGAG. Based on the higher levels of GAG in CF human bronchial cells and tissues, GAG remodeling has been associated to CF airways inflammation and tissue damage (Revees et al., 2011). These recent discoveries and the paucity of studies in the CF field prompted us to analyze GAG species present in the lung during chronic infection in agar beads mouse model. We observed that the persistence of the CF-adapted variant AA43 in the lung pellet of wt mice induced the prevalence of the monosulphated disaccharides over the other HEP/HS products detected. In the lung, GAG are distributed in the ECM, encompassing the interstitial space lying between the capillary endothelium and the alveolar epithelium (Suki et al., 2005), in the subepithelial tissue, bronchial walls and airways secretion. The lower level of GAG detected in lung supernatant than in the pellet of mice suggests that the long-term chronic infection increased the presence of GAG in the structural lung component probably altering their physiologic structural roles (e.g. antigen recognition or interaction of GAG with inflammatory molecules). Then we extended the analysis of GAG profile in CF mice during chronic infection. In this contest we observed more digestion products in supernatants of CF mice than wt mice and the most represented disaccharide, characterized by 2 sulphates and 1 acetyl, was absent in wt mice. These results indicate that CFTR background could influence the levels of released GAG and those present in the structural component. In addition, the higher sulphation may be probably correlated to the excessive inflammation observed in CF. Indeed, it has been demonstrated that the increased expression of GAG and subsequent binding to IL-8, MCP-1, RANTES and MIP-1β increased the half-life and activity of these cytokines and this process has been linked to the sustained inflammatory response and continued recruitment of neutrophils in CF bronchial tissue (Solic et al., 2005; Lau et al., 2004). However the role and the contribution of GAG in the host response and in the progression of tissue damage during *P. aeruginosa* infections in CF patients remains to be investigate and clarified.

Overall these results showed the evidence that the mouse model of *P. aeruginosa* long-term chronic infection proposed in this work mirrors human CF pathology, so it is useful to further study

CF lung disease pathogenesis and progression. The development of animal models that are able to reproduce features of CF lung disease is an open debate. It is well known that CF mice do not fully recapitulate the natural progression of CF lung disease seen in human patients (Fisher et al., 2011). The presence in mice of a significant calcium activated chloride secretory pathway alternative to CFTR protein and the lack of spontaneous lung infection with familiar CF organisms has dampened the enthusiasm of many investigators for this model (Clarke et al., 1994; Egan ME, 2009). In this context, the use of the agar beads model is essential for creating chronic lung infection in mice. Models of chronic infections have been described but, until now, no experimental studies have managed to achieve the progressive advanced-stage of lung pathology induced by chronic bacterial colonization that strictly mimics human CF infection (e.g., chronic *Pseudomonal* endobrochitis). The purpose of embedding *P. aeruginosa* within the beads is to retain the bacteria physically in the airways: the growth of the bacteria is slow within the beads which is comparable to that in biofilm in the CF lung. Inoculating mice with *P. aeruginosa*-laden agar beads better resembles the chronic lung infection of CF demonstrating both bronchial and parenchymal changes microscopically (e.g. squamous metaplasia and matrix remodeling.) Furthermore proliferation of BALT-like structures occurred in the peribronchial area adjacent to bead-containing airways, and consisted almost entirely of lymphocytes. This immunopathology is notably similar to the clinical description of human CF lung disease, mirroring chronic *Pseudomonal* endobronchitis of the CF population.

Despite distinct pathophysiological mechanisms underlying other respiratory diseases, such as bronchiectasis, advanced COPD, asthma and IPF, these pathologies share several common features with CF (e.g inflammation, *P. aeruginosa* persistence, anti-protease/protease imbalance, airway remodeling and fibrosis). Taking this into account, the chronic infection model in mice could be extended to reproduce other human respiratory pathologies, to study the course of the diseases and to develop therapeutic strategies.

Based on these considerations and the emerging relevance of GAG in CF pathogenesis (Reeves et al., 2011), also confirmed by our studies during long-term chronic infection in mice (Cigana et al., 2016), in the second part of this work we decided to test competitors of GAG present in the lung (GAG mimetics) to clarify the role of GAG in the host response and in the progression of tissue damage during *P. aeruginosa* infection in the mouse model. GAG mimetics belong to the class of heparins and low-molecular-weight heparins (LMWH), widely used as anticoagulants for more

than 50 years (Hostettler et al., 2007). However, heparin and LMWH are not just mere anticoagulants, rather complex sulfated GAG with several biological functions (Lever et al., 2002). The chemical modification of heparin and its derivatives, especially de-O-and de-N-sulfation, usually results in a net reduction of the overall charge density and also tends to reduce structural complexity, and attenuate undesired anticoagulant activities. Exogenously non-anticoagulant administered heparin and LMWH have been shown to exert beneficial effects in cancer (Yip et al., 2006; Lazo-Langner et al., 2007; Casu et al., 2008) and inflammation (Lever and Page, 2002; Young, 2008; Rek et al., 2009). The anti-tumor and anti-inflammatory properties of heparin and related species are thought to be largely associated with the influence on pathological functions of HS chains of HS proteoglycan (HSPGs), an "ubiquitous" component of cell surfaces and ECM (Casu B et al., 2010). In fact, GAG-based drugs can conceivably be designed to interfere with HS–protein interactions to compete with functions of HS chains (Lindahl, 2007; Lindahl and Li, 2009). Our hypothesis was that the compounds tested in this work could act as competitor of endogenous GAG replacing the pathologic effect of GAG remodeling (high level of GAG concentration and sulphation) that we previously observed during long-term chronic *P. aeruginosa* infection in wt and ko mice. In this study the N-acetylated C23 and the glycol-splitted C3 GAG mimetics were synthetized and previously characterized for their ability to interact with other proteins leading to anti-inflammatory effects (Guimond, Turbull and Yates, 2006). N-acetylation and glycol-split modifications of compounds facilitated the interaction with other protein and reduced the anticoagulant activity, demonstrating that these modifications can be useful to reduce undesired side effects without altering the substitution pattern of heparin (Casu et al., 2004). Firstly, compounds were screened for their ability to inhibit neutrophils elastase and modulate inflammation in *in vitro* tests. We observed that C23 inhibited the HNE of 25/30% while the C3 inhibition level reached 50/60% as the reference molecule heparin. We could speculate that this attenuation of elastase activity, rather than its complete inhibition, is desirable to contain and confine bacterial infection *in vivo.* Nevertheless, C23 also matched this inhibition of HNE with a significantly ability to diminish concentration of TNF-α, involved in inflammatory response. These results indicated that these compounds could be promising in reducing inflammation and tissue damage during acute and chronic *P. aeruginosa* infection in mice.

When we administered these molecules in a murine model of acute lung infection we found that C23 was able to reduce neutrophil numbers and the concentration of a panel of chemokines/cytokines in *P. aeruginosa*-infected animals in comparison to untreated mice (Ctrl

mice). This result suggested the positive impact of this GAG mimetic treatment on inflammatory response. Interestingly, the reduction of neutrophils recruitments could be ascribed not only to the reduced amount of chemokines, but also to the ability of GAG mimetics to inhibit the L-selectin-dependent cell rolling of leukocytes, mediated by HS, during leukocytes extravasation on the site of infection (Koenig et al., 1998; Hostettler et al., 2007). Interestingly, a similar reduction of inflammation observed with C3 was associated with a significant bacterial proliferation in the lungs in comparison to Ctrl mice. This result is in line with previous reports indicating that a strong anti-inflammatory treatment can deplete neutrophil numbers to such an extent that the infecting microorganisms could replicate in the lung and contribute to the symptoms of acute pulmonary exacerbations (Doring et al., 2014). For this reason, caution should be taken when administering anti-inflammatory compounds. Then we extended the analysis of C23 and C3 effect in the chronic infection model by challenging mice with CF-adapted variants AA43 for one month. As previously described, this model represents a precious tool and has been used for pre-clinical testing of candidate anti-bacterial and anti-inflammatory molecules (Paroni et al., 2013; Doring et al., 2014; Cigana et al., 2016). The treatment of mice was started a week after infection, when chronic infection was stably established. We decided to use this protocol to allow the establishment of the infection in the lung with a stable bacterial load (10^4/10^5 CFU), mimicking the treatment in a patient already chronically colonized by *P. aeruginosa.* We observed that both compounds attenuated the number of total leukocytes, including neutrophils and the concentration of inflammatory mediators including IL-1β, KC and MIP-1α compared with Ctrl mice. Furthermore we observed that C3 was able to preserve significantly elastin degradation in the lung, probably due not only to the inhibition of HNE by this GAG mimetic previously described *in vitro*, but also to the low concentration of MMP-9 (Jackson et al., 2010). In this experiment, the bacterial load, that was a critical aspect during acute infection, was reduced by both C23 and C3, likely due to the *in vitro* anti-biofilm activity of both compounds. This effect of C23 and C3 could be probably ascribed to their potential ability to create electrostatic interaction with basic amino acid or interfere with polysaccharides useful for the initial step of biofilm matrix formation. This hypothesis merits further investigation in the future. We also tested other glycol-split GAG mimetics, that differ for their molecular weight and percentage of N-acetyl substitution in D-glucosamine (GlcA) residues, in the mouse models of *P. aeruginosa* acute and chronic infection. These compounds did not show any inhibitory effect on markers of inflammation and/or tissue damage (data not shown). Overall,

these results further confirm the effectiveness of C3 and C23 in containing inflammation, tissue damage and the infection severity.

Future studies will further investigate the efficacy of these compounds taking into consideration both different routes of administration, including those more used in CF patients (e.g. nebulization), and pharmacokinetic/pharmacodynamics studies to improve the schedule of treatments. In addition, the compounds identified offer a starting point for future drug development, opening-up the possibility of the synthesis of GAG mimetics or analogues with lower molecular weight, capable of acting on multiple targets simultaneously, while minimizing unwanted side-effects. However, a deeper knowledge of their mechanisms of action is needed to optimize the drug candidates and to ensure that they hit the selected targets. Overall these results highlight the concept that the evaluation of potential therapies in murine models of chronic infection provides the greatest opportunity to optimally translate results obtained to the clinical care of patients. The encouraging results obtained so far with GAG mimetics support further development in translational application.

F. References

Akira S, Uematsu S, et al. (2006). Pathogen recognition and innate immunity. Cell 124 (4):783-801.

Amaral MD (2015). Novel personalized therapies for cystic fibrosis: treating the basic defect in all patients. J Intern Med 277(2):155-66.

Amin R, Dupuis A, et al. (2010). The effect of chronic infection with Aspergillus fumigatus on lung function and hospitalization in patients with cystic fibrosis. Chest **2010** 137(1):171-6

Andersson DI and Hughes D (2014). Microbiological effects of sublethal levels of antibiotics. Nat Rev. Microbiol 12, 465–478.

Armstrong DS, Grimwood K, et., et al (1997). Lower airway inflammation in infants and young children with cystic fibrosis. Am J Respir Crit Care Med 156:1197–1204.

Armstrong DS, Nixon GM, et al. (2002). Detection of a widespread clone of *Pseudomonas aeruginosa* in a pediatric cystic fibrosis clinic. Am J Respir Crit Care Med 1;166(7):983-7.

Athanazio R (2012). Airway disease: similarities and differences between asthma, COPD and bronchiectasis. Clinics (Sao Paulo) 67(11):1335-43.

Atkinson JJ and Senior RM (2003). Matrix metalloproteinase-9 in lung remodeling. Am J Respir Cell Mol Biol 28(1):12-24.

Baici A, Diczhazi C, et al. (1993). Inhibition of the human leukocyte endopeptidases elastase and cathepsin G and of porcine pancreatic elastase by N-oleoyl derivatives of heparin. Biochem. Pharmacol 46, 1545–1549.

Becker M, Franz G and Alban S (2003). Inhibition of PMN-elastase activity by semisynthetic glucan sulfates. Thromb Haemost 89, 915–925.

Bergin DA, Hurley K, et al. (2013). Airway inflammatory markers in individuals with cystic fibrosis and non-cystic fibrosis bronchiectasis. J Inflamm Res 6:1-11.

Bianchi SM, Prince LR, et al. (2008). Impairment of apoptotic cell engulfment by pyocyanin, a toxic metabolite of *Pseudomonas aeruginosa*. Am J Respir Crit Care Med 177(1):35–43.

Bianconi I, Milani A, Cigana C, et al. (2011). Positive signature-tagged mutagenesis in *Pseudomonas aeruginosa*: tracking patho-adaptive mutations promoting airways chronic infection. PLoS Pathog 7(2):e1001270.

Bilton D (2008). Update on non-cystic fibrosis bronchiectasis. J R Soc Med 101 Suppl 1:S6-9

Birrer P, McElvaney NG, et al. (1994). Protease-antiprotease imbalance in the lungs of children with cystic fibrosis. Am J Respir Crit Care Med 150, 207–213.

Bittar F and Rolain JM (2010). Detection and accurate identification of new or emerging bacteria in cystic fibrosis patients. Clin Microbiol Infect 16(7):809-20.

Bondí R, Messina M, et al. (2014). Affecting *Pseudomonas aeruginosa* Phenotypic Plasticity by Quorum Sensing Dysregulation Hampers Pathogenicity in Murine Chronic Lung Infection. PLoS ONE 9(11): e112105.

Bodini A, D'Orazio C, et al. (2005). Biomarkers of neutrophilic inflammation in exhaled air of cystic fibrosis children with bacterial airway infections. Pediatr Pulmonol 40(6): 494–9.

Borsig L (2004). Selectins facilitate carcinoma metastasis and heparin can prevent them. News Physiol Sci 19, 16-21.

Boucher JC, Yu H, Mudd MH and Deretic V (1997). Mucoid *Pseudomonas aeruginosa* in cystic fibrosis: characterization of muc mutations in clinical isolates and analysis of clearance in a mouse model of respiratory infection. Infect Immun 65: 3838–3846.

Boucher RC (2004). New concepts of the pathogenesis of cystic fibrosis. Eur Respir J 23(1):146-58. Review.

Bousquet J, Jeffery PK, et al. (2000). Asthma. From bronchoconstriction to airways inflammation and remodeling. Am J Respir Crit Care Med 161(5):1720-45.

Bragonzi A, Paroni M, et al. (2009). *Pseudomonas aeruginosa* microevolution during cystic fibrosis lung infection establishes clones with adapted virulence. Am J Respir Crit Care Med 180(2):138-45.

Bragonzi A (2010). Murine models of acute and chronic lung infection with cystic fibrosis pathogens. Int J Med Microbiol 300(8):584-93.

Brightling CE, Monteiro W, et al. (2000). Sputum eosinophilia and short-term response to prednisolone in chronic obstructive pulmonary disease: a randomised controlled trial. Lancet 356(9240):1480-5.

Brinkmann V, Reichard U, et al. (2004). Neutrophil extracellular traps kill bacteria. Science 303(5663):1532–5.

Brocker C, Thompson DC and Vasiliou V (2012). The role of hyperosmotic stress in inflammation and disease. Biomol. Concepts 3, 345–364.

Bruscia E, Zhang PX, et al. (2009). Macrophages directly contribute to the exaggerated inflammatory response in cystic fibrosis transmembrane conductance regulator-/- mice. Am J Respir Cell Mol Biol 40(3):295–304.

Buczek-Thomas JA and Nugent MA (1999). Elastase-mediated release of heparan sulfate proteoglycans from pulmonary fibroblast cultures. A mechanism for basic fibroblast growth factor (bFGF) release and attenuation of bfgf binding following elastase-induced injury. J Biol Chem 274, 25167–25172.

Burns JL, Gibson RL, et al. (2001). Longitudinal assessment of *Pseudomonas aeruginosa* in young children with cystic fibrosis. J Infect Dis 183(3):444-52.

Cantin AM, Hartl D, Konstan MW and Chmiel JF (2015). Inflammation in cystic fibrosis lung disease: Pathogenesis and therapy. J Cyst Fibros 14(4):419-30.

Casu B, Guerrini M, Guglieri S, Naggi A, et al. (2004). Undersulfated and glycol-split heparins endowed with antiangiogenic activity. J Med Chem 47(4):838-48.

Casu B, Vlodavsky I and Sanderson RD (2008). Non-anticoagulant heparins and inhibition of cancer. Pathophysiol Haemost Thromb 36:195–203.

Casu B, Naggi A and Totti G (2010). Heparin-derived heparan sulfate mimics that modulate inflammation and cancer. Matrix Biol 29(6): 442–452.

Chan YR, Chen K, et al. (2013). Patients with cystic fibrosis have inducible IL-17 + IL-22+ memory cells in lung draining lymph nodes. J Allergy Clin Immunol 131:1117–29.

Charo IF, and Ransohoff RM (2006). The many roles of chemokines and chemokine receptors in inflammation. N Engl J Med 354(6):610-21.

Chawla K, Vishwanath S, et al. (2015). Influence of *Pseudomonas aerugin*osa on exacerbation in patients with bronchiectasis. J Glob Infect Dis 7(1):18-22.

Cigana C, Curcurù L, et al. (2009). *Pseudomonas aeruginosa* exploits lipid A and muropeptides modification as a strategy to lower innate immunity during cystic fibrosis lung infection. PLoS One 4(12):e8439.

Cigana C, Lorè NI, Bernardini ML and Bragonzi A (2011). Dampening host sensing and avoiding recognition in *Pseudomonas aeruginosa* pneumonia. J Biomed Biotechnol 2011:852513.

Cigana C, Lorè NI, Riva C, et al. (2016). *Tracking the immunopathological response to Pseudomonas aeruginos*a during respiratory infections. Sci Rep 6:21465.

Clarke LL, Grubb BR, et al. (1994). Relationship of a noncystic fibrosis transmembrane conductance regulator-mediated chloride conductance to organ level disease in cftr (-/-) mice. Proc Natl Acad Sci USA 91:479-483.

Cystic Fibrosis Foundation Patient Registry Annual Report 2013.

Cystic fibrosis Foundation Patient Registry Annual Report 2014.

Cohen TS and Prince A (2012). Cystic fibrosis: a mucosal immunodeficiency syndrome. Nat Med 509-519.

Court CS, Cook DG and Strachan DP (2002). Comparative epidemiology of atopic and non-atopic wheeze and diagnosed **asthma** in a national sample of English adults. Thorax 57(11):951-7.

Cukic V, Lovre V, Dragisic D and Ustamujic A (2012). Asthma and Chronic Obstructive Pulmonary Disease (COPD). Differences and Similarities. Mater Sociomed 24(2):100-5.

Decraene A, Willems-Widyastuti A, et al. (2010). Elevated expression of both mRNA and protein levels of IL-17A in sputum of stable cystic fibrosis patients. Respir Res 11:177.

Decramer M, Janssens W and Miravitlles M (2012). Chronic obstructive pulmonary disease. Lancet 379: 1341–51.

Del Porto P, Cifani N, et al. (2011). Dysfunctional CFTR alters the bactericidal activity of human macrophages against *Pseudomonas aeruginosa*. PLoS One 6(5):e19970.

Deretic V, Schurr MJ and Yu H (1995). *Pseudomonas aeruginosa*, mucoidy and the chronic infection phenotype in cystic fibrosis. Trends Microbiol 3: 351–356.

Donlan RM and Costerton JW (2002). Biofilms: survival mechanisms of clinically relevant microorganisms. Clin Microbiol Rev 15(2):167–93.

Doring G, Taccetti et al., (2006). Eradication of *Pseudomonas aeruginosa* in cystic fibrosis patients Eur Resp J 27, 653 (2006).

Doring, G, Parameswaran IG and Murphy TF (2011). Differential adaptation of microbial pathogens to airways of patients with cystic fibrosis and chronic obstructive pulmonary disease. FEMS Microbiol 35 (1):124-146.

Doring G, Bragonzi A, et al. (2014). BIIL 284 reduces neutrophil numbers but increases P. aeruginosa bacteremia and inflammation in mouse lungs. J Cyst Fibros 13(2):156-63.

Egan ME (2009). How useful are cystic fibrosis mouse model? Drug Discovery Today 6(2)35-41.

Emerson J, Rosenfeld M, et al. (2002). *Pseudomonas aeruginosa* and other predictors of mortality and morbidity in young children with cystic fibrosis. Pediatr Pulmonol 34(2):91-100.

Facchini M, De Fino I, Riva C, Bragonzi A (2014). Long term chronic *Pseudomonas aeruginosa* airway infection in mice. J Vis Exp (85):51019.

Fath MA, Wu X, Hileman RE, et al. (1998). Interaction of secretory leukocyte protease inhibitor with heparin inhibits proteases involved in asthma. J Biol Chem 273, 13563–13569.

Feldman C (2011). Bronchiectasis: new approaches to diagnosis and management. Clin Chest Med 32(3):535-46.

Fisher JT, Zhang Y and Engelhardt JF (2011). Comparative biology of cystic fibrosis animal models. Methods Mol Biol 742:311-34.

Fodor AA, Klem ER et al. (2012). The adult cystic fibrosis airway microbiota is stable over time and infection type, and highly resilient to antibiotic treatment of exacerbations. PLoS ONE 7, e45001.

Folkesson A, Jelsbak L, et al. (2012). Adaptation of *Pseudomonas aeruginosa* to the cystic fibrosis airway: an evolutionary perspective. Nat Rev Microbiol 10(12):841-51.

Fryer, A. et al. (1997). Selective O-desulfation produces nonanticoagulant heparin that retains pharmacological activity in the lung. J Pharmacol Exp Ther 282, 208–219.

Furukawa S, Kuchma SL and O'Toole GA (2006). Keeping their options open: acute versus persistent infections. J Bacteriol 188(4):1211-7.

Gadsby DC, Vergani P and Csanády L (2006). The ABC protein turned chloride channel whose failure causes cystic fibrosis. Nature.;440(7083):477-83. Review.

Gaggar A, Li Y, et al. (2007). Matrix metalloprotease-9 dysregulation in lower airway secretions of cystic fibrosis patients. Am J Physiol Lung Cell Mol Physiol 293, L96-L104.

Gaggar A, Jackson PL, et al. (2008). A novel proteolytic cascade generates an extracellular matrix-derived chemoattractant in chronic neutrophilic inflammation. J Immunol 180, 5662-5669.

Gaggar A, Hector A, et al. (2011). The role of matrix metalloproteinases in cystic fibrosis lung diesase. Eu Respir J 38, 721-727.

Gandhi NS and Macera RL (2010). Heparin/heparan sulphate-based drugs. Drug Discovery Today 15(23/24):1058-1069.

Gellatly SL and Hancock RE (2013). *Pseudomonas aeruginosa*: new insights into pathogenesis and host defenses. Pathog Dis 67(3):159-73.

Geraghty P., Greene C.M. et al. (2007). Secretory leucocyte protease inhibitor inhibits interferon-gamma-induced cathepsin S expression. J Biol Chem 282, 33389– 33395.

Gibson RL, Burns JL and Ramsey BW (2003). Pathophysiology and management of pulmonary infections in cystic fibrosis. Am J Respir Crit Care Med 168(8):918-51.

Gosens R, Bos IS, et al. (2005). Protective effects of tiotropium bromide in the progression of airway smooth muscle remodeling. Am J Respir Crit Care Med 171(10):1096-1102.

Griese M., Latzin P, et al. (2007). Alpha1- antitrypsin inhalation reduces airway inflammation in cystic fibrosis patients. Eur Respir J 29, 240–250.

Greene CM, McElvaney NG, O'Neill SJ and Taggart CC (2004). Secretory leucoprotease inhibitor impairs Toll-like receptor 2- and 4-mediated responses in monocytic cells. Infect Immun 72(6): 3684-7.

Guimond SE, Turnbull JE and Yates EA (2006). Engineered bio-active polysaccharides from heparin. Macromol Biosci 6(8):681-6.

Hancock RE, Mutharia LM, et al. (1983). *Pseudomonas aeruginosa* isolates from patients with cystic fibrosis: a class of serum-sensitive, nontypable strains deficient in lipopolysaccharide O side chains. Infect Immun 42: 170–177.

Hansen CR, Pressler T, et al. (2010). Inflammation in *Achromobacter xylosoxidans* infected cystic fibrosis patients. J Cyst Fibros 9(1):51-8.

Harris WT, Muhlenbach MS et al. (2011). Plasma TGF-β_1 in pediatric cystic fibrosis: potential biomarker of lung disease and response to therapy. Pediatr Pulmonol. 46(7):688-95.

Harris WT, Kelly DR, et al. (2013). Myofibroblast differentiation and enhanced TGF-B signaling in cystic fibrosis lung disease. PLoS One 8, e70196.

Hartl D, Griese M, et al. (2006). Pulmonary T(H)2 response in *Pseudomonas aeruginosa*-infected patients with cystic fibrosis. J Allergy Clin Immunol 117(1):204–11.

Hartl D, Latzin P, et al (2007). Cleavage of CXCR1 on neutrophils disables bacterial killing in cystic fibrosis lung disease. Nat Med Dec 13(12):1423-30.

Hartl D, Gaggar A, et al. (2012). Innate immunity in cysic fibrosis lung disease. J Cyst Fibros 11(2012) 363-382.

Hassett DJ, Cuppoletti J et al. (2002). Anaerobic metabolism and quorum sensing by Pseudomonas aeruginosa biofilms in chronically infected cystic fibrosis airways: rethinking antibiotic treatment strategies and drug targets. Adv Drug Deliv Rev 54(11):1425-43. Review.

Hauser AR, Jain M, Bar-Meir M, McColley SA (2011). Clinical significance of microbial infection and adaptation in **cystic fibrosis**. Clin Microbiol Rev 24(1):29-70.

Hector A, Griese M and Hartl D (2014). Oxidative stress in cystic fibrosis lung disease: an early event, but worth targeting? Eur Respir J 44, 17–19.

Hirota N and Martin JG (2014). Mechanisisms of airway remodeling. Chest 144(3):1026-1032.

Hilliard TN, Regamey N, et al. (2007). Airway remodelling in children with cystic fibrosis. Thorax 62, 1074-1080.

Høiby N, Frederiksen B, Pressler T (2005). Eradication of early *Pseudomonas aeruginosa* infection. J Cyst Fibros 4 Suppl 2:49-54.

Hogardt M, Roeder M, et al. (2004). Expression of *Pseudomonas aeruginosa* exoS is controlled by quorum sensing and RpoS. Microbiology 150: 843–851.

Hogardt M, Hoboth C, et al. (2007). Stage-specific adaptation of hypermutable *Pseudomonas aeruginosa* isolates during chronic pulmonary infection in patients with cystic fibrosis. J Infect Dis 195: 70–80.

Hostettler N, Naggi A, et al. (2007). P-selectin- and heparanase-dependent antimetastatic activity of non-anticoagulant heparins. FASEB J 21(13):3562-72.

Hurley MN, Forrester DL and Smyth AR (2010). Antibiotic adjuvant therapy for pulmonary infection in cystic fibrosis. Cochrane Database Syst Rev 10:CD008037.

Ikpa PT, Bijvelds MJC, de Jonge H (2013). Cystic fibrosis: toward personalized therapies. Inter J Bioch & Cell Biol 52(2914) 192-200.

Jackson PL, Xin Xu, et al. (2010). Human neutrophil elastase-mediated cleavage sites of MMP-9 and TIMP-1: implications to cystic fibrosis proteolytic dusfuncyion. Mol Med 16(5-6): 159-166.

Jain M, Ramirez D, et al. (2004). Type III secretion phenotypes of Pseudomonas aeruginosa strains change during infection of individuals with cystic fibrosis. J Clin Microbiol 42: 5229–5237.

Jesaitis AJ, Franklin MJ, et al. (2003). Compromised host defense on *Pseudomonas aeruginosa* biofilms: characterization of neutrophil and biofilm interactions. J Immunol 171(8):4329–39.

Kang JY, Rhee CK, et al. (2012). Effect of tiotropium bromide on airway remodeling in a chronic asthma model. Ann Allergy Asthma Immunol 109(1):29-35.

Kelly E, Greene CM and McElvaney N.G. (2008). Targeting neutrophil elastase in cystic fibrosis. Expert Opin Ther Targets 12, 145–157.

Khatri IA, Bhaskar KR, et al. (2003). Effect of chondroitinase ABC on purulent sputum from cystic fibrosis and other patients. Pediatr Res 53, 619–627.

King Jr TE, Annie P and Selman M (2011). Idiopathic pulmonary fi brosis. Lancet 378: 1949–61.

King P, Lomovskaya O, et al. (2010). In vitro pharmacodynamics of levofloxacin and other aerosolized antibiotics under multiple conditions relevant to chronic pulmonary infection in cystic fibrosis. Antimicrob Agents Chemother 54(1):143–8.

Klockgether J, W¨urdemann D, et al. (2007). Diversity of the abundant pKLC102/PAGI-2 family of genomic islands in *Pseudomonas aeruginosa*. J Bacteriol 189: 2443–2459.

Koenig A, Norgard-Sumnicht K et al. (1998). Differential interactions of heparin and heparan sulfate glycosaminoglycans with the selectins. Implications for the use of unfractionated and low molecular weight heparins as therapeutic agents. J Clin Invest 101(4):877-89.

Konstan MW, Schluchter MD, et al. (2007). Clinical use of Ibuprofen is associated with slower FEV1 decline in children with cystic fibrosis. Am J Respir Crit Care Med 176:1084–9.

Konstan MW (2008). Ibuprofen therapy for cystic fibrosis lung disease: revisited. Curr Opin Pulm Med 14:567–73.

Laguna TA and Wagner BD (2009). Sputum desmosine during hospital admission for pulmonary exacerbation in cystic fibrosis. Chest 136(6):1561-8.

Lands LC, Milner R, et al. (2007). High-dose ibuprofen in cystic fibrosis: Canadian safety and effectiveness trial. J Pediatr 151:249–54.

Langereis JD and Hermans PW (2013). Novel concepts in nontypeable *Haemophilus influenzae* biofilm formation. FEMS Microbiol Lett 346(2):81–9.

Lau E, Paavola CD, et al. (2004). Identification of the glycosaminoglycans binding site of the CC chemokine,MCP-1: implications for structure and function in vivo. J Biol Chem 279(21):22294-305.

Lazo-Langner A, Goss GD, et al. (2007). The effect of low-molecular- weight heparin on cancer survival. A systematic review and meta-analysis of randomized trials. J Thromb Haemost 5:729–737.

Lee DG, Urbach JM, et al. (2006). Genomic analysis reveals that *Pseudomonas aeruginosa* virulence is combinatorial. Genome Biol 7: R90.

Lee VT, Smith RS, et al. (2005). Activities of *Pseudomonas aeruginosa* effectors secreted by the Type III secretion system in vitro and during infection. Infect Immun 73: 1695–1705.

Lämmermann T, Afonso PV, et al. (2013). Neutrophil swarms require LTB4 and integrins at sites of cell death in vivo. Nature 498(7454):371–5.

Lever R and Page CP (2002). Novel drug development opportunities for heparin. Nat Rev Drug Discov 1(2):140-8.

Lindahl U (2007). Heparan sulfate–protein interactions: a concept for drug design? Thromb Haemost 98, 109–115.

Lindahl U and Li JP (2009). Interactions between heparan sulfate and proteins-design and functional implications. Int Rev Cell Mol Biol 276:105-59.

Lopes SP, Azevedo NF and Pereira MO (2014). Microbiome in cystic fibrosis: shaping polymicrobial interactions for advances in antibiotic therapy. Crit. Rev. Microbiol. 41, 353–565.

Lopes SP, Azevedo NF and Pereira MO (2014). Emergent bacteria in cystic fibrosis: invitro biofilm formation and resilience under variable oxygen conditions. Biomed Res Int 2014:678301.

Lorè NI, Cigana C, De Fino I, Riva C, et al., (2012). Cystic fibrosis-niche adaptation of *Pseudomonas aeruginosa* reduces virulence in multiple infection hosts. PLoS One 7(4):e35648.

Lory S, Merighi M and Hyodo M (2009). Multiple activities of c-di- GMP in *Pseudomonas aeruginosa*. Nucleic Acids Symp Ser 53: 51–52.

Luzar MA, Thomassen MJ and Montie TC (1985). Flagella and motility alterations in *Pseudomonas aeruginosa* strains from patients with cystic fibrosis: relationship to patient clinical condition. Infect Immun 50: 577–582.

Lyczak JB, Cannon CL and Pier GB (2000). Establishment of *Pseudomonas aeruginosa* infection: lessons from a versatile opportunist. Microbes Infect 2(9):1051-60.

Mall M, Grubb BR, et al. (2004). Increased airway epithelial Na+ absorption produces cystic fibrosis-like lung disease in mice. Nat Med 10(5):487-93.

Mall Ma and Hartl D (2014). CFTR: cystic fibrosis and beyond. Eur Respir J 44(4):1042-54.

Mantovani A, Cassatella MA, et al. (2011). Neutrophils in the activation and regulation of innate and adaptive immunity. Nat Rev Immunol 11(8):519-31.

Martinez FD and Vercelli D (2013). Asthma. Lancet 19;382(9901):1360-72.

McKeon DJ, Cadwallader KA, et al. (2010). Cystic fibrosis neutrophils have normal intrinsic reactive oxygen species generation. Eur Respir 35(6):1264-72.

Medzhitov R, Schneider DS and Soares MP (2012). Disease tolerance as a defense strategy. Science. 335(6071):936-41.

Meers P, Neville M, et al (2008). Biofilm penetration, triggered release and in vivo activity of inhaled liposomal amikacin in chronic *Pseudomonas aeruginosa* lung infections. J Antimicrob Chemother 61(4):859–68.

Mogayzel Jr PJ, Naureckas ET, et al (2013). Cystic fibrosis pulmonary guidelines. Chronic medications for maintenance of lung health. Am J Respir Crit Care Med 187: 680–9.

Molyneaux PL and **Maher** TM (2013). The role of infection in the pathogenesis of idiopathic pulmonary fibrosis. Eur Respir Rev 22(129):376-81.

Moser C, Kjaergaard S, et al. (2000). The immune response to chronic *Pseudomonas aeruginosa* lung infection in cystic fibrosis patients is predominantly of the Th2 type. APMIS 108(5):329–35.

Moser C, Jensen PØ, et al. (2002). Improved outcome of chronic *Pseudomonas aeruginosa* lung infection is associated with induction of a Th1-dominated cytokine response. Clin Exp Immunol 127(2):206–13.

Munck A, Bonacorsi S et al. (2001). Genotypic characterization of *Pseudomonas aeruginosa* strains recovered from patients with cystic fibrosis after initial and subsequent colonization. Pediatric Pulmonol 32, 288-292.

Nguyen D and Singh PK (2006). Evolving stealth: genetic adaptation of *Pseudomonas aeruginosa* during cystic fibrosis infections. Proc Natl Acad Sci U S A 103(22):8305-6.

Noth I, Zhang Y et al (2013). Genetic variants associated with idiopathic pulmonary fibrosis susceptibility and mortality: a genome-wide association study. Lancet Respir Med 1(4):309-1.

Noble PW, Albera C, et al. (2011). Pirfenidone in patients with idiopathic pulmonary fi brosis (CAPACITY): two randomised trials. Lancet 377: 1760–69.

Owen C (2001). Chemokine receptors in airway disease: which receptors to target? Pulm Pharmacol Ther 14(3):193-202.

O'Donnell AE (2008). Bronchiectasis. Chest 134(4):815-23.

O'Sullivan BP, Freedman SD (2009). Cystic fibrosis. Lancet. 30;373(9678):1891-904.

Paroni M, Moalli F, et al. (2013). *Response of CFTR-deficient mice to long-term chronic Pseudomonas aeruginosa* infection and PTX3 therapy. J Infect Dis 208(1):130-8.

Parkins MD and Elborn JS (2011). Tobramycin inhalation powder: a novel drug delivery system for treating chronic *Pseudomonas aeruginosa* infection in cystic fibrosis. Expert Rev Respir Med 5(5):609–22.

Pazos MA, Pirzai W, et al. (2015). Distinct cellular sources of hepoxilin a3 and leukotriene b4 are used to coordinate bacterial-induced neutrophil transepithelial migration. J Immunol 194(3):1304–15.

Pera T, Zuidhof et al. (2011). Tiotropium inhibits pulmonary inflammation and remodelling in a guinea pig model of COPD. Eur Resp J 38(4):789-796.

Pillarisetti N, Williamson E, et al. (2011). Infection, inflammation, and lung function decline in infants with cystic fibrosis. Am J Respir Crit Care Med 184(1):75-81.

Raghu G, Collard HR, Egan J, et al. (2011). An official ATS/ERS/JRS/ALAT statement: idiopathic pulmonary fi brosis: evidence-based guidelines for diagnosis and management. Am J Respir Crit Care Med 183: 788–824

Ratjen F, Hartog CM, et al. (2002). Matrix metalloproteases in BAL fluid of patients with cystic fibrosis and their modulation by treatment with dornase alpha. Thorax 57(11):930-4.

Rau MH, Hansen SK, et al (2010). Early adaptive developments of *Pseudomonas aeruginosa* after the transition from life in the environment to persistent colonization in the airways of human cystic fibrosis hosts. Environ Microbiol 12(6):1643-58.

Reeves EP, Bergin DA, et al. (2011). The involvement of glycosaminoglycans in airway disease associated with cystic fibrosis. ScientificWorldJournal 11:959-71.

Regamey N, Jeffery, PK, et al. (2011). Airway remodelling and its relationship to inflammation in cystic fibrosis. Thorax 66, 624-629.

Rek A, Krenn E and Kungl AJ (2009). Therapeutically targeting protein–glycan interactions. Brit J Pharmacol 157:686–694.

Ren CL, Morgan WJ, et al. (2007). Presence of methicillin resistant Staphilococcus aureus in respiratory cultures from cystic fibrosis patients is associated with lower lung function. Pediatric pulmonology 42(6): 513-8.

Roderfeld M, Rath T et al. (2009). Serum matrix metalloproteinases in adult CF patients: Relation to pulmonary exacerbation. J Cyst Fibros 8(5):338-47.

Rostand KS and Esko JD (1997). Microbial adherence to and invasion through proteoglycans. Infect Immun 65(1):1-8.

Rossol M, Heine H et al. (2011). LPS-induced cytokine production in human monocytes and macrophages. Crit Rev Immunol 31(5):379-446. Review.

Sabra W, Lunsdorf H and Zeng AP (2003). Alterations in the formation of lipopolysaccharide and membrane vesicles on the surface of *Pseudomonas aeruginosa* PAO1 under oxygen stress conditions. Microbiology 149: 2789–2795.

Sagel SD and Accurso FJ (2002). Monitoring inflammation in CF. Cytokines. Clin Rev Allergy Immunol 23(1):41-57.

Saiman L, Tabibi S, et al. (2001). Cathelicidin peptides inhibit multiply antibiotic-resistant pathogens from patients with cystic fibrosis. Antimicrob Agents Chemother 45(10): 2838–44.

Salipante SJ, Sengupta DJ et al. (2013). Rapid 16S rRNA next-generation sequencing of polymicrobial clinical samples for diagnosis of complex bacterial infections. PLoS One 29;8(5):e65226.

Schuster M, Tschernig T, et al. (2000). Lymphocytes migrate from the blood into the bronchoalveolar lavage and lung parenchyma in the asthma model of the brown Norway rat. Am J Respir Crit Care Med 161(2):558-66.

Sethi S, Wrona C , et al. (2008). Inflammatory profile of new bacterial strain exacerbations of chronic obstructive pulmonary disease. Am J Respir Crit Care Med 177: 491–97.

Silo-Suh L, Suh SJ, Phibbs PV and Ohman DE (2005). Adaptations of *Pseudomonas aeruginosa* to the cystic fibrosis lung environment can include deregulation of zwf, encoding glucose-6-phosphate dehydrogenase. J Bacteriol 187: 7561–7568.

Silby, M.W. Winstanley C, et al. (2011). *Pseudomonas* genomes: diverse and adaptable. FEMS Microbiol Rev ;35(4):652-80.

Sibley CD, Sibley KA, et al. (2010). The *Streptococcus milleri* population of a cystic fibrosis clinic reveals patient specificity and intraspecies diversity. Clin Microbiol 48(7):2592-4.

Sissi C, Lucatello L, Naggi A, et al. (2006). Interactions of low-molecular-weight semisynthetic sulfated heparins with human leukocyte elastase and human cathepsin G. Biochem Pharmacol 71, 287–93.

Skerrett SJ, Wilson CB, et al. (2007). Redundant Toll-like receptor signaling in the pulmonary host response to *Pseudomonas aeruginosa*. Am J Physiol Lung Cell Mol Physiol 292(1):L312–22.

Smith EE, Buckley DG, et al. (2006). Genetic adaptation by *Pseudomonas aeruginosa* to the airways of cystic fibrosis patients. Proc Natl Acad Sci USA **103**, 8487-8492.

Snelgrove RJ, Jackson PL (2010). A critical role for LTA4H in limiting chronic pulmonary neutrophilic inflammation. Science 330(6000):90-4.

Solic N, Wilson J, et al. (2005). Endothelial activation and increased heparan sulfate expression in cystic fibrosis. Am J Respir Crit Care Med 172, 892–898.

Speert DP (2002). Molecular epidemiology of *Pseudomonas aeruginosa*. Front Biosci 1;7:e354-61. Review.

Spencer JL, Stone PJ and Nugent MA (2006). New insights into the inhibition of human neutrophil elastase by heparin. Biochemistry 45, 9104–9120.

Starkey M, Hickman JA, Ma L et al. (2009). *Pseudomonas aeruginosa* Rugose Small-Colony Variants Have Adaptations That Likely Promote Persistence in the Cystic Fibrosis Lung. J Bacteriol 191: 3492–3503.

Stoltz DA, Meyerholz DK and Welsh MJ (2015). Origins of cystic fibrosis lung disease. N Engl J Med **372**, 351-362.

Stover CK, Pham XQ, et al. (2000). Complete genome sequence of *Pseudomonas aeruginosa* PAO1, an opportunistic pathogen. Nature 406(6799):959-64.

Suh SJ, Silo-Suh L, et al. (1999). Effect of rpoS mutation on the stress response and expression of virulence factors in *Pseudomonas aeruginosa*. J Bacteriol 181: 3890–3897.

Suki B, Ito S, et al. (2005). Biomechanics of the lung parenchyma: critical roles of collagen and mechanical forces. J Appl Physiol 98, 1892–1899.

Taggart CC, Greene CM, McElvaney NG and O'Neill S (2002). Secretory leucoprotease inhibitor prevents lipopolysaccharide-induced IkappaBalpha degradation without affecting phosphorylation or ubiquitination. J Biol Chem 277(37): 33648-53.

Taggart CC, Cryan SA, et al. (2005). Secretory leucoprotease inhibitor binds to NF-kappaB binding sites in monocytes and inhibits p65 binding. J Exp Med 202(12): 1659-68.

Taniguchi H, Ebina M, Kondoh Y, et al (2010). Pirfenidone in idiopathic pulmonary fi brosis. Eur Respir J 35: 821–29.

Tepper MA, Zurier RB and Burstein SH (2014). Ultrapure ajulemic acid has improved CB2 selectivity with reduced CB1 activity. Bioorg Med Chem 22(13):3245-51.

Thomas SR, Ray A, Hodson ME et al. (2000). Increased sputum amino acid concentrations and auxotrophy of *Pseudomonas aeruginosa* in severe cystic fibrosis lung disease. Thorax 55: 795–797.

Tian Y, Gebitekin C, et al. (1995). Influence of heparin thromboprophylaxis on plasma leucocyte elastase levels following lobectomy for lung carcinoma. Blood Coagul Fibrinolysis 6, 527–530.

Tirouvanziam R (2006). Neutrophilic inflammation as a major determinant in the progression of cystic fibrosis. Drug News Perspect 19(10): 609-14.

Tiringer K, Treis A, et al. (2013). A Th17- and Th2-skewed cytokine profile in cystic fibrosis lungs represents a potential risk factor for *Pseudomonas aeruginosa* infection. Am J Respir Crit Care Med 187(6):621–9.

Trevani AS, Chorny A, et al. (2003). Bacterial DNA activates human neutrophils by a CpG-independent pathway. Eur J Immunol 33(11):3164–74.

Tschernig T, Boeke K, et al. (1997). The lung as a source and a target organ for T- and B-lymphocytes. Am J Respir Cell Mol 17(4):414-21.

Veraldi N, Hughes AJ, et al. (2015). Heparin derivatives for the targeting of multiple activities in the inflammatory response. Carbohydr Polym 117:400-7.

Volpi N (1996). Inhibition of human leukocyte elastase activity by heparins: influence of charge density. Biochim Biophys Acta 1290, 299–307.

Walsh RL, Dillon, TJ, Scicchitano, R and McLennan G (1991). Heparin and heparan sulphate are inhibitors of human leucocyte elastase. Clin. Sci. (Lond.) 81, 341–346.

Wadström T and Ljungh A (1999). Glycosaminoglycan-binding microbial proteins in tissue adhesion and invasion: key events in microbial pathogenicity. J Med Microbiol 48(3):223-33.

Wadsworth SJ and Sandford AJ (2013). Personalised medicine and asthma diagnostics/management. Curr Allergy Asthma Rep 13(1):118-29.

Wang L, Fuster M et al. (2005). Endothelial heparan sulphate deficiency impairs L-selectin and chemokine mediated neutrophils trafficking during inflammatory response. Nat Immunol 6, 902-910.

Waters V and Smyth A (2015). Cystic fibrosis microbiology: Advances in antimicrobial therapy. J Cyst Fibros 14(5):551-60.

Weathington NM, van Houwelingen AH, et al. (2006). A novel peptide CXCR ligand derived from extracellular matrix degradation during airway inflammation. Nat Med 12(3):317-23.

Wiehlmann L, Wagner G, et al., (2007). Population structure of *Pseudomonas aeruginosa*. P Natl Acad Sci USA 104: 8101–8106.

Winkler M (2003). Role of cytokines and other inflammatory mediators. BJOG 110 (20):118-23.

Winstanley C, O'Brien S and Brockhurst MA (2016). *Pseudomonas aeruginosa* evolutionary adaptation and diversification in cystic fibrosis chronic lung infections. Trends Microbiol 24(5):327-37.

Wood SR, Firoved AM et al. (2007). Nitrosative stress inhibits production of the virulence factor alginate in mucoid *Pseudomonas aeruginosa*. Free Radic Res 41, 208–215.

Woods DE, Schaffer MS, et al. (1986). Phenotypic comparison of *Pseudomonas aeruginosa* strains isolated from a variety of clinical sites. J Clin Microbiol 24: 260–264.

Worlitzsch D, Tarran R, et al. (2002). Effects of reduced mucus oxygen concentration in airway Pseudomonas infections of cystic fibrosis patients. J Clin Invest 109: 317–325.

Wootton SC, Kim DS, et al (2011). Viral infection in acute exacerbation of idiopathic pulmonary fibrosis. Am J Respir Crit Care Med 183: 1698–1702.

Wyatt HA, Dhawan A, et al. (2002). Serum hyaluronic acid concentrations are increased in cystic fibrosis patients with liver disease. Arch Dis Child 86, 190–193.

Ying QL, Kemme M, et al. (1997). Glycosaminoglycans regulate elastase inhibition by oxidized secretory leukoprotease inhibitor. Am J Physiol 272, L533–541.

Yip GW, Smollich M and Götte M (2006). Therapeutic value of glycosaminoglycans in cancer. Mol Cancer Ther 5:2139–2148.

Yonker LM, Cigana C, Hurley BP and Bragonzi A (2015). Host-pathogen interplay in the respiratory environment of cystic fibrosis. J Cyst Fibros 14(4):431-9.

Young E (2008). The anti-inflammatory effects of heparin and related compounds. Thromb Res 122:743–752.

Yu Q and Stamenkovic I (2000). Cell surface-localized matrix metalloproteinase-9 proteolytically activates TGF-beta and promotes tumor invasion and angiogenesis. Genes Dev. ;14(2):163-76.

Zemanick ET, Harris JK, et al., (2013). Inflammation and airway microbiota during cystic fibrosis pulmonary exacerbations. PLoS One 8(4):e62917.

Zhang Q, Illing R, et al. (2012). Bacteria in sputum of stable severe asthma and increased airway wall thickness. Respir Res 18;13:35.

Zimmermann S, Wagner C, et al. (2006). Induction of neutrophil chemotaxis by the quorum-sensing molecule N-(3-oxododecanoyl)-L-homoserine lactone. Infect Immun 74(10):5687–92.

www.nature.com/scientificreports

OPEN

Received: 20 November 2015
Accepted: 19 January 2016
Published: 17 February 2016

Tracking the immunopathological response to *Pseudomonas aeruginosa* during respiratory infections

Cristina Cigana[1,*], Nicola Ivan Lorè[1,*], Camilla Riva[1], Ida De Fino[1], Lorenza Spagnuolo[1], Barbara Sipione[1], Giacomo Rossi[2], Alessandro Nonis[3], Giulio Cabrini[4] & Alessandra Bragonzi[1]

Repeated cycles of infections, caused mainly by *Pseudomonas aeruginosa*, combined with a robust host immune response and tissue injury, determine the course and outcome of cystic fibrosis (CF) lung disease. As the disease progresses, *P. aeruginosa* adapts to the host modifying dramatically its phenotype; however, it remains unclear whether and how bacterial adaptive variants and their persistence influence the pathogenesis and disease development. Using *in vitro* and murine models of infection, we showed that *P. aeruginosa* CF-adaptive variants shaped the innate immune response favoring their persistence. Next, we refined a murine model of chronic pneumonia extending *P. aeruginosa* infection up to three months. In this model, including CFTR-deficient mice, we unveil that the *P. aeruginosa* persistence lead to CF hallmarks of airway remodelling and fibrosis, including epithelial hyperplasia and structure degeneration, goblet cell metaplasia, collagen deposition, elastin degradation and several additional markers of tissue damage. This murine model of *P. aeruginosa* chronic infection, reproducing CF lung pathology, will be instrumental to identify novel molecular targets and test newly tailored molecules inhibiting chronic inflammation and tissue damage processes in pre-clinical studies.

The genetic defect underlying cystic fibrosis (CF) disrupts lung function by obstruction with thick, sticky secretions which predispose to infections, as those by *Pseudomonas aeruginosa*[1]. Early in life CF lungs are characterized by intermittent airway bacterial infections and excessive neutrophil-dominated inflammation[2]. Later, chronic infection with *P. aeruginosa* fuels a sustained, exuberant inflammatory response that progressively destroys the lungs and ultimately results in respiratory failure. Structural changes in CF lungs include bronchiectasis, airway mucus plugging, microabscesses, peribronchial inflammation, fibrosis -associated with increased levels of metalloproteinases (MMPs)[3–5] and glycosaminoglycans (GAG)[6–8]- and vascular changes, all indicating extensive remodeling that contributes to the lung function decline[9–11].

Long-term chronic infection is carried on by *P. aeruginosa* variants characterized by adaptive traits[12,13]. Indeed the genetic and phenotypic properties of persisting bacterial cells in CF airways differ greatly from those that initiated the infections[12]. The findings that chronic infection in CF patients progresses with bacteria lacking invasive virulence functions open the questions whether: i) *P. aeruginosa* CF-adapted variants live life-long in the lung avoiding host immune response and/or ii) their persistence triggers pathways relevant for tissue remodelling, that finally lead to lung function decline. These issues are difficult to approach in humans due to confounding factors such as the diverse polymicrobial community, unknown environmental factors and host genetic variability.

Several animal models of *P. aeruginosa* infection as well as CF mouse models have been generated[14]. Most of them are focused on modelling the acute phases of the *P. aeruginosa* infection, while others use immobilizing agent such as agar, agarose, or seaweed alginate to monitor certain aspects of the chronic infection in mice[15].

[1]Division of Immunology, Transplantation and Infectious Diseases, IRCCS San Raffaele Scientific Institute, Milano, Italy. [2]School of Biosciences and Veterinary Medicine, University of Camerino, Italy. [3]University Center for Statistics in the Biomedical Sciences (CUSSB), Vita-Salute San Raffaele University, Milan, Italy. [4]Department of Pathology and Diagnostics, University Hospital, Verona, Italy. *These authors contributed equally to this work. Correspondence and requests for materials should be addressed to C.C. (email: cigana.cristina@hsr.it) or A.B. (email: bragonzi.alessandra@hsr.it)

However, at the time of this writing no experimental studies have managed to model the advanced-stage of lung pathology that strictly mimics human CF infection[14]. Pulmonary damage, remodeling and fibrosis are more difficult to be reproduced. While these pathological traits of human disease can be induced by causative agents (e.g. bleomycin), they have not been reproduced following bacterial pneumonia in mice. As a consequence, the cascade of events mediated by *P. aeruginosa* persistence in the pathogenesis of chronic airways infection has been difficult to address.

Using models of infection, we demonstrated that *P. aeruginosa* CF-adapted isolates shape innate immunity to favor their persistence. Remarkably, we succeeded in reproducing the advanced stage of chronic infection lasting for three months with stable bacterial load and traits of the CF human airway disease in mice, including airway remodeling and damage.

Results

P. aeruginosa CF-adapted variants shape the host immune response during the progression of infection. To track the host response with *P. aeruginosa* variants, acute (planktonic bacteria) and chronic (agar-bead embedded bacteria) infections were established in C57BL/6NCrlBR mice with CF-adapted AA43 and AA44 in comparison with AA2 clonal isolate. In particular, AA43 and AA44 were, respectively, mucoid and non-mucoid variants with adaptive phenotypes, including absence of swimming motility, low twitching motility and production of protease, while AA2 expressed a wide series of virulence factors including swimming motility, twitching motility and protease secretion (Fig. S1)[16,17]. AA2 either disseminated systemically and induced death or was cleared by the host in both acute[17] and chronic murine models of lung infection confirming previous data[16] (Fig. 1A,B). Planktonic bacteria of AA43 and AA44 CF-adapted variants were cleared after acute infection[17], while bacteria embedded in agar-beads retained their capacity to persist in murine lungs. Here, chronic colonization was extended up to three months with bacterial loads stabilizing at $\approx 10^4$ colony forming units (CFU)/lung. Thus, the susceptibility to *P. aeruginosa* chronic infection is isolate-dependent in our murine model.

Immunofluorescent staining for *P. aeruginosa* and Haematoxylin and Eosin (H&E) on day 2 localized the infection to bronchial lumens in the agar-beads (Fig. 1C). In the initial phases, infection with the AA43 and AA44 CF-adapted variants yielded lower recruitment of innate immune cells, including neutrophil and macrophage (Fig. 2A,B), and less MIP-2, KC, MIP-1α, IL-6, MCP-1 and TNF-α cytokines/chemokines production than AA2 (Fig. 3A–F). After 28 and 90 days, the persistent AA43 and AA44 CF-adapted variants, irrespective of mucoid phenotype, were localized as macrocolonies in the beads remaining in the bronchial lumen and in biofilm-like structures (Fig. 1C). At this stage, cytokines/chemokines decreased further, but were still detectable in mice retaining infection with AA43 and AA44 isolates (Fig. 3A–F). The persistence of CF-adapted variants promoted an adaptive immune response characterized also by the formation of bronchus-associated lymphoid tissue (BALT)-like structures (Fig. 2A,C,D). Overall, *P. aeruginosa* variants with CF-adapted phenotype determine a weakening of the innate immune recognition and a shift in the immune response during the course of airway diseases.

Differential cell host response to _P. aeruginosa_ phenotypic variants. Next, we conducted *in vitro* analysis to exclude the confounding variables (e.g. different bacterial load) during the course of the infection that cannot be controlled in mouse models. Thus, RNA macroarray analysis[18] of human IB3-1 cells infected with AA2 and CF-adapted AA43 and AA44 variants was performed to investigate the host response mediated by bronchial epithelial cell models widely investigated in CF inflammation. We identified a total of 20 genes whose transcription was changed more than 2-fold in cells infected with different *P. aeruginosa* variants but with equal bacterial load (Fig. 4A, Table S1). Only five genes were up-regulated after infection with the AA43 and AA44 CF-adapted variants in respect to AA2 infection, while the majority (15 out of 20) were down-regulated, including several chemokines and cytokines and their receptors (TNF-α, Gro-β and γ, IP-10, IL-8, FPR2, CCR6, CCR7, CCR9), and adhesion molecules involved in the process of leukocytes extravasation and recruitment (VCAM-1 and ICAM-1). In addition, although AA2 isolate induced higher expression of elastase 2, liable for collagen-IV and elastin proteolysis, AA43 and AA44 induced much higher expression of the matrix metalloprotease 9 (MMP-9), suggesting a contribution of *P. aeruginosa* CF-adapted variants in matrix degradation. Validation of results by real time PCR and/or ELISA for selected targets (IL-8, TNF-α, IP-10, VCAM-1, ICAM-1, Gro-β, MMP-9) has been carried out in different cell types (IB3-1, C38 and THP-1) (Fig. 4B–I).

Next, we extended our investigation to additional *P. aeruginosa* CF-adaptive variants (Fig. 4B–H). Selection was based on previous characterization: KK71 and KK72 showed phenotypic traits of CF-adaptation absent in KK1 and KK2 clonal variants (Fig. S1)[16,17]. Results confirmed the lower pro-inflammatory potential of CF-adapted KK71 and KK72 in comparison with KK1 and KK2 variants. Overall, these results unravel that *P. aeruginosa* CF-adapted variants rewrite the host response in CF bronchial epithelial cell lines and in particular attenuate the expression of a set of genes involved in inflammation, confirming our hypothesis with additional *P. aeruginosa* variants.

P. aeruginosa persistence promotes airway tissue damage in mice that mirrors human CF pathology. Next, we investigated whether and to what extent chronic persistence by *P. aeruginosa* CF-adapted variants recapitulates human CF lung disease (Fig. 5). Mice, retaining infection with AA43 and AA44 CF-adapted variants for one month, displayed hallmarks of CF chronic lung pathology: intraluminal and peribronchial inflammation, epithelial hyperplasia and structure degeneration, goblet cell metaplasia, collagen deposition and elastin degradation (Fig. 5A–C). Biochemical markers of tissue damage in CF disease such as MMP-9 activity and protein, TGF-β_1 protein and sulphated GAG (sGAG) increased progressively during

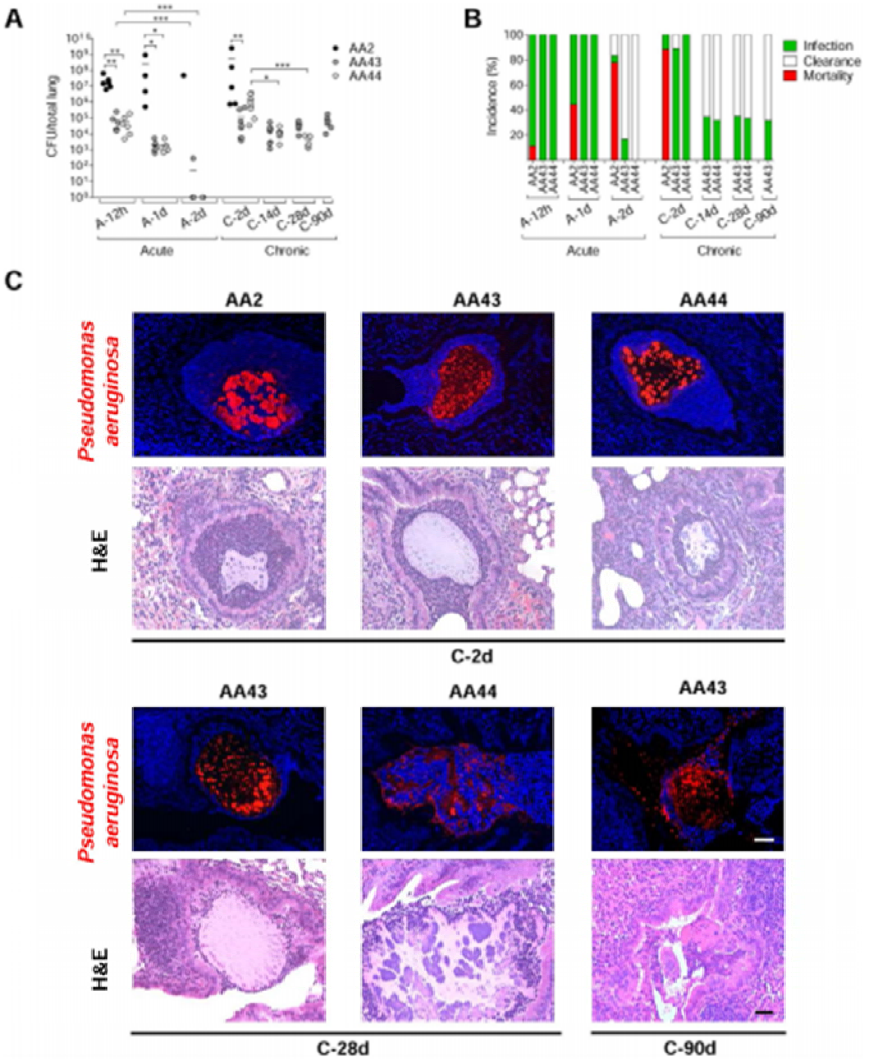

Figure 1. Virulence of *P. aeruginosa* isolates and bacterial localization in murine models of airways infection. Two groups of minimum five C57Bl/6NCrlBR mice were infected with 5×10^6 CFU/lung of planktonic bacteria for the acute infection (data modified from Fig. 5P included in Lorè NI *et al.* PLoS One 2012;7(4):e35648.) and with 1 to 2×10^6 CFU/lung of isolates embedded in agar beads for the chronic infection and analyzed during a time course post-infection (12 hours, 1 and 2 days of acute infection and 2, 14, 28 and 90 days of chronic lung infection). **(A)** CFUs were evaluated in total lung. Dots represent CFUs in individual mice and horizontal lines represent median values. The data are pooled from at least two independent experiments ($n = 1–9$). Statistical significance is indicated: $^*p < 0.05$, $^{**}p < 0.01$, $^{***}p < 0.001$. **(B)** The incidences of mortality induced by bacteremia (red), clearance (white) and airway infection (green) were determined. The data are pooled from at least two independent experiments ($n = 8–24$). **(C)** Bacterial and agar-beads localization in the lung were evaluated on challenged mice by immunofluorescence (with specific antibody against *P. aeruginosa*, stained in red, and with 4,6-Diamidino-2-phenylindole dihydrochloride, stained in blue) and H&E staining. Scale bar: 25μm.

long-term infection with AA43 and AA44 CF-adapted variants (Fig. 6A–F). So for the first time, the above described mouse model of long-term airway chronic infection established with *P. aeruginosa* CF-adapted variants reproduced several traits of human CF lung pathology.

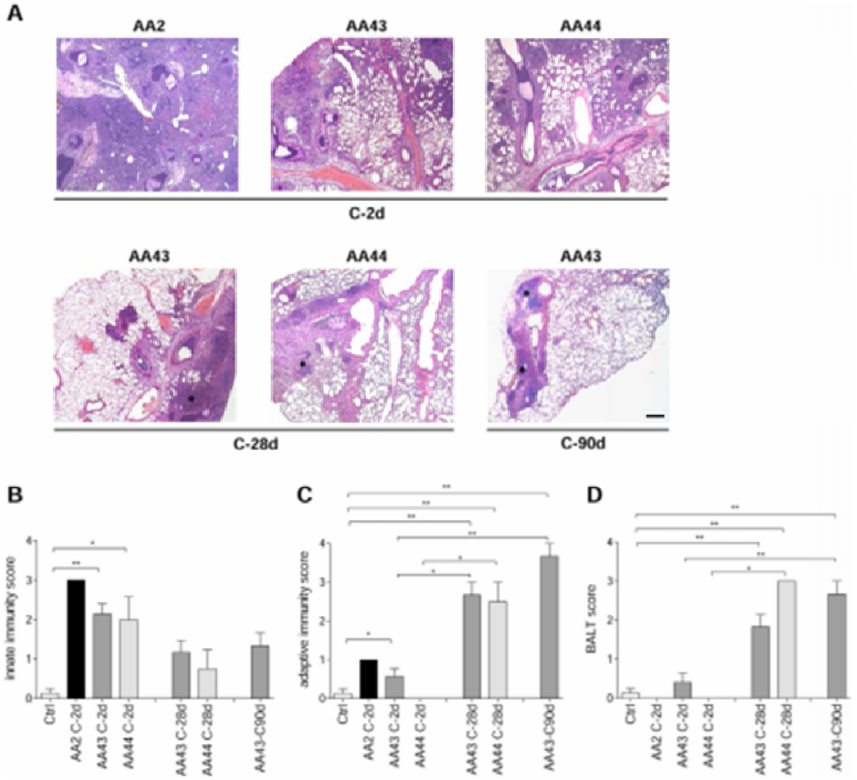

Figure 2. Lung histology and histopathological score of immune cells recruitment in the murine model of *P. aeruginosa* chronic airways infection. C57Bl/6NCrlBR mice were infected with 1 to 2 × 10^6 CFU/lung of isolates embedded in agar beads for the chronic infection and analyzed during a time course post-infection (2, 28 and 90 days). (**A**) Lung histopathology was performed on challenged mice by H&E staining. Scale bars: 200 µm. BALT-like structures are indicated by asterisks. Innate (**B**) and adaptive (**C**) immune cells infiltration and BALT activation (**D**) were scored in tissue section of murine lungs stained with H&E. The data are pooled from at least two independent experiments (n = 2–7). Values represent the mean ± standard error of the mean (SEM). Statistical significance is indicated: $^*p < 0.05$, $^{**}p < 0.01$.

Taking into consideration the emerging relevance of MMPs to pulmonary remodelling and impaired lung function in CF patients[6,13,20], and MMP-9 activation in our chronic infection model and cell culture, we investigated host response to chronic infection by AA43 CF-adapted isolate in MMP-9 deficient mice. Lower collagen levels were found in *Mmp-9*$^{-/-}$ mice compared to the isogenic counterpart (Fig. 6G) while no differences in terms of bacterial load, inflammatory cells recruitment, sGAG and TGF-β_1 after one month were recorded (Fig. S2). These findings suggest a role of MMP-9 in the process of collagen deposition during *P. aeruginosa* chronic persistence.

Contribution of CFTR-deficiency to the pathogenesis of *P. aeruginosa* infection. To determine whether the CFTR-deficiency could exacerbate the inflammatory response or tissue damage after chronic *P. aeruginosa* infection, we infected gut-corrected CFTR-deficient [C57Bl/6 Cftr^{tm1UNC}TgN(FABPCFTR)#Jaw] and their congenic wt mice with the AA43 CF-adapted variant. The percentage of *P. aeruginosa* infection and bacterial load were similar between CF and wt mice, revealing the capacity of *P. aeruginosa* AA43 CF-adapted isolate to persist in murine lungs regardless of the CF genetic background (Fig. 7A,B). However, at the early time point the inflammatory response following *P. aeruginosa* infection in the bronchoalveolar lavage fluid (BALF) was higher in CF mice, in terms of total cells, neutrophils, macrophages and MIP-2 levels, compared to wt mice (Fig. 7C–F). KC, MIP-1α, IL-6, MCP-1 and TNF-α in BALF were similar between CF and isogenic wt mice (Fig. 7G–K). The chronic BALF response was similar in CF and wt animals. In the lung homogenate, the levels of all of the above-mentioned chemokines/cytokines were similar between CF and wt mice at both the early and late chronic time points. At an advanced stage of chronic infection, CF and wt mice differed in terms of goblet cell metaplasia. Histology and pathological scores revealed a higher number of goblet cells in the lung tissue of CF

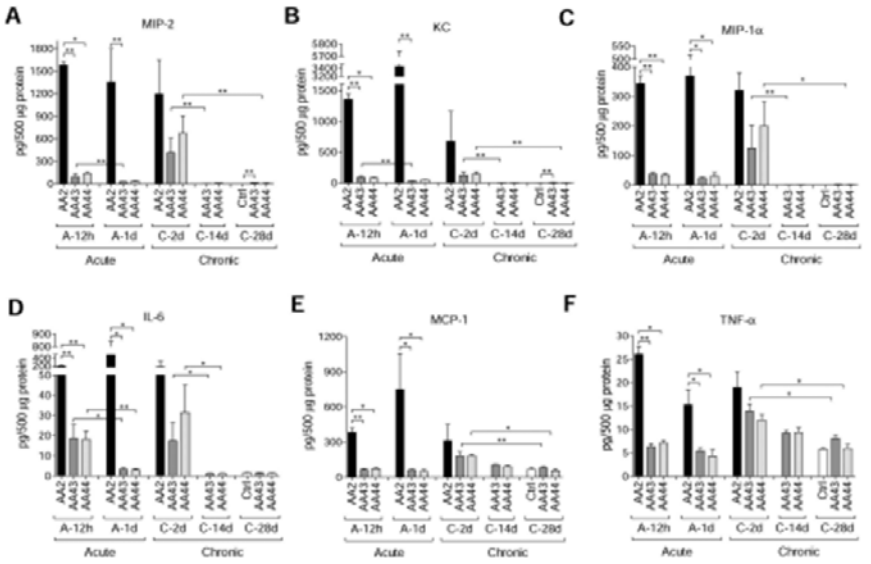

Figure 3. Cytokines/chemokines profiles in murine models after *P. aeruginosa* infection. C57Bl/6NCrlBR mice were infected with 5×10^6 CFU/lung of planktonic bacteria for the acute infection or 1 to 2×10^6 CFU/lung of strains embedded in agar beads for the chronic infection and analyzed during a time course post-infection (12 hours and 1 day of acute infection and 2, 14 and 28 days of chronic lung infection). Cytokines and chemokines, including MIP-2 (**A**), KC (**B**), MIP-1α (**C**), IL-6 (**D**), MCP-1 (**E**) and TNF-α (**F**), were measured by Bioplex in lung homogenates. The data are pooled from at least two independent experiments (n = 3–6). Values represent the mean ± SEM. Statistical significance is indicated: $^*P < 0.05$, $^{**}P < 0.01$.

mice compared to wt, indicating greater mucus production (Figs 7L and S3A). Other markers of tissue damage, such as collagen deposition, elastin degradation, MMP-9 activity, sGAG and TGF-β_1, were similarly increased in CF and wt mice (Fig. S3B–F). Furthermore, no differences were detected in recruitment of innate and adaptive immune cells, and BALT formation (data not shown). Overall, these data indicate that, in mice, alteration of the immune response and subsequent tissue remodeling during *P. aeruginosa* chronic infection are mostly independent of the presence of functional CFTR.

Discussion

Current debates on CF pathogenesis recognize that multifactorial variables contribute to the outcome of lung disease; these include host factors and the bacterial pathogenic potential[21,22]. Dissection of these factors and their causal associations in humans are complicated by confounding variables that cannot be controlled individually. Here, using well established *in vitro* and *in vivo* models of infection we demonstrated that *P. aeruginosa* CF-adapted variants shape the innate immune response to favor their persistence. However, the previous lack of a suitable animal model of long-term chronic infection has limited understanding of the consequence of *P. aeruginosa* persistence on host response. In this study, we refined the agar-beads mouse model approaching the advanced stage of chronic pneumonia. This model was instrumental in demonstrating the contribution of *P. aeruginosa* long-term persistence in activating relevant pathways for tissue remodeling and damage. Surprisingly, *P. aeruginosa* persistence had a greater effect on inflammation and damage profile rather than the *Cftr* mutation itself. These findings have real importance to understanding CF airways disease pathogenesis and progression.

For this study, we used *P. aeruginosa* isolates sampled at the onset of infection and after years of chronic colonization; they were selected for their diversity determined in previous characterization[16,17,23]. The *P. aeruginosa* CF-adapted isolates were genetically characterized by genome rearrangements, mutations, and variations in pathogenic islands, and phenotypically by altered motility, mucoidy, and changes in virulence factors. Thus, the selected *P. aeruginosa* isolates display features commonly associated with bacterial adaptation to CF lung[12,13,16]. When we investigated *P. aeruginosa*/host interaction in mice, the *P. aeruginosa* isolate equipped with virulence factors either disseminated systemically resulting in death or was cleared by a strong host inflammatory response, while CF-adapted variants diminished the innate immune response to allow long-term persistence. Indeed, by measuring cytokines/chemokines at acute/early phases of infection, we found lower pro-inflammatory response induced by *P. aeruginosa* adapted variants. One factor of major interest was that the host response of *P. aeruginosa* adapted variants did not appear to be dependent only on a particular bacterial phenotype or clonal variants. Different *P. aeruginosa* patho-adaptive variants (e.g. mucoid and a non-mucoid) or belonging to different patients, showed a similar capacity to shape the host immune response.

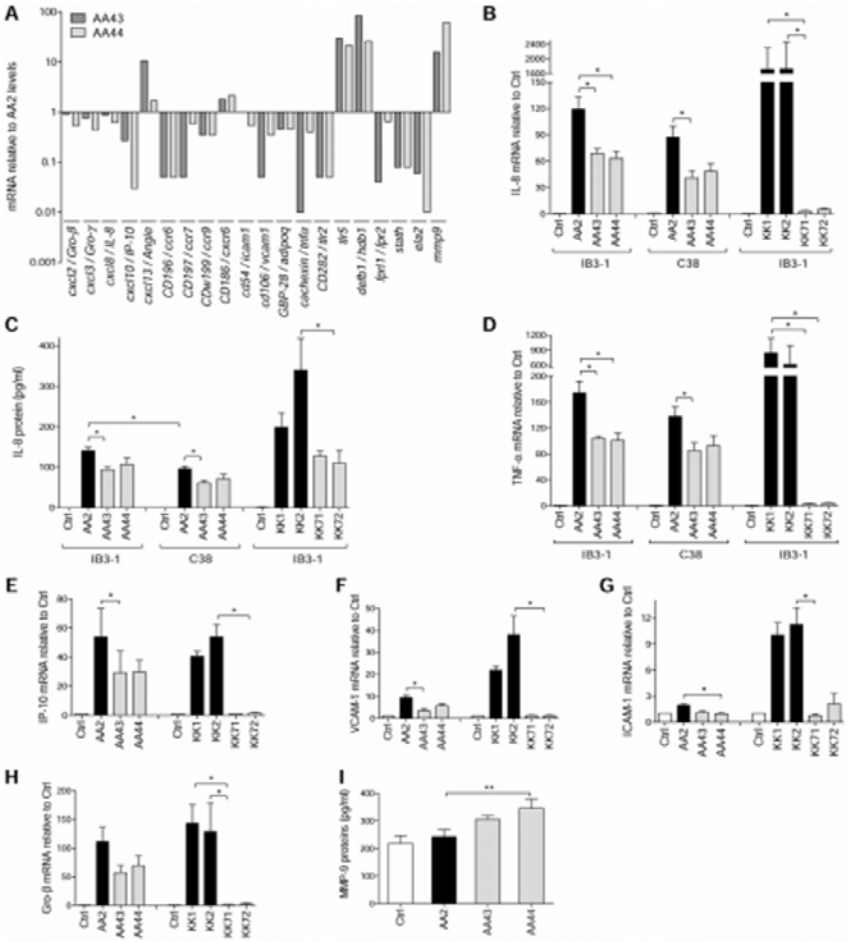

Figure 4. Expression/release of markers of inflammation and tissue damage in cell lines after infection with *P. aeruginosa* phenotypic variants. Bronchial epithelial CF cells IB3-1 were infected for 4 hours with *P. aeruginosa* AA2-AA43-AA44 isolates, RNA extracted and retrotranscribed, and macroarray conducted. (**A**) Genes expression is expressed after normalization on expression induced by AA2. Validation of gene expression was performed by real time PCR in IB3-1 (**B**,**D**–**H**) and isogenic non-CF cells C38 (**B**,**D**) after infection with AA2, AA43, AA44, KK1, KK2, KK71 and KK72. (**C**) Validation of IL-8 protein release was performed by ELISA in culture medium of IB3-1 and C38 after infection with isolates mentioned above. (**I**) Macrophagic-like cells THP-1 were infected for with *P. aeruginosa* AA2, AA43 and AA44 isolates (MOI 1), and MMP-9 release was measured in the culture supernatants by ELISA. Values represent the mean ± SEM. The data are pooled from at least three independent experiments. Statistical significance is indicated: $^{*}p < 0.05$, $^{**}p < 0.01$.

Although mice deficient for *Cftr*[24], or overexpressing the β-ENaC channel[25], have been available for many years, these models do not completely mimic the advanced human pathology[26–29]. Infection of CF mice with *P. aeruginosa* has been performed and resulted in a heightened inflammatory response[30], but high mortality or resolution of the infection have typically limited pathogen persistence for long time. Lung pathology in β-ENaC mice reflects undeniably several hallmarks of CF airways disease, including mucus hyperproduction, goblet cells metaplasia, neutrophilic inflammation and poor bacterial clearance[31,32]. However, they do not reproduce spontaneously the advanced stage of CF lung disease, including chronic *P. aeruginosa* infection, the development of the adaptive immune response and a considerable tissue damage (e.g. elastin degradation and collagen deposition). Models of chronic infections have been described but, at the time of writing, no experimental studies have managed to achieve the progressive advanced-stage of lung pathology induced by chronic bacterial colonization that

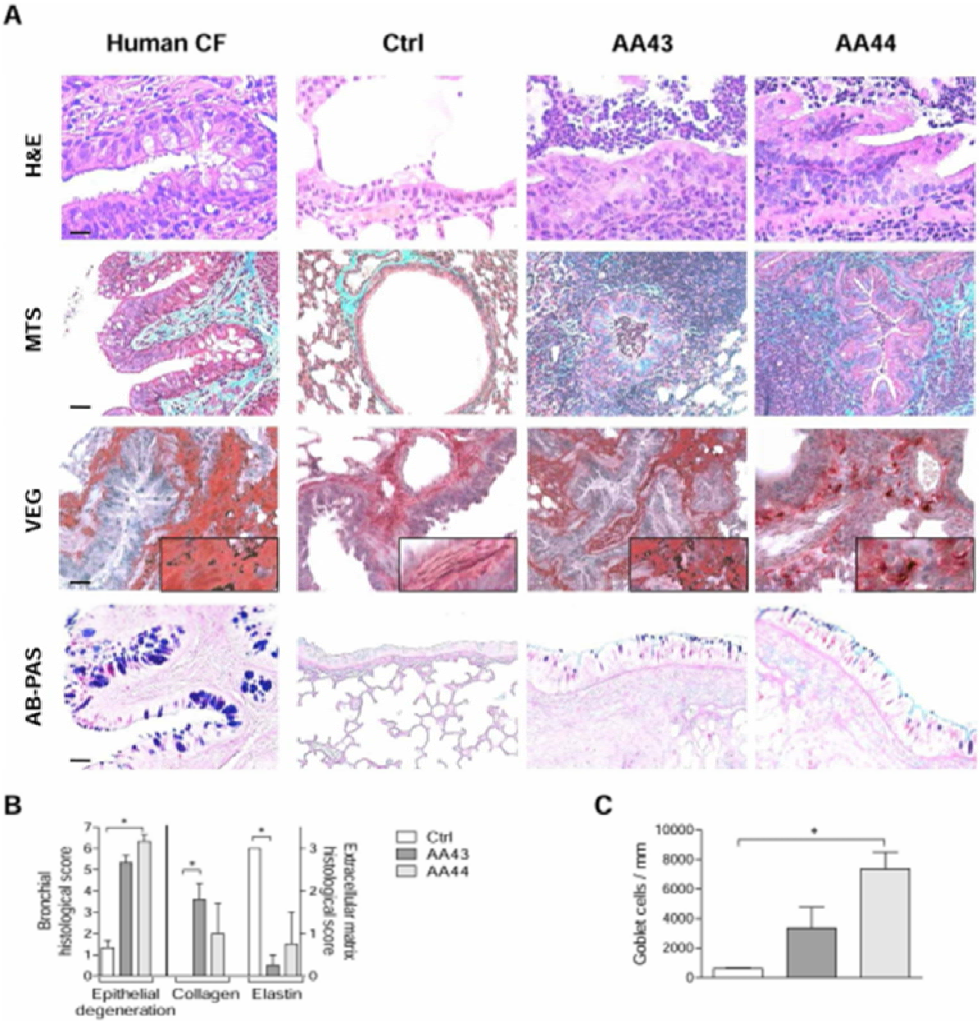

Figure 5. Lung histology and histopathological score of tissue damage in murine lung after infection with *P. aeruginosa*. C57Bl/6NCrlBR mice were infected with 1 to 2×10^6 CFU/lung of isolates embedded in agar beads and analyzed 28 days post-infection. Sections of air ways from transplanted CF patients and from C57Bl/6NCrlBR infected with CF-adapted isolates AA43 and AA44 and sterile beads were stained with H&E, MTS for collagen, VEG for elastic fibers and AB/PAS for mucopolysaccarides, according to the standard procedures (**A**). Scale bars: 12.5 µm for H&E, 25 µm for MTS, VEG and AB-PAS. Scorings of bronchial epithelial degeneration, collagen deposition and elastin degradation (**B**) were performed on slices stained with H&E, MTS and VEG, respectively. Goblet cells numbers were evaluated on slices stained with AB-PAS (**C**). The data are pooled from at least two independent experiments ($n = 2$–6). Values represent the mean ± SEM. Statistical significance is indicated: $^*p < 0.05$.

strictly mimics human CF infection (e.g., chronic Pseudomonal endobronchitis). Although models of long-term chronic infection have been described and are undeniably useful to study several features of CF lung disease including *P. aeruginosa* evolution or chronic inflammation, they show some weaknesses, such as the absence of a stable bacterial load over the course of the infection or the use of mechanical devices as catheters that render, the model not-physiological[33,34]. The previous lack of an accessible CF animal model has limited not only a satisfactory evaluation of the host adaptive immune response, but also the understanding of tissue damage and remodeling processes observed during chronic pneumonia, as described in CF disease[3,35]. We successfully reproduced the long-term chronic infection with stable bacterial titers up to three months and the presence of bacteria in

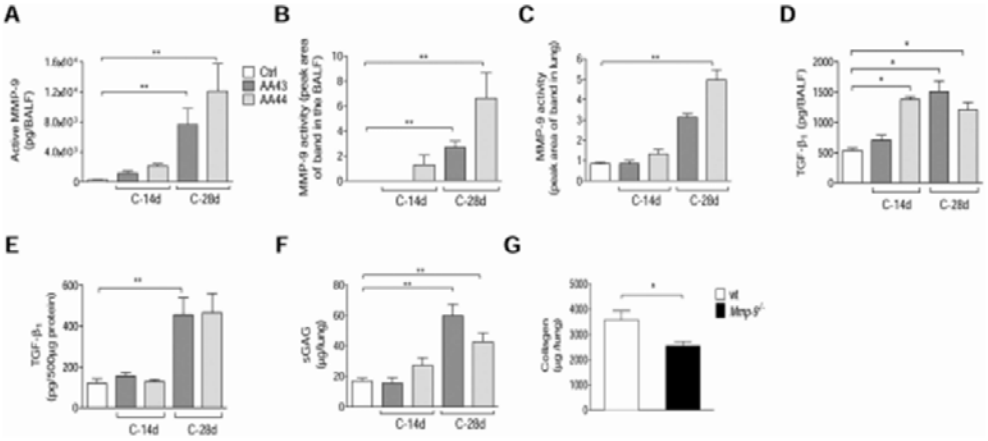

Figure 6. Tissue damage markers, including MMP-9, in murine models after *P. aeruginosa* infection. C57Bl/6NCrlBR mice were infected with 1 to 2×10^6 CFU/lung of CF-adapted isolates embedded in agar beads for 14 and 28 days. Levels of MMP-9 protein (**A**) in BALF by ELISA, MMP-9 activity (**B**) in BALF and (**C**) lung homogenate by zymography, TGF-β_1 (**D**) in BALF and (**E**) lung homogenate by Bioplex and sGAG (**F**) in lung homogenate by a dye-binding colorimetric assay were measured after 14 and 28 days of chronic lung infection. Values represent the mean ± SEM. The data are pooled from at least two independent experiments (n = 3–12). **G)** B6.FVB(Cg)-Mmp9tm1Tvu/J and congenic mice were infected with 2×10^6 CFU/lung of AA43 strain embedded in agar beads. Collagen levels were evaluated by a dye-binding assay in lung homogenate after 28 days of chronic lung infection with the *P. aeruginosa* CF-adapted isolate AA43. Values are represented as mean ± SEM. The data derive from one experiment (n = 6–7). Statistical significance is indicated: * $p < 0.05$, ** $p < 0.01$.

biofilm-like structures. In this model, a long-term consequence of *P. aeruginosa* chronic infection is the formation of BALT-like structures. Moreover, the degeneration of the epithelial structure, collagen deposition, elastin degradation, increased factors associated with matrix remodeling (MMP-9 activity, sGAG and TGF-β_1) and goblet cell metaplasia were also observed in murine airways. This immunopathology is notably similar to the clinical descriptions of human CF lung disease, mirroring chronic Pseudomonal endobronchitis of the CF population.

In our CF mouse model, we found that the CFTR deficiency was associated with a higher inflammatory response to *P. aeruginosa* at the early phases of infection which is in agreement with previous observations[15]. When we extended the infection to the advanced stage, tissue remodeling and damage were partially independent of the *Cftr* murine background. Interestingly, our data showed that pathological traits developed similarly in both wt and CF mice, with further increase of goblet cell metaplasia in the CF host. In this context, the pro-inflammatory environment of the lung can impair and decrease CFTR function as demonstrated in chronic obstructive pulmonary disease (COPD)[36,37]. Furthermore, recent observations indicate that TGF-β_1 and hypoxic environments down-regulate the expression and activity of CFTR[38,39]. Thus, it could be speculated that chronic inflammatory profile and high levels of TGF-β_1 after long-term *P. aeruginosa* infection in wt mice may undermine CFTR function and dampen the differences between wt and CF mice. Further studies are required to strengthen these hypotheses. Most important, the findings that CFTR function could be impaired by *P. aeruginosa* infection, its virulence factors and the associated-chronic inflammation[40] may further explain the similar pathological events developed independently of the CFTR deficiency in our murine model. Overall our data strongly suggest that *P. aeruginosa* persistence is a key driver of the pathogenesis of CF chronic lung disease. Relevance of these studies may be extended to other chronic endobronchitis including advanced COPD, where some hallmarks observed in CF, such as high inflammation, tissue remodeling and *P. aeruginosa* persistence, have been described[41].

New therapeutic approaches to preserve airway structure and pulmonary function are a clinical need. Taking into consideration the emerging relevance of MMPs to pulmonary remodelling in CF patients[6,19,20] and MMP-9 link to *P. aeruginosa* persistence, observed in this work, we further investigated its role in the pathophysiology of the chronic disease. Results obtained in *Mmp-9*$^{-/-}$ mice demonstrated that this metalloprotease contributes to collagen deposition during *P. aeruginosa* chronic infection, while it does not exert any harmful effect on host defense. In agreement with other recent studies[42], our results may support the exploitation of this target in CF.

In conclusion, our study demonstrates that *P. aeruginosa* CF-adaptive variants shape the host response favoring their persistence within the lung. Furthermore, the *P. aeruginosa* persistence contributes to modulate pathways relevant for airway structural changes, reproducing human pathology in mice. Notably, the mouse model, refined in this study, is an invaluable tool for studying the pathogenesis and progression of infection in CF and other chronic airway diseases (such as advanced COPD) and may be an ideal platform for testing novel therapies. In addition, our findings emphasize that the development of new therapeutic interventions (e.g., drug/

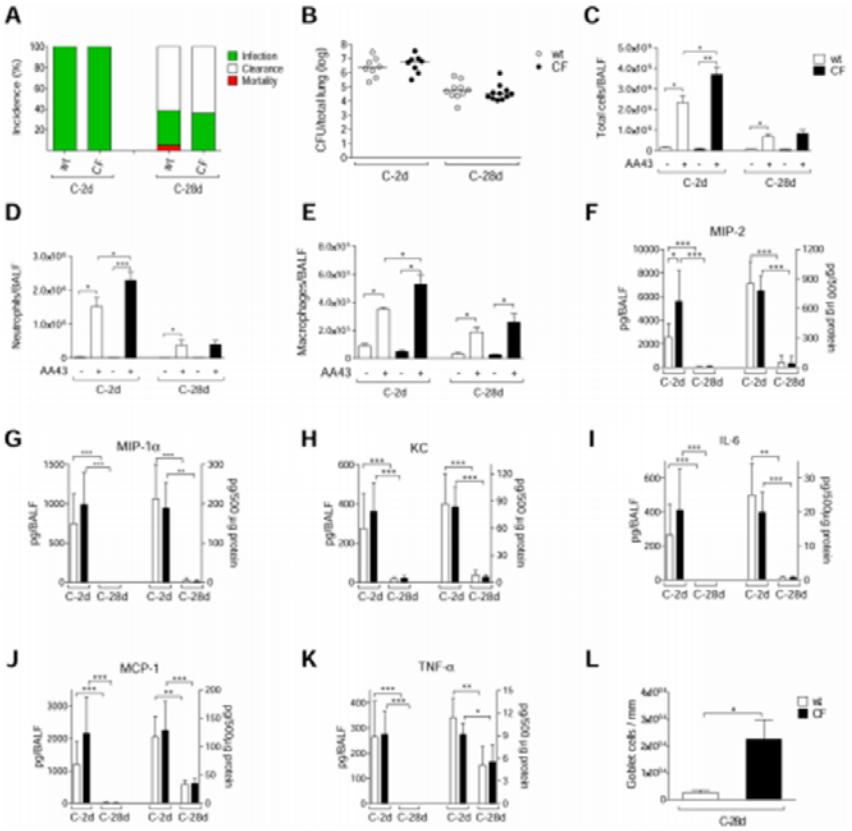

Figure 7. Bacterial virulence and lung inflammatory response in CF and congenic wt mice after *P. aeruginosa* chronic lung infection. Gut-corrected CFTR-deficient C57Bl/6 Cftr^{tm1UNC}TgN(FABPCFTR)#Jaw and congenic wt mice were infected with 2×10^6 CFU/lung of *P. aeruginosa* AA43 strain embedded in agar beads and analyzed after 2 and 28 Days. **A)** The incidences of mortality induced by bacteremia (red), clearance (white) and airway infection (green) were determined. The data are pooled from two independent experiments (n = 8–28). **B)** CFU were evaluated in total lung. Dots represent individual mice measurements and horizontal lines represent the median values reported in a log scale (n = 8–11). The number of total cells (**C**) and in particular of neutrophils (**D**) and macrophages (**E**) in the airways were analyzed in BALF of mice. Cytokines/chemokines, including MIP-2 (**F**), MIP-1α (**G**), KC (**H**), IL-6 (**I**), MCP-1 (**J**) and TNF-α (**K**), were measured by Bioplex in murine BALF (left side of the graph) and lung homogenates (right side of the graph). Sections of murine lungs infected with AA43 for 28 days were stained with AB/PAS for mucopolysaccharides, according to the standard procedure. Goblet cells numbers were evaluated on slices stained with AB-PAS (**L**). Values represent the mean ± SEM. The data are pooled from at least two independent experiments (n = 3–11). Statistical significance is indicated: $^*p < 0.05$, $^{**}p < 0.01$, $^{***}p < 0.001$.

pharmacological) for CF should target tissue remodeling and damage and account for immune changes that manifest in the setting of chronic infection.

Methods

Ethics Statement. Animal studies were conducted according to protocols adhering strictly to the Italian Ministry of Health guidelines for the use and care of experimental animals (IACUC protocols #402 and 502) and approved by the San Raffaele Scientific Institute (Milan, Italy) Institutional Animal Care and Use Committee (IACUC).

The use of human bronchi, obtained from patients undergoing lung transplant, was approved by the Ethical Committee of the Gaslini Institute (Genova, Italy), in accordance with the guidelines of the Italian Ministry of Health. Each patient provided written informed consent to the study using a form that was also approved by the Ethical Committee (approval #13).

Research with the longitudinal bacterial isolates from CF individuals (AA2, AA43, AA44, KK1, KK2, KK71 and KK72), used for *in vitro* and animal experiments, has been approved by the Ethics Commission of Hannover Medical School, Germany. The patients and parents gave informed consent before the sample collection. Approval for storing of biological materials was obtained by the Ethics Commission of Hannover Medical School, Germany.

Bacterial strains. Sequential *P. aeruginosa* isolates from CF patients were chosen from a strain collection, previously characterized for genotypic and phenotypic traits, and virulence[16,17,23]. AA2, KK1 and KK2, expressing virulence factors, were isolated at the onset of chronic infection, while AA43, AA44, KK71 and KK72, showing different adaptive phenotypes, including mucoidy for AA43, were collected after 7 to 13 years after colonization.

Mouse strains. C57Bl/6 (C57Bl/6NCrlBR, Charles River), MMP-9$^{-/-}$ (B6.FVB(Cg)-Mmp9tm1Tvu/J, Jackson Laboratory) and congenic mice (C57Bl/6J, Jackson Laboratory), 8 to 10 weeks old, and CF [gut-corrected CFTR-deficient C57Bl/6 Cftr^{tm1UNC}TgN(FABPCFTR)#Jaw] and congenic wild-type (wt) mice (originally obtained from Case Western Reserve University and maintained at San Raffaele Scientific Institute, Milan, Italy)[43], 11 to 16 weeks old, were maintained in specific pathogen-free conditions.

Mouse model of acute and chronic *P. aeruginosa* infection. Mice were injected intratracheally with 5×10^6 CFU of planktonic *P. aeruginosa* or with $1–2 \times 10^6$ CFU, embedded in agar beads, following established procedures[16,17,44]. The bacterial load was previously set-up as the minimum inoculum to establish chronic infection[45]. BALF and lung were recovered and processed, as previously described[44].

Histological examination. Sections of murine and human lungs for histological analysis were collected and stained by Haematoxylin and Eosin (H&E), Acid Schiff (AB-PAS), Masson's trichrome (MTS), Verhoeff's elastic (VEG) and immunofluorescence (IF) stainings and were examined blindly and scored by a pathologist, as detailed in Supplementary Information.

Cell lines. IB3-1 cells, an adeno-associated virus-transformed human bronchial epithelial cell line derived from a CF patient (ΔF508/W1282X), and C38 cells, the cell line which expresses a plasmid encoding functional CFTR, and non-adherent human myelomonocytic THP1 cells were obtained from LGC Promochem. IB3-1 cells were grown as previously described[17]. *In vitro* infection was performed as described in Supplementary Information.

Macroarray analysis. Macroarray analysis was performed by using TaqMan Low Density Array (TLDA) platform (Applied Biosystems, Foster City, CA), as detailed in Supplementary Information.

Evaluation of Cytokines/chemokines and markers associated to tissue damage. Cytokines/chemokines and growth factors, MMP-9 active levels, sGAG and collagen, and MMP-9 activity were respectively measured by Bioplex, ELISA, colorimetric dye-binding assay and zymography, according to the manufacturer's instructions as detailed in Supplementary Information.

Statistics. Data analysis was performed using a nonparametric two-taled Mann-Whitney U test for single comparison when comparing data induced by a specific strain at two time points during acute infection (e.g. cytokines/chemokines levels) or comparison of data from wt and CF mice at each time-point. To compare data induced by CF-adapted variants to AA2 or Ctrl data at one time-point and data induced by a specific strain across multiple time-points a nonparametric Kruskal-Wallis test was used followed by post-hoc Dunn test to correct for multiple comparisons. Mortality and percentage of infection were compared using Fisher exact test. $P < 0.05$ was considered significant.

References

1. Barinaga, M. Knockout mice offer first animal model for CF. *Science* 257, 1046–1047 (1992).
2. Cohen, T. S. & Prince, A. Cystic fibrosis: a mucosal immunodeficiency syndrome. *Nat Med* 18, 509–519, doi: 10.1038/nm.2715 (2012).
3. Devereux, G. *et al.* An observational study of matrix metalloproteinase (MMP)-9 in cystic fibrosis. *J Cyst Fibros* 13, 557–563, doi: 10.1016/j.jcf.2014.01.010 (2014).
4. Gaggar, A. *et al.* A novel proteolytic cascade generates an extracellular matrix-derived chemoattractant in chronic neutrophilic inflammation. *J Immunol* 180, 5662–5669, doi: 180/8/5662 (2008).
5. Weathington, N. M. *et al.* A novel peptide CXCR ligand derived from extracellular matrix degradation during airway inflammation. *Nat Med* 12, 317–323, doi: nm1361 (2006).
6. Hilliard, T. N. *et al.* Airway remodelling in children with cystic fibrosis. *Thorax* 62, 1074–1080, doi: 10.1136/thx.2006.074641 (2007).
7. Reeves, E. P., Bergin, D. A., Murray, M. A. & McElvaney, N. G. The involvement of glycosaminoglycans in airway disease associated with cystic fibrosis. *ScientificWorldJournal* 11, 959–971, doi: 10.1100/tsw.2011.81 (2011).
8. Solic, N., Wilson, J., Wilson, S. J. & Shute, J. K. Endothelial activation and increased heparan sulfate expression in cystic fibrosis. *Am J Respir Crit Care Med* 172, 892–898, doi: 10.1164/rccm.200409-1207OC (2005).
9. Regamey, N., Jeffery, P. K., Alton, E. W., Bush, A. & Davies, J. C. Airway remodelling and its relationship to inflammation in cystic fibrosis. *Thorax* 66, 624–629, doi: 10.1136/thx.2009.134106 (2011).
10. Hamutcu, R. *et al.* Clinical findings and lung pathology in children with cystic fibrosis. *Am J Respir Crit Care Med* 165, 1172–1175, doi: 10.1164/ajrccm.165.8.2104090 (2002).
11. Harris, W. T. *et al.* Myofibroblast differentiation and enhanced TGF-B signaling in cystic fibrosis lung disease. *PLoS One* 8, e70196, doi: 10.1371/journal.pone.0070196 (2013).
12. Smith, E. E. *et al.* Genetic adaptation by Pseudomonas aeruginosa to the airways of cystic fibrosis patients. *Proc Natl Acad Sci USA* 103, 8487–8492, doi: 10.1073/pnas.0602138103 (2006).
13. Marvig, R. L., Sommer, L. M., Molin, S. & Johansen, H. K. Convergent evolution and adaptation of Pseudomonas aeruginosa within patients with cystic fibrosis. *Nat Genet* 47, 57–64, doi: 10.1038/ng.3148 (2015).

14. Soltz, D. A., Meyerholz, D. K. & Welsh, M. J. Origins of cystic fibrosis lung disease. *N Engl J Med* **372**, 351–362, doi: 10.1056/NEJMra1300109 (2015).
15. Bragonzi, A. Murine models of acute and chronic lung infection with cystic fibrosis pathogens. *Int J Med Microbiol* **300**, 584–593, doi: 10.1016/j.ijmm.2010.08.012 (2010).
16. Bragonzi, A., *et al.* Pseudomonas aeruginosa microevolution during cystic fibrosis lung infection establishes clones with adapted virulence. *Am J Respir Crit Care Med* **180**, 138–145, doi: 10.1164/rccm.200812-1943OC (2009).
17. Lore, N. I. *et al.* Cystic fibrosis-niche adaptation of Pseudomonas aeruginosa reduces virulence in multiple infection hosts. *PLoS One* **7**, e35648, doi: 10.1371/journal.pone.0035648 (2012).
18. Dechecchi, M. C. *et al.* Modulators of sphingolipid metabolism reduce lung inflammation. *Am J Respir Cell Mol Biol* **45**, 825–833, doi: 10.1165/rcmb.2010-0457OC (2011).
19. Sagel, S. D., Kapsner, R. K. & Osberg, I. Induced sputum matrix metalloproteinase-9 correlates with lung function and airway inflammation in children with cystic fibrosis. *Pediatr Pulmonol* **39**, 224–232, doi: 10.1002/ppul.20165 (2005).
20. Gaggar, A. *et al.* Matrix metalloprotease-9 dysregulation in lower airway secretions of cystic fibrosis patients. *Am J Physiol Lung Cell Mol Physiol* **293**, L96–L104, doi: 10.1152/ajplung.00492.2006 (2007).
21. Cigana, C., Lore, N. I., Bernardini, M. L. & Bragonzi, A. Dampening Host Sensing and Avoiding Recognition in Pseudomonas aeruginosa Pneumonia. *Journal of biomedicine & biotechnology* **2011**, 852513, doi: 10.1155/2011/852513 (2011).
22. Guillot, L. *et al.* Lung disease modifier genes in cystic fibrosis. *The international journal of biochemistry & cell biology* **52**, 83–93, doi: 10.1016/j.biocel.2014.02.011 (2014).
23. Cigana, C. *et al.* Pseudomonas aeruginosa exploits lipid A and muropeptides modification as a strategy to lower innate immunity during cystic fibrosis lung infection. *PLoS One* **4**, e8439, doi: 10.1371/journal.pone.0008439 (2009).
24. Snouwaert, J. N. *et al.* An animal model for cystic fibrosis made by gene targeting. *Science* **257**, 1083–1088 (1992).
25. Mall, M., Grubb, B. R., Harkema, J. R., O'Neal, W. K. & Boucher, R. C. Increased airway epithelial Na^+ absorption produces cystic fibrosis-like lung disease in mice. *Nat Med* **10**, 487–493, doi: 10.1038/nm1028 (2004).
26. Kent, G. *et al.* Lung disease in mice with cystic fibrosis. *J Clin Invest* **100**, 3060–3069, doi: 10.1172/JCI119861 (1997).
27. Durie, P. R., Kent, G., Phillips, M. J. & Ackerley, C. A. Characteristic multiorgan pathology of cystic fibrosis in a long-living cystic fibrosis transmembrane regulator knockout murine model. *Am J Pathol* **164**, 1481–1493, doi: 10.1016/S0002-9440(10)63234-8 (2004).
28. Guilbault, C., Saeed, Z., Downey, G. P. & Radzioch, D. Cystic fibrosis mouse models. *Am J Respir Cell Mol Biol* **36**, 1–7, doi: 10.1165/rcmb.2006-0184TR (2007).
29. Wilke, M. *et al.* Mouse models of cystic fibrosis: phenotypic analysis and research applications. *J Cyst Fibros* **10** Suppl 2, S152–171, doi: 10.1016/S1569-1993(11)60020-9 (2011).
30. Heeckeren, A. *et al.* Excessive inflammatory response of cystic fibrosis mice to bronchopulmonary infection with Pseudomonas aeruginosa. *J Clin Invest* **100**, 2810–2815, doi: 10.1172/JCI119828 (1997).
31. Mall, M., Grubb, B. R., Harkema, J. R., O'Neal, W. K. & Boucher, R. C. Increased airway epithelial Na^+ absorption produces cystic fibrosis-like lung disease in mice. *Nat Med* **10**, 487–493, doi: 10.1038/nm1028 (2004).
32. Gehrig, S. *et al.* Lack of neutrophil elastase reduces inflammation, mucus hypersecretion, and emphysema, but not mucus obstruction, in mice with cystic fibrosis-like lung disease. *Am J Respir Crit Care Med* **189**, 1082–1092, doi: 10.1164/rccm.201311-1932OC (2014).
33. Fothergill, J. L., Neill, D. R., Loman, N., Winstanley, C. & Kadioglu, A. Pseudomonas aeruginosa adaptation in the nasopharyngeal reservoir leads to migration and persistence in the lungs. *Nat Commun* **5**, 4780, doi: 10.1038/ncomms5780 (2014).
34. Yanagihara, K. *et al.* Role of elastase in a mouse model of chronic respiratory Pseudomonas aeruginosa infection that mimics diffuse panbronchiolitis. *J Med Microbiol* **52**, 531–535, doi: 10.1099/jmm.0.05154-0 (2003).
35. Zhou, Z. *et al.* The ENaC-overexpressing mouse as a model of cystic fibrosis lung disease. *J Cyst Fibros* **10** Suppl 2, S172–182, doi: 10.1016/S1569-1993(11)60021-0 (2011).
36. Raju, S. V. *et al.* Impact of heterozygote CFTR mutations in COPD patients with chronic bronchitis. *Respir Res* **15**, 18, doi: 10.1186/1465-9921-15-18 (2014).
37. Bodas, M., Min, T., Mazur, S. & Vij, N. Critical modifier role of membrane-cystic fibrosis transmembrane conductance regulator-dependent ceramide signaling in lung injury and emphysema. *J Immunol* **186**, 602–613, doi: 10.4049/jimmunol.1002850 (2011).
38. Sun, H. *et al.* Tgf-beta downregulation of distinct chloride channels in cystic fibrosis-affected epithelia. *PLoS One* **9**, e106842, doi: 10.1371/journal.pone.0106842 (2014).
39. Guimbellot, J. S. *et al.* Role of oxygen availability in CFTR expression and function. *Am J Respir Cell Mol Biol* **39**, 514–521, doi: 10.1165/rcmb.2007-0452OC (2008).
40. Trinh, N. T. *et al.* Deleterious impact of Pseudomonas aeruginosa on cystic fibrosis transmembrane conductance regulator function and rescue in airway epithelial cells. *Eur Respir J* **45**, 1590–1602, doi: 10.1183/09031936.00076214 (2015).
41. Doring, G., Parameswaran, I. G. & Murphy, T. F. Differential adaptation of microbial pathogens to airways of patients with cystic fibrosis and chronic obstructive pulmonary disease. *FEMS Microbiol Rev* **35**, 124–146, doi: 10.1111/j.1574-6976.2010.00237.x (FMR237 (2011).
42. Gaggar, A. *et al.* The role of matrix metalloproteinases in cystic fibrosis lung disease. *Eur Respir J* **38**, 721–727, doi: 10.1183/09031936.00173210 (2011).
43. van Heeckeren, A. M., Schluchter, M. D., Drumm, M. L. & Davis, P. B. Role of Cftr genotype in the response to chronic Pseudomonas aeruginosa lung infection in mice. *Am J Physiol Lung Cell Mol Physiol* **287**, L944–952, doi: 10.1152/ajplung.00387.2003 (2004).
44. Kukavica-Ibrulj, I., Facchini, M., Cigana, C., Levesque, R. C. & Bragonzi, A. Assessing Pseudomonas aeruginosa virulence and host response using murine models of acute and chronic lung infection. *Methods Mol Biol* **1149**, 757–771, doi: 10.1007/978-1-4939-0473-0_58 (2014).
45. Bragonzi, A. *et al.* Nonmucoid Pseudomonas aeruginosa expresses alginate in the lungs of patients with cystic fibrosis and in a mouse model. *J Infect Dis* **192**, 410–419, doi: JID33931 (2005).

Acknowledgements

The authors thank B. Tümmler (Medizinische Hochschule Hannover, Germany) for supplying *P. aeruginosa* clinical strains, L. J. Galietta (Gaslini Institute, Genova, Italy) for bronchial samples from transplanted CF patients, G. B. Pier (Harvard Medical School, Boston, Massachusetts, USA) for *P. aeruginosa* antibody, W. T. Harris (University of Alabama, Birmingham, Alabama, USA) and J. K. Kolls (University of Pittsburgh Medical Center, Pittsburgh, Pennsylvania, USA) for critical review of the manuscript. This study was supported to A. Bragonzi by Ministero della Salute (project GR/2009/1579812) and to C. Cigana by Italian Cystic Fibrosis Research Foundation (FFC# 20/2011 and 14/2013), with the contribution of the Delegazioni FFC di Milano, Bergamo Villa d'Almè, di Sondrio Valchiavenna, di Fermo, Cosenza 2, Amici della Ricerca di Milano, Latteria Montello 70° compleanno nonno Armando, and ESCMID (#19/2012). The funders had no role in study design, data collection and analysis, decision to publish, or preparation of the manuscript.

Author Contributions

C.C., N.I.L. and A.B. conceived and designed the experiments; C.C., N.I.L., C.R., I.D.F., L.S., B.S. and G.R. performed experiments; C.C., N.I.L., C.R., I.D.F., L.S., B.S. and G.R. analyzed data; A.N. performed statistical analysis; C.C. and N.I.L. interpreted the experiments results; C.C. and N.I.L. prepared the figures; C.C., N.I.L., G.C. and A.B. wrote the manuscript. All authors reviewed the manuscript.

Additional Information

Supplementary information accompanies this paper at http://www.nature.com/srep

Competing financial interests: The authors declare no competing financial interests.

How to cite this article: Cigana, C. *et al.* Tracking the immunopathological response to *Pseudomonas aeruginosa* during respiratory infections. *Sci. Rep.* **6**, 21465; doi: 10.1038/srep21465 (2016).

www.nature.com/scientificreports

SCIENTIFIC REPORTS

OPEN

IL-17A impairs host tolerance during airway chronic infection by *Pseudomonas aeruginosa*

Received: 28 January 2016
Accepted: 22 April 2016
Published: xx xx xxxx

Nicola Ivan Lorè[1,*], Cristina Cigana[1,*], Camilla Riva[1], Ida De Fino[1], Alessandro Nonis[1], Lorenza Spagnuolo[1], Barbara Sipione[1], Lisa Cariani[1], Daniela Girelli[1], Giacomo Rossi[1], Veronica Basso[1], Carla Colombo[1], Anna Mondino[1] & Alessandra Bragonzi

Resistance and tolerance mechanisms participate to the interplay between host and pathogens. IL-17-mediated response has been shown to be crucial for host resistance to respiratory infections, whereas its role in host tolerance during chronic airway colonization is still unclear. Here, we investigated whether IL-17-mediated response modulates mechanisms of host tolerance during airways chronic infection by *P. aeruginosa*. First, we found that IL-17A levels were sustained in mice at both early and advanced stages of *P. aeruginosa* chronic infection and confirmed these observations in human respiratory samples from cystic fibrosis patients infected by *P. aeruginosa*. Using *IL-17a*$^{-/-}$ or *IL-17ra*$^{-/-}$ mice, we found that the deficiency of IL-17A/IL-17RA axis was associated with: i) increased incidence of chronic infection and bacterial burden, indicating its role in the host resistance to *P. aeruginosa*; ii) reduced cytokine levels (KC), tissue innate immune cells and markers of tissue damage (pro-MMP-9, elastin degradation, TGF-β_1), proving alteration of host tolerance. Blockade of IL-17A activity by a monoclonal antibody, started when chronic infection is established, did not alter host resistance but increased tolerance. In conclusion, this study identifies IL-17-mediated response as a negative regulator of host tolerance during *P. aeruginosa* chronic airway infection.

Two evolutionarily conserved host defense strategies to narrow disease severity have been described in host-pathogens interplay: resistance aims to contrast and eventually eradicate pathogenic bacteria, whereas tolerance limits the consequences of productive infections[1–3]. Altered mechanisms of resistance and tolerance can contribute to the aberrant inflammatory response during chronic airways diseases. In this context, persistent infections by *Pseudomonas aeruginosa* together with chronic inflammatory responses and progressive tissue damage are all hallmarks of chronic respiratory disease, such as cystic fibrosis (CF) and advanced chronic obstructive pulmonary disease (COPD)[4–6]. The pathophysiological mechanisms that control host resistance and/or tolerance in chronic airways diseases remain to be deciphered.

Interleukin 17A (IL-17A) and IL-17 cytokines family have been suggested to participate to the pathogenesis of several respiratory diseases[7–12]. The IL-17-induced host response contributes to resistance mechanisms by playing a protective role at the mucosal barriers against pathogens such as *Staphylococcus aureus*, *Citrobacter rodentium* or *Klebsiella pneumonia*[13]. Recent data suggest that IL-17 pathway may play a key role in resistance and modulation of the inflammatory response during *P. aeruginosa* acute infection[14–17]. In addition, the IL-17-mediated host response has been shown to increase the secretion of matrix metalloproteinases (MMP)[18], involved in tissue remodeling. All together these evidences suggest that type 17 immunity may be involved in the pathogenesis of chronic respiratory diseases, modulating both host resistance and tolerance.

Clinical proofs support the idea of a role for IL-17 in the pathogenesis of chronic respiratory diseases[12]. Indeed, IL-17 levels are elevated in several inflammatory lung diseases, such as CF and COPD[19,20]. In particular,

[1]Infections and Cystic Fibrosis Unit, Division of Immunology, Transplantation and Infectious Diseases, IRCCS San Raffaele Scientific Institute, Milano, Italy. [2]University Center for Statistics in the Biomedical Sciences (CUSSB), Vita-Salute San Raffaele University, Milano, Italy. [3]Cystic Fibrosis Microbiology Laboratory, Fondazione IRCCS Ca' Granda, Ospedale Maggiore Policlinico, Milano, Italy. [4]School of Biosciences and Veterinary Medicine, University of Camerino, Italy. [5]Cystic Fibrosis Center, Fondazione IRCCS Ca' Granda, Ospedale Maggiore Policlinico, Milano, Italy. [6]Lymphocytes Activation Unit, Division of Immunology, Transplantation and Infectious Diseases, IRCCS San Raffaele Scientific Institute, Milano, Italy. *These authors contributed equally to this work. Correspondence and requests for materials should be addressed to N.I.L. (email: lore.nicolaivan@hsr.it) or A.B. (email: bragonzi.alessandra@hsr.it)

in CF, IL-17 levels have been found to negatively correlate with FEV_1, suggesting its role in the decline of the lung function[21]. Among the potential cellular sources, IL-17 producing $CD4^+$ T cells have been increasingly described in CF[22]. Thus, these data prompt the hypothesis that CF could be a IL-17-mediated disease[11,22,23].

To date, the relative contribution of IL-17 to mechanisms of host resistance and tolerance during advanced chronic airways infections remains to be clarified[12]. Here, we addressed these issues in mice chronically infected for long term and in CF patients infected by *P. aeruginosa*. In the experimental murine model, we found that IL-17A levels were sustained over the course of *P. aeruginosa* chronic infection. In respiratory samples from CF patients, we confirmed that increased IL-17A levels were associated to both early and advanced stages of *P. aeruginosa* infection, strengthening the importance of the IL-17A-mediated response in the overall progression of chronic airways disease. Mechanistically, using *IL-17a*$^{-/-}$ and *IL-17ra*$^{-/-}$ mice, we demonstrated that the IL-17A/IL-17RA axis plays a dual role during chronic infection by *P. aeruginosa*: while it contributes to the host resistance, it weakens host tolerance, promoting immunopathology, during chronic airways infection. Moreover, targeting IL-17A when chronic infection is already established limits immunopathology, without compromising resistance to *P. aeruginosa* respiratory infection. Thus, our results indicate the role of IL-17A in modulating host tolerance during *P. aeruginosa* persistent infections and propose it as a potential target to modulate host tolerance in the context of chronic airways diseases.

Results

Host responses to *P. aeruginosa* during early and advanced chronic infection. While previous mechanistic studies in murine models attributed a role to IL-17 and IL-17 producing cells during acute early phases of *P. aeruginosa* infection[14–16], here we focused on advanced *P. aeruginosa* chronic infection (28 days) in comparison with early acute phase (2 days). We adopted the *P. aeruginosa* AA43 isolate, which can establish chronic infection in C57Bl/6 mice with an incidence of colonization around 30–40%[24,25]. Cytokines typical of the immune response (IL-1β, IL-2, IFN-γ, IL-4, IL-17A) were analyzed at 2 and 28 days after infection. Although the bacterial burdens did not change among the early and advanced phases of infection (Fig. 1A), IL-1β levels significantly differed. IL-1β was acutely induced at day 2. By day 28, IL-1β levels had decreased, despite remaining significantly higher than those found in uninfected mice (Fig. 1B). While IL-4, indicative of type 2 immunity, was almost not detectable, IFN-γ, linked to type 1 immunity, was induced at the early stage and returned at basal levels at day 28 (Fig. 1C). Differently, IL-17A levels increased by day 2 and remained high over the course of *P. aeruginosa* infection (Fig. 1D).

Next, we analysed IL-17A, IFN-γ and IL-4 levels in sputa from patients with CF. The samples were collected from a cohort of 55 clinically stable CF patients recruited during routine care plans (Table S1), regardless of *P. aeruginosa* presence in the microbiological cultures. To evaluate whether IL-17A levels change according to the stage of *P. aeruginosa* infection, we distinguished CF patients into three categories: i) free, ii) "early" (intermittent *P. aeruginosa* infection and chronic colonization for up to two years) iii) "late" (chronic colonization for more than four years). IL-17A levels were significantly increased in both "early" and "late" patients in comparison to free patients (Fig. 1E), showing a similar trend to that observed in mice during *P. aeruginosa* chronic infection. As to IFN-γ and IL-4, their levels did not differ (Fig. 1F,G). Moreover the sera of CF patients colonized by *P. aeruginosa* revealed low or undetectable levels of IL-17A (Table S2), suggesting IL-17A release to be restricted to the lung compartment rather than systemic. Thus, while type 1 and 2 immunities do not seem to participate to the advanced stages of *P. aeruginosa* infection in the lung compartment, IL-17A-mediate response might play a critical role during the advanced stage of chronic infection in both humans and mice.

Type 17 immunity is sustained during *P. aeruginosa* chronic infection. Lung infiltrating cells were further dissected by FACS analysis and immunohistochemistry in murine models. The number of infiltrating leukocytes was significantly higher in samples recovered from infected mice at both day 2 and 28 post-infection when compared to controls (Fig. 2A). While alveolar and interstitial macrophages were not enriched for, both neutrophils and dendritic cells (DC) were accumulated in infected lungs. However, neutrophils counts decreased by day 28, whereas DC numbers remained high at the advanced phase of *P. aeruginosa* chronic infection (Fig. 2B–E). Also T and B cell representations were significantly different in control and infected mice. While T cells, comprising both $CD4^+$ and $CD8^+$ subsets, were significantly enriched for both at day 2 and day 28 and $CD4^+$ subsets further increased at day 28 (Fig. 2F–H), B cell numbers were significantly higher only at the advanced stage of chronic infection (Fig. 2I). This was in agreement with a selective enrichment of $CD4^+$ IL-17A$^+$ T cell, but not of $CD4^+$ IL-4$^+$ and $CD4^+$ IFN-γ$^+$ T cells (Fig. 2J). Differently, $CD8^+$ T cells capable of IFN-γ or IL-17A did not change over the course of chronic *P. aeruginosa* infection (Fig. 2K) and those secreting IL-4 were not detectable. By immunohistochemistry we found that T and B cells co-localized in bronchus-associated lymphoid tissue (BALT)-like structures at day 28 (Fig. 2L), likely indicating an active adaptive immune response in the airways. The distribution of cytokine-secreting $CD4^+$ T cells did not differ in the spleen of infected and not infected mice (Table S3), supporting the existence of tissue-restricted events in *P. aeruginosa*-infected mice. Together these data highlight the potential impact of type 17 immunity in the airways disease progression during *P. aeruginosa* chronic infection.

Depletion of the IL-17A/IL-17RA axis reduces host resistance while favoring tolerance to *P. aeruginosa* infection. To directly establish the role of the IL-17A/IL17-RA axis in host resistance and/or tolerance to *P. aeruginosa* colonization, we infected *IL-17a*$^{-/-}$ and *IL-17ra*$^{-/-}$ in comparison with wt congenic mice. Bacterial burden, inflammation and tissue damage were evaluated at day 28 after infection. *P. aeruginosa* lung infection did not lead to mortality in *IL-17a*$^{-/-}$ and *IL-17ra*$^{-/-}$ mice, similarly to wt mice (data not shown). Higher bacterial load was observed in *IL-17ra*$^{-/-}$ but not in *IL-17a*$^{-/-}$ mice (Fig. 3A). However, the incidence of colonization was increased in both *IL-17a*$^{-/-}$ and *IL-17ra*$^{-/-}$ mice (Fig. 3B). Overall, these results suggest that

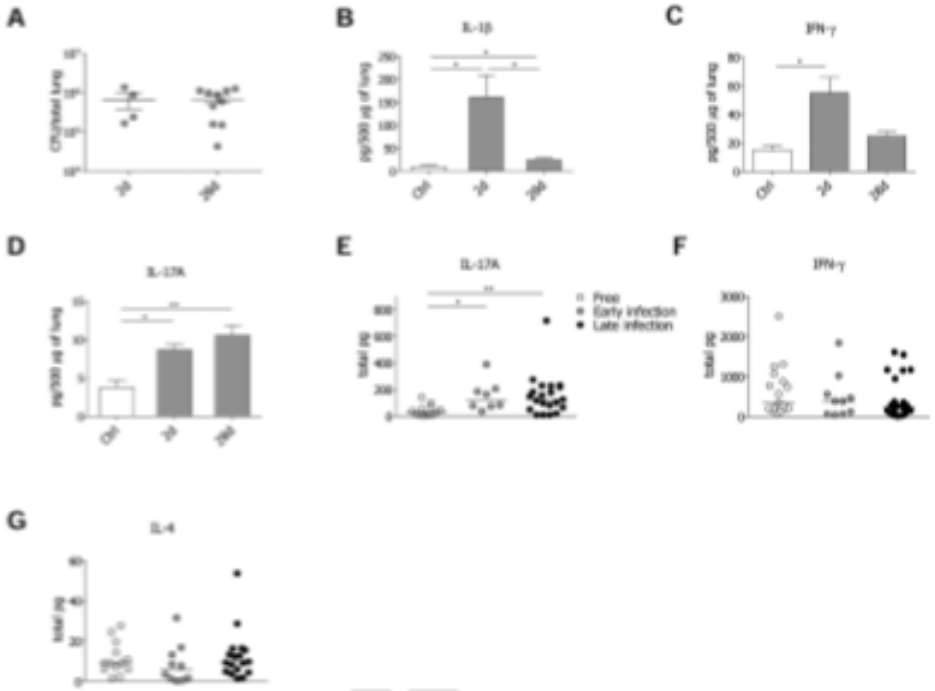

Figure 1. ***P. aeruginosa*** **infection and markers of immune response in the murine model of chronic airways infection and CF patients.** Two groups of minimum five C57Bl/6 mice were infected with 1 to 2×10^6 CFU/lung of the *P. aeruginosa* strain AA43 embedded in agar beads and analyzed after 2 and 28 days of infection. Control (Ctrl) mice were treated with sterile agar-beads. (**A**) CFU were evaluated in total lung. Dots represent CFU in individual mice, horizontal lines represent mean values and the error bars represent the standard error of the mean (SEM). The data are pooled from at least two independent experiments (n = 4–12). Cytokines and chemokines, including IL-1β (**B**), IFN-γ (**C**), and IL-17A (**D**), were measured by Bioplex in murine lung homogenates. The data are pooled from at least two independent experiments (n = 3–9). Values represent the mean ± SEM. Levels of IL-17A (**E**), IFN-γ (**F**) and IL-4 (**G**) in sputa from CF patients never colonized by *P. aeruginosa* (free), with intermittent or chronic colonization up to two years (early) and with chronic colonization for at least four years (late) are compared. Dots represent values in individual patients and horizontal lines represent median values. Statistical significance is indicated: $^*p < 0.05$, $^{**}p < 0.01$, $^{***}p < 0.001$.

host resistance to *P. aeruginosa* infection can be principally ascribed to the IL-17RA downstream signaling, rather than to IL-17A alone.

By studying cytokines/chemokines profile in lung homogenates, we found higher levels of IL-17F in *IL-17a*$^{-/-}$ mice, and of IL-17A in *IL-17ra*$^{-/-}$ mice, likely due to compensatory mechanisms (Fig. 3C,D). In addition, we also found higher levels of type 17 cytokines, such as IL-21, IL-22 and IL-23 in *IL-17a*$^{-/-}$ mice, and comparable trends in *IL-17ra*$^{-/-}$ mice (Fig. 3E–G). Of note, while IFN-γ levels decreased in deficient mice, IL-4 levels were significantly increased (Fig. 3H,I). IL-1β levels were comparable between wt and deficient mice (Fig. 3M). Of note, KC levels were significantly reduced in *IL-17a*$^{-/-}$ mice, with a similar trend in *IL-17ra*$^{-/-}$ mice (Fig. 3K) despite a higher bacterial load. Accordingly, the number of lung infiltrating neutrophils and macrophages as representative of the innate immune response, and the inflammation severity, in terms of infiltrating inflammatory cells combined to alveolar damage, were significantly reduced in *IL-17a*$^{-/-}$ mice, with a similar trend in *IL-17ra*$^{-/-}$ mice (Fig. 3L,M). Thus, deficiency of the IL-17A/IL-17RA axis modulates the immune response, regardless of the bacterial burden, suggesting a potential role of the axis in mediating tolerance mechanisms.

Given observed differences, we quantified markers associated to tissue damage trying to prove the role of IL-17 mediated response in the modulation of host tolerance mechanisms. Elastin degradation, levels of pro-MMP-9 and TGF-β_1 were significantly reduced in *IL-17a*$^{-/-}$ mice (Fig. 4A–D). Similar trends were also observed in *IL-17ra*$^{-/-}$ mice, confirming that deficiency of the IL-17A/IL-17RA axis is associated to tissue preservation. Thus, together the data indicate that chronic IL-17-induced responses propagate local immune manifestations and induce tissue damage in response to persistent *P. aeruginosa* infection by hindering tolerance mechanisms.

IL-17A targeting improves tolerance during *P. aeruginosa* chronic airways infection. Next, we investigated whether targeting the IL-17A/IL-17RA axis rescues tolerance mechanisms during *P. aeruginosa* chronic infection. Taking into consideration the noxious effect of *IL-17ra* deficiency on host resistance, in term of bacterial burden, we adopted blocking anti-IL-17A mAb. Schedule of treatment with anti-IL-17A mAb was set-up

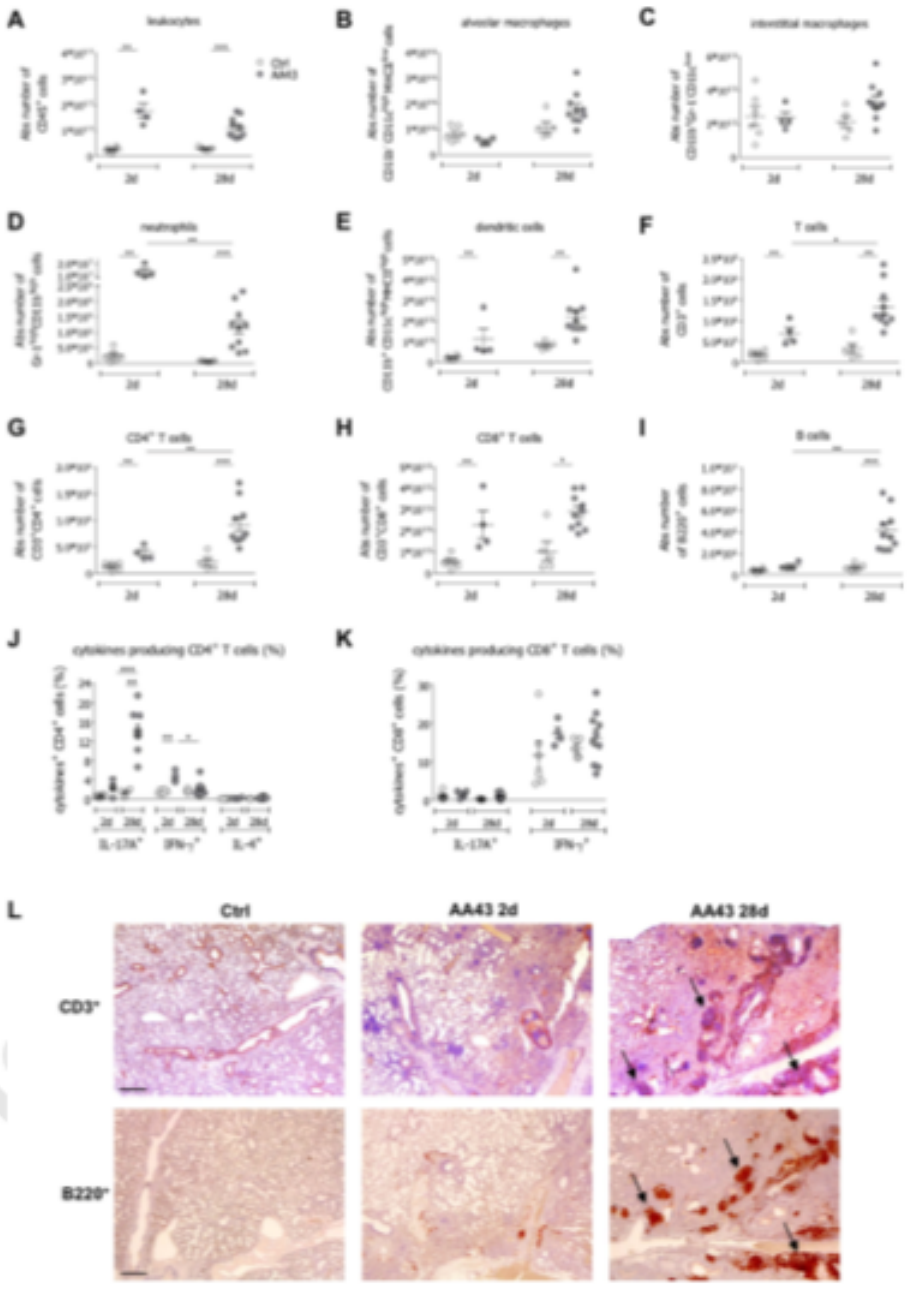

Figure 2. Adaptive immune response in the murine model of chronic airways infection with *P. aeruginosa*. C57Bl/6 mice were infected with 1 to 2 × 10^6 CFU/lung of the *P. aeruginosa* strain AA43 embedded in agar beads and analyzed after 2 and 28 days of infection. Ctrl mice were treated with sterile agar-beads. The absolute numbers of leukocytes (A), alveolar macrophages (B), interstitial macrophages (C), neutrophils (D), dendritic cells (E), T cells (F), $CD4^+$ T cells (G), $CD8^+$ T cells (H) and B cells (I) were measured by flow cytometric analysis in cell suspensions of murine lungs. The frequency of IL-17A-, IFN-γ- and IL-4-producing $CD4^+$ T (J) and $CD8^+$ (K) T cells were measured in lung cell suspensions after PMA/ionomycin stimulation, by flow cytometric analysis. The data are pooled from at least two independent experiments (n = 4–12). Dots represent cells in individual mice, horizontal lines represent mean values and the error bars represent the SEM. Statistical significance is indicated: $^*p < 0.05$, $^{**}p < 0.01$, $^{***}p < 0.001$. (L) Lung immunohistochemistry was performed on challenged mice by staining with anti-CD3 and anti-B220 antibodies. Scale bars: 400 μm. Some BALT-like structures are indicated by arrows.

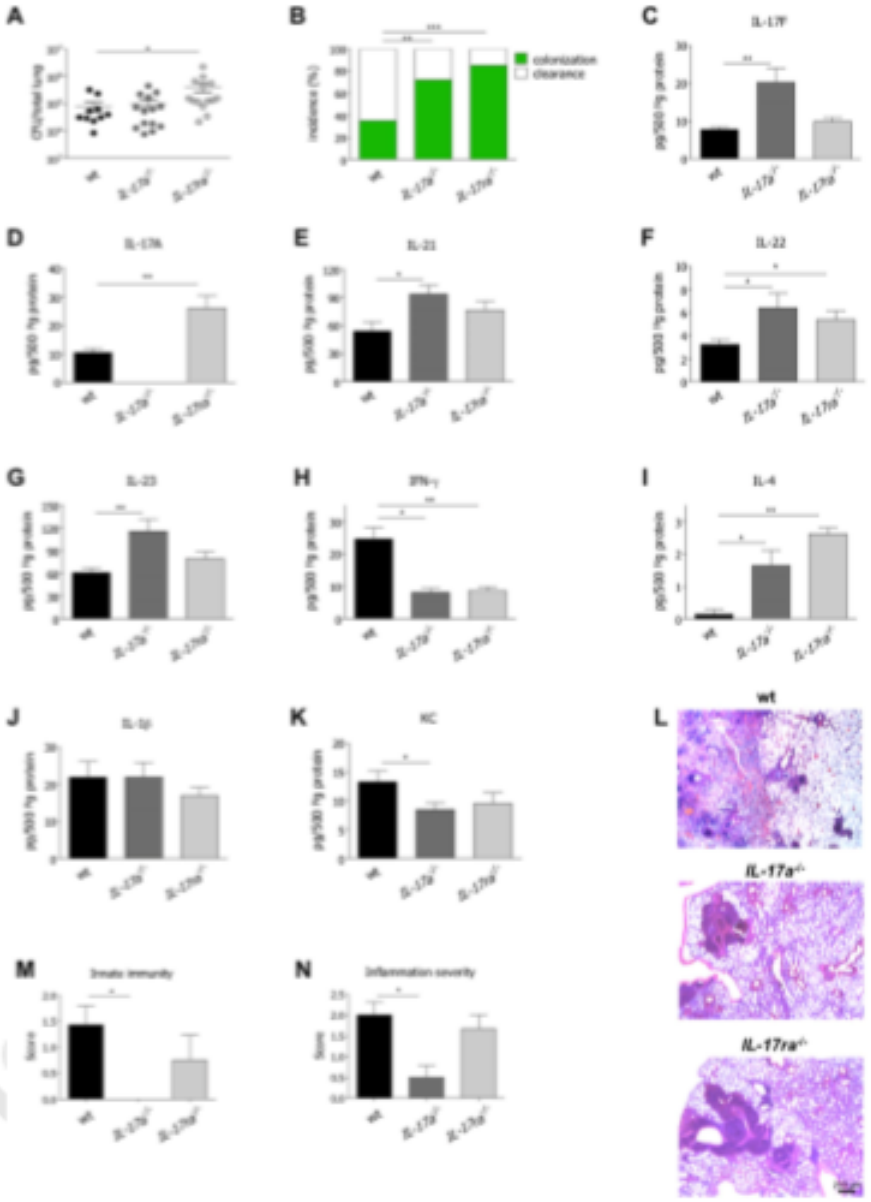

Figure 3. Virulence of *P. aeruginosa* and host immune response to chronic airways infection in *IL-17a*$^{-/-}$, *IL-17ra*$^{-/-}$ and congenic wt mice. Two groups of minimum five *IL-17a*$^{-/-}$, *IL-17ra*$^{-/-}$ and congenic wt C57Bl/6 mice were infected with 1 to 2×10^6 CFU/lung of the *P. aeruginosa* strain AA43 embedded in agar beads and analyzed 28 days post-infection. Ctrl mice were treated with sterile agar-beads. (A) CFU were evaluated in total lung. Dots represent CFU in individual mice, horizontal lines represent mean values and the error bars represent the SEM. The data are pooled from at least two independent experiments (n = 10–14). (B) Bacterial clearance (white) and incidence of colonization (green) were determined. The data are pooled from at least two independent experiments (n = 17–29). Cytokines and chemokines, including IL-17F (C), IL-17A (D), IL-21 (E), IL-22 (F), IL-23 (G), IFN-γ (H), IL-4 (I), IL-1β (J) and KC (K), were measured by Bioplex in lung homogenates of mice after 28 days of chronic lung infection with *P. aeruginosa*. The data are pooled from at least two independent experiments (n = 3–14). Values represent the mean ± SEM. Sections of airways from mice infected with AA43 for 28 days were stained with H&E, according to the standard procedure (L). Scale bars: 200 μm. Innate immune cells infiltration (M) and inflammation severity (N) were scored in tissue sections. Values represent the mean ± SEM. The data are pooled from two independent experiments (n = 3–5). Statistical significance is indicated: *$p < 0.05$, **$p < 0.01$, ***$p < 0.001$.

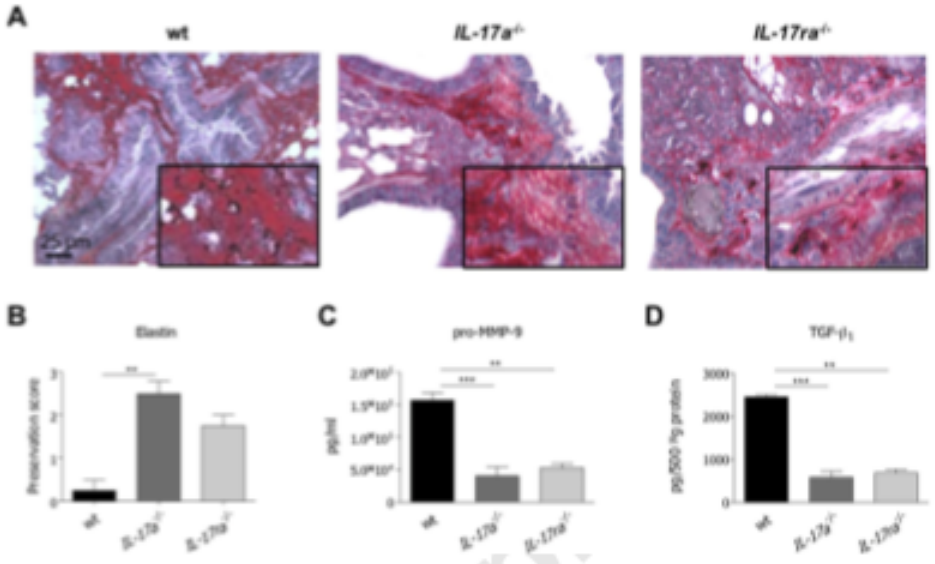

Figure 4. Tissue damage after *P. aeruginosa* chronic airways infection in *IL-17a*$^{-/-}$, *IL-17ra*$^{-/-}$ and congenic wt mice. Two groups of minimum five *IL-17a*$^{-/-}$, *IL-17ra*$^{-/-}$ and congenic wt C57Bl/6 mice were infected with 1 to 2 × 10^6 CFU/lung of the *P. aeruginosa* strain AA43 embedded in agar beads and analyzed 28 days post-infection. Ctrl mice were treated with sterile agar-beads. (**A**) Sections of airway from mice infected with AA43 were stained with VEG for elastic fibers, according to the standard procedure. Scale bars: 25 μm. Scoring of elastin preservation was performed on slices stained with VEG (**B**). Levels of pro-MMP-9 (**C**) and TGF-β_1 (**D**) were measured by ELISA and Bioplex respectively in lung homogenates after 28 days of chronic lung infection. Values represent the mean ± SEM. The data are pooled from at least two independent experiments (n = 3–10). Statistical significance is indicated: *p < 0.05, **p < 0.01, ***p < 0.001.

from 10 days post infection to distinguish IL-17A contributions to the lung pathology during advanced *P. aeruginosa* chronic infection (Fig. 5A) from those determined at the early/acute phase of infection in *IL-17a*$^{-/-}$ mice. At day 28, mice treated with isotype IgG control and anti-IL-17A mAb showed comparable bacterial load and colonization incidence (Fig. S1A). Also leukocyte (interstitial macrophages, alveolar macrophages, B cells and cytotoxic T cells) (Fig. S1B–E) and T cell numbers, along with CD4$^+$ T cells, IL-17A and IFN-γ producing CD4$^+$ T cells were comparable in isotype IgG and anti-IL-17A-treated mice (Fig. 5B–F), while IL-4 producing CD4$^+$ T cells were undetectable. Moreover, IL-17A and IFN-γ levels were comparable in mice treated with isotype IgG control and anti-IL-17A mAb (data not shown). Nevertheless, we found that IL-17A blockade decreased neutrophils infiltration (Fig. 5G), likely due to reduced KC levels (Fig. 5H). Remarkably, mice treated with anti-IL-17A mAb displayed also lower levels of pro-MMP-9 (Fig. 5I) and TGF-β_1 (Fig. 5J), indicating lower production of markers promoting tissue remodeling and damage. Results suggest that IL-17A neutralization does not provoke bacterial spreading, and instead promotes host tolerance mechanisms, narrowing exacerbated pulmonary neutrophilia and tissue damage associated with chronic *P. aeruginosa* airways infection.

Discussion

The mechanisms underlying the exaggerated inflammation and tissue damage, associated to un-resolved airways infections, in CF[4] and others chronic lung diseases, such as COPD[26,27], are thought to be associated with an inappropriate host response. Here we demonstrate that type 17 immunity is central to the exaggerated and detrimental host response to *P. aeruginosa* chronic infection. Indeed, while previous data indicated a role for IL-17A in resistance to microbial insults in the acute/early phases of infection[12], our results underline its involvement in impairing host tolerance during advanced chronic *P. aeruginosa* airways infection.

Using mouse models of short term infection by *P. aeruginosa*, previous studies demonstrated that IL-17 and IL-17$^+$ cells contribute to the host response in the acute phase, mediating neutrophils and T cells recruitment[10]. During the early/acute phases of *P. aeruginosa* infection, γδ T or pILC3 (Type 3 pulmonary Innate Lymphoid Cells) cells were found to be the main cellular sources of IL-17 cytokines[12,16,28]. To investigate the previously unexplored role for IL-17A during advanced chronic *P. aeruginosa* airways infection we took advantage of the agar-beads mouse model[25,29], and characterized innate and adaptive immune responses at the early and advanced phases of infection. We found that type 1 and type 17 cytokine responses could all be detected at early phases of infection. However, while IFN-γ cytokines returned to background levels in chronically infected mice, IL-17A levels remained high. In support of our experimental evidences, we found elevated IL-17A levels in CF human respiratory samples at both early and late phases of *P. aeruginosa* infection, fostering the concept that the type 17 immunity is involved during the overall course of chronic infection by *P. aeruginosa*.

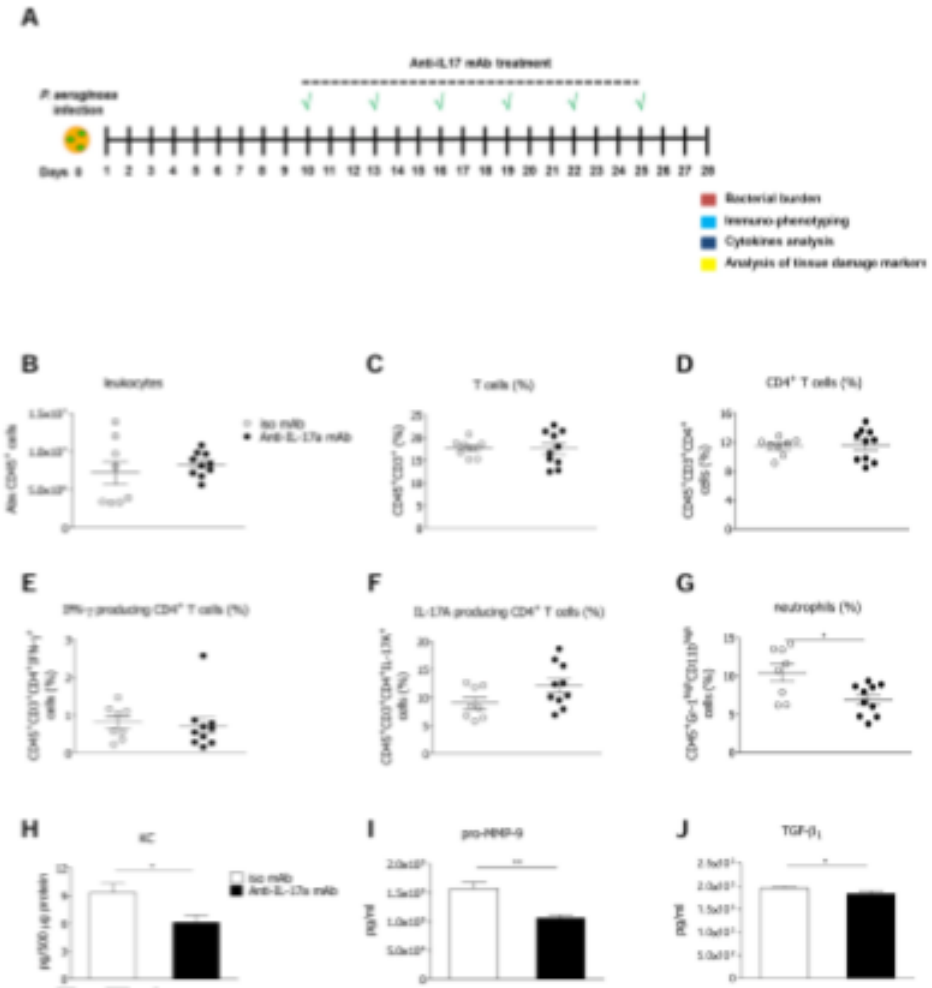

Figure 5. Anti-IL-17A mAb treatment in the murine model of chronic airways infection by *P. aeruginosa*. C57Bl/6 mice were infected with 1 to 2×10^6 CFU/lung of the *P. aeruginosa* strain AA43 embedded in agar beads. Every three days starting from the tenth day from infection, a group of mice was treated i.p. with 100 µg/mouse of anti-IL-17A mAb, while the other group was treated i.p. with 100 µg/mouse of control isotypic IgG and analyzed after 28 days of infection. Schematic view of the treatment schedule is shown (A). Leukocytes (B), T cells (C), $CD4^+$ T cells (D), the frequency of IFN-γ- (E) and IL-17A-producing $CD4^+$ T cells (F) after PMA/ionomycin stimulation, and neutrophils (G) were measured by flow cytometric analysis in cell suspensions of murine lungs. Dots represent cells in individual mice, horizontal lines represent mean values and the error bars represent the SEM. KC levels (H) were measured by Bioplex in the supernatants of murine lung cellular suspensions. Levels of pro-MMP-9 (I) by ELISA and TGF-β_1 (J) by Bioplex were measured in the supernatants of murine lung cellular suspensions. Values represent the mean ± SEM. The data are pooled from at least two independent experiments (n = 8–10). Statistical significance is indicated: $^*p < 0.05$, $^{**}p < 0.01$.

Next, we dissected the inflammatory response by FACS analysis. We proved that $CD4^+$ IL-$17A^+$ cells were greatly increased, suggesting their involvement in chronic inflammation, while we did not find neutrophils secreting IL-17A (data not shown) at the advanced stage of infection. However, we cannot exclude that other cellular sources (ILCs or γδ T cells) may be involved during *P. aeruginosa* long-term chronic infection in our mouse model. Further studies are needed to explore this possibility. In addition to T cells, B cells and DC were found in association to the presence of BALT like-structure, likely indicative of active local responses. Interestingly, the absence of IL-$17A^+$ T cells in murine spleens indicated that T cell differentiation in response to pathogenic insults is tissue specific rather than systemically activated, supporting other studies on chronic lung diseases (e.g. severe COPD)[30].

The role of IL-17 in protective versus detrimental immunity has been debated[8,31]. Recent evidences indicate that the IL-17 pathway exerts a protective effect in the airways by favoring the clearance of several pathogens[8,32].

IL-17A and IL-17F cytokines may have a redundant function in host defense through the heterodimeric receptor complex formed by IL-17RA and IL-17RC[33]. To validate the hypothesis that IL-17A-mediated response may have a role in modulating host resistance during chronic *P. aeruginosa* infection, *IL-17a* and *IL-17ra* deficient mice were explored. Moreover, we took advantage of a *P. aeruginosa* isolate, namely AA43, known to establish stable chronic infection in the 30–40% of challenged mice[24,25]. This choice was fundamental to uncover that the incidence of chronic colonization was increased in both *IL-17a* and *IL-17ra* deficient mice when compared to wt mice. Differently, bacterial burdens were altered only by *IL-17ra* deficiency. This suggests that host resistance to *P. aeruginosa* is mediated by IL-17A and IL-17F, through IL17RA, rather than only by IL-17A.

In addition to resistance, several evidences suggested the IL-17 pathway as detrimental to chronic inflammatory airways diseases[34,35]. Indeed, blockade of IL-17A in bleomycin-induced acute inflammation promoted the resolution of inflammation[36]. IL-17 was associated with airways hyperresponsiveness and to increased mucus production in murine model of respiratory syncytial virus disease or allergic disease[31,37]. Other studies demonstrated the contribution of IL-17A in remodeling processes, such as the development of chronic fibroproliferative disease[38]. Expanding this notion in the context of chronic inflammatory processes mediated by persistent *P. aeruginosa* infection, our findings showed that IL-17A pathway affects the host tolerance, increasing leukocytes recruitment and causing tissue damage. Although the bacterial burden did not change in *IL-17a*, but even increased in the *IL-17ra* deficient mice, markers of tissue remodeling and damage, such as elastin degradation, and levels of pro-MMP-9 and TGF-β_1 were decreased. Thus, our findings demonstrated that prolonged local release of IL-17A affects host tolerance favoring the development of excessive immunopathology during chronic *P. aeruginosa* infection.

Experimental evidences of a detrimental role of IL-17A in chronic *P. aeruginosa* infection prompted us to evaluate whether neutralizing IL-17A might provide a valuable strategy in the effort of limiting pathogen-associated tissue damage, without altering host resistance. To avoid an exacerbation of bacterial lung burden in the early phase of infection[39,40], we decided to interfere with IL-17A, leaving the IL-17F and IL-17RA able to operate during the advanced stage of chronic infection. We found that anti-IL-17A mAb treatment did not increase the bacterial burden, while it significantly reduced local inflammatory response and tissue remodeling and damage. Interestingly, the finding that IL-17A targeting partially reduced neutrophils infiltration and did not affect other immune cells suggests that IL-17F may have a complementary function in modulating immune response, as previously described for other pathogens[8,13]. Given the notion that IL-17 contributes to the pathogenesis of several chronic diseases and inhibitors have been identified[12,34], it is tempting to speculate that IL-17A neutralization might be a critical target in *P. aeruginosa* infected patients, in particular those chronically infected, to ameliorate their lung function.

In conclusion, our work has elucidated the role of IL-17A during chronic airways infection by *P. aeruginosa* and may provide the ground for designing novel immunotherapy strategies, modulating mechanisms of resistance and tolerance. We indeed proved that IL-17-mediated immunity plays a double-edged activity during chronic airways infection: on one side, it contributes to the control of *P. aeruginosa* burden, modulating host resistance, while, on the other, it alters host tolerance, propagating exacerbated pulmonary neutrophilia and tissue remodeling. Inhibition of the IL-17 pathway in a time-specific fashion represents a novel potential host-based intervention to ameliorate lung physiology and function without compromising host resistance against pathogens during chronic airways infection.

Methods

Ethics statement. Animal studies were conducted according to protocols approved by the San Raffaele Scientific Institute (Milan, Italy) Institutional Animal Care and Use Committee (IACUC) and adhered strictly to the Italian Ministry of Health guidelines for the use and care of experimental animals (IACUC protocol #505), following the guidelines included in the D. Lgs. 04-03-2014 n. 26. Research with AA43 bacterial strain, used for animal experiments, has been approved by the Ethics Commission of Hannover Medical School, Germany. The patient and parents gave informed consent before the sample collection. Approval for storing of biological materials was obtained by the Ethics Commission of Hannover Medical School, Germany. The study on human samples from the Regional CF Center of Lombardia was approved by the Ethical Committees of San Raffaele Scientific Institute and Fondazione IRCCS Ca' Granda, Ospedale Maggiore Policlinico, Milan, Italy, and written informed consent was obtained from patients enrolled or their parents according to the Ethical Committee rules, in accordance with the laws of the Italian Ministero della Salute (approval #1874).

Bacterial strains. The *P. aeruginosa* isolate, AA43, from a CF patient, was chosen from a strain collection, previously characterized for genotypic and phenotypic traits and virulence[24,25,41].

Mouse strains and model of chronic *P. aeruginosa* infection. C57Bl/6 (Charles River), *IL-17a*$^{-/-}$ and *IL-17ra*$^{-/-}$ mice (background C57Bl/6), male, 8–10 weeks old, were maintained in specific pathogen-free conditions. Mice were injected intratracheally with 1–2 × 10^6 CFU of *P. aeruginosa*, embedded in agar beads, following established procedures[25,29].

Lung dissociation and processing for analysis of cytokines and markers of tissue damage. Mice were sacrificed by CO_2 administration. Lungs were removed and homogenized[29]. Samples were plated for CFU count. Recovery of >1000 CFU from lung cultures was indicative of chronic infection. Lung homogenates were then centrifuged at 14000 rpm for 30 min at 4 °C and the supernatants (SN) were stored at −80 °C for quantification of total protein content with Bradford's assay (Bio-RAD) and analysis of inflammatory and tissue damage markers.

APC antibodies panel	T cells antibodies panel	Intracellular T cells panel
anti-CD45	anti-CD45	anti-CD3
anti-GR-1	anti-CD3	anti-CD4
anti-CD11B	anti-CD4	anti-CD8
anti-CD11C	anti-CD8	anti-IL-17A
anti-MHCII	anti-CD44	anti-IFN-Y
anti-B220		anti-IL4

Table 1. Antibodies used for FACS analysis and intracellular staining are indicated.

Flow cytometry and intracellular cytokines staining. Mechanical dissociation was used to prepare single cells suspensions from lung and spleen. Antibody staining was performed as previously described[42,43]. Briefly, after Fc blocking treatment, cells harvested from lungs and spleen were washed and stained for 20 minutes with appropriate dilutions of antibodies from the antigen-presenting cell (APC) panel and lymphoid cells (T cell) panel (Table 1) in FACS staining buffer (PBS, 2% FBS, 0,2% NaN_3). Then cells were washed twice, fixed (PBS 4% formaldehyde) and resuspended in FACS staining buffer. For intracellular staining, cells harvested from lungs and spleens were washed, incubated 2 hours with phorbol 12-myristate 13-acetate (PMA, 10 ng/ml, Sigma) and Ionomycin (1 μg/ml, Sigma), then brefeldin A (BFA) was added (5 μg/ml, Sigma). After 2 hours, samples were washed with FACS staining buffer, and, after Fc blocking treatment, cells were incubated with appropriate dilutions of antibodies from intracellular lymphoid cells panel (Table 1). Cells were washed twice. Fixation and permeabilization for cytokine intracellular staining were performed according to the manufacturer's instruction. Anti-IL-17A, anti-IL-4 and anti-IFN-γ antibodies were used. For each antibody, a control isotype was used for compensation. Doublets were removed by gating on a plot of forward-scatter area versus forward-scatter height. Acquisition and analyses were performed using FACSCanto cytometer (BD Biosciences) and FlowJo Software (Tree Star).

Inhibitory treatment in mice. Rat anti–IL-17A monoclonal antibody (Cat.# 506923) and isotype control were purchased from Biolegend. Animals were treated every 3 days with intraperitoneal (i.p.) injection of 100 μg/mouse of antibodies starting 10 days post infection, when chronic airways infection was stably settled[44].

Histological examination. Murine lungs were removed, fixed in formalin, and embedded in paraffin. Consecutive sections from the middle of the five lung lobes were used for histological and immunohistochemical examination. Sections were collected and stained by anti-CD3 mAb or anti-B220 mAb, Haematoxylin and Eosin (H&E) and Verhoeff's elastic (VEG) staining and were examined blindly and scored by a pathologist. Histological score analysis of murine lungs was performed to grade the amount of innate immune cells infiltration (macrophages and neutrophils) and inflammation severity (evaluating both innate and adaptive immune cells recruitment, and the extent of alveolar damage). Histological examination primarily scored the number of immune cells (mononuclear cells, such as macrophages, lymphocytes, plasma cells, and neutrophils) at a magnification of ×400. The results are reported as the mean for the entire specimen[45]. Immune cells were classified as absent (score of 0) when there were no or fewer than 19 cells per high-power field (HPF) (at a magnification of ×400), mild (score of 1) for 20 to 49 cells per HPF, moderate (score of 2) for 50 to 99 cells per HPF, marked or severe (score of 3) for 100 to 200 cells or more per HPF. Histological criteria for normal pulmonary characteristics included detection of no or only a few mononuclear cells per HPF and no or only a few scattered neutrophils in bronchioli and alveoli without tissue changes (no interstitial thickening or aggregates of lymphocytic infiltrates, and airways free from exudate). The number of inflammatory cells, assessed at ×400 and ×100 magnification respectively, was scored and customized as described by Martino *et al.*[46].

VEG was used for assessing and quantifying the elastin architecture in lung interstitial and peribrochial areas. The degree of fragmentation and the amount of the elastic fibers were examined by the pathologist, blinded to the treatment group, who scored each slide using an arbitrary combined scoring system that counted the number of "islands of damage" within a lung cross-section from each mouse. An island of damage was defined as an isolated area of lung's interstitium or peribronchus, where two adjacent elastic fibers were fragmented with interposed excessive connective tissue matrix, evaluated randomly on the cross-section at 400x. Three evaluations/lung were performed. The method was extrapolated from McLoughlin *et al.*[47].

CF patients and study design. Sputum was recovered from 55 CF patients at the regional CF centre of Lombardia (Fondazione IRCCS Ca' Granda – Ospedale Maggiore Policlinico, Milan, Italy).

Inclusion criteria were: a) diagnosis after neonatal screening or after symptoms onset and followed since birth in the centre; b) complete clinical history available in the computerized database; c) at least two visits yearly since diagnosis; d) availability of at least four yearly sputum cultures for microbiological ascertainment; e) at least one CT every year; f)at least one respiratory function test/year after the age of 5 years.

Exclusion criteria were i) positive culture for *Burkholderia cepacia complex*, methicillin-resistant *Staphylococcus aureus, Achromobacter xylosoxidans, Stenotrophomonas maltophilia, Scedosporium* spp, and ii) acute pulmonary exacerbation (APE). APE was determined by the presence of at least four of the following criteria: 10% or greater decrease in baseline FEV_1, increased cough or sputum production, change in sputum character, dyspnea, tachypnea, fever, weight loss, 5% or greater decrease in O_2 saturation, new or worsening crackles

on lung auscultation, or findings on chest X-ray consistent with pneumonia. The clinical procedures were applied for usual care plans. Data on age, gender, *cftr* genotype (ΔF508 homozygous) *P. aeruginosa* status and years of colonization, and presence of pathogens other than *P. aeruginosa*, were collected. The characteristics of the CF patients are summarized in the Table S1.

CF patients sputum processing. Samples used to evaluate immune markers diluted in PBS to a final volume of 5 ml and they were centrifuged at 350 g for 10 min at 4 °C and SN collected and stored at −80 °C.

Human respiratory samples microbiology. Respiratory samples were plated on chocolate agar with bacitracine, Columbia CNA Agar with 5% Sheep Blood, Mannitol salt agar, MacConkey II Agar, Cepacia Medium Agar and Sabouraud Dexstrose Agar. Microbic species were identified with MicroScan WalkAway plus System.

Evaluation of markers associated to tissue damage and inflammation. Multiplex immunoassays (Bio-Rad) based on Luminex technology were used for the quantification of cytokines, chemokines and growth factors in murine and human samples, according to the manufacturer's instruction. A mouse Bio-Plex custom mix was used to analyze KC, IL-1β, IL-4, IL-17A, IL-17F, IL-21, IL-22, IL-23, and IFN-γ in murine lungs. A human Bio-Plex custom mix was used to analyze IL-4, IL-17A, IFN-γ. The three isoforms of TGF-β (TGF-β_1, TGF-β_2 and TGF-β_3) were analyzed with Bio-Plex Pro™ TGF-β 3-plex panel in murine BAL fluid and lung homogenates. Data were measured on Bio-Plex 200 System and calculated using Bio-Plex Manager 6.0 and 6.1 software. Murine pro-MMP-9 was measured by ELISA (R&D DuoSet ELISA Development System), according to the manufacturer's instructions.

Statistics. Statistics were performed with GraphPad Prism and R environment for statistical computing. When comparing data at a specific time-point a nonparametric two-taled Mann–Whitney U test was performed. To compare data in different murine strains and human samples in comparing groups of patients at different stage of infection ("free", "early" and "late") a nonparametric Kruskal–Wallis test was used followed by post-hoc Dunn test to correct for multiple comparisons. Incidences of colonization were compared using Fisher exact test. Statistical analyses were considered significant at $p < 0.05$.

References

1. Medzhitov, R., Schneider, D. S. & Soares, M. P. Disease tolerance as a defense strategy. *Science* 335, 936–941, doi: 10.1126/science.1214935 (2012).
2. Schneider, D. S. & Ayres, J. S. Two ways to survive infection: what resistance and tolerance can teach us about treating infectious diseases. *Nat Rev Immunol* 8, 889–895, doi: 10.1038/nri2432 (2008).
3. Raberg, L., Graham, A. L. & Read, A. F. Decomposing health: tolerance and resistance to parasites in animals. *Philos Trans R Soc Lond B Biol Sci* 364, 37–49, doi: 10.1098/rstb.2008.0184 (2009).
4. Cohen, T. S. & Prince, A. Cystic fibrosis: a mucosal immunodeficiency syndrome. *Nat Med* 18, 509–519, doi: 10.1038/nm.2715 (2012).
5. Hassett, D. J., Borchers, M. T. & Panos, R. J. Chronic obstructive pulmonary disease (COPD): evaluation from clinical, immunological and bacterial pathogenesis perspectives. *J Microbiol* 52, 211–226, doi: 10.1007/s12275-014-4068-2 (2014).
6. Gallego, M. *et al.* Pseudomonas aeruginosa isolates in severe chronic obstructive pulmonary disease: characterization and risk factors. *BMC Pulm Med* 14, 103, doi: 10.1186/1471-2466-14-103 (2014).
7. Isailovic, N., Daigo, K., Mantovani, A. & Selmi, C. Interleukin-17 and innate immunity in infections and chronic inflammation. *J Autoimmun* 60, 1–11, doi: S0896-8411(15)00059-1 (2015).
8. Jin, W. & Dong, C. IL-17 cytokines in immunity and inflammation. *Emerg Microbes Infect* 2, e60, doi: 10.1038/emi.2013.58 (2013).
9. McAleer, J. P. & Kolls, J. K. Directing traffic: IL-17 and IL-22 coordinate pulmonary immune defense. *Immunol Rev* 260, 129–144, doi: 10.1111/imr.12183 (2014).
10. Reynolds, J. M., Angkasekwinai, P. & Dong, C. IL-17 family member cytokines: regulation and function in innate immunity. *Cytokine Growth Factor Rev* 21, 413–423, doi: 10.1016/j.cytogfr.2010.10.002 (2010).
11. Tan, H. L. & Rosenthal, M. IL-17 in lung disease: friend or foe? *Thorax* 68, 788–790, doi: 10.1136/thoraxjnl-2013-203307 (2013).
12. Lorè, N. I., Bragonzi, A. & Cigana, C. The IL-17A/IL-17RA axis in pulmonary defence and immunopathology. *Cytokine and Growth Factor Reviews*, doi: 10.1016/j.cytogfr.2016.03.009 (2016).
13. Ishigame, H. *et al.* Differential roles of interleukin-17A and -17F in host defense against mucoepithelial bacterial infection and allergic responses. *Immunity* 30, 108–119, doi: 10.1016/j.immuni.2008.11.009 (2009).
14. Dubin, P. J. *et al.* Interleukin-23-mediated inflammation in Pseudomonas aeruginosa pulmonary infection. *Infection and Immunity* 80, 398–409, doi: 10.1128/IAI.05821-11 (2012).
15. Xu, X. *et al.* Role of interleukin-17 in defense against pseudomonas aeruginosa infection in lungs. *Int J Clin Exp Med* 7, 809–816 (2014).
16. Liu, J. *et al.* The responses of gammadelta T-cells against acute Pseudomonas aeruginosa pulmonary infection in mice via interleukin-17. *Pathog Dis* 68, 44–51, doi: 10.1111/2049-632X.12043 (2013).
17. Mutr, R. *et al.* Innate Lymphoid Cells are the Predominant Source of Interleukin-17A During the Early Pathogenesis of Acute Respiratory Distress Syndrome. *Am J Respir Crit Care Med*, doi: 10.1164/rccm.201410-1782OC (2015).
18. Fogli, L. K. *et al.* T cell-derived IL-17 mediates epithelial changes in the airway and drives pulmonary neutrophilia. *J Immunol* 191, 3100–3111, doi: 10.4049/jimmunol.1301360 (2013).
19. Dubin, P. J. & Kolls, J. K. IL-17 in cystic fibrosis: more than just Th17 cells. *Am J Respir Crit Care Med* 184, 155–157, doi: 10.1164/rccm.201104-0617ED (2011).
20. Kolls, J. K. Helper T-cell type 17 cytokines and immunity in the lung. *Ann Am Thorac Soc* 11 Suppl 5, S284–286, doi: 10.1513/AnnalsATS.201403-109AW (2014).
21. Tiringer, K. *et al.* A Th17- and Th2-skewed cytokine profile in cystic fibrosis lungs represents a potential risk factor for Pseudomonas aeruginosa infection. *Am J Respir Crit Care Med* 187, 621–629, doi: 10.1164/rccm.201206-1150OC (2013).
22. Tan, H. L. *et al.* The Th17 pathway in cystic fibrosis lung disease. *Am J Respir Crit Care Med* 184, 252–258, doi: 10.1164/rccm.201102-0236OC (2011).
23. Brodlie, M., Corris, P. A., Lordan, J. & Ward, C. Interleukin-17 and cystic fibrosis lung disease. *Am J Respir Crit Care Med* 185, 108–109; author reply 109–110, doi: 185/1/108.a (2012).
24. Bragonzi, A. *et al.* Pseudomonas aeruginosa microevolution during cystic fibrosis lung infection establishes clones with adapted virulence. *Am J Respir Crit Care Med* 180, 138–145, doi: 10.1164/rccm.200812-1943OC (2009).

25. Cigana, C. *et al.* Tracking the immunopathological response to Pseudomonas aeruginosa during respiratory infections. *Sci Rep* **6**, 21465, doi: 10.1038/srep21465 (2016).
26. Doring, G., Parameswaran, I. G. & Murphy, T. F. Differential adaptation of microbial pathogens to airways of patients with cystic fibrosis and chronic obstructive pulmonary disease. *FEMS Microbiol Rev* **35**, 124–146, doi: 10.1111/j.1574-6976.2010.00237.x (2011).
27. Holtzman, M. J., Byers, D. E., Alexander-Brett, J. & Wang, X. The role of airway epithelial cells and innate immune cells in chronic respiratory disease. *Nat Rev Immunol* **14**, 686–698, doi: 10.1038/nri3739 (2014).
28. Dubin, P. J., McAllister, F. & Kolls, J. K. Is cystic fibrosis a TH17 disease? *Inflamm Res* **56**, 221–227, doi: 10.1007/s00011-007-6187-2 (2007).
29. Kukavica-Ibrulj, I., Facchini, M., Cigana, C., Levesque, R. C. & Bragonzi, A. Assessing Pseudomonas aeruginosa virulence and the host response using murine models of acute and chronic lung infection. *Methods Mol Biol* **1149**, 757–771, doi: 10.1007/978-1-4939-0473-0_58 (2014).
30. Bryant, D. M. & Mostov, K. E. From cells to organs: building polarized tissue. *Nat Rev Mol Cell Biol* **9**, 887–901, doi: 10.1038/nrm2523 (2008).
31. Kudo, M. *et al.* IL-17A produced by alphabeta T cells drives airway hyper-responsiveness in mice and enhances mouse and human airway smooth muscle contraction. *Nat Med* **18**, 547–554, doi: 10.1038/nm.2684 (2012).
32. Wozniak, K. L., Hardison, S. E., Kolls, J. K. & Wormley, F. L. Role of IL-17A on resolution of pulmonary C. neoformans infection. *PLos one* **6**, e17204, doi: 10.1371/journal.pone.0017204 (2011).
33. Gaffen, S. L. Structure and signalling in the IL-17 receptor family. *Nat Rev Immunol* **9**, 556–567, doi: 10.1038/nri2586 (2009).
34. Miossec, P. & Kolls, J. K. Targeting IL-17 and TH17 cells in chronic inflammation. *Nat Rev Drug Discov* **11**, 763–776, doi: 10.1038/nrd3794 (2012).
35. Bartlett, H. S. & Million, R. P. Targeting the IL-17-T(H)17 pathway. *Nat Rev Drug Discov* **14**, 11–12, doi: 10.1038/nrd4518 (2015).
36. Mi, S. *et al.* Blocking IL-17A promotes the resolution of pulmonary inflammation and fibrosis via TGF-beta1-dependent and -independent mechanisms. *J Immunol* **187**, 3003–3014, doi: 10.4049/jimmunol.1004081 (2011).
37. Mukherjee, S. *et al.* IL-17-induced pulmonary pathogenesis during respiratory viral infection and exacerbation of allergic disease. *Am J Pathol* **179**, 248–258, doi: 10.1016/j.ajpath.2011.03.003 (2011).
38. Ivanov, S. & Linden, A. Interleukin-17 as a drug target in human disease. *Trends Pharmacol Sci* **30**, 95–103, doi: 10.1016/j.tips.2008.11.004 (2009).
39. Doring, G. *et al.* BIIL 284 reduces neutrophil numbers but increases P. aeruginosa bacteremia and inflammation in mouse lungs. *J Cyst Fibros* **13**, 156–163, doi: 10.1016/j.jcf.2013.10.007 (2014).
40. Konstan, M. W. *et al.* A randomized double blind, placebo controlled phase 2 trial of BIIL 284 BS (an LTB4 receptor antagonist) for the treatment of lung disease in children and adults with cystic fibrosis. *J Cyst Fibros* **13**, 148–155, doi: 10.1016/j.jcf.2013.12.009 (2014).
41. Lore, N. I. *et al.* Cystic fibrosis-niche adaptation of Pseudomonas aeruginosa reduces virulence in multiple infection hosts. *PLos one* **7**, e35648, doi: 10.1371/journal.pone.0035648 (2012).
42. Zaynagetdinov, R. *et al.* Identification of Myeloid Cell Subsets in Murine Lungs Using Flow Cytometry. *Am J Resp Cell Mol* **49**, 180–189, doi: DOI 10.1165/rcmb.2012-0366MA (2013).
43. Price, A. E., Reinhardt, R. L., Liang, H. E. & Locksley, R. M. Marking and quantifying IL-17A-producing cells *in vivo*. *PLos one* **7**, e39750, doi: 10.1371/journal.pone.0039750 (2012).
44. Bragonzi, A. Murine models of acute and chronic lung infection with cystic fibrosis pathogens. *Int J Med Microbiol* **300**, 584–593, doi: 10.1016/j.ijmm.2010.08.012 (2010).
45. Cersini, A., Martino, M. C., Martini, I., Rossi, G. & Bernardini, M. L. Analysis of virulence and inflammatory potential of Shigella flexneri purine biosynthesis mutants. *Infect Immun* **71**, 7002–7013 (2003).
46. Martino, M. C. *et al.* Mucosal lymphoid infiltrate dominates colonic pathological changes in murine experimental shigellosis. *J Infect Dis* **192**, 136–148, doi: JID33751 (2005).
47. McLoughlin, D. *et al.* Pravastatin reduces Marfan aortic dilation. *Circulation* **124**, S168–173, doi: 10.1161/CIRCULATIONAHA.110.012187 (2011).

Acknowledgements

The authors thank B. Tümmler (Medizinische Hochschule Hannover, Germany) for supplying *P. aeruginosa* clinical strain AA43, L. Romani (University of Perugia, Perugia, Italy) for providing *IL-17a*$^{-/-}$ and *IL-17ra*$^{-/-}$ mice, A. Biffi (Ospedale Maggiore Policlinico, Milano, Italy) for support in human protocol, M. Rocchi and F. Sanvito (Department of Pathology, San Raffaele Scientific Institute, Milano, Italy) for the mouse histopathology preparations and the San Raffaele Microscopy facility (Alembic) for images acquisition.

Author Contributions

Conceiving and designing the experiments: N.I.L., C.Ci. and A.B.; performing experiments: N.I.L., C.Ci., C.R., I.D.F., L.S., B.S., L.C., D.G. and V.B.; analyzing data: N.I.L., C.C., C.R., I.D.F., L.S., B.S., G.R., A.M. and A.B.; performing statistical analysis: A.N.; interpretation of the experiments results: N.I.L. and C.Ci.; recruitment of patients and providing informed consent: C.Co.; preparing figures: N.I.L. and C.Ci.; writing the manuscript: N.I.L., C.Ci., A.M. and A.B.

Additional Information

Supplementary information accompanies this paper at http://www.nature.com/srep

Competing financial interests: The authors declare no competing financial interests.

How to cite this article: Lorè, N. I. *et al.* IL-17A impairs host tolerance during airway chronic infection by *Pseudomonas aeruginosa*. *Sci. Rep.* **6**, 25937; doi: 10.1038/srep25937 (2016).

AAC
JournalsASM.org

Thymidine-Dependent *Staphylococcus aureus* Small-Colony Variants Are Induced by Trimethoprim-Sulfamethoxazole (SXT) and Have Increased Fitness during SXT Challenge

Andre Kriegeskorte,[a] Nicola Ivan Lorè,[b] Alessandra Bragonzi,[b] Camilla Riva,[b] Marco Kelkenberg,[a] Karsten Becker,[a] Richard A. Proctor,[c] Georg Peters,[a,d] Barbara C. Kahl[a]

Institute of Medical Microbiology, University Hospital of Münster, Münster, Germany[a]; Infections and Cystic Fibrosis Unit, Division of Immunology, Transplantation and Infectious Diseases, San Raffaele Scientific Institute, Milan, Italy[b]; Department of Microbiology and Immunology, University of Wisconsin—Madison, Madison, Wisconsin, USA[c]; Interdisciplinary Centre for Clinical Research, University of Münster, Münster, Germany[d]

Trimethoprim-sulfamethoxazole (SXT) is a possible alternative for the treatment of community- and hospital-acquired methicillin-resistant *Staphylococcus aureus* (MRSA) due to the susceptibility of most MRSA strains to the drug. However, after long-term treatment with SXT, thymidine-dependent (TD) SXT-resistant small-colony variants (SCVs) emerge. In TD-SCVs, mutations of thymidylate synthase ([TS] *thyA*) occur. Until now, it has never been systematically investigated that SXT is triggering the induction and/or selection of TD-SCVs. In our study, we performed induction, reversion, and competition experiments *in vitro* and *in vivo* using a chronic mouse pneumonia model to determine the impact of SXT on the emergence of TD-SCVs. SCVs were characterized by light and transmission electron microscopy (TEM) and auxotrophism testing. Short-term exposure of *S. aureus* to SXT induced the TD-SCV phenotype in *S. aureus* SH1000, while selection of TD-SCVs with *thyA* mutations occurred after long-term exposure. In reversion experiments with clinical and laboratory TD-SCVs, all revertants carried compensating mutations at the initially identified mutation site. Competition experiments *in vitro* and *in vivo* revealed a survival and growth advantage of the Δ*thyA* mutant under low-thymidine availability and SXT exposure although this advantage was less profound *in vivo*. Our results show that SXT induces the TD-SCV phenotype after short-term exposure, while long-term exposure selects for *thyA* mutations, which provide an advantage for TD-SCVs under specified conditions. Thus, our results further an understanding of the dynamic processes occurring during SXT exposure with induction and selection of *S. aureus* TD-SCVs.

Staphylococcus aureus is an important human pathogen which causes a variety of infections in healthy and hospitalized patients (1). The increase of methicillin-resistant *S. aureus* (MRSA) isolates not only in hospitals but also in the community threatens the use of β-lactam antibiotics, which are most efficient for the treatment of *S. aureus* infections. Since more than 90% of community-acquired (CA-MRSA) and hospital acquired (HA-MRSA) strains are still susceptible to trimethoprim-sulfamethoxazole (TMP-SMX, or SXT) (2–5), new attention has been drawn to this old drug. For example, two recent randomized placebo-controlled studies evaluated the effect of SXT in skin abscesses after incision and drainage in children and adults mostly caused by CA-MRSA (6–8). Furthermore, De Angelis et al. suggested the use of SXT and clindamycin as first-line drugs as a therapeutic option in patients suffering from CA-MRSA infections (9). In contrast, the role of SXT in infections associated with tissue damage and extracellular available thymidine was questioned by Proctor (10) because *S. aureus* can bypass the inhibitory effect of SXT by external uptake of thymidine.

However, if patients were treated with SXT for extended periods, the emergence of thymidine-dependent (TD) small-colony variants (SCVs) of *S. aureus* has been reported (11–13). TD-SCVs were recovered from patients with chronic infections, such as soft tissue infection, bronchitis, peritonitis, endocarditis, and septicemia, and in particular with a high prevalence from the airways of cystic fibrosis (CF) patients, often in combination with an isogenic normal phenotype (11, 12, 14, 15). Just recently, Wolter et al. reported a high prevalence of SCVs in children with CF (24%), and most of these (95%) were TD-SCVs (16). A detailed characterization of clinical *S. aureus* TD-SCVs is given in Kahl et al. (17–19), where special features including gross morphological changes, impaired cell separation, and altered transcription patterns of important metabolism and virulence genes as well as of virulence regulators are described. TD-SCVs grow unaffected in the presence of SXT if TD-SCVs have access to extracellular thymidine such as that present in infected tissues and purulent airway secretions (13, 20).

The antibacterial effects of SXT are due to the interference of the drug with the bacterial folate pathway by competitive inhibition of dihydropteroate synthase and dihydrofolate reductase, two proteins involved in the synthesis and conversion of tetrahydrofolic acid (THF). THF acts as a cofactor for thymidylate synthase ([TS] *thyA*), which is essential for the *de novo* thymidylate biosynthesis (21, 22) required for DNA synthesis and bacterial replica-

Received 31 March 2015 Returned for modification 11 May 2015
Accepted 4 September 2015
Accepted manuscript posted online 14 September 2015
Citation Kriegeskorte A, Lorè NI, Bragonzi A, Riva C, Kelkenberg M, Becker K, Proctor RA, Peters G, Kahl BC. 2015. Thymidine-dependent *Staphylococcus aureus* small-colony variants are induced by trimethoprim-sulfamethoxazole (SXT) and have increased fitness during SXT challenge. Antimicrob Agents Chemother 59:7265–7272. doi:10.1128/AAC.00742-15.
Address correspondence to Barbara C. Kahl, kahl@uni-muenster.de.
Supplemental material for this article may be found at http://dx.doi.org/10.1128/AAC.00742-15.

TABLE 1 Analysis of the *thyA* genes from revertant strains in comparison to genes of their parent isolates

Parent strain and variant	TD phenotype[a]	Alteration(s) in *thyA*[b]	Predicted alteration or point mutation (position)[c]	Reference or source
Normal-5	−	G561T	Trp → Tyr (188)	1
SCV-5	+	T564G	Trp → stop (188)	1
Revertant-5	−	T562C, T564G	Trp → Gln (188)	This study
Normal-6	−			1
SCV-6	+	C941A	Ala → Asp (314)	1
Revertant-6	−	C941T	Ala → Phe (314)	This study
Normal-7	−			24
SCV-7	+	C705A	Ser → Arg (235)	24
Revertant-7	−			This study
Newman WT	−			24
Newman SCV	+	G748T	Glu → stop (249)	24
Newman revertant	−	G748A	Glu → Lys (249)	This study

[a] TD, thymidine-dependent.
[b] Only nonsynonymous mutations in *thyA* compared to the *thyA* gene of *S. aureus* 8325-4 are shown.
[c] Amino acid position.

tion. We along with others have shown that mutations in *thyA* are responsible for thymidine dependency of *S. aureus* TD-SCVs and that the emergence of these SCVs is associated with SXT treatment (21, 22).

However, until now the emergence of TD-SCVs has never been studied systematically, which we aimed to do in this study.

MATERIALS AND METHODS

Ethics statement. Animal studies were conducted according to protocols approved by the San Raffaele Scientific Institute (Milan, Italy) Institutional Animal Care and Use Committee (IACUC) and adhered strictly to the Italian Ministry of Health guidelines for the use and care of experimental animals.

Bacterial strains and plasmids. Strains and plasmids used in this study are listed in Table 1. *S. aureus* SH1000, a *sigB*-positive variant (*rsbU*$^+$) of *S. aureus* 8325-4 (23), and its Δ*thyA* mutant (24) were used for competition experiments. Three clinical strain pairs of *S. aureus*, consisting of TD-SCVs and the respective isogenic normal phenotype, were isolated from airway secretions of CF patients who were treated long term with SXT (24).

Media and growth conditions. For cultivation of *S. aureus*, tryptic soy agar (BD, Heidelberg, Germany), Columbia blood agar (BD), Mueller-Hinton (MH) agar (Heipha Dr. Müller GmbH, Eppelheim, Germany), brain heart infusion (BHI) broth (Merck, Darmstadt, Germany), chemically defined medium to determine auxotrophisms of SCVs (25), and Luria-Bertani (LB) broth (BD) were used.

DNA extraction and sequencing. *S. aureus* cells were lysed with lysostaphin (WAK Chemie Medical GmbH, Steinbach/Ts, Germany). Chromosomal DNA was prepared using a PrestoSpin D kit (Molzym GmbH and Co. KG, Bremen, Germany). All *thyA* sequences were cloned in the vector pQE30Xa (Qiagen, Hilden, German) using the primers thyA-fwd (TTG AAT TCA TTT GAT GCA GCA TAT CAC) and thyA-rev (TCA GGA TCC CTA CAC TGC TAT TGG AGC) as described before (25) and sequenced at Eurofins MWG Operon (Martinsried, Germany) using the primers pQE-for (GTA TCA CGA GGC CCT TTC GTC T) and pQE-rev (CAT TAC TGG ATC TAT CAA CAG GAG).

Induction of TD-SCVs by SXT. To induce/select for TD-SCVs, the laboratory *S. aureus* strain Newman was cultured with SXT (240 μg/ml) in BHI broth (10 ml of medium in 100-ml baffled flasks at 160 rpm and 37°C) for several days. After each overnight (ON) culture, appropriate dilutions were streaked on Columbia blood agar. Small colonies were selected, subcultured, and tested for thymidine auxotrophism (11).

Reversion experiments. First, the background frequency of mutation was determined by assessing the mutation rate of normal SCVs and TD-SCVs subjected to rifampin treatment (26). Briefly, one bacterial colony was resuspended in 20 ml of BHI broth and incubated overnight at 37°C at 160 rpm. Bacterial cells were collected by centrifugation at 3,000 rpm for 5 min and resuspended in 1 ml of BHI broth. A 100-μl sample of this suspension was further diluted and plated onto BHI agar plates with and without rifampin. The same dilutions were plated on MH agar plates, which are low in thymidine, to test for reversion of TD-SCVs. After 48 h, CFU were enumerated, and the mutation frequency was determined by dividing the number of CFU on the rifampin plates by the number of bacteria on BHI agar without rifampin. The reversion frequency was determined as the number of CFU on MH agar.

Competition experiments. To investigate which conditions would select for TD-SCVs, we performed competition experiments with the wild type (WT) and a constructed stable Δ*thyA* mutant (24). After individual overnight cultures of the Δ*thyA* mutant, which is erythromycin resistant, and the WT in BHI broth under aerobic conditions (shaking at 160 rpm), both phenotypes were combined and inoculated to a final optical density at 578 nm (OD_{578}) of 0.1, consisting of 0.05 OD units of each strain in fresh medium. The medium was BHI broth (i) without SXT or thymidine, (ii) with 240 μg/ml SXT, (iii) with 240 μg/ml SXT and 100 μg/ml thymidine, and (iv) with 100 μg/ml thymidine. After 24 h, cultures were transferred into fresh broth (OD of 0.1) with the respective substrates, and 100 μl of appropriate diluted aliquots were streaked on Columbia blood agar with (to select for the mutant) and without erythromycin and on MH agar for colony counting. This procedure was repeated for 5 days.

Transmission electron microscopy. Samples were prepared for ultrastructure analysis as described previously (18). Ultrathin sections were visualized on a transmission electron microscope (Philips EM201) equipped with a digital imaging system (Ditabis, Pforzheim, Germany). Normal and SCV phenotypes of cocci were counted on the various images.

Chronic pneumonia mouse model. The agar bead chronic pneumonia mouse model was used for competition experiments between the WT (*S. aureus* SH1000) and the Δ*thyA* mutant (27). A starting amount of 5×10^9 Δ*thyA* mutant cells/WT bacteria, mixed at a 1:1 ratio, was used for inclusion in the agar beads prepared according to a method described previously for *P. aeruginosa*, with modifications (28, 29). Briefly, *S. aureus* strains were cultured in BHI broth with erythromycin (2.5 μ/ml) for the mutant and without erythromycin for the WT overnight at 37°C, adjusted to a starting OD_{600} of 0.1, grown for an additional 3 h (SH1000) and 5 h (Δ*thyA* mutant) to allow agar bead preparation. Briefly, the bacteria were harvested by centrifugation and resuspended in 1 ml of phosphate-buffered saline (PBS; pH 7.4). Bacteria were added to 9 ml of BHI agar (BD), prewarmed to 45°C. This mixture was pipetted forcefully into 150 ml of heavy mineral oil at 45°C and stirred rapidly with a magnetic stirring bar for 6 min at room temperature, followed by cooling at 4°C with continuous slow stirring for 35 min. The oil-agar mixture was centrifuged at 4,000 rpm for 20 min to sediment the beads and washed six times in PBS. The size of the beads was verified microscopically, and only the preparations containing beads of 100 μm to 200 μm in diameter were used as inocula for animal experiments. The number of *S. aureus* CFU in the beads was determined by plating serial dilutions of the homogenized bacteria-bead suspension on Columbia blood agar plates with or without erythromycin (2.5 μl/ml). The inoculum was prepared by diluting the bead suspension with PBS to 1×10^7 CFU/ml.

Groups of 12 to 13 C57BL/6 male mice (20 to 22 g; Charles River Laboratories) were infected with 5×10^5 CFU of *S. aureus* as described previously (27, 30). After anesthesia and exposure of the trachea, mice were inoculated with 50 μl of agar bead suspension into the lung. After inoculation, all incisions were closed by suture. All mice were maintained under specific-pathogen-free conditions in sterile cages, which were put

into a ventilated isolator. Twenty-four hours after infection, mice were treated with SXT (Cotrim-ratiopharm Ampullen SF; Ratiopharm) (20 mg of the TMP component/kg of body weight intraperitoneally [i.p.]) or with saline as a control by intraperitoneal injection once a day. Antibiotic treatment and dose were established according to previous papers (31, 32). Twelve days after infection and repeated antibiotic treatments, the murine lungs were excised, homogenized, and plated onto BHI agar plates in the presence and absence of erythromycin (2.5 μ/ml).

The mean of the competition index (CI) was calculated as the ratio between the number of Δ*thyA* mutant and WT CFU recovered from the murine lungs at 12 days postinfection, adjusted by the input ratio of the inoculum of each animal (*in vivo* CI) (29, 33).

Statistical analysis. Statistical analyses for the *in vivo* experiments were performed by Mann-Whitney U tests for unpaired samples, using GraphPad software. Tests were considered statistically significant at a significance level of ≤0.05.

RESULTS

SXT-induced *S. aureus* TD-SCVs. To verify the impact of SXT on the emergence of TD-SCVs, we set up induction/selection experiments *in vitro*. We tried to select TD-SCVs by cultivating the laboratory *S. aureus* strain Newman, SH1000, and USA300 with SXT (240 μg/ml) in BHI broth for several days. (SXT MICs for the strains were 0.38 mg/liter, 0.047 mg/liter, and 0.064 mg/ml). After three overnight cultures with SXT, appropriate dilutions were streaked on Columbia blood agar. Small colonies were selected and subcultured. Only after several repetitions of these experiments were we able to isolate one particular SCV in strain Newman but not in *S. aureus* strain SH1000 or USA300. The strain Newman SCV failed to grow on MH agar plates and was determined to be thymidine dependent by auxotrophism testing. To confirm thymidine dependency of this isolate also on the molecular level, we sequenced the *thyA* gene of this strain and identified a point mutation at position 748 leading to a premature stop codon (Table 1). It was not possible to retrieve TD-SCVs directly after one ON culture with SXT on agar plates. Therefore, it was not possible to determine the exact *thyA* mutation frequency. Since the background mutation rate of strain Newman was 9.44×10^{-10} cells per generation, as determined in three independent experiments using the rifampin mutation frequency assay, we could only estimate the induction frequency as being approximately less than 1×10^{-10} cells per generation.

Primary mutational events in *thyA* of TD-SCVs were compensated in revertants. It is known that clinical SCVs are often not stable and revert back to the normal phenotype (34, 35). Therefore, we aimed to study reversion of TD-SCVs systematically. Three consecutive overnight cultures in BHI broth of clinical TD-SCVs and an *in vitro*-induced TD-SCV of strain Newman (Table 1) were performed. Serial dilutions of each passage were streaked on Columbia blood agar. We were able to recover revertants for SCVs with point mutations (Table 1) but not for TD-SCVs with deletions in *thyA* (data not shown). We tried to estimate the reversion frequency of SCVs by plating the samples after overnight culture in addition to BHI with and without rifampin also on MH agar to assess reversion frequency. While TD-SCVs are not able to grow on MH agar, which contains small amounts of thymidine, revertants can grow on this agar. Since SCVs are impaired in their replication, not all of the SCVs yield high numbers of bacteria after overnight culture. Therefore, it was not possible to determine the mutation frequency for all TD-SCVs. We were able to get a high enough density for one of the clinical TD-SCVs with 6.45×10^8 CFU/ml. For this TD-SCV we determined a background mutation rate of 1.55×10^{-9} with no growth on MH agar. From these results we estimated the reversion frequency of this TD-SCV as being lower than 1×10^{-9}. Sequence analysis of the *thyA* genes of all revertants revealed second point mutations at the initially identified mutation site leading back to *thyA* of the WT strain or to a novel sequence leading to another amino acid exchange (Table 1).

SXT exposure induced the SCV phenotype morphologically in normal *S. aureus* cells. To analyze the effects of SXT on *S. aureus*, we exposed *S. aureus* WT (SH1000) and the Δ*thyA* mutant (24) strains to SXT (240 μg/ml). We analyzed the effects on *S. aureus* morphology by light microscopy (see Fig. S1 in the supplemental material) and by transmission electron microscopy (TEM). In BHI broth, the Δ*thyA* mutant showed significantly enlarged cocci with multiple and partially incomplete cross walls in contrast to the homogenous morphology of the WT (Fig. 1A). If thymidine was added to BHI broth, the sizes of the cocci decreased, with a mixture of normal and enlarged cells in the mutant, while the phenotype of the WT did not change (Fig. 1B). Challenge with SXT did not affect the morphology of the TD-SCV (Fig. 1C) but caused enlarged cocci with impaired cell division in the WT strain comparable to the phenotype of the mutant (Fig. 1C). Further addition of thymidine to the medium containing SXT caused changes in both strains almost leading back to the normal morphology (Fig. 1D). The prevalences of normal and SCV phenotypes were determined for the respective images (Table 2). During SXT exposure, 46% of cocci of the WT exhibited the SCV phenotype, while 69% of the cocci of the Δ*thyA* mutant showed this phenotype. Addition of thymidine under SXT challenge caused reversion to the normal phenotype in 94% of cocci of the WT and in 79% of the cocci of the mutant. Using light microscopy analysis (37) of Gram stainings (see Fig. S1 in the supplemental material), the sizes of 100 cocci of three biological replicates of each condition were measured and showed the same effects: the sizes of the TD-SCVs were significantly smaller with additional thymidine in the medium, with or without SXT, while the sizes of the WT cells were significantly larger under SXT challenge, a characteristic which was reverted by the addition of thymidine (Fig. 2).

Advantage of the Δ*thyA* mutant under SXT exposure *in vitro*. To assess both the relative fitness of the Δ*thyA* mutant compared to that of its parent strain and the conditions which would select for TD-SCVs, we performed competition experiments exposing the Δ*thyA* mutant and the WT strain to SXT with and without additional thymidine in BHI broth (Fig. 3). By adding thymidine to BHI broth, we expected a growth advantage for the WT under SXT challenge. The WT showed a considerably higher growth rate than the Δ*thyA* mutant in BHI broth without SXT (data not shown) and comparable growth to that of the Δ*thyA* mutant under SXT challenge. As expected, the WT was the predominant phenotype under three of the four tested conditions (BHI, BHI plus SXT plus thymidine, and BHI plus thymidine) after 5 days of serial subcultures (data not shown). Only under low-thymidine conditions, as with BHI broth and SXT exposure (BHI plus SXT), the Δ*thyA* mutant outcompeted the WT and almost entirely displaced the WT within 5 days of serial subcultures (Fig. 3).

Advantage of the Δ*thyA* mutant in a chronic murine pneumonia model under SXT treatment. To further investigate the

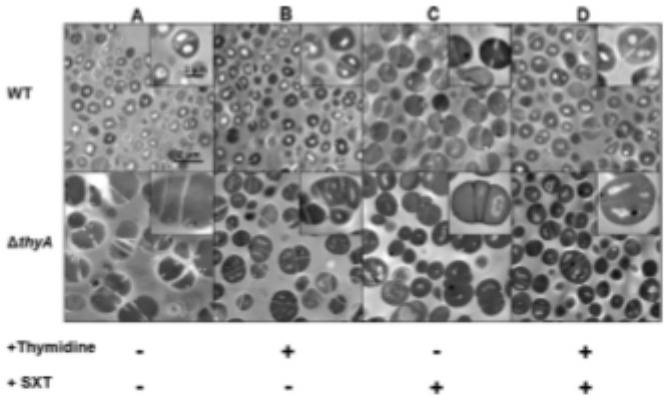

FIG 1 WT *S. aureus* SH1000 and the Δ*thyA* mutant under SXT challenge with and without thymidine. Strains were cultured in BHI broth under SXT exposure with and without additional thymidine. TEM was performed to analyze the phenotypic changes of the wild-type (SH1000) and the mutant (Δ*thyA* strain) under different conditions, as follows: BHI, showing the typical phenotypes of WT *S. aureus* and the Δ*thyA* mutant, which is characterized by enlarged cocci with several division planes (A); BHI broth plus 100 μg/ml thymidine, showing that the WT phenotype did not change but that the mutant was partially complemented with smaller cocci than in culture with BHI broth without additional thymidine (B); BHI broth plus 240 μg/ml SXT, which demonstrates that the WT resembles the mutant under these conditions, with enlarged cocci, while the phenotype of the mutant did not change (C); BHI plus 100 μg/ml thymidine plus 240 μg/ml SXT, where adding thymidine to SXT-challenged bacteria almost reverts both SCV phenotypes back to the normal phenotypes in the WT and in the mutant (D).

relative fitness of the Δ*thyA* mutant in comparison with that of the WT under *in vivo* conditions, we performed competition experiments in a chronic murine pneumonia model with or without SXT treatment (Fig. 4). First, the WT has a significantly better fitness in the murine lung than the Δ*thyA* mutant. After antibiotic treatment for 12 days, the total number of bacteria present in lung samples was lower (Fig. 4, top), indicating the therapeutic benefit of SXT to reduce bacterial infection. However, SXT treatment was more efficient in reducing bacterial counts of the WT than of the Δ*thyA* mutant strain. As already observed for other pathogens, the antibiotic treatment failed to completely eradicate chronic infection under these experimental conditions (33). Thus, significant reduction of the WT population was observed under treated conditions compared to the level of the untreated condition ($P < 0.05$), while bacterial counts of the Δ*thyA* mutant were unchanged. In terms of the competition index (CI), the nontreated group showed a CI value of 0.95×10^{-1}, indicating an advantage of the WT over the Δ*thyA* mutant strain, whereas the treated group increased the CI to 0.78, resulting in almost comparable fitness levels of the mutant and the WT under this condition (Fig. 4, bottom). These results show that during SXT challenge the fitness of the mutant, but not of the WT, increased (CI, $P < 0.05$).

TABLE 2 Frequency of normal and SCV phenotypes of the WT and the Δ*thyA* mutant strains under different conditions

Strain and phenotype	No. of cocci (%) for the indicated Fig. 1 panel and treatment			
	A (none)	B (+ thymidine)	C (+ SXT)	D (+ thymidine, + SXT)
WT				
Normal	100 (100)	92 (100)	18 (54)	50 (94)
SCV	0 (0)	0 (0)	15 (46)	3 (6)
Δ*thyA* strain				
Normal	3 (18)	19 (58)	8 (31)	31 (79)
SCV	14 (82)	14 (52)	18 (69)	8 (21)

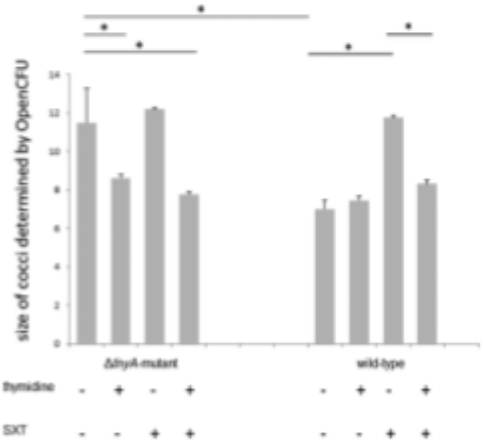

FIG 2 Size analysis of SH1000 and the Δ*thyA* mutant cocci under SXT challenge with and without thymidine by light microscopy. The WT and the Δ*thyA* mutant were cultured under the same conditions as described in the legend of Fig. 1. The overnight culture was centrifuged, resuspended in 1 ml of BHI broth, and subjected to Gram staining and size analysis of each 100 cocci using OpenCFU. Data are shown for three biological replicates with means and standard deviations. The significance of differences in sizes of cocci was calculated by a *t* test (*, $P < 0.05$).

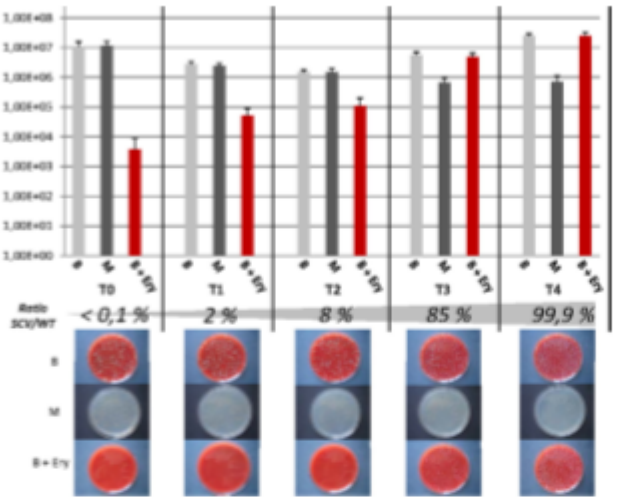

FIG 3 *In vitro* competition assay of the SH1000 WT and the Δ*thyA* mutant under low-thymidine conditions (in BHI broth). After individual overnight cultures in BHI broth (37°C and 160 rpm), the strains were combined and inoculated to a final OD of 0.1 consisting of 0.05 OD units of each strain in fresh medium (BHI plus 240 μg/ml SXT). After 24 h of coincubation, an aliquot of the culture (corresponding to an OD of 0.1) was transferred into fresh medium. One hundred microliters of appropriate dilutions (10^{-1} to 10^{-6}) were streaked on Columbia blood agar (B), on which all bacteria grow, on Columbia blood agar with erythromycin (B + Ery), on which only the mutant grows, and on Mueller-Hinton agar (M), which allows growth of only the WT and not of the mutant, which needs additional thymidine. CFU/ml was determined by colony counting (see graphs). The ratio of the number of the SH1000 Δ*thyA* mutant CFU to the number of the SH1000 WT CFU was calculated. Images of the agar plates show the growth of the WT and mutant. At the beginning only low numbers of the mutant were detected on cultures plated on Columbia blood agar with erythromycin compared to numbers of the WT plated on Mueller-Hinton agar (5.0×10^5 CFU versus 1.0×10^7 CFU), while after 5 days of SXT challenge more CFU of the mutant than of the WT were cultured (1.3×10^7 CFU versus 8.0×10^5 CFU), indicating that the mutant outcompeted the WT under these conditions. T0 to T4, time period day 1 to day 5 of coincubation.

DISCUSSION

For more than a decade, it has been shown that the emergence of *S. aureus* TD-SCVs is associated with prolonged SXT treatment (11). However, the reasons why TD-SCVs emerge and why they are especially associated with chronic *S. aureus* infections are not known. This study showed for the first time that SXT exposure induced, selected, and conferred a survival and growth advantage to TD-SCVs in low-thymidine-containing environments and that mutational inactivation of *thyA* is the molecular mechanism leading to the clinical TD-SCV phenotype.

Having shown earlier that mutations in *thyA* caused inactivity of the protein (24), we aimed to induce TD-SCVs with *thyA* mutations *in vitro* by SXT challenge. This was only possible after prolonged exposure of *S. aureus* to SXT in BHI broth as shown here for the widely used laboratory *S. aureus* strain Newman but not for strain SH1000 or USA300. After several attempts of induction, we isolated a typical TD-SCV which did not grow on MH agar and which was thymidine dependent. Such a low mutation frequency might be due to the high fitness costs that thymidine dependency causes for the bacteria, indicating that selection of TD-SCVs requires long-term exposure. Such results are in line with earlier studies in CF patients, which showed that TD-SCVs were isolated after approximately 18 months of SXT treatment (11). The induced TD-SCV in the *S. aureus* strain Newman carried a point mutation in *thyA*, leading to a premature stop codon. Similar mutations were already seen in clinical TD-SCVs (21, 22, 24).

The fact that TD-SCVs were isolated from patients *in vivo* who were treated with SXT for long periods (11–13, 16, 24, 36) indicates that particular conditions seem to favor the emergence of TD-SCVs. To simulate such clinical conditions, we performed competition experiments comparing the WT and the Δ*thyA* mutant during SXT exposure *in vitro* and *in vivo*. In the *in vitro* experiments, the Δ*thyA* mutant had a clear growth and survival advantage under SXT exposure compared to that of the WT in one out of four tested conditions. Only in BHI broth plus SXT, which contains low but sufficient amounts of thymidine, did the mutant out-compete the WT. Low concentrations of thymidine, such as those present in BHI broth, are supposed to be available in chronically infected tissues in contrast to conditions in acute infections, with large amounts of thymidine present due to cell detritus, pus, and DNA degradation (20). Only these conditions favored the selection of TD-SCVs. In addition, the *in vitro* results were supported by our *in vivo* competition experiments.

In the *in vivo* competition experiments using a chronic pneumonia model, which compared SXT-treated to nontreated mice, we show that the WT was the dominant phenotype in the nontreated group. However, SXT treatment reduced the number of the WT cells significantly but not the numbers of the Δ*thyA* mutant cells, indicating an advantage of the mutant in this model under antibiotic treatment. Although we established for the first time a 2-week mouse pneumonia infection model for *S. aureus*, this extended period still seems to be too short to reflect real long-

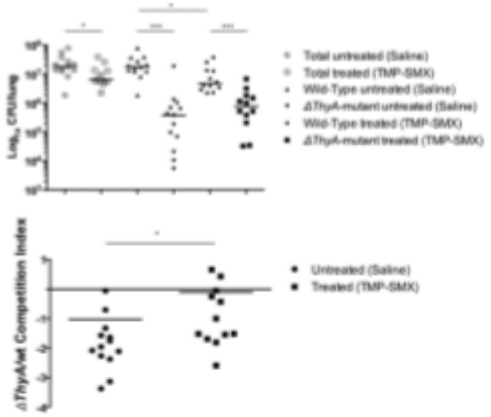

FIG 4 *In vivo* competition between the Δ*thyA* mutant and the WT *S. aureus* strain in C57BL/6 mice. The Δ*thyA* mutant and the WT *S. aureus* strain SH1000 were embedded in agar beads and used to infect 12 to 13 C57BL/6 mice/group. Chronic infection was sustained for 12 days with and without treatment by SXT, and the numbers of CFU per lung were evaluated on erythromycin-selective plates to distinguish the two competitors (top). CI was calculated by dividing the ratio of the number of CFU of the Δ*thyA* mutant/number of CFU of the WT strain recovered from the lungs by the ratio of the number of the CFU of the Δ*thyA* mutant/number of the CFU of the WT strain of the inoculum for each animal (bottom). Dots represent individual measurements, and horizontal lines represent the geometric means. A CI of <1 indicated a disadvantage for the Δ*thyA* mutant in being maintained *in vivo* compared with the WT strain SH1000. Statistical analysis was calculated for each *in vivo* competition between the two treated groups with and without SXT (*, $P < 0.05$; *** $P < 0.01$, Mann-Whitney two-tailed test). The results show that during SXT challenge, the fitness of the mutant but not of the WT increased. TMP-SMX, trimethoprim-sulfamethoxazole (SXT).

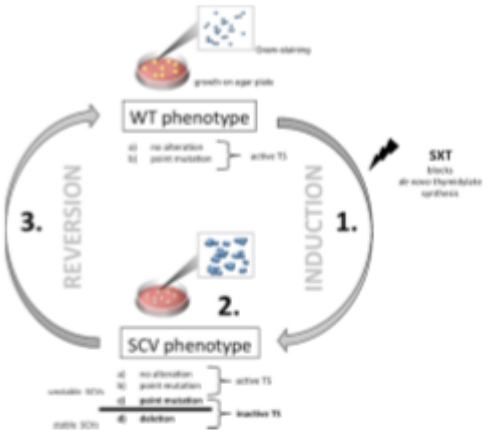

FIG 5 A model for the dynamics of TD-SCVs. A three-step model explains the dynamics of TD-SCV formation and reversion. In a low-thymidine environment, treatment with SXT will induce the formation of SCV phenotypes in the whole *S. aureus* population by blocking thymidylate *de novo* synthesis (step 1). Two types of functional inactivation of *thyA* are possible: (i) point mutations, leading to single amino acid substitutions, and (ii) deletions, leading to frameshift or in-frame mutations (step 2). TD-SCVs with point mutations can revert back to the WT phenotype representing unstable SCVs, while TD-SCVs with deletions are very unlikely to revert, therefore representing a stable TD-SCV population (step 3). Once the strains are no longer exposed to SXT, induced SCVs and TD-SCVs with point mutations revert back to the WT phenotype.

term infections in humans with CF, which can go on for months or even years.

However, the *in vitro* and *in vivo* results of our competition experiments indicate that our results can be directly transferred to the *in vivo* situation, in which treatment with SXT causes selection of TD-SCVs at sites where sufficient amounts of thymidine are available. Zander et al. demonstrated that thymidine is available in various human specimens (20), showing that thymidine is provided by pus and cell detritus and thereby allows growth and survival of TD-SCVs.

Our results allow us to propose a three-step model for the dynamics of TD-SCV formation and reversion (Fig. 5). If thymidine availability is low, as at some infection sites, short-term challenge by SXT induces the formation of SCV phenotypes in the whole *S. aureus* population, as shown by TEM (Fig. 1), due to blocking *de novo* thymidylate synthesis. If SXT is present for extended periods, such conditions will favor a thymidine-dependent phenotype based on random mutations within *thyA*, leading to inactivity of the TS protein. Two types of functional inactivation of *thyA* are possible: (i) point mutations, leading to single amino acid substitutions, and (ii) deletions, leading to frameshift or in-frame mutations. If SXT exposure is halted (e.g., end of antibiotic treatment), TD-SCVs with point mutations may revert, while TD-SCVs with deletions are very unlikely to revert, thereby representing a stable TD-SCV population. Once the population is no longer exposed to SXT, phenotypically induced SCVs revert back to the WT phenotype while stable TD-SCVs (with mutations in *thyA*) will remain. However, treatment with SXT favors TD-SCVs *in vivo* and *in vitro*, and one could speculate that several episodes of treatment will lead to a diversification of the whole *S. aureus* population. This population then consists of WT phenotypes including revertants with and without point mutations in *thyA* and TD-SCVs, which can revert or are stable, depending on the underlying mutational event.

In summary, our results provide for the first time clear evidence that short-term SXT exposure induces the TD-SCV phenotype in WT *S. aureus* and that long-term exposure drives the selection of mutations in *thyA*, resulting in TD-SCVs which have a survival advantage in a specific environment with low thymidine availability. Thus, our results help further an understanding of the dynamic processes of *S. aureus* phenotypic adaptation and selection during SXT challenge.

ACKNOWLEDGMENTS

We thank S. Deiwick, D. Kuhn, and E. Leidig (Institute of Medical Microbiology, University Hospital of Muenster, Muenster, Germany) for excellent technical assistance. We thank Wolfgang Völker (Leibniz Institute of Atherosclerosis Research, University Hospital of Muenster, Muenster, Germany) for excellent transmission electron microscopy. We thank Melisa Zengin, a summer student from Hacettepe University, Ankara, Turkey, for performing Gram stainings and size analysis of cocci.

This project was funded partly by grants of the German Research Foundation (Deutsche Forschungsgemeinschaft [DFG]; KA 2249/1-3,

DFG Spp 1316, and BE 2546/1-2), the Interdisciplinary Center for Clinical Research (IZKF Münster; Kah2/024/09), the Transregional Collaborative Research Center 34 (C7), and the Bundesministerium für Bildung und Forschung (BMBF Medizinische Infektionsgenomik; 0315829B).

There are no conflicts of interest for any of the authors.

REFERENCES

1. Lowy FD. 1998. *Staphylococcus aureus* infections. N Engl J Med 339:520–532. http://dx.doi.org/10.1056/NEJM199808203390806.
2. Chua K, Laurent F, Coombs G, Grayson ML, Howden BP. 2011. Antimicrobial resistance: not community-associated methicillin-resistant *Staphylococcus aureus* (CA-MRSA)! A clinician's guide to community MRSA—its evolving antimicrobial resistance and implications for therapy. Clin Infect Dis 52:99–114. http://dx.doi.org/10.1093/cid/ciq067.
3. Talan DA, Krishnadasan A, Gorwitz RJ, Fosheim GE, Limbago B, Albrecht V, Moran GJ. 2011. Comparison of *Staphylococcus aureus* from skin and soft-tissue infections in US emergency department patients, 2004 and 2008. Clin Infect Dis 53:144–149. http://dx.doi.org/10.1093/cid/cir308.
4. Hanaki H, Cui L, Ikeda-Dantsuji Y, Nakae T, Honda J, Yanagihara K, Takesue Y, Matsumoto T, Sunakawa K, Kaku M, Tomono K, Fukuchi K, Kusachi S, Mikamo H, Takata T, Otsuka Y, Nagura O, Fujitani S, Aoki Y, Yamaguchi Y, Tateda K, Kadota J, Kohno S, Niki Y. 2014. Antibiotic susceptibility survey of blood-borne MRSA isolates in Japan from 2008 through 2011. J Infect Chemother 20:527–534. http://dx.doi.org/10.1016/j.jiac.2014.06.012.
5. Levesque S, Bourgault AM, Galarneau LA, Moisan D, Doualla-Bell F, Tremblay C. 2015. Molecular epidemiology and antimicrobial susceptibility profiles of methicillin-resistant *Staphylococcus aureus* blood culture isolates: results of the Quebec Provincial Surveillance Programme. Epidemiol Infect 143:1511–1518. http://dx.doi.org/10.1017/S095026881400209X.
6. Schmitz GR, Bruner D, Pitotti R, Oldenburg C, Livengood T, Williams J, Huebner K, Lightfoot J, Ritz B, Bates C, Schmitz M, Mete M, Deye G. 2010. Randomized controlled trial of trimethoprim-sulfamethoxazole for uncomplicated skin abscesses in patients at risk for community-associated methicillin-resistant *Staphylococcus aureus* infection. Ann Emerg Med 56:283–287. http://dx.doi.org/10.1016/j.annemergmed.2010.03.002.
7. Duong M, Markwell S, Peter J, Barenkamp S. 2010. Randomized, controlled trial of antibiotics in the management of community-acquired skin abscesses in the pediatric patient. Ann Emerg Med 55:401–407. http://dx.doi.org/10.1016/j.annemergmed.2009.03.014.
8. Pallin DJ, Binder WD, Allen MB, Lederman M, Parmar S, Filbin MR, Hooper DC, Camargo CA, Jr. 2013. Clinical trial: comparative effectiveness of cephalexin plus trimethoprim-sulfamethoxazole versus cephalexin alone for treatment of uncomplicated cellulitis: a randomized controlled trial. Clin Infect Dis 56:1754–1762. http://dx.doi.org/10.1093/cid/cit122.
9. De Angelis G, Cipriani M, Cauda R, Tacconelli E. 2011. Treatment of skin and soft tissue infections due to community-associated methicillin-resistant *Staphylococcus aureus* in Europe: the role of trimethoprim-sulfamethoxazole. Clin Infect Dis 52:1471–1472. http://dx.doi.org/10.1093/cid/cir247.
10. Proctor RA. 2008. Role of folate antagonists in the treatment of methicillin-resistant *Staphylococcus aureus* infection. Clin Infect Dis 46:584–593. http://dx.doi.org/10.1086/525536.
11. Kahl B, Herrmann M, Everding AS, Koch HG, Becker K, Harms E, Proctor RA, Peters G. 1998. Persistent infection with small colony variant strains of *Staphylococcus aureus* in patients with cystic fibrosis. J Infect Dis 177:1023–1029. http://dx.doi.org/10.1086/515238.
12. Besier S, Smaczny C, von Mallinckrodt C, Krahl A, Ackermann H, Brade V, Wichelhaus TA. 2007. Prevalence and clinical significance of *Staphylococcus aureus* small-colony variants in cystic fibrosis lung disease. J Clin Microbiol 45:168–172. http://dx.doi.org/10.1128/JCM.01510-06.
13. Besier S, Zander J, Siegel E, Saum SH, Hunfeld KP, Ehrhart A, Brade V, Wichelhaus TA. 2008. Thymidine-dependent *Staphylococcus aureus* small-colony variants: human pathogens that are relevant not only in cases of cystic fibrosis lung disease. J Clin Microbiol 46:3829–3832. http://dx.doi.org/10.1128/JCM.01440-08.
14. Yagci S, Hascelik G, Dogru D, Ozcelik U, Sener B. 2013. Prevalence and genetic diversity of *Staphylococcus aureus* small-colony variants in cystic fibrosis patients. Clin Microbiol Infect 19:77–84. http://dx.doi.org/10.1111/j.1469-0691.2011.03742.x.
15. Gilligan PH, Gage PA, Welch DF, Muszynski MJ, Watt KR. 1987. Prevalence of thymidine-dependent *Staphylococcus aureus* in patients with cystic fibrosis. J Clin Microbiol 25:1258–1261.
16. Wolter DJ, Emerson JC, McNamara S, Buccat AM, Qin X, Cochrane E, Houston LS, Rogers GB, Marsh P, Prehar K, Pope CE, Blackledge M, Deziel E, Bruce KD, Ramsey BW, Gibson RL, Burns JL, Hoffman LR. 2013. *Staphylococcus aureus* small-colony variants are independently associated with worse lung disease in children with cystic fibrosis. Clin Infect Dis 57:384–391. http://dx.doi.org/10.1093/cid/cit270.
17. Kahl BC, Belling G, Becker P, Chatterjee I, Wardecki K, Hilgert K, Cheung AL, Peters G, Herrmann M. 2005. Thymidine-dependent *Staphylococcus aureus* small colony variants are associated with extensive changes in regulator and virulence gene expression profiles. Infect Immun 73:4119–4126. http://dx.doi.org/10.1128/IAI.73.7.4119-4126.2005.
18. Kahl BC, Belling G, Reichelt R, Herrmann M, Proctor RA, Peters G. 2003. Thymidine-dependent small-colony variants of *Staphylococcus aureus* exhibit gross morphological and ultrastructural changes consistent with impaired cell separation. J Clin Microbiol 41:610–613. http://dx.doi.org/10.1128/JCM.41.1.410-413.2003.
19. Chatterjee I, Herrmann M, Proctor RA, Peters G, Kahl BC. 2007. Enhanced post-stationary-phase survival of a clinical thymidine-dependent small-colony variant of *Staphylococcus aureus* results from lack of a functional tricarboxylic acid cycle. J Bacteriol 189:2936–2940. http://dx.doi.org/10.1128/JB.01444-06.
20. Zander J, Besier S, Saum SH, Dehghani F, Loitsch S, Brade V, Wichelhaus TA. 2008. Influence of dTMP on the phenotypic appearance and intracellular persistence of *Staphylococcus aureus*. Infect Immun 76:1333–1339. http://dx.doi.org/10.1128/IAI.01075-07.
21. Besier S, Ludwig A, Ohlsen K, Brade V, Wichelhaus TA. 2007. Molecular analysis of the thymidine-auxotrophic small colony variant phenotype of *Staphylococcus aureus*. Int J Med Microbiol 297:217–225. http://dx.doi.org/10.1016/j.ijmm.2007.02.003.
22. Chatterjee I, Kriegeskorte A, Fischer A, Deiwick S, Theimann N, Proctor RA, Peters G, Herrmann M, Kahl BC. 2008. In vivo mutations of thymidylate synthase (*thyA*) are responsible for thymidine dependency in clinical small colony variants (TD-SCVs) of *Staphylococcus aureus*. J Bacteriol 190:834–842. http://dx.doi.org/10.1128/JB.00912-07.
23. Horsburgh MJ, Aish JL, White IJ, Shaw L, Lithgow JK, Foster SJ. 2002. σ^B modulates virulence determinant expression and stress resistance: characterization of a functional *rsbU* strain derived from *Staphylococcus aureus* 8325-4. J Bacteriol 184:5457–5467. http://dx.doi.org/10.1128/JB.184.19.5457-5467.2002.
24. Kriegeskorte A, Block D, Drescher M, Windmuller N, Mellmann A, Baum C, Neumann C, Lore NI, Bragonzi A, Liebau E, Hertel P, Seggewiss J, Becker K, Proctor RA, Peters G, Kahl BC. 2014. Inactivation of *thyA* in *Staphylococcus aureus* attenuates virulence and has a strong impact on metabolism and virulence gene expression. mBio 5:e01447–14. http://dx.doi.org/10.1128/mBio.01447-14.
25. van de Rijn I, Kessler RE. 1980. Growth characteristics of group A streptococci in a new chemically defined medium. Infect Immun 27:444–448.
26. Besier S, Zander J, Kahl BC, Kraiczy P, Brade V, Wichelhaus TA. 2008. The thymidine-dependent small-colony-variant phenotype is associated with hypermutability and antibiotic resistance in clinical *Staphylococcus aureus* isolates. Antimicrob Agents Chemother 52:2183–2189. http://dx.doi.org/10.1128/AAC.01395-07.
27. Bragonzi A, Worlitzsch D, Pier GB, Timpert P, Ulrich M, Hentzer M, Andersen JB, Givskov M, Conese M, Doring G. 2005. Nonmucoid *Pseudomonas aeruginosa* expresses alginate in the lungs of patients with cystic fibrosis and in a mouse model. J Infect Dis 192:410–419. http://dx.doi.org/10.1086/431516.
28. Bragonzi A, Farulla I, Paroni M, Twomey KB, Pirone L, Lore NI, Bianconi I, Dalmastri C, Ryan RP, Bevivino A. 2012. Modelling co-infection of the cystic fibrosis lung by *Pseudomonas aeruginosa* and *Burkholderia cenocepacia* reveals influences on biofilm formation and host response. PLoS One 7:e52330. http://dx.doi.org/10.1371/journal.pone.0052330.
29. Montanari S, Oliver A, Salerno P, Mena A, Bertoni G, Tummler B, Cariani L, Conese M, Doring G, Bragonzi A. 2007. Biological cost of hypermutation in *Pseudomonas aeruginosa* strains from patients with cystic fibrosis. Microbiology 153:1445–1454. http://dx.doi.org/10.1099/mic.0.2006/003400-0.
30. Bragonzi A, Paroni M, Nonis A, Cramer N, Montanari S, Rejman J, Di SC, Doring G, Tummler B. 2009. *Pseudomonas aeruginosa* microevolution during cystic fibrosis lung infection establishes clones with adapted

virulence. Am J Respir Crit Care Med 180:138–145. http://dx.doi.org/10.1164/rccm.200812-1943OC.
31. Bhagwat SP, Wright TW, Gigliotti F. 2010. Anti-CD3 antibody decreases inflammation and improves outcome in a murine model of *Pneumocystis* pneumonia. J Immunol 184:497–502. http://dx.doi.org/10.4049/jimmunol.0901864.
32. Disney MD, Stephenson R, Wright TW, Haidaris CG, Turner DH, Gigliotti F. 2005. Activity of Hoechst 33258 against *Pneumocystis carinii* f. sp. *muris*, *Candida albicans*, and *Candida dubliniensis*. Antimicrob Agents Chemother 49:1326–1330. http://dx.doi.org/10.1128/AAC.49.4.1326-1330.2005.
33. Alcala-Franco B, Montanari S, Cigana C, Bertoni G, Oliver A, Bragonzi A. 2012. Antibiotic pressure compensates the biological cost associated with *Pseudomonas aeruginosa* hypermutable phenotypes in vitro and in a murine model of chronic airways infection. J Antimicrob Chemother 67:962–969. http://dx.doi.org/10.1093/jac/dkr587.
34. Proctor RA, von Eiff C, Kahl BC, Becker K, McNamara P, Herrmann M, Peters G. 2006. Small colony variants: a pathogenic form of bacteria that facilitates persistent and recurrent infections. Nat Rev Microbiol 4:295–305. http://dx.doi.org/10.1038/nrmicro1384.
35. Tuchscherr L, Medina E, Hussain M, Volker W, Heitmann V, Niemann S, Holzinger D, Roth J, Proctor RA, Becker K, Peters G, Loffler B. 2011. *Staphylococcus aureus* phenotype switching: an effective bacterial strategy to escape host immune response and establish a chronic infection. EMBO Mol Med 3:129–141. http://dx.doi.org/10.1002/emmm.201000115.
36. Vergison A, Denis O, Deplano A, Casimir G, Claeys G, DeBaets F, DeBoeck K, Donat N, Franckx H, Gigi J, Ieven M, Knoop C, Lebeque P, Lebrun F, Malfroot A, Pauquay F, Pierard D, Van Eldere J, Struelens MJ. 2007. National survey of molecular epidemiology of *Staphylococcus aureus* colonization in Belgian cystic fibrosis patients. J Antimicrob Chemother 59:893–899. http://dx.doi.org/10.1093/jac/dkm037.
37. Geissmann Q. 2013. OpenCFU, a new free and open-source software to count cell colonies and other circular objects. PLoS One 8:e54072. http://dx.doi.org/10.1371/journal.pone.0054072.

jove Journal of Visualized Experiments www.jove.com

Video Article

Long Term Chronic *Pseudomonas aeruginosa* Airway Infection in Mice

Marcella Facchini[1,2], Ida De Fino[1,2], Camilla Riva[1,2], Alessandra Bragonzi[1]

[1]Infections and Cystic Fibrosis Unit, Division of Immunology, Transplantation and Infectious Diseases, San Raffaele Scientific Institute
[2]Italian Cystic Fibrosis Research Foundation

Correspondence to: Alessandra Bragonzi at bragonzi.alessandra@hsr.it

URL: http://www.jove.com/video/51019
DOI: doi:10.3791/51019

Keywords: Infection, Issue 85, Opportunistic Infections, Respiratory Tract Infections, Inflammation, Lung Diseases, Cystic Fibrosis, *Pseudomonas aeruginosa*

Date Published: 3/17/2014

Citation: Facchini, M., De Fino, I., Riva, C., Bragonzi, A. Long Term Chronic *Pseudomonas aeruginosa* Airway Infection in Mice. *J. Vis. Exp.* (85), e51019, doi:10.3791/51019 (2014).

Abstract

A mouse model of chronic airway infection is a key asset in cystic fibrosis (CF) research, although there are a number of concerns regarding the model itself. Early phases of inflammation and infection have been widely studied by using the *Pseudomonas aeruginosa* agar-beads mouse model, while only few reports have focused on the long-term chronic infection *in vivo*. The main challenge for long term chronic infection remains the low bacterial burden by *P. aeruginosa* and the low percentage of infected mice weeks after challenge, indicating that bacterial cells are progressively cleared by the host.

This paper presents a method for obtaining efficient long-term chronic infection in mice. This method is based on the embedding of the *P. aeruginosa* clinical strains in the agar-beads *in vitro*, followed by intratracheal instillation in C57Bl/6NCrl mice. Bilateral lung infection is associated with several measurable read-outs including weight loss, mortality, chronic infection, and inflammatory response. The *P. aeruginosa* RP73 clinical strain was preferred over the PAO1 reference laboratory strain since it resulted in a comparatively lower mortality, more severe lesions, and higher chronic infection. *P. aeruginosa* colonization may persist in the lung for over three months. Murine lung pathology resembles that of CF patients with advanced chronic pulmonary disease.

This murine model most closely mimics the course of the human disease and can be used both for studies on the pathogenesis and for the evaluation of novel therapies.

Video Link

The video component of this article can be found at http://www.jove.com/video/51019/

Introduction

Cystic fibrosis (CF) is a genetic disease caused by mutations in the cystic fibrosis transmembrane conductance regulator (CFTR) gene. This gene encodes for a chloride channel expressed on the membrane of most epithelial cells. Bronchiectasis, mucus plugging and parenchymal destruction caused mainly by *Pseudomonas aeruginosa* infections progressively lead to severe lung disease and mortality in most of the CF patients[1]. Understanding CF pathogenesis and further development of novel therapies rely on animal model with characteristic features of CF. Several mice, genetically modified for the *Cftr* gene, have been generated, but limitations in the ability of these species to recapitulate CF-like lung disease and several other organ abnormalities seen in CF patients have been widely documented[2].

Development of infection is one of the major challenges in CF animal model. The literature clearly suggests that a chronic infection lasting more than one month can be achieved only if mice are inoculated with bacteria embedded in an immobilizing agent such as agar, agarose, or seaweed alginate[3-5]. These immobilizing agents provide the microaerobic/anaerobic conditions that allow bacteria to grow in the form of microcolonies, similarly to the growth in the mucus of CF patients[6]. This model of chronic infection leads to the persistence of the bacteria in the lungs causing airway inflammation and damage[7]. However, depending on the method used, the bacterial strain and the dose inoculated in the lungs, the percentage of chronic infected mice and the bacterial load recovered in the lungs at different time points can differ considerably. In particular, the main challenge for long-term chronic infection remains the low bacterial burden by *P. aeruginosa* and the low percentage of infected mice weeks after challenge, indicating that bacterial cells are progressively cleared by the host. By selecting the *P. aeruginosa* RP73 clinical strain from a collection of CF isolates[8] we successfully obtained low mortality, more severe lesions, and high percentage of chronic infection with a stable bacterial load up to one month in C57Bl/6NCrl mice.

This paper details the methodology for embedding *P. aeruginosa* in the agar beads; we have infected mice by intratracheal instillation, measured the bacterial load and cytokines in lungs, collected BAL fluid and performed histological examination. Overall, this protocol will aid researchers in addressing fundamentally important questions on pathogenesis[9,10] and testing novel therapies against *P. aeruginosa* chronic infection[10,11].

Protocol

1. Preparing Bacteria for Chronic Infection (Three and Two Days prior to Mouse Challenge)

1. Select the appropriate *P. aeruginosa* strain to be tested.
2. Inoculate a loopful of *P. aeruginosa* from a -80 °C stock culture to a Trypticase Soy Agar (TSA) plate and incubate at 37 °C overnight.
3. Pick a single colony and inoculate into 5 ml Trypticase Soy Broth (TSB) in a 15 ml snap-capped tube and incubate at 37 °C overnight in a shaking incubator at 200 rpm.

2. Embedding Bacteria in Agar Beads for Chronic Infection (One Day prior to Infection)

1. Take a small aliquot of bacterial overnight culture, dilute 1:50 in phosphate buffered saline (PBS) and measure the optical density (OD) at 600 nm.
2. Dilute the overnight bacterial culture by adding 2 OD in a new snap-capped tube containing 20 ml of fresh TSB.
3. Incubate at 37 °C for approximately 3-4 hr to log phase in a shaking incubator at 200 rpm, until a total of 10-15 OD is reached.
4. In the meantime, prepare the TSA, made of TSB with 1.5% agar, autoclave and equilibrate at 50 °C in a water bath. Equilibrate 150 ml of preautoclaved heavy mineral oil in an Erlenmeyer flask at 50 °C in a water bath.
5. Once *P. aeruginosa* reaches the log phase, collect the bacterial cells by centrifugation at 2,700 x g for 15 min at 4 °C and discard the supernatant.
6. Resuspend the bacterial pellet in 1 ml of sterile PBS and vortex thoroughly to resuspend the pellet completely.
7. Mix 1 ml bacterial suspension with 9 ml of liquid TSA pre-equilibrated at 50 °C.
8. Add the 10 ml TSA-*P. aeruginosa* mixture to heavy mineral oil (prewarmed at 50 °C) and immediately stir for 6 min at room temperature. The agitation must produce a visible vortex in the oil.
9. Cool the mixture to 4 °C, stirring at the minimum speed for 35 min (**Figure 1**).
10. Rest the agar-beads-oil mixture in ice for an additional 20 min.
11. Transfer the agar-beads into 50 ml Falcon tubes and centrifuge at 2,700 x g for 15 min at 4 °C.
12. Accurately remove mineral oil and wash with sterile PBS six times, as described in step 2.11. After three washes, the beads can be pelleted by gravity instead of using the centrifuge. After the last wash, resuspend the agar-beads in 20-30 ml PBS.
13. Take an aliquot of the beads (approximately 0.5 ml) and aseptically homogenize.
14. Take 100 µl of the homogenized beads and dilute in 900 µl of sterile PBS. Serially dilute 1:10 down to 10^{-6}.
15. Plate serial dilution on TSA plates, including undiluted sample down to 10^{-4} and incubate plates at 37 °C.
16. Measure the bead diameter using an inverted light microscope in several fields. The bead diameter must be between 100-200 µm (**Figure 1**).
17. Store the beads overnight at 4 °C.

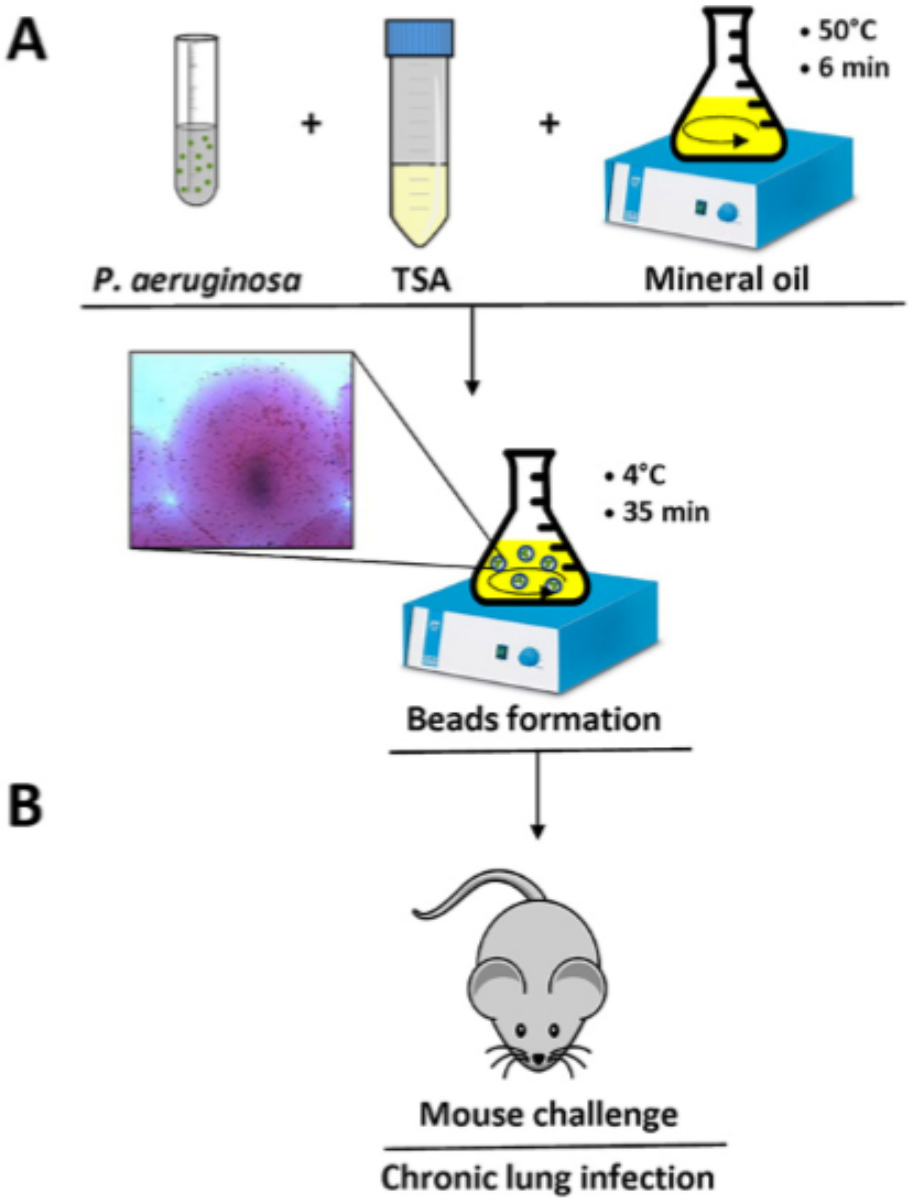

Figure 1. Overview of the agar beads preparation and mouse infection. *P. aeruginosa* cells are resuspended in 1 ml of PBS and added to 9 ml of liquid TSA (50 °C). This mixture is added to 150 ml heavy mineral oil at 50 °C in a flask and stirred at high speed for 6 min at room temperature. When the flask is cooled to 4 °C with a slow stirring for 35 min, the agar solidifies creating beads, and bacteria present in the mixture are embedded into the agar beads. Detail of an agar bead containing bacterial cells is shown (A). After removing the mineral oil with several washes using sterile PBS, the agar-beads suspension is ready for inoculation in the lungs of mice by an intratracheal injection (B). Click here to view larger image.

3. Mice Challenge with Agar-beads

Ethics Statement: This protocol and experimentation follow the guidelines from the animal care and ethics committee of San Raffaele Scientific Institute.

1. Count the number of Colony Forming Units (CFU) on the TSA plates to determine the number of CFU/ml in the agar-beads suspension. Dilute the agar-beads with sterile PBS to 2-4 x 10^7 CFU/ml to reach an optimal inoculum of 1-2 x 10^6 in 50 µl.
2. Anesthetize C57Bl/6NCr (20-22 g, 6-8 weeks old) male mice with ketamine (50 mg/ml) and xylazine (5 mg/ml) in 0.9 % NaCl administered at a volume of 0.002 ml/g body weight by intraperitoneal injection.

   NOTE: Anesthesia is considered adequate when the animal stays still quietly, is unresponsive to external stimuli, and has constant heart and respiratory rates.
3. Place the mouse in supine position. Disinfect the coat of the mouse with 70% ethanol.
4. Expose the trachea by a vertical cut of the skin and intubate the trachea with a sterile, flexible 22 G 0.9 mm x 25 mm I.V. catheter, keeping attention to remove the stylette while moving down into the trachea. Insert the catheter not too deep into the trachea. Stop before reaching the carina (bifurcation).
5. Immediately take a volume of 50 µl of agar bead suspension by a 1 ml syringe and attach it to the catheter. Gently push the plunger of the syringe, allowing the beads to be implanted into the lung. Close the incision using suture clips.
6. Place the animal on a heating pad until fully awake.

4. Mice Evaluation

1. Observe the mice daily for clinical signs including coat quality, posture, ambulation, and hydration status. Monitor daily body weight. Mice that lose ≈20% body weight must be euthanized.
2. Follow Point 5 for collection of bronchoalveolar lavage fluid (BAL) and Points 6 or 7 for the collection of lungs and the analysis of total CFU, histological analysis, inflammatory response in terms of total and differential cell count in the BAL, cytokine analysis, and myeloperoxidase (MPO) activity.

5. BAL Fluid Collection and Analysis

1. Euthanize the mice by CO_2 inhalation.
2. Place the mouse in the supine position. Disinfect the coat of the mouse with 70% ethanol.
3. Expose the trachea and the thoracic cage by a vertical cut of the skin. Expose the lungs by cutting the diaphragm.
4. Insert a suture thread under the trachea using tweezers and intubate the trachea with a sterile, flexible 22 g 0.9 mm x 25 mm I.V. catheter. Pull the two ends of the suture thread to bind the catheter to the trachea and knot the thread around the trachea.
5. Take a volume of 1 ml of RPMI 1640 using a 1 ml syringe and attach it to the catheter. Push the plunger of the syringe to wash the lungs and immediately recover the liquid, storing it in a 15 ml tube.

   NOTE: If cytokines are to be analyzed, add protease inhibitors to RPMI 1640.
6. Repeat this step three times with a total of 3 ml of RPMI. From now on, store the BAL fluid on ice. Go to step 6 for the collection and analysis of lungs.

   NOTE: Please note that not all of the liquid will be retrieved (2.8 ml maximum).
7. For quantification of bacteria present in the BAL fluid, sample a small aliquot (300 µl), serially dilute 1:10 in sterile PBS, plate on TSA plates and incubate at 37 °C overnight.
8. Count total cells using an inverted light optical microscope diluting an aliquot of the BAL fluid 1:2 with Tuerk solution in a Burker cell count chamber.
9. Centrifuge the remaining BAL fluid at 330 x g for 8 min at 4 °C. Take the supernatant for ELISA cytokine analysis, storing it at -80 °C. Follow steps 5.10-5.13 for differential cell count by cytospin.
10. If the pellet is red, lyse the erythrocytes resuspending the pellet in 250-300 µl of RBC lysis buffer diluted 1:10 in ultra-pure distilled water for 3 min. Neutralize with 2 ml PBS and centrifuge at 330 x g for 8 min at 4 °C.
11. Discard the supernatant and resuspend the pellet in RPMI 10% fetal bovine serum (FBS). Use a volume that will provide 1 x 10^6 cells/ml, based on the total cell count.
12. Place microscope slides and filters into appropriate slots in the cytospin with the cardboard filters facing the center of the cytospin. Pipette 150 µl of each sample into the appropriate wells of the cytospin and centrifuge in a cytocentrifuge at 300 x g for 5 min.
13. Stain slides by Romanowsky staining using a commercial kit, according to the manufacturer's instructions and as described previously[12]. Follow steps 5.14-5.17 for MPO activity analysis.
14. Centrifuge the remaining volume of BAL at 380 x g for 5 min at 4 °C. Discard the supernatant and resuspend the pellet in 250 µl of Hexadecyltrimethylammonium chloride 0.5% in ultra-pure distilled water to lyse the cells. The suspension can be frozen at -20 °C for several days before performing the assay.
15. Centrifuge at 16,000 x g for 30 min at 4 °C and use the supernatant to perform MPO assay in 96-well plates, adding the sample in duplicate to each well and if needed, also proper dilutions of the sample.
16. Add to each sample in the wells an equal volume of 3,3',5,5'-tetramethylbenzidine (TMB) as a substrate for peroxidase. Allow the reaction to take place in the dark for at least 5 min and until there is no further development in the color.
17. Stop the reaction by adding 2 M H_2SO_4 and measure the OD at 450 nm. The OD value will be directly proportional to peroxidase activity.

6. Measurement of Bacterial Load in Lung and Cytokine Analysis

1. Immediately after BAL fluid collection, excise lungs from the mouse, rinse them in sterile PBS, separate lobes, put them in a round-bottom tube with 2 ml of sterile PBS and store on ice.

   NOTE: If cytokines are to be analyzed, add protease inhibitors to PBS to the tubes.
2. Aseptically homogenize lungs, take a small aliquot (300 µl) from the homogenate, serially dilute 1:10 in PBS, plate on TSA plates and incubate at 37 °C overnight. Please note that the total airway bacterial load will be the sum of the CFUs found in BAL fluid and lung.
3. Centrifuge the remaining homogenate at 16,000 x g for 30 min at 4 °C. Take the supernatant for ELISA cytokine analysis, and store at -80 °C.

7. Histological Examination

1. Perform histological analysis only on the lungs in which BAL fluid has not been collected, to preserve lung aspect and properties.
2. Euthanize the mouse by CO_2 inhalation.
3. Expose the thoracic cage by a vertical cut of the skin, expose the lungs by cutting the diaphragm.
4. Excise lungs, rinse them in PBS, separate the lobes, put them in a tube containing 5-10 ml 10% neutral buffered formalin (4% formaldehyde) and store at 4 °C protected from light.
5. Embed lungs in paraffin, using standard procedures.
6. Cut 5 µm thick sections using a microtome.
7. Stain slides with hematoxylin and eosin and cover the slides with a coverslip, according to standard procedures.
8. Examine slides using an inverted brightfield microscope and acquire images by connecting the microscope to a camera.

Representative Results

When the protocol is done correctly, the *P. aeruginosa* agar-beads will measure between 100-200 µm and can be observed with an inverted light microscope by pipetting a small volume of the agar-beads suspension on a slide. Single bacterial cells are visible in the agar beads, as shown in detail in **Figure 1**.

The choice of *P. aeruginosa* strain used in the agar-beads preparation is critical. **Figure 2** and **Table 1** show the data obtained following the infection of mice with *P. aeruginosa* PAO1 reference laboratory strain compared to RP73 clinical isolate. Mortality, observed within the first 3 days of infection, is low for both strains, but higher for PAO1 (**Figures 2A** and **2B**). Considerable differences in terms of the percentage of chronic infection in the surviving mice can be observed between PAO1 and RP73 challenged mice. While at 3 days post-infection, all mice were still infected by both *P. aeruginosa* strains, after this time-point some mice cleared the bacteria and others developed a stable chronic infection. From 7 days onwards the percentage of chronically-infected mice remained stable up to 28 days for both the strains. PAO1 leads to chronic infection in a percentage of mice that ranged between 20-27.8% (**Figure 2A**), while for RP73 the percentage was 75-87.1% (**Figure 2B**), indicating that the *P. aeruginosa* clinical strain was more efficient in establishing a chronic infection compared to the PAO1 laboratory strain. Numbers of bacteria at 3 days post-infection were higher for PAO1 (5×10^7 CFU/lung) (**Figure 2C** and **Table 1**) compared to RP73 (1.3×10^6 CFU/lung) (**Figure 2D**), then from 7 days onwards, when chronic infection was established, the bacterial load stabilizes at between 10^4 and 10^5 CFU/lung for both strains. Once chronic infection is established, the number of CFU/lung does not change significantly over one month. Moreover, the bacterial load in the airways is similar among mice challenged with different bacterial strains[6,17].

Other read-outs, including the host inflammatory response and histopathology, can be measured at different time-points from challenge. **Figure 3** shows the inflammatory response in terms of leukocyte recruitment in mouse BAL fluid 7 days from challenge with *P. aeruginosa* RP73 clinical strain embedded in agar-beads. RP73-infected mice were compared to uninfected mice. Differential cell count included neutrophils, macrophages, and lymphocytes. The number of total cells is considerably higher in RP73-infected mice compared to uninfected mice. Neutrophils, in particular, almost completely absent in the BAL fluid of not-infected mice, were the most represented cellular type in RP73-infected mice, indicating a considerable response by the innate immune system to chronic infection.

The histopathological analysis of lungs from mice, chronically infected with *P. aeruginosa* RP73, shows that the infection is pluri-focal. **Figures 4C** and **4F** show one lobe that is more involved than other lobes that are unaffected or marginally involved (**Figures 4B** and **4E**). Beads can be observed in bronchial lumen and microcolonies of bacterial cells are visible in the beads (**Figures 4C** and **4F**). Lung histopathology in the areas involved by infection showed inflammatory lesions in the bronchia and in the pulmonary parenchyma. The bronchia were filled by a massive neutrophil inflammation surrounding the beads, whereas the parenchyma was infiltrated by macrophages, lymphocytes and some neutrophils. Histology of a uninfected mouse was used as a control; both parenchyma and bronchia were clear from inflammatory cells (**Figures 4A** and **4D**).

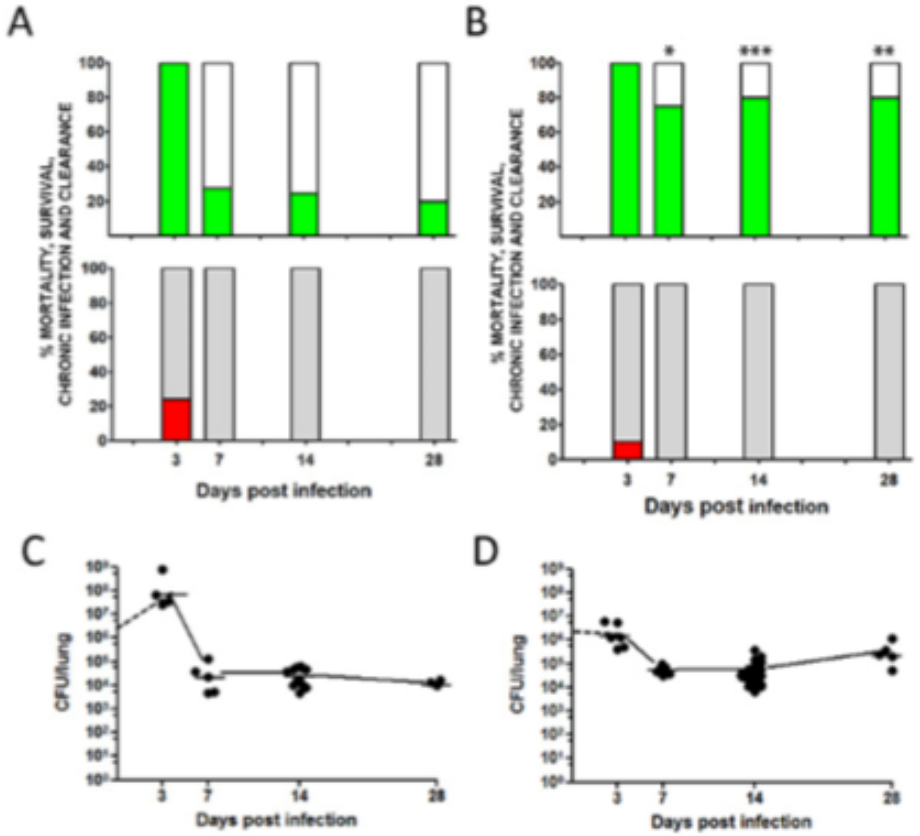

Figure 2. Time course of *P. aeruginosa* chronic infection with PAO1 reference strain and RP73 clinical strain. C57BL/6NCrl (20-22 g) male mice were infected by intratracheal injection with 1 to 5 x 10^6 CFU of *P. aeruginosa* strain PAO1 (A and C) or RP73 (B and D) embedded in agar-beads. For each time-point, histograms represent the percentage mortality induced by bacteremia (*red*) and survival (*grey*) or the percentage of animals that cleared the infection (*white*) and those able to establish a chronic infection (*green*) (A and B). Surviving mice were euthanized at the indicated time-points, and the lungs were harvested, homogenized, and cultured on TSA plates to determine the bacterial load. The growth curves of PAO1 and RP73 strains in murine lungs are shown (C and D). Dots represent individual measurements and horizontal lines represent median values. Statistical significance by Fisher's test is indicated: * $p<0.05$, ** $p<0.01$, *** $p<0.001$. Click here to view larger image.

Strain	Days post infection	Mortality % (No. of dead/ total mice)	Chronic infection % (No. of infected/ surviving mice)	CFU/lung of infected mice (n)
PAO1	3	24.2 (16/66)	100 (4/4)	$5*10^7$ (4)
	7	0 (0/54)	27.8 (5/18)	$2.3*10^4$ (5)
	14	0 (0/54)	24.1 (13/54)	$2.8*10^4$ (13)
	28	0 (0/20)	20 (4/20)	$1.1*10^4$ (4)
RP73	3	10.3 (7/68)	100 (8/8)	$1.3*10^6$ (6)
	7	0 (0/61)	75 (9/12) *	$4.8*10^6$ (7)
	14	0 (0/61)	87.1 (27/31) ***	$3.5*10^4$ (25)
	28	0 (0/61)	80 (8/10) **	$2.7*10^5$ (6)

Table 1. Time course of *P. aeruginosa* chronic infection with PAO1 reference strain and RP73 clinical strain. Percentages of mortality and of chronic infection of PAO1 and RP73 infected mice and number of CFUs per lung (median) are shown. Values are selected from 2-4 different experiments. *n*, no. of pooled mice analyzed for each condition. Statistical significance by Fisher's test is indicated: * $p<0.05$, ** $p<0.01$, *** $p<0.001$. Click here to view larger image.

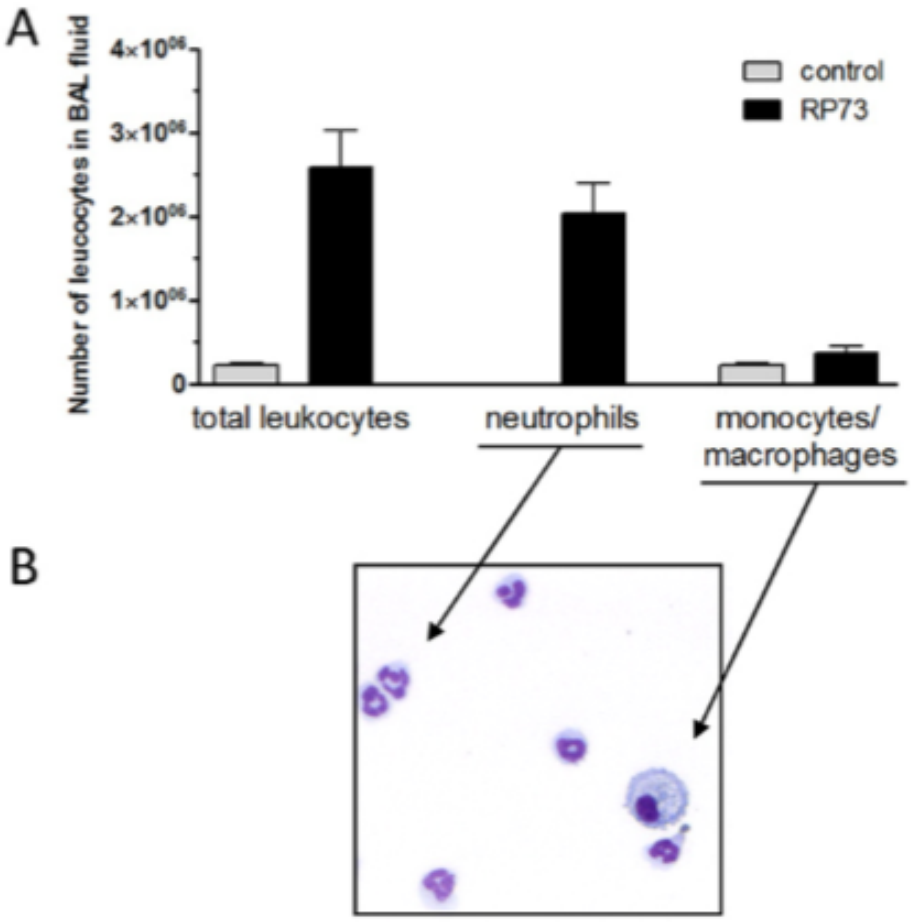

Figure 3. Evaluation of inflammation in BAL fluid after 7 days of chronic infection with RP73 clinical strain. (A) The graph shows the content of total leukocytes, neutrophils and monocytes/macrophages recovered in the BAL fluid of RP73 chronically infected mice after 7 days from challenge compared to uninfected mice (control). Mean values and SEM are represented. (B) In the box below arrows indicate neutrophils and a macrophage as seen in a spot on a slide after cytospin. Click here to view larger image.

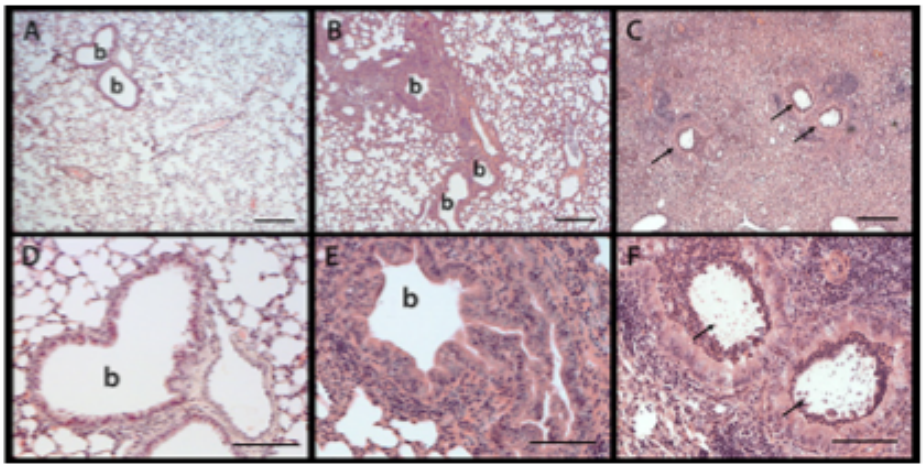

Figure 4. Hematoxylin and eosin staining on histological sections of lungs after 7 days of chronic infection with RP73 clinical strain. The panel shows hematoxylin and eosin staining of lung sections of uninfected mice (A and D) and of mice challenged with agar-beads containing RP73 (B, C, E, F). The infection is pluri-focal and generally involves one or more lung lobes (C and F), whereas the others are unaffected or marginally involved (B and E). Arrows indicate agar beads deposited in the bronchial lumen (b). Lines (A, B, C) 250 µm; lines (D, E, F) 100 µm. Click here to view larger image.

Discussion

The critical steps in the *P. aeruginosa*-beads preparation and mouse challenge are reported below.

The P. aeruginosa strain used for mice challenge is critical. Mortality, chronic infection or clearance may differ significantly depending on the bacterial strain used for the challenge. The *P. aeruginosa* RP73 clinical strain was preferred over the PAO1 reference laboratory strain since it resulted in a comparatively lower mortality, more severe lesions, and higher chronic infection. Drug testing in preclinical studies should be performed with *P. aeruginosa* strains selected for their high efficiency in establishing long-term chronic infection. This minimizes the number of mice that are consistent with the requirements of scientific validation and statistical analysis[10,11].

The individual *P. aeruginosa* agar-bead preparations vary in size and in CFU/ml. An average diameter of 150 µm with 2 x 10^7 CFU/ml is considered optimal. Bead size is affected by the stirring rate during the cooling phase (step 2.9). Beads stirred at top speed are small and spherical (<50 µm) while those stirred very slowly are large and amorphous (>1 mm). In addition, when the final dilution for challenge is prepared, beads with a low bacterial load can be sticky while those with high bacterial load can be excessively diluted. Inoculation of mice with sticky beads is associated with high mortality due to mice choking soon after challenge, while excessively diluted beads may result in an absence of chronic infection. The optimal volume of intratracheal injection is 50 µl but higher volumes of up to 100 µl can be inoculated. Differences in mortality or chronic infection of mice are rarely observed when the inoculated dose ranges between 5 x 10^5 and 5 x 10^6 CFU/mouse.

Appropriate bacterial growth medium must be used for agar beads formation. In this instance, *P. aeruginosa* was embedded in TSA; other papers reported that, *Burkholderia cenocepacia* was included in nutrient broth agar[9,12]. Agar beads should provide a microanaerobic environment with essential nutrients available for bacterial proliferation from single cells to microcolonies[9].

Respiratory effort differs depending on the anesthetic and dose used, and affects mortality after surgery. Ketamine at a dose of 0.1 mg/g body weight and xylazine at a dose of 0.01 mg/g body weight are the optimal choices. Respiration is normal when mice are intubated with the catheter and visibly shallower when mice are inoculated by *P. aeruginosa* agar-beads. Ideally, the injection of *P. aeruginosa* agar-beads should be performed slowly with an optimal volume of 50 µl. Higher volumes of up to 100 µl could result in higher mortality and greater difficulties in mice recovery. All mice are adequately infected when challenged by intratracheal surgery.

The *P. aeruginosa* RP73 agar bead-induced chronic pneumonia indicates that in this model the infection is pluri-focal and generally involves one or more lung lobes without compromising the entire lung. Consequently, evaluation of bacterial load and inflammatory response must be carried out on total lung. The analysis of selective lobes does not produce valid results. An uninfected group of mice should be added as a control and compared to infected mice to detect any potential abnormality in cell recruitment in BAL fluid or in the histology of the lung due to contaminations or mistake in the procedure. This model was established in a BSL-2 laboratory with all laboratory personnel should be trained in the appropriate skills for mouse observation. The mice were monitored twice per day for the following parameters: piloerection, attitude, locomotion, breathing, curiosity, nasal secretion, grooming and dehydration. Mice that lost ≥20% body weight and showed evidence of severe clinical disease, such as scruffy coat, inactivity, loss of appetite, poor locomotion, or painful posture, were euthanized before the termination of the experiment. Mice infected with *P. aeruginosa* RP73 agar-beads showed lower signs of discomfort within three days from infection when compared to PAO1-infected mice. After this time point some mice cleared the bacteria and others developed a stable chronic infection, lasting up to 28 days.

We demonstrated that the model of chronic infection we propose in this paper is able to induce a stable *P. aeruginosa* chronic infection in mice. This method has been optimized to study the molecular mechanisms underlying the pathogen virulence and host defense[8,9,15] or for drug testing of antibacterial and anti-inflammatory molecules[10,11]. The preclinical validation of these compounds in appropriate animal models is essential for future therapeutic interventions for lung infections in patients with CF.

Disclosures

The authors declare that they have no competing financial interests.

Acknowledgements

Research in Bragonzi's laboratory has been funded by the Italian Cystic Fibrosis Foundation (CFaCore) and EU-F7-2009-223670. Part of this work was carried out in ALEMBIC, an advanced microscopy laboratory, and mouse histopathology was performed in the Unit of Pathological Anatomy (San Raffaele Scientific Institute).

References

1. Gibson, R., Burns, J.L., Ramsey, B.W. Pathophysiology and management of pulmonary infections in cystic fibrosis. *Am. J. Respir. Crit. Care Med.* **168**, 918-951 (2003).
2. Bragonzi, A. Murine models of acute and chronic lung infection with cystic fibrosis pathogens. *IJMM.* **300**, 584-593 (2010).
3. Cash, H.A., McCullough, B., Johanson, W.G. Jr., Bass, J.A. A rat model of chronic respiratory infection with *Pseudomonas aeruginosa*. *Am. Rev. Respir. Dis.* **119**, 453-459 (1979).
4. Starke, J.R., Langston, C., Baker, C.J. A mouse model of chronic pulmonary infection with *Pseudomonas aeruginosa* and *Pseudomonas cepacia*. *Pediatr. Res.* **22**, 698-702 (1987).
5. Pedersen, S.S., Hansen, B.L., Hansen, G.N. Induction of experimental chronic *Pseudomonas aeruginosa* lung infection with *P. aeruginosa* entrapped in alginate microspheres. *APMIS.* **98**, 203-211 (1990).
6. Bragonzi, A. *et al.* Nonmucoid *Pseudomonas aeruginosa* expresses alginate in the lungs of patients with cystic fibrosis and in a mouse model. *J. Infect. Dis.* **192**, 410-419 (2005).
7. van Heeckeren, A.M. Murine models of chronic *Pseudomonas aeruginosa* lung infection. *Lab. Anim.* **36**, 291-312 (2002).
8. Bragonzi, A. *et al. Pseudomonas aeruginosa* microevolution during cystic fibrosis lung infection establishes clones with adapted virulence *AJRCCM.* **180**, 138-145 (2009).
9. Kukavica-Ibrulj, I., Facchini M, Cigana C, Levesque RC, Bragonzi A. Assessing *Pseudomonas aeruginosa* virulence and the host response using murine models of acute and chronic lung infection. *In: Filloux A, Ramos JL, editors. Methods in Pseudomonas aeruginosa: Humana Press.* (2014).
10. Moalli, F. *et al.* The Therapeutic Potential of the Humoral Pattern Recognition Molecule PTX3 in Chronic Lung Infection Caused by *Pseudomonas aeruginosa*. *J. Immunol.* **186**, 5425-534 (2011).
11. Paroni, M. Response of CFTR-deficient mice to long-term *Pseudomonas aeruginosa* chronic infection and PTX3 therapeutic treatment. *J. Infect. Dis.* **In press** (2012).
12. Maxeiner, J., Karwot, R., Hausding, M., Sauer, K.A., Scholtes, P., Finotto, S. A method to enable the investigation of murine bronchial immune cells, their cytokines and mediators. *Nat. Protoc.* **2**, 105-112 (2007).
13. Bragonzi, A. *et al. Pseudomonas aeruginosa* microevolution during cystic fibrosis lung infection establishes clones with adapted virulence. *AJRCCM.* **In press** (2009).
14. Pirone, L. *et al.* Burkholderia cenocepacia strains isolated from cystic fibrosis patients are apparently more invasive and more virulent than rhizosphere strains. *Environ. Microbiol.* **10**, 2773-2784 (2008).
15. Bragonzi, A. *et al.* Modelling co-infection of the cystic fibrosis lung by *Pseudomonas aeruginosa* and *Burkholderia cenocepacia* reveals influences on biofilm formation and host response. *PLoS One.* **7**, e52330 (2012).
16. Bianconi, I. *et al.* Positive signature-tagged mutagenesis in *Pseudomonas aeruginosa*: tracking patho-adaptive mutations promoting long-term airways chronic infection. *PLoS Pathog.* **7**, e1001270 (2011).

Published in final edited form as:
Biochim Biophys Acta. 2014 January ; 1840(1): 586–594. doi:10.1016/j.bbagen.2013.10.018.

Anti-inflammatory action of lipid nanocarrier-delivered Myriocin: therapeutic potential in Cystic Fibrosis

Anna Caretti[1], **Alessandra Bragonzi**[2], **Marcella Facchini**[2], **Ida De Fino**[2], **Camilla Riva**[2], **Paolo Gasco**[3], **Claudia Musicanti**[3], **Josefina Casas**[4], **Gemma Fabriàs**[4], **Riccardo Ghidoni**[1], and **Paola signorelli**[1]

[1]Department of Health Sciences, University of Milan, San Paolo Hospital, Italy

[2]Infections and Cystic Fibrosis Unit, San Raffaele Scientific Institute, Milan, Italy

[3]Nanovector S.r.l. Turin, Italy

[4]Research Unit on BioActive Molecules, Department of Biomedicinal Chemistry, Catalan Institute of Advanced Chemistry (IQAC/CSIC), Barcelona, Spain

Abstract

Background—Sphingolipids take part in immune response and can initiate and/or sustain inflammation. Various inflammatory diseases have been associated with increased ceramide content, and pharmacological reduction of ceramide diminishes inflammation damage *in vivo*. Inflammation and susceptibility to microbial infection are two elements in a vicious circle. Recently, sphingolipid metabolism inhibitors were used to reduce infection. Cystic Fibrosis (CF) is characterized by a hyper-inflammation and an excessive innate immune response, which fails to evolve into adaptive immunity and to eradicate acute infection. This results in chronic infections, lung damage, and patient morbidity. Indeed, ceramide content in mucosa airways is higher in CF mouse models and in patients than in control mice or healthy subjects.

Methods—The potential of the *de novo* ceramide synthesis inhibitor myriocin in CF therapy was investigated in cells and mice models.

Results—We treated CF human respiratory epithelial cells with myriocin, an inhibitor of the rate limiting enzyme involved in *de novo* ceramide synthesis Serine Palmitoyl Transferase (SPT). This treatment resulted in reduced basal, as well as TNFα -stimulated, inflammation. In turn, TNFα induced an increase in SPT in these cells, linking *de novo* synthesis of ceramide and inflammation in a noxious loop. Furthermore, myriocin-loaded nanocarrier, injected intratrachea prior to *P.aeruginosa* challenge, allowed a significant reduction of lung infection and reduced inflammation.

Corresponding author: Paola Signorelli, Department of Health Sciences, University of Milan, San Paolo Hospital, Via A. di Rudinì 8, 20142 Milan, Italy, Phone ++39 02 50323257, Fax ++39 02 50323245, paola.signorelli@unimi.it.

Conclusion—The presented data suggest that *de novo* sphingolipid synthesis is constitutively enhanced in CF mucosa and that it can be envisaged as pharmacological target for modulating inflammation and restoring effective innate immunity against acute infection.

General significance—Myriocin stands as a powerful immunomodulatory agent for inflammatory and infectious diseases.

Introduction

Sphingolipids (SPL) are a broad class of membrane components and signaling mediators involved in cell survival and function. It is becoming increasingly apparent that SPL take part to inflammation and to host innate response upon infection (1-3). The sphingolipid ceramide is highly effective in the activation of inflammation related transcription factors, such as NF-kB (4) and AP1(5) and in receptors clustering /signaling upon inflammatory stimula (6). Patients suffering from chronic inflammation such as irritable bowel syndrome (7), emphysema lung injury and chronic obstructive pulmonary disease (8-10), exhibit increased levels of mucosal ceramide as compared to controls. A vicious loop relates the excessive inflammation to the susceptibility to microbial infection. Hyper-inflammation associates with the inability to clear infections at their early stage, as well as to mature the adaptive immune response, thus allowing the chronic establishment of pathogens communities. Ceramide accumulation may derive from increased synthesis *de novo* or from altered metabolism of complex sphingolipids such as sphingomyelin or glycosphingolipids. The role of sphingomyelinases, neutral and acidic, in inflammation has been extensively investigated (11; 12). The hydrolysis of plasma-membrane sphingomyelin is responsible for ceramide-rich membrane platforms formation and required for signal transduction of inflammatory stimula, such as TNFα, ILβ, INFγ (6; 8; 13; 14), increased vascular permeability (15; 16) as well as for the internalization of microorganisms (13; 17). On the other side, only a few reports underscore the involvement of *de novo* synthesis of ceramide in the inflammatory responses (10; 18-20). Thus, emphysema lung damage (10) and immune-reactivity in murine dorsal horn of the lumbar spinal cord were reduced by Fumonisin B1, an inhibitor of ceramide synthase (18). Furthermore, mice feeding with Myriocin (Myr), an inhibitor of Serine Palmitoyl Transferase (SPT), decreased radiation-induced inflammation and fibrosis (21). A recent finding demonstrated that reduced *de novo* ceramide synthesis by fenretinide, associated with the increase of its precursor dihydroceramide, impairs bacterial infection in macrophages (19).

Cystic Fibrosis (CF) is an inherited autosomal recessive disease caused by CF transmembrane conductance regulator (CFTR) mutations. CF patients develop mucus viscosity, impaired mucociliary transport, hyper- inflammation and severe alteration of all mucosal functions with lung disease (22; 23) and chronic opportunistic infections (mainly *Pseudomonas aeruginosa*, *Bhurkolderia cepacia complex*, and *Staphylococcus aureus*) remaining the main cause of morbidity and mortality (24; 25). Inflammation is an independent risk factor for CF disease progression. Even the uninfected CF lungs of foetuses or two years old infants, develop a pathological inflammatory condition (26-29), confirming the severe immune alteration of mucosa in the respiratory tract.

In mouse models of CF, an age-related accumulation of ceramide in respiratory epithelium was associated to the pathological inflammatory state and infection susceptibility. Sphingomyelinase (9; 30; 31), or ceramide synthase (9) inhibition, or fenretinide, an inhibitor of ceramide formation from its precursor dihydro-ceramide (32), reduced inflammation and infection in CF mice.

Similarly, in CF patients, increased ceramide content was found in nasal respiratory epithelium and lungs (30; 33; 34). Amitriptyline, an inhibitor of acid sphingomyelinase used in a phase II study, reduced ceramide levels in the respiratory epithelial cells of treated patients and this was accompanied by a significant increase in lung function (30; 31).

In spite of the increased ceramide mass in CF mucosa, there is no evidence on what is the rate of ceramide synthesis *versus* its release from membrane sphingomyelin. We hypothesized that preventing *de novo* sphingolipid synthesis with Myr could reduce excessive lung inflammation in CF and allow an efficient innate response to acute infection. In this article we demonstrated that Myr reduces IL-8 and IL6 release in human CF respiratory epithelium. Given the hydrophobicity of the compound, we sought to deliver Myr *in vivo*, in murine airways, by means of Solid Lipid Nanoparticles (SLN) (35). We demonstrated that Myr- loaded SLN are able to reduce inflammation and infection in CF mice lung.

Materials and Methods

Reagents and Antibodies

Myr was purchased from Fermentek LTD (Israel), MTT and bovine serum albumin (BSA) were from Sigma-Aldrich (US). LHC Basal, LHC-8 w/o gentamicin culture media (Gibco, US), Penicillin and streptomycin (Invitrogen) were purchased from Life Technologies Italia (Italy). Fetal bovine serum (FBS) and the chemiluminescence system LiteAbLot were purchased from EuroClone Life Science Division (Italy). Human Fibronectin and Bovine Collagen were from Becton-Dickinson Italia (Italy). Human and mouse IL-8, IL-6 mini EDK and Human TNF-α were from Peprotech (UK). The synthetic oligonucleotides used in this study were purchased from M-Medical (Italy). All reagents were of the maximal available purity degree.

Myriocin stock solution preparation

Myr powder was weighted and dissolved in DMSO by warming up at 37°C, to a final concentration of 2 mM. Solution was sterile filtered (0.22 μm pore diameter, Nalgene) and stored at 4°C until used. This stock solution was diluted in medium for cell treatment (final treatment concentration: 10 μM) and in sterile saline for animal treatments (final treatment concentration: 420 μM, equal to 11,95 μg of Myr *per* mouse).

Myriocin loaded-Solid Lipid Nanoparticles (SLN) used for mice treatment

Treatment of mice with Myr was achieved by using Myr-loaded SLNs (Nanovector srl, Italy) prepared as previously described (35). SLN loaded with drug were measured for Myr content and a 1 mM Myr-SLN stock solution was prepared. This solution was diluted 1:12

in sterile saline and 75 μl (1.7 μg of Myr and 8% SLN) were used for each mouse administration in the airways.

Cell lines and treatments

IB3-1 cells, an adeno-associated virus-transformed human bronchial epithelial cell line derived from a CF patient (ΔF508/W1282X) and its isogenic C38 cells, corrected by insertion of CFTR, have been both obtained from LGC Promochem (US) and kindly provided by the Cystic Fibrosis animal Core Facility (CFaCore, San Raffaele Hospital, Milan, Italy). Cells were grown in LHC-8 media supplemented with 5% FBS. Both culture flasks and plates were coated with a solution of LHC-basal medium containing 35 μg/ml bovine collagen, 1 μg/ml bovine serum albumin and 10 μg/ml human fibronectin as described (36). For experiments, cells were seeded in 6 multi-wells plate or 100 mm petri dishes at 3×10^5 and 2×10^6 cells/plate respectively. Twenty four h after seeding, when cells reached about 60% confluence, medium was replaced with fresh one, containing either Myr (10 μM) or vehicle (DMSO). Eight h after Myr treatment, human TNFα (20ng/ml) was added to both treated and untreated cells. Incubation proceeded for further 18 h and then samples were collected for analyses.

MTT assay

Cell proliferation was examined in triplicate samples by the MTT assay as previously described (37). Proliferation index represents fold increase proliferation over vehicle-treated cells at time zero.

ELISA

Released IL-8 and IL-6 were determined in supernatants collected from the cell cultures using ELISA kits according to the manufacturer's instructions (Vinci Biochem, Italy). Values were normalized to 10^6 cells. KC and IL-6 concentration were determined in lung homogenates by ELISA, according to manufacturer's instructions.

LC–MS analysis

Sphingolipid extracts from both mice lungs and treated cells, fortified with internal standards (*N*-dodecanoylsphingosine, *N*-dodecanoylglucosylsphingosine, *N*-dodecanoylsphingosyl phosphorylcholine, C17-sphinganine (0.2 nmol each) and C17-sphinganine-1-phosphate (0.1 nmol), were prepared and analysed as reported (38).

Western blotting

Cells were scraped in ice-cold phosphate buffered saline (PBS) containing proteases inhibitors (Roche Italia, Milan, Italy) and spun at 1,200 × g for 5 min at 4°C. An aliquot was used for protein quantification; the remaining cells were resuspended in Laemmli buffer, boiled for 8 min and stored at -20°C. Cytosolic and nuclear extracts were obtained by NE-PER Nuclear and Cytoplasmic Extraction Reagents (Pierce, US), according to manufacturer protocols. Equal amount of proteins (20 μg for SPT and 15μg for NF-kB 40μg for IK-Bα) were separated on 10% acrylamide gels by SDS-electrophoresis and transferred onto nitrocellulose membranes. After blocking unspecific binding sites with 5% dry skimmed

milk in PBS-Tween 0.1% (PBST), the membranes were incubated (47°C/overnight) with primary antibodies (Anti-Serine Palmitoyltransferase, anti-SPTLC 1 and 2, antibodies were kindly provided by Dr. T. Hornemann University Hospital Zürich, Switzerland; anti IK-Bα and anti NF-kB p65 were from Calbiochem, US) diluted 1:1,000 in PBST-3% BSA, followed by incubation (room temperature/2 h) with the appropriate HRP-secondary antibodies (Jackson Laboratories US) diluted 1:10,000 in PBST-3% BSA. The same membranes were immunoblotted against β-actin (dilution 1:5,000) for data normalization. Proteins were detected by chemiluminescence and bands intensity was quantified by Gel Doc 2000, using Quantity One Software (BioRad Life Science, US).

RNA extraction and quantitative RT-PCR

RNA extraction and quantitative RT-PCR for murine KC and IL-6 and human IL-8 and IL-6 were performed as previously reported (39). Human SPTLC 1 and 2 transcripts (mRNA) were evaluated by RT-PCR as previously reported (40).

Mice treatment and infection

Fourteen weeks old gut-corrected CFTR deficient mice B6.129P2-$Cftr^{tm1UNC}$TgN(FABPCFTR) (group KO) and congenic wild-type (Case Western Reserve University, Cleveland, Ohio, USA) (group WT) male and female mice were used (41; 42).

Mice were housed in filtered cages under specific-pathogen conditions and permitted unlimited access to food and water. Once a deep stage of anesthesia with 2,2,2,-tribromoethanol (Avertin, Sigma-Aldrich, US) was reached, Myr either dissolved in DMSO or uploaded in SLN, was intra-trachea instilled by means of MicroSprayer® Aerosolizer – Model IA1C, attached to "FMJ-250 High Pressure Syringe" (Penn-Century Inc., US). Control animals were treated with the corresponding empty vehicle. The total volume introduced in lungs was 75 μl, in mice of approximately 30 gr each. This volume contained either 11.95 μg of compound/mouse in 10%DMSO-saline solution or 1.75 μg of compound/mouse in 8%SLN-saline solution. 24 h after treatment, animals (both KO and WT) were infected with 3-10 × 10^5 CFU of *P. aeruginosa* strain PAO1 planktonic cells, as previously described (43). After 18 h post-infection, mice were euthanized and lungs were perfused with PBS and homogenized in 1 ml of PBS containing protease inhibitors (Roche Italia, Italy). Part of the lung homogenates was centrifuged at 13,000 rpm for 30 minutes at 4°C and the supernatants were stored at −20°C for cytokine analysis. The remaining lung homogenate was divided in two aliquots: one part was lyophilized and lipids were extracted for LC–MS analysis; the other aliquot was serially diluted 1:10 in PBS and plated onto TSA plates to determine lung bacterial load. All experiments were performed with a minimum of five animals per group.

Ethics Statement

Animal studies were conducted according to protocols approved by the San Raffaele Scientific Institute (Milan, Italy) Institutional Animal Care and Use Committee (IACUC) and adhered strictly to the Italian Ministry of Health guidelines for the use and care of experimental animals.

Statistical analysis

Data significance was evaluated by unpaired two-tailed Student t-test ($P < 0.05$) or by one-way ANOVA followed by the Bonferroni multiple comparisons test when significant ($P < 0.05$). Data are expressed as mean ±SEM.

Results

1. Myriocin differently affects proliferation of IB3 *vs* C38 cells

To assess whether IB3 cells (a cystic fibrosis cell line, Δ508/W128X) and C38 cells (a cell line derived from IB3, but stably expressing the wild-type CFTR) respond to sphingolipid *de novo* synthesis inhibitor, we evaluated the proliferation rate of cells treated with Myr *vs* untreated control cells (DMSO vehicle only) for different times. Myr inhibitory effect on proliferation was significantly lower (50%) on IB3 with respect to C38 cells, at 48 and at 72 h (Figure 1A and B). In order to exclude that sphingolipid synthesis inhibition was affecting cell survival, we performed a Trypan blue exclusion test in IB3 and C38 cells treated with Myr. As shown in Figure 1C, percentage of alive cells was not affected by Myr treatment at any time point (24, 48, 72 h).

2. Inflammation increases ceramide *de novo* synthesis and Myriocin reduces the inflammatory response in IB3 cells

To understand the above reported different behaviour of the two cell lines upon sphingolipid *de novo* synthesis inhibition, we measured ceramide in Myr pre-treated (8 h) and/or TNFα treated (24 h) cells. First of all, we observed a higher content of ceramide in IB3 than in C38 unstimulated cells (Figure 2A). The higher ceramide levels found in IB3 may account for their reduced sensitivity to the anti-proliferative effect of sphingolipid synthesis inhibition (see Figure 1 A). Second, we observed that ceramide was elevated by two folds in TNFα treated IB3 but not in C38 cells (Figure 2A), indicating that *de novo* synthesis of ceramide is hyper-stimulated in the CFTR mutant cells upon inflammatory stimulation. As expected, Myr treatment drastically reduced ceramide levels in both IB3 and C38 cell lines. Notably, in TNFα stimulated IB3 cells, Myr reduced ceramide levels from 900 ± 68.3 to 187 ± 62.7 pmoles/mg protein. To further assess the correlation between sphingolipid *de novo* synthesis and inflammatory signalling, we stimulated IB3 and C38 cells with TNFα and measured SPT (the sphingolipid synthesis rate-limiting enzyme, SPT1 and 2 subunits) transcription by Real Time PCR. TNFα induced an increase in SPT 1 and 2 mRNA levels. Such an increase was significantly higher in IB3 than in C38 cells (Figure 2B). The transcript increase was confirmed by an augmented protein expression of both subunits of the enzyme (Figure 2 C and 2 D).We then evaluated if sphingolipid synthesis inhibition was able to modulate cytokines release upon TNFα stimulation. IB3 and C38 cells were treated with TNFα (24 h), either alone or in combination with a pre-treatment with Myr (8 h). Myr significantly reduced TNFα stimulated IL-8 mRNA expression and protein release in IB3 cells, whereas cytokines expression and release was slightly affected in C38 treated cells (Figure 3 A and C). IL-6 mRNA expression was down-regulated by Myr alone both in C38 and IB3 cells. When cells were stimulated with TNFα, Myr was able to reduce (about 2 folds) the IL-6 mRNA in IB3 but no significant reduction was observed in C38 cell line (Figure 3 B). IL-6 protein release was not affected by either TNFα or by Myr stimulation in C38 cells.

Whereas Myr alone did not alter the levels of secreted IL-6 protein in IB3 cells, it was effective in decreasing cytokines release induced by TNFα in IB3 (Figure 3 D).

3. Myriocin downregulates NF-kB activation in IB3 cells

Human and murine CF epithelium was demonstrated to sustain inflammatory signaling via NF-kB activation (44-46).Therefore we investigated on Myr ability to alter NF-kB activation in human CF epithelial cell line. IB3 cells were treated with TNFα (24 h) either alone or in combination with Myr pre-treatment (8 h). Cytosolic fractions were separated from nuclear fractions. We observed that TNFα-induced degradation of the cytosolic Ik-Bα (the NF-kB inhibitor, Figure 4 A and B) and nuclear accumulation of NF-kB p65 (Figure 4 C and D), were both reversed by Myr.

4. Myriocin modulates *P. aeruginosa* airways inflammation in $Cftr^{tm1UNC}TgN(FABPCFTR)$ mice

At the aim of validating the results obtained on human cell lines in an *in vivo* model, *$Cftr^{tm1UNC}TgN(FABPCFTR)$* mice (KO) and congenic control (WT) mice were treated with Myr dissolved in 10% DMSO, by intra-tracheal micro-sprayer nebulisation for 24 h prior to infection with *P. aeruginosa* (PAO1) by intra-tracheal injection. Animals were sacrificed 18 h after infection. Myr treatment was significantly effective in reducing lungs Cer level in infected KO mice (from 722 ± 9 to 313.3 ± 6.9 pmoles/mg protein) and small reduction was detected in infected WT mice lungs (from 784.5 ± 60.5 to 612.5 ± 129.5 pmoles/mg protein) (Figure 5).

On the contrary, sphingolipid synthesis inhibition was associated to a reduced KC mRNA content (Figure 6 A) as well as in KC protein level (Figure 6 C), both in KO and in WT mice lungs homogenate. IL-6 mRNA was down-modulated by Myr in both KO and WT animals and IL-6 protein release was reduced in both animal groups (Figure 6 B and D, respectively). All animal experiments have been repeated three times.

5. SLN delivery of Myriocin enhances its effects on infection and inflammation in murine airways

Myr is highly lipophilic and poorly soluble, even in a 10% DMSO solution. At the aim of optimizing lungs delivery and prolonging the effect of the inhibitor by increasing its half-life in the lungs, Myr was loaded into SLN and injected as aerosol solution, by intra-tracheal microsprayer nebulisation, 24 h prior to infection with *P. aeruginosa*. Animals were sacrificed at 18 h post infection. SLN- mediated Myr delivery ensured a high efficacy on sphingolipid synthesis inhibition as demonstrated by 37% or 60% of lungs ceramide reduction in WT and KO infected animals respectively (Figure 7 A). The inhibition of *de novo* ceramide synthesis in CF mouse airways was associated to a marked reduction of glucosyl-galactosyl ceramide pool. No changes were detected in the overall content of sphingomyelins (supplementary Figure 1). This suggests that in CF models, *de novo* generated ceramide can be preferentially metabolized by glycosylation. This hypothesis is in line with the anti-inflammatory effect of miglustat, an inhibitor of ceramide glycosylation, obtained by Dechecchi and coworkers (39).

Notably, SLN- mediated Myr delivery reduced *P.aeruginosa* lung colonies 6 times in treated KO treated compared to untreated KO mice, while no differences were found between treated and untreated WT mice (Figure 7 B). Sphingolipid synthesis inhibition *via* Myr-loaded SLN was associated to a significant reduction in lungs KC and IL-6 mRNA expression (Figure 8 A and B). Lung KC and IL-6 protein levels were similarly down-regulated by Myr both in KO and WT infected mice. All animal experiments have been repeated three times.

Discussion

The role of sphingolipid *de novo* synthesis pathway in inflammation is still largely unexplored. The data presented in this article demonstrate for the first time that *de novo* sphingolipid synthesis is enhanced during inflammation and, in turn, it promotes the production of inflammatory mediators (Figure 2 and 4). In CF mice model, we proved that blocking SPL *de novo* synthesis can reduce hyper-inflammation favouring the recovery of an effective response to *P.aeruginosa* infection in the respiratory tract. It is important to consider that CF is a chronic inflammatory disease, prior to become an infective chronic disease: noteworthy even CF uninfected infants exhibit high levels of pulmonary inflammation (27). Hence, it is mandatory to cure innate immunity in CF patients and immunomodulatory agents are required to reduce the persistent inflammation that favours infection stabilization. From literature evidences it is clear that acute and chronic inflammation modulate sphingolipids and are, in turn, tuned by sphingolipid metabolites (2; 31; 39; 47). Accordingly, in CF human cells we showed: i) a basal higher amount of endogenously synthesized ceramide, that provides the cells with the ability to partially overcome the antiproliferative effect of sphingolipid *de novo* synthesis inhibition; ii) an increased expression of the rate limiting enzyme of sphingolipid *de novo* synthesis upon TNFα stimulation (Figure 2 B). We also proved that *de novo* sphingolipid synthesis inhibition in this cells reduced NF-kB activation (Figure 4) and IL8 and IL6 release (Figure 3) upon TNFα stimulation. These evidences demonstrate the existence of a noxious loop between ceramide *de novo* synthesis and inflammation in CF. Gulbins and colleagues demonstrated first in CF mice and then in CF human patients, that inhalation of an acid sphingomyelinase inhibitor reduces ceramide accumulation and lung burden of inflammation and infection (31). On the other side, in pulmonary infections, rapid acid sphingomyelinase activation and formation of ceramide-enriched membrane platforms was shown to be required for the internalization/clearence of different bacteria, including *P.aeruginosa* (17; 48). It was also found that infection of acid sphingomyelinase-deficient mice with P. aeruginosa caused increased bacterial load, cytokine storm (49) and finally death of the mice (50). Thus the activity of acid sphingomylinase seems to be required for a proper inflammatory response and for pathogens clearance (48; 51), casting doubt on a long term use of acid sphingomyelinase inhibitor, which may negatively impact on the immunity system of the respiratory tract. Petrache and co-workers demonstrated that increased rate of sphingolipid *de novo* synthesis is associated with inflammation and, importantly, with an increase in the secretion of acid sphingomyelinase, which is responsible for a high release of ceramide in respiratory mucosa of COPD mice. This ceramide contributes to mucus thickness and inflammation (10). Our hypothesis is that CFTR mutation, possibly by

inducing endogenous stress, associates with an enhanced rate of *de novo* sphingolipid synthesis and with an increase in the content of ceramide within the respiratory mucosa. In addition to the block of ceramide release from secreted sphingomyelinase activity by amitriphteline, the correction of the hyper-stimulated *de novo* synthesis, which may be responsible of increased sphingomyelinase activity (10) by Myr, is able to counteract the excessive inflammatory reaction upon infection and to favour bacteria clearance.

Sphingolipid targeting for human therapy has the problem of hydrophobicity of most of the known metabolism inhibitors. Lipophilic ceramide was previously delivered *in vivo* by means of liposomes carriers (52). Recently, the use of solid lipid nanocarriers was successfully experienced in mouse eye, by external administration of eye drops containing Myr-loaded SLN (35). We here demonstrate that surfactant like containing nanoparticles allow a good uptake and delivery of Myr. Comparing the efficacy of the compound in terms of ceramide content reduction, we observed approximately a 7 fold decrease in the effective drug concentration when using SLN delivery in respect to the concentration required when Myr was dissolved in DMSO and directly diluted into saline. It is feasible that aqueous suspensions and perhaps dry powder formulations of SLN can be used for pulmonary inhalation. We think that SLN may be a very important tool for any drug targeting sphingolipid metabolism *in vivo*.

Supplementary Material

Refer to Web version on PubMed Central for supplementary material.

Acknowledgments

We thank the Italian Cystic Fibrosis Research Fundation for financial, technical, administrative support and post-doctoral fellowship. We thank Dr Horneman University Hospital Zürich, Switzerland for kindly providing us with anti-SPT antibodies. We thank Dr. Marco Trinchera, Università dell'Insubria, Italy for kind support and advices. We thank Eva Dalman for her excellent technical assistance. We thank Dr.Giovanna Riccio for setting up HPLC-RI method for myriocin analysis and quantitation and for her valuable technical contribution to the project. Financial support from the Institutional Grants of University of Milan and the PhD program in Molecular Medicine, Università di Milano, Italy is acknowledged. Financial support from Generalitat de Catalunya (grant SGR2009 1072), Ministerio de Economía y Competitividad (grant SAF2011 22444) and Fundació La Marató de TV3 (grant 112130) is acknowledged.

References

1. Chalfant CE, Spiegel S. Sphingosine 1-phosphate and ceramide 1-phosphate: expanding roles in cell signaling. Journal of cell science. 2005; 118:4605–12. [PubMed: 16219683]
2. El Alwani M, Wu BX, Obeid LM, Hannun YA. Bioactive sphingolipids in the modulation of the inflammatory response. Pharmacol Ther. 2006; 112:171–83. [PubMed: 16759708]
3. Miyake Y, Kozutsumi Y, Nakamura S, Fujita T, Kawasaki T. Serine palmitoyltransferase is the primary target of a sphingosine-like immunosuppressant, ISP-1/myriocin. Biochemical and biophysical research communications. 1995; 211:396–403. [PubMed: 7794249]
4. Schutze S, Potthoff K, Machleidt T, Berkovic D, Wiegmann K, Kronke M. TNF activates NF-kappa B by phosphatidylcholine-specific phospholipase C-induced "acidic" sphingomyelin breakdown. Cell. 1992; 71:765–76. [PubMed: 1330325]
5. Sawai H, Okazaki T, Yamamoto H, Okano H, Takeda Y, et al. Requirement of AP-1 for ceramide-induced apoptosis in human leukemia HL-60 cells. The Journal of biological chemistry. 1995; 270:27326–31. [PubMed: 7592995]

26. Verhaeghe C, Delbecque K, de Leval L, Oury C, Bours V. Early inflammation in the airways of a cystic fibrosis foetus. Journal of cystic fibrosis: official journal of the European Cystic Fibrosis Society. 2007; 6:304–8. [PubMed: 17223612]
27. Khan TZ, Wagener JS, Bost T, Martinez J, Accurso FJ, Riches DW. Early pulmonary inflammation in infants with cystic fibrosis. American journal of respiratory and critical care medicine. 1995; 151:1075–82. [PubMed: 7697234]
28. Muhlebach MS, Noah TL. Endotoxin activity and inflammatory markers in the airways of young patients with cystic fibrosis. American journal of respiratory and critical care medicine. 2002; 165:911–5. [PubMed: 11934713]
29. Gangell C, Gard S, Douglas T, Park J, de Klerk N, et al. Inflammatory responses to individual microorganisms in the lungs of children with cystic fibrosis. Clinical infectious diseases: an official publication of the Infectious Diseases Society of America. 2011; 53:425–32. [PubMed: 21844026]
30. Riethmuller J, Anthonysamy J, Serra E, Schwab M, Doring G, Gulbins E. Therapeutic efficacy and safety of amitriptyline in patients with cystic fibrosis. Cellular physiology and biochemistry: international journal of experimental cellular physiology, biochemistry, and pharmacology. 2009; 24:65–72.
31. Becker KA, Riethmuller J, Luth A, Doring G, Kleuser B, Gulbins E. Acid sphingomyelinase inhibitors normalize pulmonary ceramide and inflammation in cystic fibrosis. American journal of respiratory cell and molecular biology. 2010; 42:716–24. [PubMed: 19635928]
32. Vilela RM, Lands LC, Meehan B, Kubow S. Inhibition of IL-8 release from CFTR-deficient lung epithelial cells following pre-treatment with fenretinide. International immunopharmacology. 2006; 6:1651–64. [PubMed: 16979119]
33. Brodlie M, McKean MC, Johnson GE, Gray J, Fisher AJ, et al. Ceramide is increased in the lower airway epithelium of people with advanced cystic fibrosis lung disease. American journal of respiratory and critical care medicine. 2010; 182:369–75. [PubMed: 20395562]
34. Teichgraber V, Ulrich M, Endlich N, Riethmuller J, Wilker B, et al. Ceramide accumulation mediates inflammation, cell death and infection susceptibility in cystic fibrosis. Nature medicine. 2008; 14:382–91.
35. Strettoi E, Gargini C, Novelli E, Sala G, Piano I, et al. Inhibition of ceramide biosynthesis preserves photoreceptor structure and function in a mouse model of retinitis pigmentosa. Proceedings of the National Academy of Sciences of the United States of America. 2010; 107:18706–11. [PubMed: 20937879]
36. Zeitlin PL, Lu L, Rhim J, Cutting G, Stetten G, et al. A cystic fibrosis bronchial epithelial cell line: immortalization by adeno-12-SV40 infection. American journal of respiratory cell and molecular biology. 1991; 4:313–9. [PubMed: 1849726]
37. Mosmann T. Rapid colorimetric assay for cellular growth and survival: application to proliferation and cytotoxicity assays. Journal of immunological methods. 1983; 65:55–63. [PubMed: 6606682]
38. Munoz-Olaya JM, Matabosch X, Bedia C, Egido-Gabas M, Casas J, et al. Synthesis and biological activity of a novel inhibitor of dihydroceramide desaturase. ChemMedChem. 2008; 3:946–53. [PubMed: 18236489]
39. Dechecchi MC, Nicolis E, Mazzi P, Cioffi F, Bezzerri V, et al. Modulators of sphingolipid metabolism reduce lung inflammation. American journal of respiratorycell and molecular biology. 2011; 45:825–33.
40. Hornemann T, Richard S, Rutti MF, Wei Y, von Eckardstein A. Cloning and initial characterization of a new subunit for mammalian serine-palmitoyltransferase. The Journal of biological chemistry. 2006; 281:37275–81. [PubMed: 17023427]
41. Bragonzi A, Paroni M, Nonis A, Cramer N, Montanari S, et al. Pseudomonas aeruginosa microevolution during cystic fibrosis lung infection establishes clones with adapted virulence. American journal of respiratory and critical care medicine. 2009; 180:138–45. [PubMed: 19423715]
42. Paroni M, Moalli F, Nebuloni M, Pasqualini F, Bonfield T, et al. Response of CFTR-Deficient Mice to Long-Term chronic Pseudomonas aeruginosa Infection and PTX3 Therapy. The Journal of infectious diseases. 2012

43. Bragonzi A. Murine models of acute and chronic lung infection with cystic fibrosis pathogens. International journal of medical microbiology: IJMM. 2010; 300:584–93. [PubMed: 20951086]
44. Finotti A, Borgatti M, Bezzerri V, Nicolis E, Lampronti I, et al. Effects of decoy molecules targeting NF-kappaB transcription factors in Cystic fibrosis IB3-1 cells recruitment of NF-kappaB to the IL-8 gene promoter and transcription of the IL-8 gene. Artificial DNA, PNA & XNA. 2012; 3:97–296.
45. Ziady AG, Sokolow A, Shank S, Corey D, Myers R, et al. Interaction with CREB binding protein modulates the activities of Nrf2 and NF-kappaB in cystic fibrosis airway epithelial cells. American journal of physiology Lung cellular and molecular physiology. 2012; 302:L1221–31. [PubMed: 22467641]
46. Venkatakrishnan A, Stecenko AA, King G, Blackwell TR, Brigham KL, et al. Exaggerated activation of nuclear factor-kappaB and altered IkappaB-beta processing in cystic fibrosis bronchial epithelial cells. American journal of respiratory cell and molecular biology. 2000; 23:396–403. [PubMed: 10970832]
47. von Bismarck P, Winoto-Morbach S, Herzberg M, Uhlig U, Schutze S, et al. IKK NBD peptide inhibits LPS induced pulmonary inflammation and alters sphingolipid metabolism in a murine model. Pulm Pharmacol Ther. 2012; 25:228–35. [PubMed: 22469869]
48. Utermohlen O, Karow U, Lohler J, Kronke M. Severe impairment in early host defense against Listeria monocytogenes in mice deficient in acid sphingomyelinase. J Immunol. 2003; 170:2621–8. [PubMed: 12594290]
49. Jbeily N, Suckert I, Gonnert FA, Acht B, Bocksneyer CL, et al. Hyperresponsiveness of mice deficient in plasma-secreted sphingomyelinase reveals its pivotal role in early phase of host response. Journal of lipid research. 2013; 54:410–24. [PubMed: 23230083]
50. Grassme H, Jendrossek V, Riehle A, von Kurthy G, Berger J, et al. Host defense against Pseudomonas aeruginosa requires ceramide-rich membrane rafts. Nature medicine. 2003; 9:322–30.
51. Schramm M, Herz J, Haas A, Kronke M, Utermohlen O. Acid sphingomyelinase is required for efficient phago-lysosomal fusion. Cellular microbiology. 2008; 10:1839–53. [PubMed: 18485117]
52. Zolnik BS, Stern ST, Kaiser JM, Heakal Y, Clogston JD, et al. Rapid distribution of liposomal short-chain ceramide in vitro and in vivo. Drug metabolism and disposition: the biological fate of chemicals. 2008; 36:1709–15. [PubMed: 18490436]

Highlights

- De novo synthesis of ceramide is increased in CF respiratory tract
- Myriocin reduces ceramide in CF respiratory tract
- Myriocin reduces inflammation in CF respiratory tract
- Nanocarriers delivery of myriocin in vivo reduces lung infection in CF mice

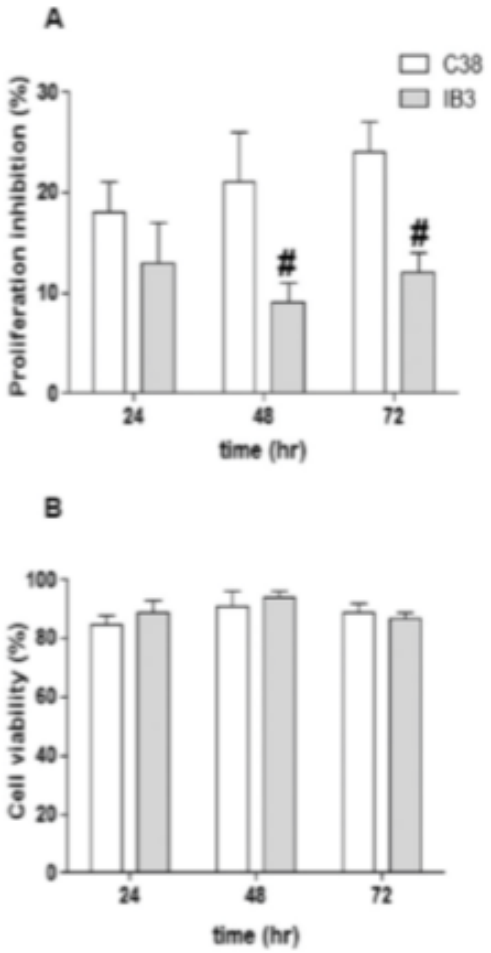

Figure 1. Myriocin differently affects proliferation of C38 *vs* IB3 cells

Inhibitory effect of Myr (10 μM) on IB3 and C38 cells proliferation at 24, 48, 72 h, expressed as percentage of proliferation inhibition in treated *vs* control (**A**). Significance was evaluated by one-way ANOVA as reported in Table 1. #, *vs* C38 cells. Cell viability, calculated as percentage of alive *vs* total cells in IB3 and C38 cells treated with Myr (10 μM) for 24, 48, 72 h (**B**).

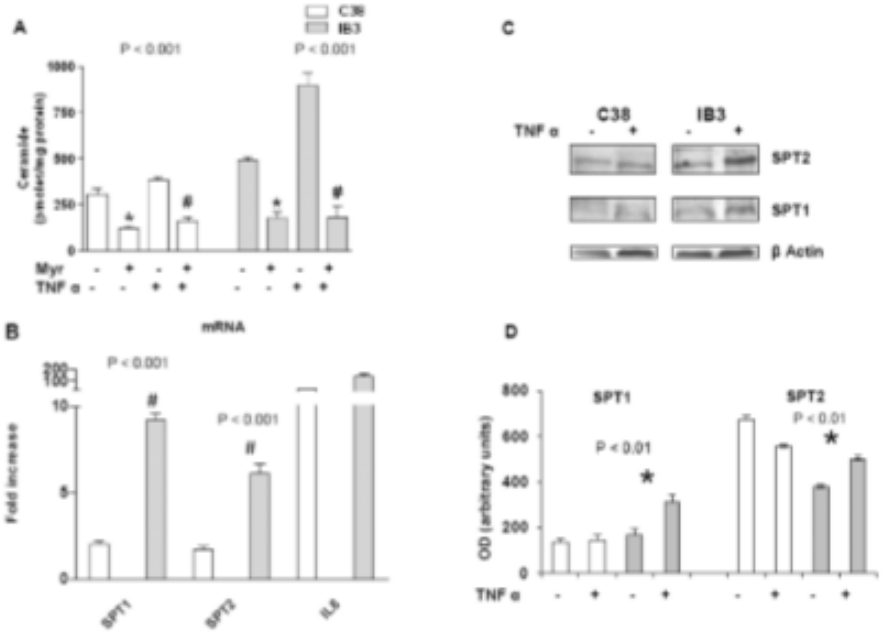

Figure 2. TNFα differently induces *de novo* ceramide synthesis in IB3 *vs* C38 cells

Cer quantitation, by LC–MS analysis, in IB3 and C38 cells stimulated with TNFα (20 ng/ml) either alone or in combination with Myr (10 μM, 8 h pre-treatment) for 24 h. Significance was evaluated by one-way ANOVA (value reported on the graphs). #, *, *vs* TNFα-treated and untreated cells (Bonferroni post-test: P <0.01 and P <0.001 in C38 and IB3, respectively) (**A**). Real time PCR of SPT 1 and 2 transcripts in C38 and IB3 cells cells stimulated with TNFα (20 ng/ml) for 24 hours. IL8 was evaluated as positive control of TNFα-induced inflammation. Data are expressed as fold increase of treated cells *vs.* untreated cells (**B**). SPT protein expression (SPT1, SPT2) in IB3 and C38 cells TNFα-treated and untreated for 24 h. β actin was used as loading control (**C**). Densitometric analysis of the SPT protein bands normalized on the corresponding β actin value. Medium value of three independent experiments. Significance was evaluated by one-way ANOVA (value reported on the graphs). SPT2: *, *vs* TNFα-treated IB3 and untreated C38 cells. SPT1: *, *vs* TNFα-treated C38 cells (Bonferroni post-test: P <0.05) (**D**).

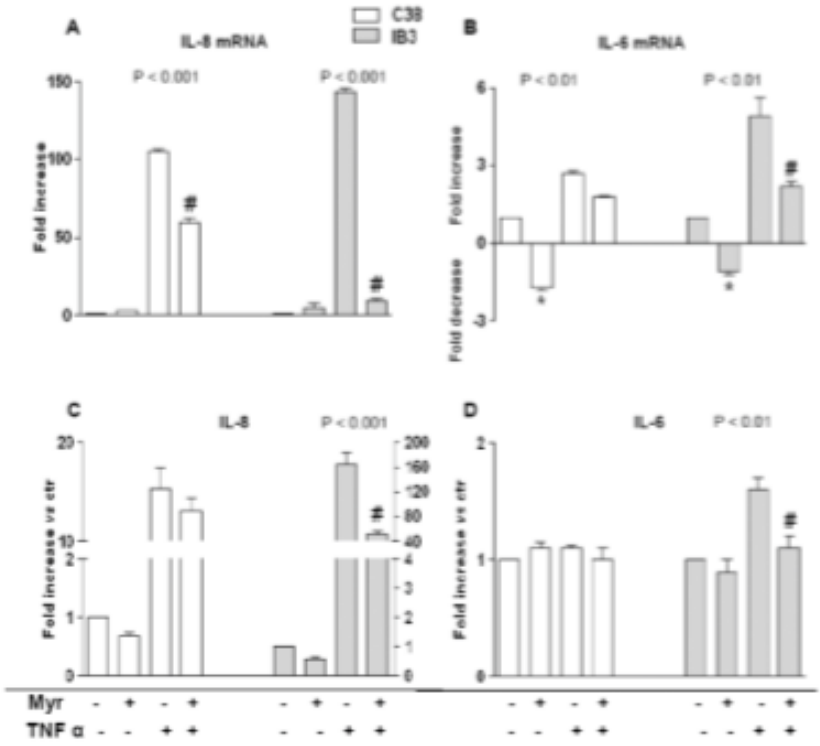

Figure 3. Myriocin effect on IL-8 and IL-6 transcription and release in TNFα–stimulated IB3 and C38 cells

IL-8 and IL-6 mRNA expression (**A** and **B**, respectively) and protein release (**C** and **D**, respectively) in IB3 and C38 cells stimulated with TNFα (20 ng/ml) either alone or in combination with Myr (10 μM, 8 h pre-treatment) for 24 h. Significance was evaluated by one-way ANOVA (value reported on the graphs). Panel **A**, **C**: #, *vs* TNFα-treated cells ($P < 0.001$, Bonferroni post-test). Panel **B**, **D**: #,*, *vs* TNFα-treated and untreated cells, respectively ($P < 0.05$, Bonferroni post-test).

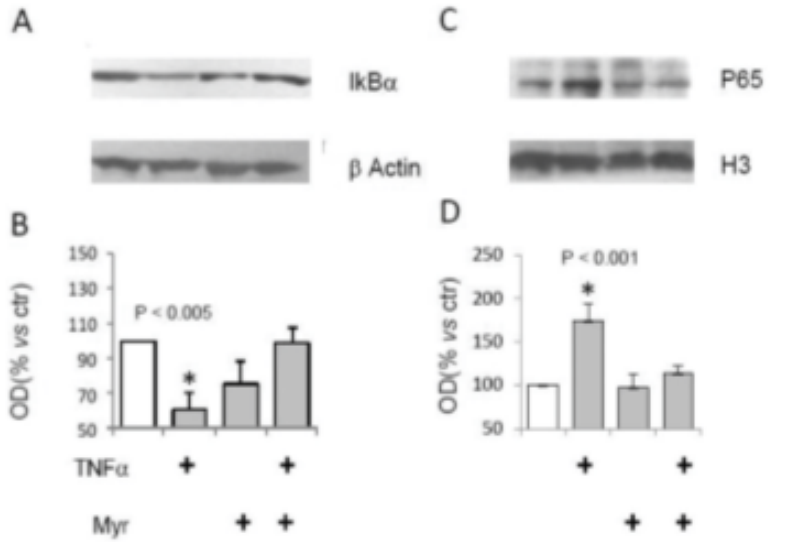

Figure 4. Myriocin effect on NF-kB activation in TNFα–stimulated IB3

IB3 cells stimulated with TNFα (20 ng/ml) for 24 h. Western blotting evaluation of I-kB from cytosolic extracts, compared to β-actin expression (A). OD from optical densitometry of 3 independent experiments was reported (B). Western blotting evaluation of NF-kB p65 from nuclear extracts, compared to histone H3. Significance was evaluated by one-way ANOVA (value reported on the graphs, P <0.001, Bonferroni post-test).

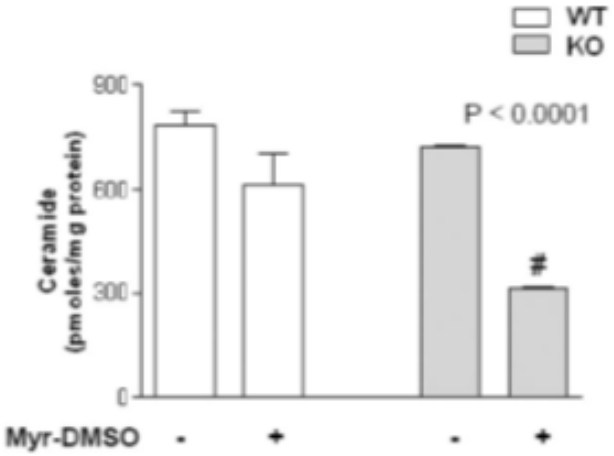

Figure 5. Myriocin effect on ceramide lung content and infection in KO and WT mice

Cer quantitation, by LC–MS analysis, in KO and WT mice treated (or untreated, DMSO vehicle only) with DMSO-solved Myr (11.95 μg of Myr/mouse lungs) 24 h prior to infection with *P. aeruginosa*. Animals were sacrificed 18 h post infection. Significance was evaluated by unpaired two-tailed Student t-test. #, *vs* untreated mice.

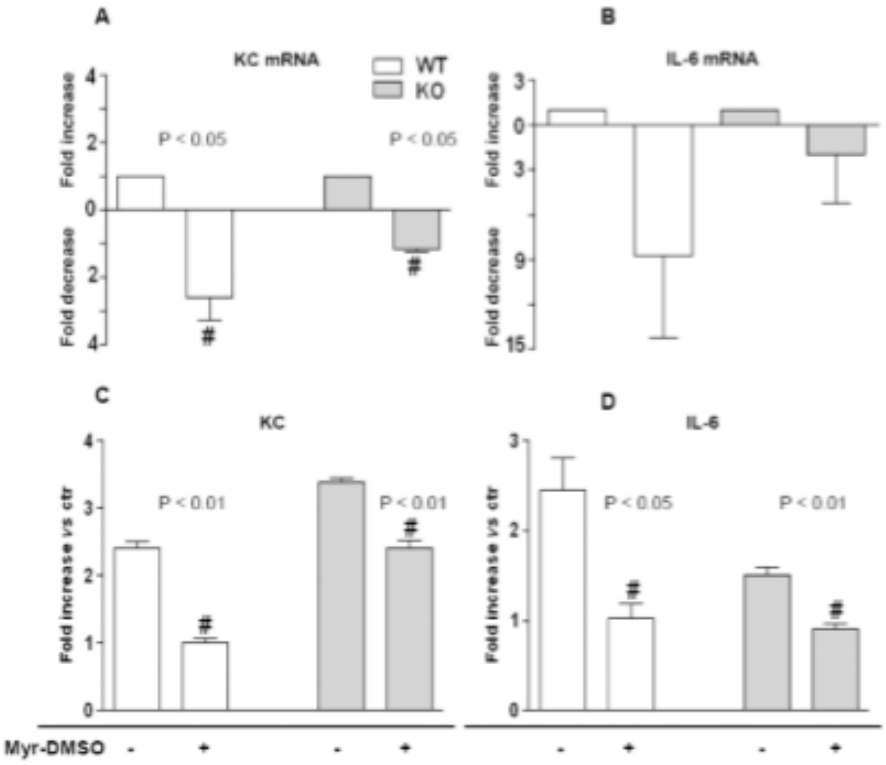

Figure 6. Myriocin effect on KC and IL-6 transcription and release in PAO1-infected lung of KO and WT mice

KC and IL-6 mRNA expression (**A** and **B**, respectively) and lung protein content (**C** and **D**, respectively) in KO and WT mice treated with DMSO-solved Myr (11.95 μg of Myr/mouse lungs) 24 h prior to infection with *P. aeruginosa* (PAO1). Animals were sacrificed 18 h post infection. mRNA values are expressed as fold change *vs* ctr (untreated mice). Protein values are expressed as fold increase *vs* ctr. Significance was evaluated by unpaired two-tailed Student t-test. #, *vs* ctr mice.

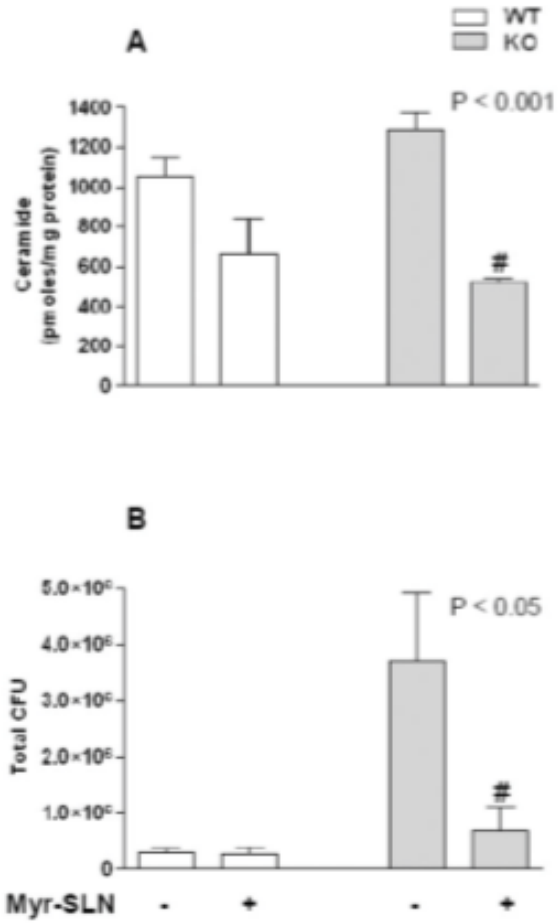

Figure 7. Myriocin-SLN effect on ceramide and infection in KO and WT mice

KO and WT mice treated with Myr-SLN (1.7 μg of Myr/mouse lungs) or untreated (empty SLN), 24 h prior to infection with *P. aeruginosa* (PAO1). Animals were sacrificed 18 h post infection. Cer quantitation, by LC–MS analysis (**A**). PAO1 colonies formation assay from lungs homogenate of infected KO and WT mice treated or untreated (**B**). Significance was evaluated by unpaired two-tailed Student t-test. #, *vs* untreated mice.

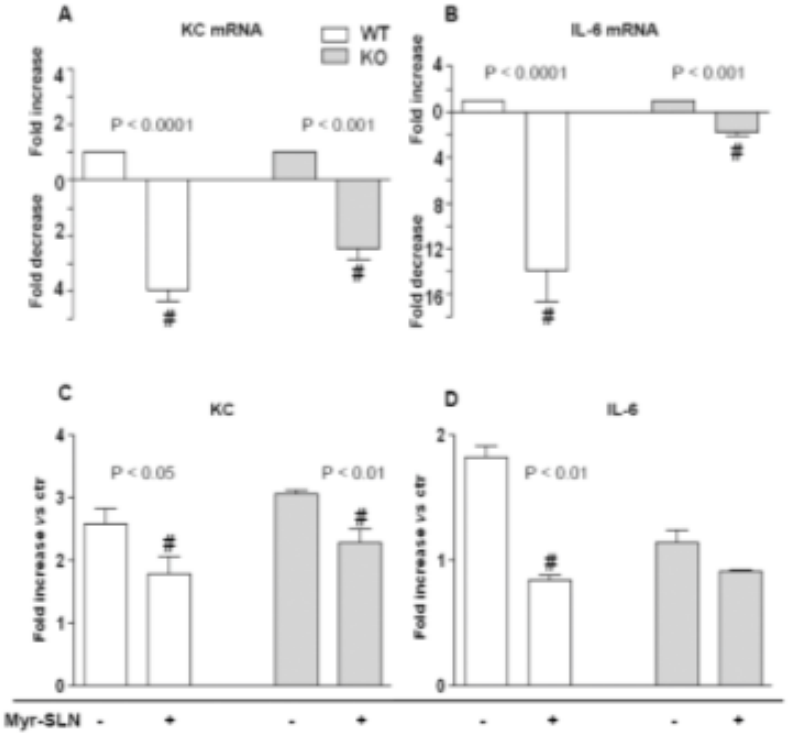

Figure 8. Myriocin-SLN effect on KC and IL-6 transcription and release in PAO1-infected lung of KO and WT mice

KO and WT mice treated with Myr-SLN (1.7 μg of Myr/mouse lungs) or untreated (empty SLN), 24 h prior to infection with *P. aeruginosa* (PAO1). Animals were sacrificed 18 h post infection. KC and IL-6 mRNA expression (**A** and **B**, respectively) and lungs protein content (**C** and **D**, respectively) in KO and WT mice. mRNA values are expressed as fold change *vs* ctr (untreated mice). Protein values are expressed as fold increase *vs* ctr. Significance was evaluated by unpaired two-tailed Student t-test. #, *vs* ctr.